Starting, braking and positioning with three-phase cage induction motors

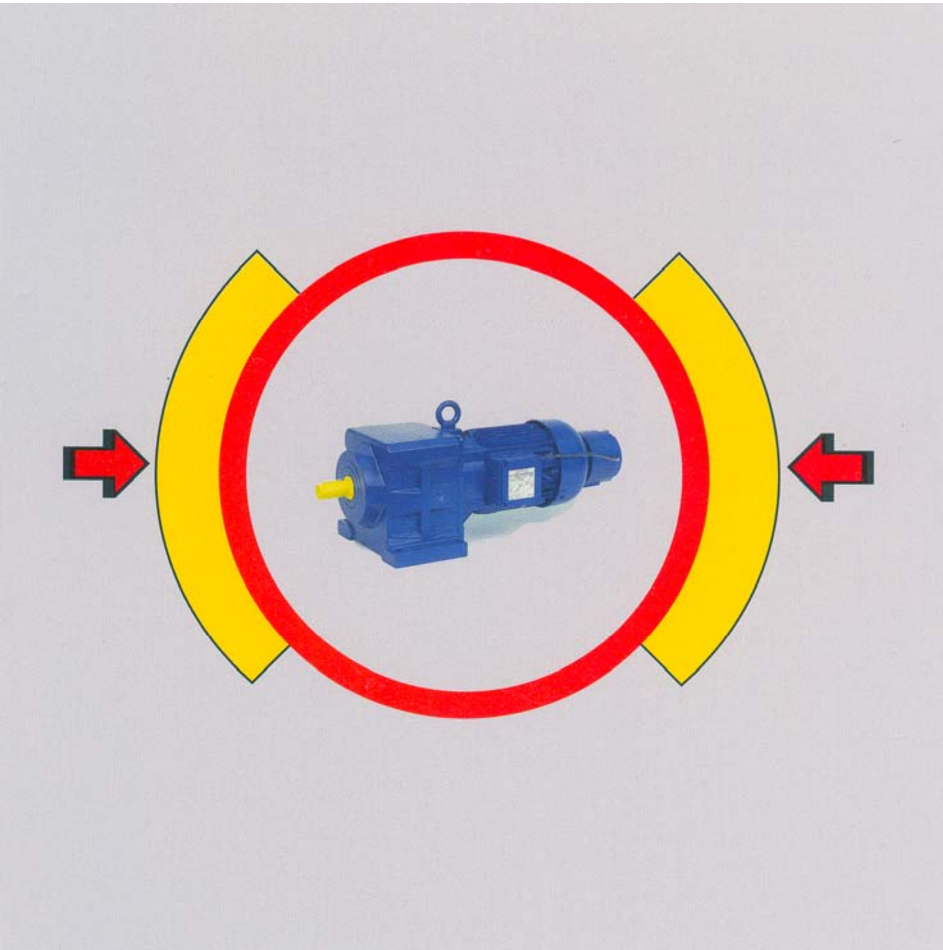

BAUER geared motors

The Gear Motor Specialist

Helmut Greiner

Starting, braking and positioning
with three-phase cage induction motors

Helmut Greiner

Starting, braking and positioning with three-phase cage induction motors

BAUER geared motors

The Gear Motor Specialist

Dipt.-Ing. (FH) Helmut Greiner (born 1929) began his electrotechnical practice in 1945 when he commenced an apprenticeship with an electrical contractor. After his studies he worked for 40 years with Bauer Antriebstechnik in Esslingen in the field of research and development of electrical motors and power transmission engineering. He is now acting as a consultant for Danfoss Bauer.

Printed in Germany
Geamtherstellung: BechtleDruckZentrum, Esslingen

Foreword

In addition to output and torque, performance characteristics are of the utmost importance in the selection of the drive for many applications involving geared motors, particularly in the fields of materials handling and robotics. The motor must accelerate softly, brake smoothly and reliably, and stop with pinpoint accuracy.

Starting, braking and positioning – these are important aspects of the duties required of electric drives in the context of automation and rationalization.

This book is aimed at all those working in the field of drive technology.
It aims to provide answers to those questions concerning drive technology which the author has most frequently encountered over his many years of experience in the planning and use of three-phase geared motors.

Aichschieß, January 2001 Helmut Greiner

TABLE OF CONTENTS

I INTRODUCTION
1 General
2 Assessment criteria for soft starting and braking
2.1 Slip on a conveyor belt
2.2 Tipping on a conveyor belt
2.3 Swinging of a load on a crane hook
2.4 Transitional behavIour of acceleration or deceleration

II STARTING
3 Torque-speed characteristic curves of the motor
4 Torque-speed characteristic curve of the load
5 Direct-on-line starting from a stiff system
6 Stepped starting by pole-changing
7 Star-delta starting
8 Part-winding starting
9 Starting transformer
10 Series resistors
10.1 Three-phase series resistors
10.2 Single-phase series resistance (KUSA resistance)
11 Electronic starting circuits
12 Frequency-controlled starting
13 Additional rotating mass
14 Special rotors with increased slip
15 Starting clutches
15.1 Centrifugal clutches
15.2 Hydrodynamic couplings
15.3 Induction couplings
16 Thermal rating of switching duty
16.1 Designation of switching duty types
16.2 Switching duty with output predominant
16.2.1 No load operating frequency Z_0
16.2.2 Permissible on-load operating frequency Z_{lim}
16.2.3 Thermally-equivalent switching frequency Z_{th}
16.2.4 Type test
16.2.5 Summary of terms used:
16.3 Switching duty with acceleration predominant
17 Determination of the run-up time
18 Classification of starting behaviour
18.1 Starting behaviour in accordance with IEC 60034-12
18.2 NEMA code letters
18.3 NEMA classification according to the torque characteristics
18.4 Starting classes

III ELECTRODYNAMIC INJECTION BRAKING
19 Hyper-synchronous regenerative braking
20 Reversing (changing the direction from full speed)
21 Plugging (reverse-field braking)
22 D.C. injection braking
22.1 Principle of D.C. injection braking
22.2 Connection of the stator winding
22.3 Rating the D.C. source
22.4 Control circuit diagram
22.5 Electronic D.C. braking units
23 Pole-changing
23.1 Production and characteristics of the braking torques
23.2 Damping the braking torques
23.3 Calculation of the braking time and braking travel
23.4 Recommended deceleration principles
23.5 SPR electronic soft deceleration

24 Frequency control
25 Thermal rating of electrodynamic methods of braking
25.1 Hyper-synchronous regenerative braking
25.2 Reversing
25.3 Plugging (reverse-field braking)
25.4 D.C. injection braking
25.5 Pole-changing
25.6 Frequency control

IV CALCULATION OF THE MASS MOMENT OF INERTIA
26 Rotor mass moment of inertia
26.1 Fixed-speed motors
26.2 Pole-changing motors
26.3 Cylindrical steel bodies
27 Homogeneous bodies with simple geometric shapes
28 Experimental determination of the mass moment of inertia
28.1 Torsional pendulum
28.2 Bar pendulum
28.3 Run-down test
29 Factor of inertia *FI*
30 Division of the torque according to the mass fractions
31 Conversion of moving masses
31.1 Rotation
31.2 Translation
31.3 Linear motion as a tangent to the circle

V MECHANICAL BRAKING
32 General
33 Braking systems
33.1 Classification of braking systems
33.2 Spring-loaded brake or magnetic brake
34 Built-on or built-in
35 Example designs
Fig. 35.1 Single-disc spring-loaded brake with D.C. solenoid release
35.2 Double-disc spring-loaded brake with D.C. solenoid release
35.3 Single-disc spring-loaded brake on the fan cowl
35.4 Double-disc spring-loaded brake on the fan cowl
35.5 Series ABR single-disc spring-loaded brake on the fan cowl
35.6 Series FBR single-disc spring-loaded brake on the fan cowl
35.7 Cone spring-loaded brake released by the motor field
35.8 Shoe spring-loaded brake with A.C. solenoid release
35.9 Multiple-disc spring-loaded brake with D.C. solenoid release
35.10 Single-disc spring-loaded brake with three-phase solenoid release
36 Electrical supply to the solenoid
36.1 One rated voltage in star or delta connection
36.2 Dual voltage winding in the ratio 1:1.73
36.3 Dual voltage winding in the ratio 1:2
36.4 Pole-changing: Dahlander connection or two separate windings
36.5 Starting devices to reduce the terminal voltage
36.6 Operation from an inverter with variable frequency
36.7 Sample cases and their preferred solutions
36.7.1 Motors with a fixed rated voltage
36.7.2 Motors with dual or variable rated voltages
36.8 Rated voltage of D.C. solenoid releases
36.8.1 Voltage spikes caused by self-inductance
36.8.2 Standardized rated D.C. voltages
36.8.3 Circuit configuration of diodes
36.9 Plug-in connection option
37 Brake release response time
37.1 Brake release using A.C. solenoids
37.2 Brake release using D.C. solenoids
37.3 Lost energy with long release time

37.3.1 Basic differences in the starting cycle
37.4 Thermal relief of the motor
38 Brake application response time
38.1 Brake application with A.C. solenoids
38.2 Brake application with D.C. solenoids
39 Mass moment of inertia of the friction discs
40 Selection according to the braking torque
40.1 Required braking torque
40.2 Run-out braking
40.3 Lifting duty
41 Selection according to the braking energy
41.1 Switching energy per braking operation
41.2 Thermally permissible switching energy
41.3 Reduction of the mechanical switching energy by electrical switching measures
41.3 Switching energy per friction element
42 Wear
43 Braking time
43.1 Deceleration
43.2 Lifting duty
43.3 Lowering duty
44 Overtravel time
44.1 Response time
44.2 Braking time
44.3 Overtravel time
45 Overtravel distance
45.1 Translation
45.2 Rotation
46 Benefits of a modular system
47 Working capacity of large brakes

VI POSITIONING
48 General remarks on positioning
49 Tolerances
49.1 Drive
49.2 Mechanical brake
49.3 Control system
49.3.1 Response times of contactors
49.3.2 Proximity switches
49.3.3 Timer relays
49.4 PLCs (programmable logic controllers)
50 Gear backlash
50.1 Guide values for standard gear units
50.2 Effect on linear motion
51 1:2 speed ratio (Dahlander connection)
51.1 External and internal current and field direction with Dahlander connection
51.2 Model utilization with Dahlander connection
51.3 Relative height of the torque characteristic curves
52 Other speed ratios (separate windings)
52.1 Terminal configuration
52.2 Possible speed ratios
52.3 Frame size utilization with separate windings
52.4 Relative height of the torque characteristic curves
52.5 Cost comparison
53 Possibilities and limits of pole-changing
54 Inverter-fed motors
55 Index positioning using SynchPos

Bibliography
Index of keywords

I INTRODUCTION

1 General

The three-phase cage induction motor owes its good reputation as a rugged, problem-free drive unit not least to its good starting characteristics. With a starting torque of 1.5 to 2.5 times its rated torque, these machines are able to start up even heavy-duty driven machinery under full load and ensure rapid acceleration.
Although this ability is of positive benefit in most applications, there are a number of driven machines where sudden acceleration can cause problems. For example, the swinging of a load on a crane hook, the tipping of bottles on a conveyor belt or the sudden over-stressing of mechanical transmission components.
Efforts to “improve the starting properties” of three-phase cage motors are therefore seldom aimed at increasing the acceleration, but are more often designed to ***reduce the run-up torque***.

The development of electric drives shows a clear trend towards ***more frequent switching*** and to ***greater precision in the positioning*** of the load. Previously, motors were designed for continuous operation and the conveyed material or the driven tools were controlled by mechanical systems which provided stepwise movement. Nowadays, braked motors can be accurately positioned by a combination of braking and pulse control. This development is particularly in evident with servo drives and stepper motors, which are required in present-day robotics. However, positioning drives are also used in the peripherals of these “robots”.

Starting, braking and positioning – these are important aspects of the duties required of electric drives in the context of automation and rationalization.

Where very high speeds and extremely accurate stopping positions are required, motors with steplessly adjustable speeds are used. For example, D.C. shunt motors with a controllable armature voltage or three-phase inverter motors where the frequency is varied by a static inverter.
In both cases the speed can be reduced to the positioning speed by a setpoint generator in the ratio of 100:1 in the case of modern inverter-fed motors and D.C. motors.
Both these methods are relatively costly and may not be justified in some instances.

There is a wide field of application for one solution that will be considered in this book in some detail, that is to say, the ***pole-changing three-phase motor*** with two fixed speeds with the maximum ratio of 10:1, controlled by conventional switchgear components.
Switching from the high speed to the low speed results from ***regenerative braking***, whereby the positioning speed is achieved within very tight tolerances without incurring any controller or regulator costs.
The switch-over times and travel distances are extremely short, which is highly beneficial in terms of rationalization. However, a transport process which is completely jolt-free and has a slower rate of deceleration is often necessary where sensitive products are to be moved.

Mechanical braking and stopping from the positioning speed is provided by an auxiliary spring-loaded ***mechanical brake***. This also works as a safety brake, securing the load in a stationary position in the event of a power loss.

2 Assessment criteria for soft starting and braking

A “soft start” or a “soft stop” is usually demanded by the manufacturer or the user of driven machinery where practical experience shows that direct-on-line (DOL) switching or braking leads to jerky operation. The designer of the drive will, in practice, find it very helpful if the “smoothness” is specified in terms of a minimum time, although this variable is not sufficient when dealing with major variations in the loading conditions, or with large difference in running speeds. The essential factor is the ***acceleration*** or ***deceleration***, as shown by the following three examples taken from the field of material handling.

Soft starting is required for instance to avoid the following:

2.1 Slip on a conveyor belt

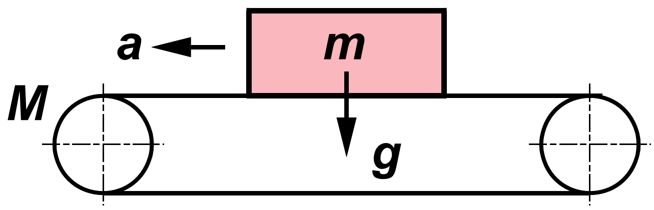	Fig. 2.1 Slip limit where force is transmitted by frictional contact
$a \leq \mu \cdot g$	*a* - acceleration in m/s² μ - friction factor *g* - acceleration due to gravity (9.81 m/s²)

2.2 Tipping on a conveyor belt

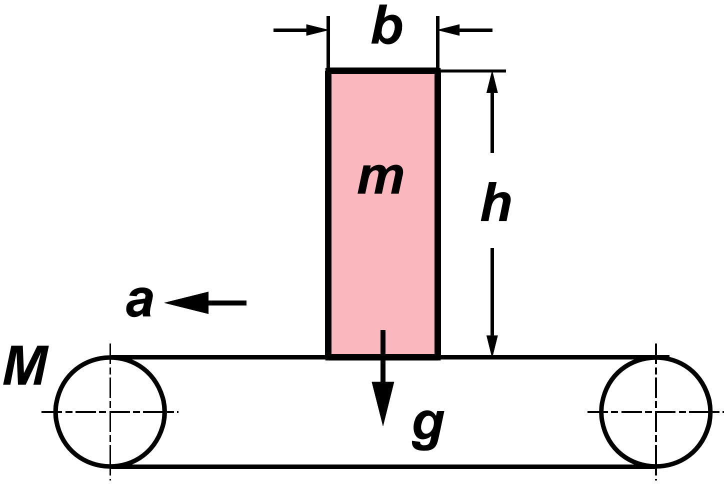	Fig. 2.2 Tipping limit relative to the height of the conveyed product
$a \leq \frac{b}{h} \cdot g$	*a* - acceleration in m/s² *b* - base width of the product in m *h* - height of the conveyed product in m *g* - acceleration due to gravity (9.81 m/s²)

2.3 Oscillation of a load on a crane hook

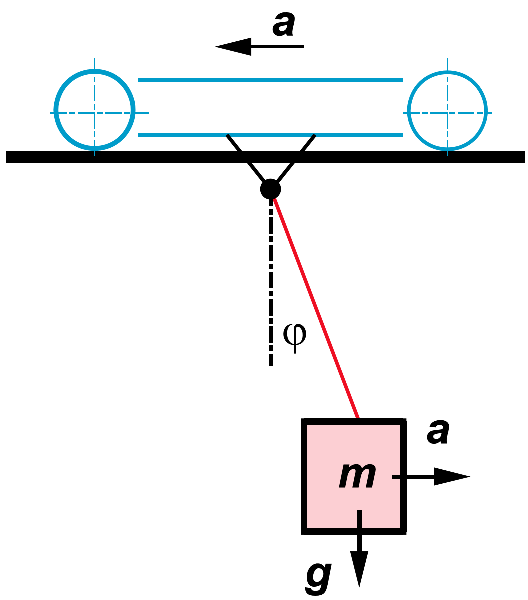	Fig. 2.3 Oscillation of a load suspended from a cable
$a \leq \tan\alpha \cdot g$	*a* - acceleration in m/s² α - angle of displacement (experience provides a maximum value of 3 °, therefore $a \leq 0.5$ m/s²) *g* - acceleration due to gravity (9.81 m/s²)

Fig. 2.4 can be used in the critical assessment of the starting behaviour of a crane's travelling gear:

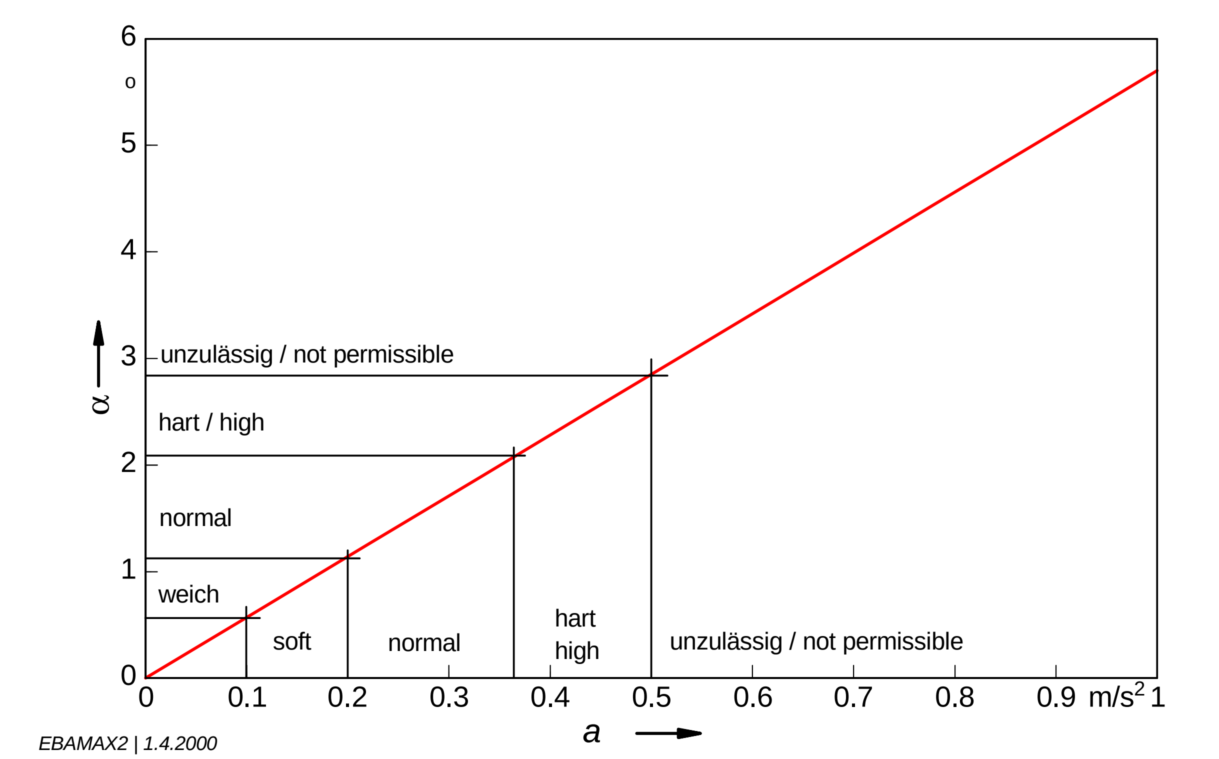

Fig. 2.4 Acceleration as an assessment criterion for starting behaviour of a crane's travelling gear

2.4 Transitional behaviour of acceleration or deceleration

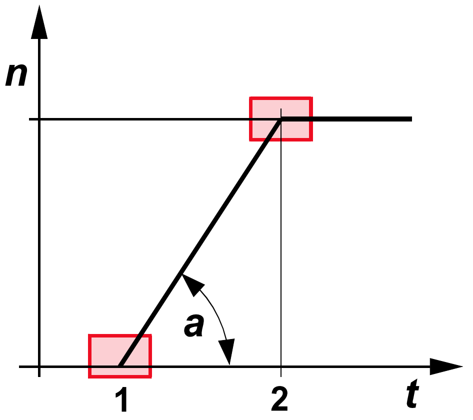

Fig. 2.4.1
Starting process

n - speed
t - time
a - degree of acceleration
1 - start of acceleration
2 - end of acceleration

The acceleration – represented by the angle *a* – can, within normal practical limits, be set as low as required, that is to say, the process is very soft according to the normal definition for starting. However, if we take a closer look at the transitional behaviour, we can see that the acceleration (angle *a*) changes suddenly at points (1) and (2) in the graph. In fact, the ***change of acceleration*** can be regarded as a ***jolt***, where:

$$r = \frac{\mathrm{d}a}{\mathrm{d}t}$$

This jolt causes pendulate oscillations and other disturbances to sensitive products when they are conveyed. The linear ramp shown in Fig. 2.4.1 is replaced by an approximation to a more or less ideal sine-shaped ramp to avoid this phenomenon on difficult drive applications. Typical applications for this would be rack drives, turntables and mobile welding robots.

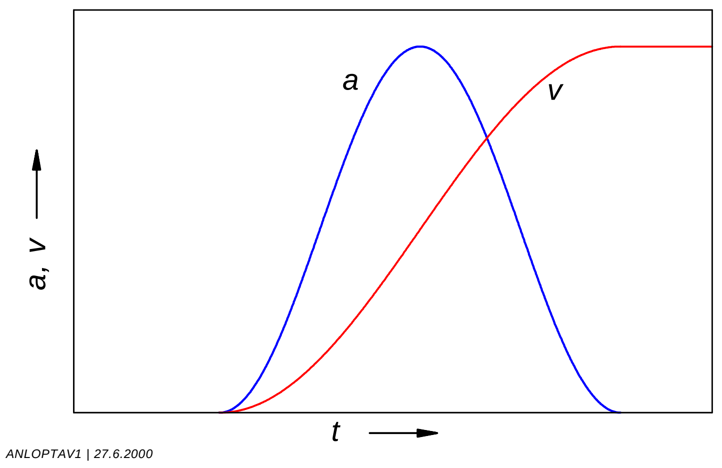

Fig. 2.4.2
Ideal acceleration profile *a* and speed *v* for jolt-free starting

Additional measures are required to obtain a “sinusoidal” profile for acceleration and speed. These are integrated into modern inverters as standard.

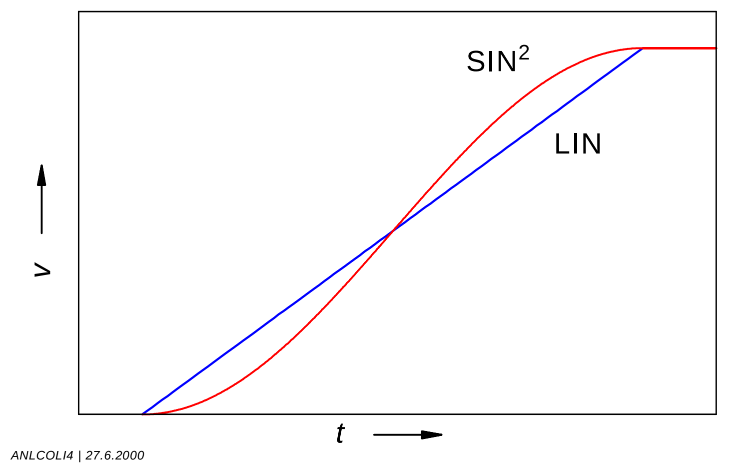

Fig. 2.4.3
Function of speed *v* with cosine or sine (SIN^2) smoothing of the speed transitions compared with a linear ramp (LIN)

Fig. 2.4.4 Overhead travelling crane used to service passenger aircraft.
Particular requirements on soft starting and stopping of the crane's travelling gear

3 Torque-speed characteristic curves of the motor

The principle of operation of the cage motor means that there are relatively high voltages and currents in the secondary circuit when the rotor is stationary with the stator field rotating at synchronous speed, i.e. with 100 % slip. This in turn can lead to high starting currents in the stator winding (Fig. 3.1).

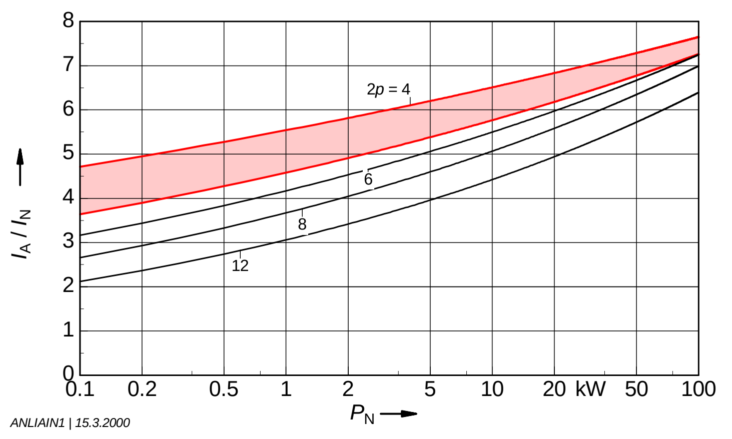

Fig. 3.1
Guide values for the relative starting current I_A/I_N for direct-on-line starting of three-phase cage motors with rated outputs of P_N = 0.1 ... 100 kW

The rotating field acting on the high rotor bar currents produces a strong breakaway torque. However, the breakaway torque is not in the ratio to the rated torque that would correspond to the increase in current. This is due to phase displacement.

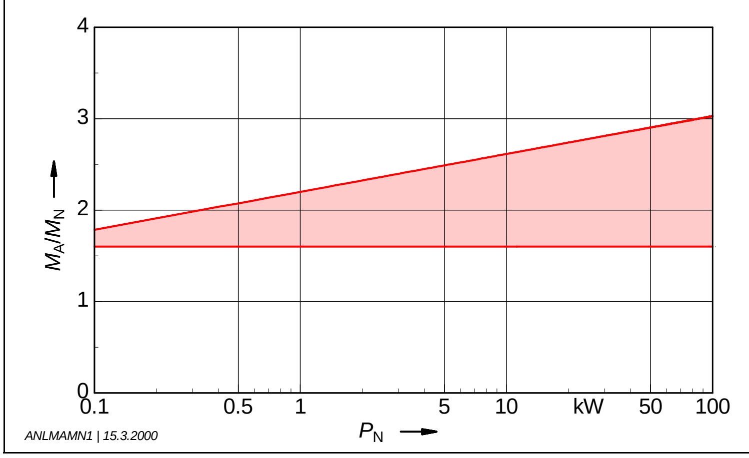

Fig. 3.2
Guide values for the relative breakaway torque M_A/M_N for direct-on-line starting of three-phase cage motors with rated outputs of P_N = 0.1 ... 100 kW

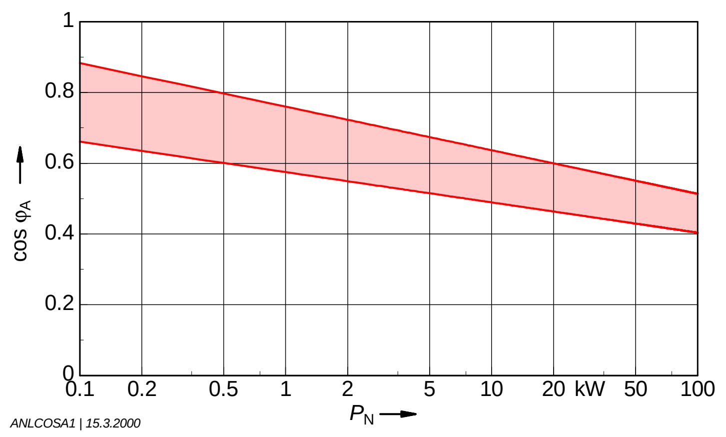

Fig. 3.3
Guide values for the locked rotor power factor cos φ_A for direct-on-line starting of three-phase cage motor with rated outputs of P_N = 0.1 ... 100 kW

The rotor resistance must be increased by ***current displacement*** for medium and higher rated outputs to reduce the starting current and increase the breakaway torque. For motors with shaft centre heights up to about 315 mm, pressure diecast rotors are available with a relatively flexible arrangement of the rotor slot shape. With larger units, the readily manufactured round slot type must be replaced by a deep slot or a double-cage design (Fig. 3.4) to obtain a smooth characteristic curve (Fig. 3.6).

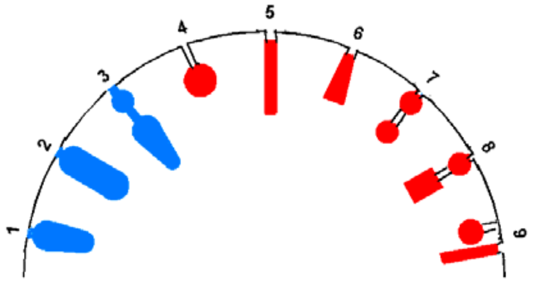

Fig. 3.4
Examples of pressure diecast cage rotor slot forms with
1 - pear-shaped slots
2 - deep slots
3 - double slots
Single-cage rotors with
4 - round bars
5 - deep bars
6 - wedge bars
Double-cage rotors 7, 8 and 9

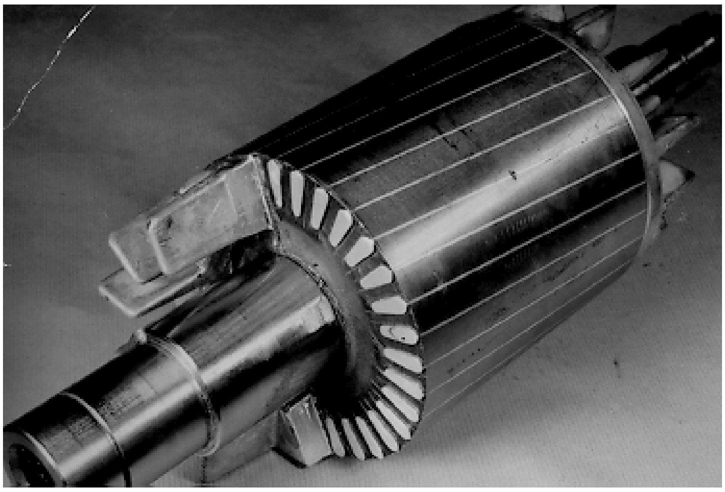

Fig. 3.5
Section through a pressure diecast cage motor with pear-shaped slots

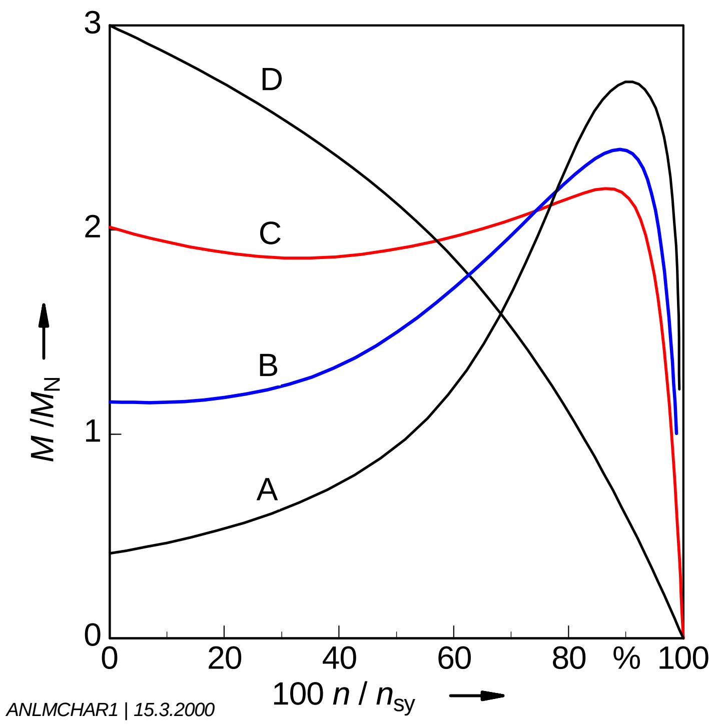

Fig. 3.6
Typical torque-speed characteristic curves of cage motors with various types of rotor design

A - round bar (4)
B - wedge bar (6), deep bar (5), pear-shaped slot (1)
C - double slot (3), double-cage (7,8,9)
D - high-resistance squirrel-cage rotor (e.g. brass, bronze, silumin)

n_{sy} - Synchronous speed

The numbers in brackets refer to Fig. 3.4

In the following discussion on this subject, a characteristic curve approximating C is assumed since this is typical for small and medium cage motors. There will be fairly considerable differences in the values mentioned where there are major deviations from this quasi-rectangular characteristic curve. Fig. 3.7 shows typical torque-speed characteristics and indicates the most important features.

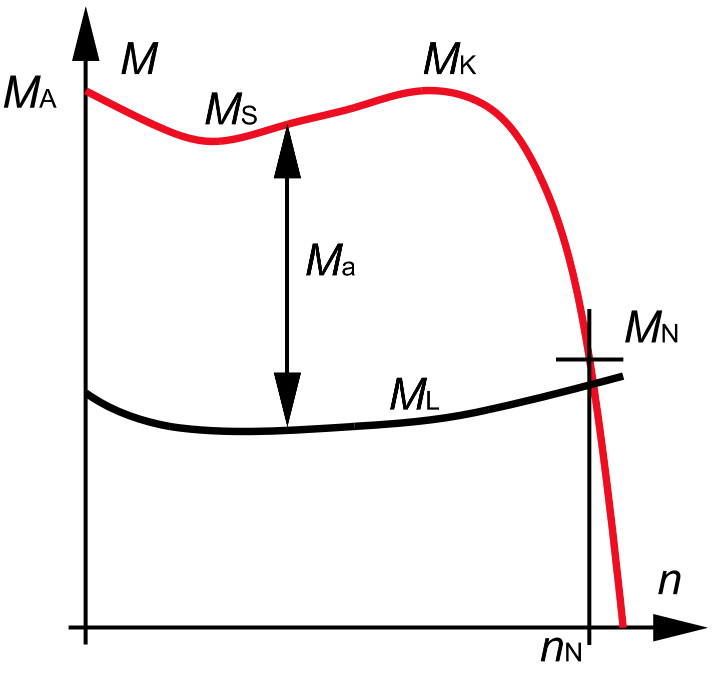

Fig. 3.7
Typical torque-speed characteristic curve of a cage motor with the characteristic values

n - speed
M - torque
M_N - rated torque
n_N - rated speed
M_A - breakaway torque (starting torque)
M_K - pull-out torque (breakdown torque)
M_S - pull-up torque
M_L - load torque
M_a - acceleration torque

4 Torque-speed characteristic curve of the load

The main influence on the starting behaviour of a drive is the relative value of the torques developed by the motor (torque-speed characteristic curve) in relation to those required by the load and the moments of inertia. The load's characteristic curve will depend on the type of driven machinery. Some typical (idealized) load characteristic curves are shown in Fig. 4. Some hybrid curves will occur in practice. These may not always have been precisely determined by the machine manufacturer for the machine in question because doing so can be a costly and complicated process. In these instances, assumptions based on experience or on the most adverse conditions have to be made. In contrast to the theoretical characteristics shown, increased "breakaway torque" must be allowed for when the motor is started from rest (relative speed 0 ... 0.1).

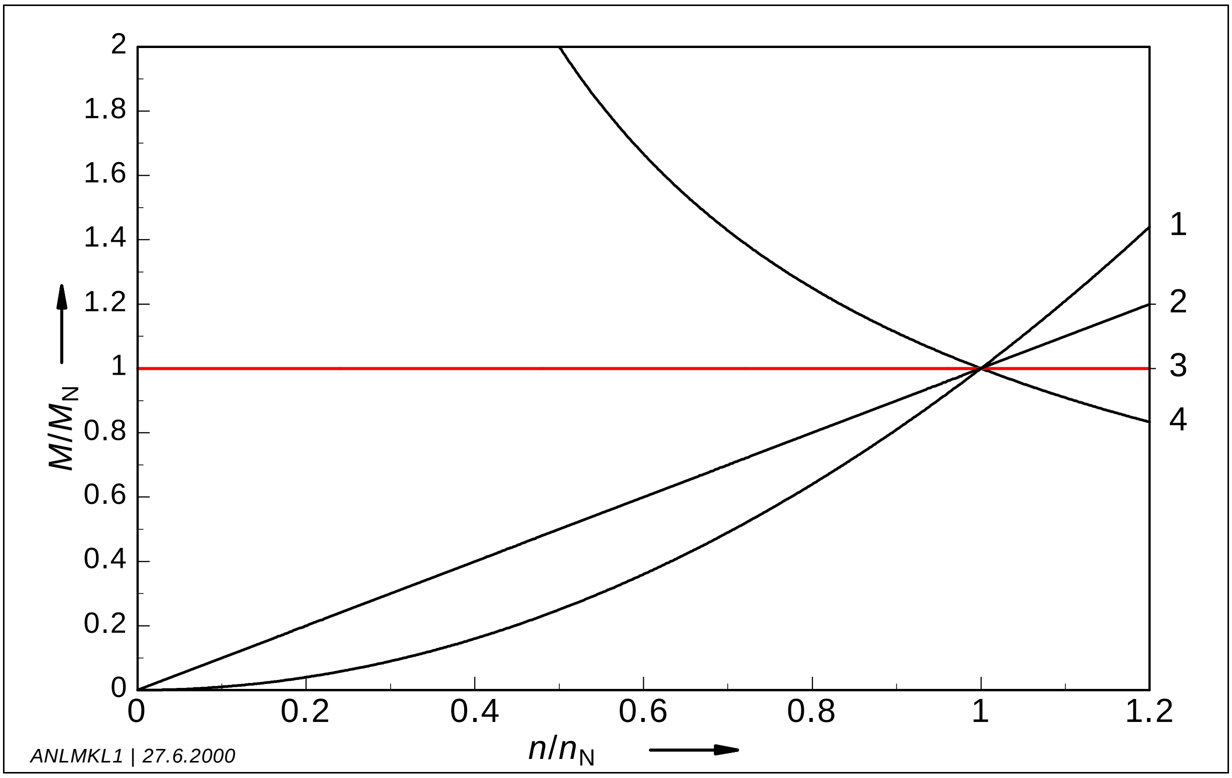

Fig. 4 Typical torque-speed characteristic curves of driven machinery.

Relationship between the torque and the relative speed:

1 - square
(pumps, fans)

2 - linear
(calenders, sheet rollers),

3 - constant
(hoists, conveyors, overcoming friction and gravitation)

4 - inverse
(coil winders, machine tools)

5 Direct-on-line starting on a stiff mains supply

A simple method of calculation is perfectly acceptable for practical purposes to determine the accelerating torque M_a for starting a typical cage motor with a “rectangular” characteristic curve (curve C in Fig. 3.5) against driven machinery with a “constant” torque (curve 3 in Fig. 4). The acceleration period is calculated as follows under these assumed conditions:

$t_a = \frac{J \cdot n}{9{,}55 \cdot M_a}$	t_a	- acceleration period in s
	J	- total mass moment of inertia in kgm²
	n	- speed in r/min
	M_a	- acceleration torque in Nm

Guide values for the ***acceleration time*** and ***run-up travel*** under no load and loaded at the rated torque are indicated in Figs 5.1 to 5.3.

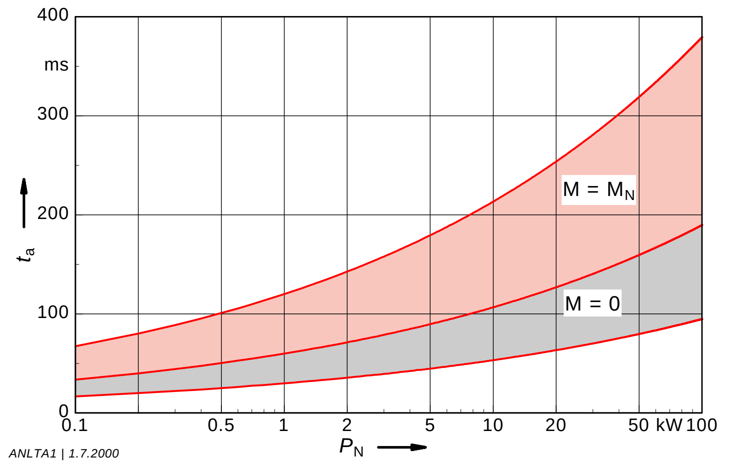

Fig. 5.1
Guide values for the acceleration time t_a of standard motor with rated outputs of
P_N = 0.1 ... 100 kW
under no load (M = 0) and
nominal load ($M = M_N$)

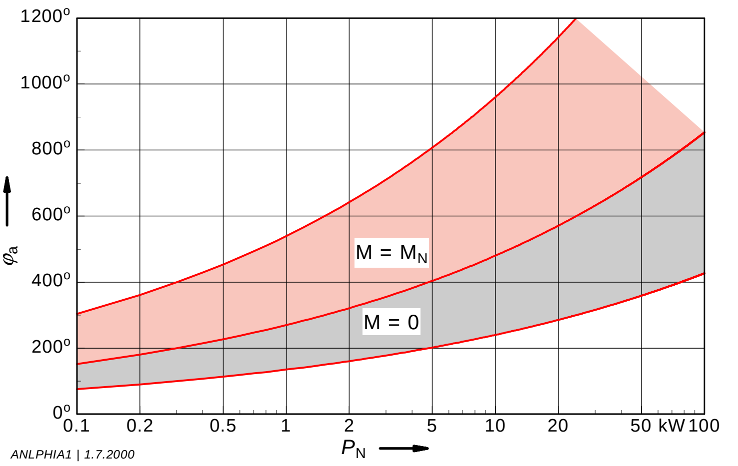

Fig. 5.2
Guide values for the angular run-up travel φ_a
of standard motors with rated outputs of
P_N = 0.1 ... 100 kW
under no load (M = 0) and
nominal load ($M = M_N$)

The following should be noted in any evaluation of these guide values:

- ☐ The shapes of the characteristic curves of the motor and load will differ to some extent from the ideal shape shown in Fig. 1.6.
- ☐ The following tolerances are permitted in accordance with EN 60034-1 [2.2]:
  M_A : –15/+25 %
  M_K : –10 %
- ☐ The rated torque M_N has been assumed for the load torque. However, most drives are not fully loaded.
- ☐ The external mass moment of inertia is not usually known to any degree of precision.

The acceleration times of standard motors are usually well under one second. The ***thermally allowable acceleration period*** – sometimes referred to in the literature as ***ART*** (allowable run-up time) – will be significantly longer (Fig. 5.3).

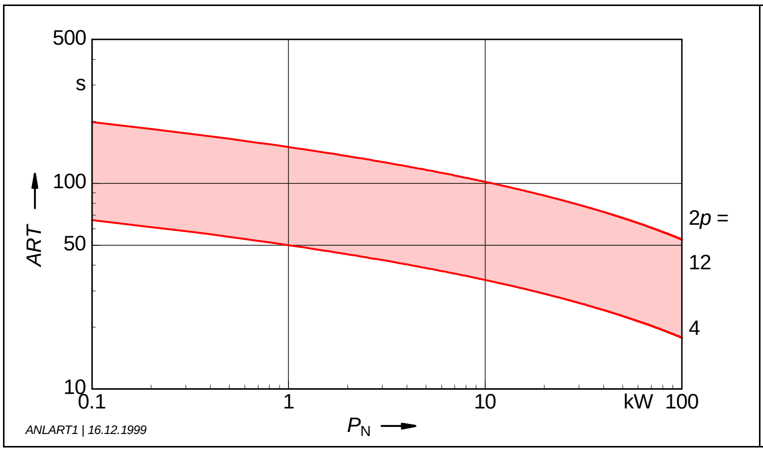

Fig. 5.3
Guide values for the thermally allowable run-up time (*ART*) of standard motors
with rated outputs of
P_N = 0.1 ... 100 kW
with pole numbers 2p = 4 ... 12

The ***pull-up torque*** of an A.C. motor is defined in EN 60034-1 subclause 2.14 as:
"The smallest value of the steady-state asynchronous torque which the motor develops between zero speed and the speed which corresponds to the breakdown torque when the motor is supplied at the rated voltage and frequency".
The minimum value of the pull-up torque is given in clause 20 of the standard:

	P_N < 100 kW	$P_N \geq$ 100 kW
Single-speed three-phase motors	0.5 M_N 0.5 M_A	0.3 M_N 0.5 M_A
Multi-speed three-phase motors	0.3 M_A	0.3 M_A

Two facts are highlighted in this table:
- ☐ Large motors have relatively low pull-up torques compared with small motors
- ☐ Pole-changing motors have lower pull-up torques than single-speed motors.

It can be assumed from this that the relatively low values specified by the standard for normal production motors will be far exceeded. Synchronous and asynchronous deflections in the torque cannot be entirely ruled out in special designs, e.g. those with unusual ratios of pole numbers. Attenuation of these dips is possible by using expensive special measures, e.g.
- ☐ Optimum slot ratio between stator and rotor (often difficult with pole changing)
- ☐ Increased skewing of the rotor slos
- ☐ Increased air gap
- ☐ Different chording in the double-layer lap winding.

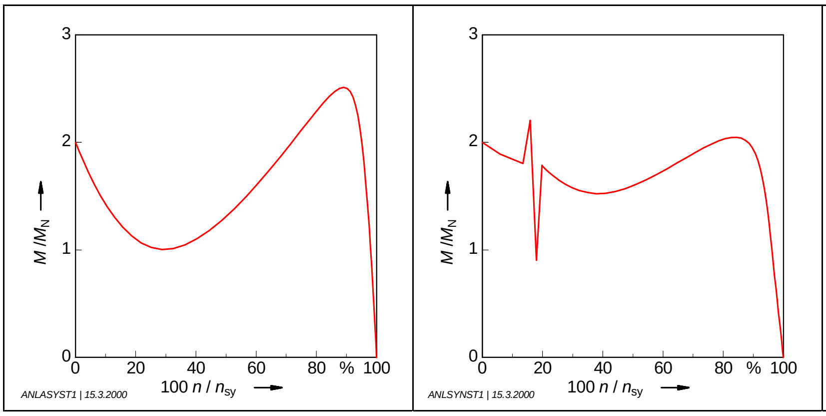

Fig. 5.4
Torque characteristics with pronounced pull-up torque deflection
Left: asynchronous
Right: synchronous

The measurement of torque dips requires some care. The torque determined with an electronic torque meter and the speed can be sent to an X-Y plotter during slow acceleration. Synchronous torque deflections may be overcome by the mass moment of inertia and will remain undetected if the speed rise is too rapid. It is often necessary to adjust to a particular suspected speed to locate the sharply-defined discontinuity in the torque curve. It will be appreciated that synchronous torque deflections are not usually discernible in practice. However, the combination of an asynchronous and a synchronous torque deflection can impede the run-up. Fig. 5.5 shows the run-up characteristic curve of a motor (M) with a pronounced asynchronous torque deflection and a load characteristic curve (L). M is dominant in the dark-shaded region: the motor can accelerate. The load L is dominant in the lightly-shaded region S: The drive remains at the same speed consuming a current virtually the same as the starting current and the mains supply will be cut by the circuit breaker before it reaches its running speed.

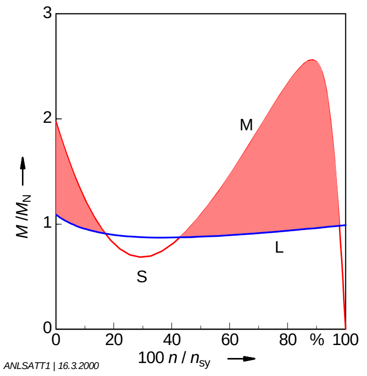

Fig. 5.5
Run-up of a motor (M) with pronounced asynchronous torque deflection (S) plotted against a load (L)

The run-up will be interrupted in the region S

In the above discussions, the quasi-steady state was assumed for the starting current and breakaway torque. The “old” German standard VDE 0530 Part 1/1.66 still defined these values as being applicable "after ***transient conditions*** had decayed". This clearly indicated that ***peak values*** before the onset of the steady state were to be ignored, although such peaks will always be present. Because the transients decay after a few half cycles, their thermal effect can be ignored. However, for very sensitive electronic or mechanical components, it is very important to know the potential magnitude of the peak values. They are extremely difficult to measure; result values fluctuate accordingly in the literature [2.8, 2.10, 2.11]:

- ☐ Peak current value I_{max} = (2 ... 5) · I_A
- ☐ Peak torque value M_{max} = (3 ... 6) · M_A

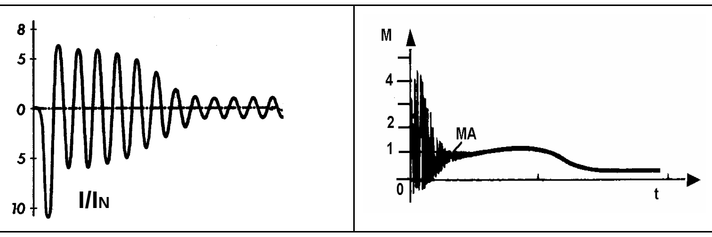

Fig. 5.6
Peak values when switching on, before the transients die away to the steady state
Left: current
Right: torque

Switching in phase opposition is a special instance of the processes described above. Power plant specifications sometimes require motors to be able to withstand a sudden switch to an independent supply in phase opposition. According to figures in the literature, this can be expected to produce a peak torque of 8 ... 10 times the rated torque. This represents an exceptionally heavy load on the mechanical transmission components. This requirement is excessive and is not justified by actual conditions found in practice since, before switching to an independent supply, the motor will be properly synchronized and even in the event of emergency switching will have been reduced to a 20° phase angle and optimized to about 40 % of the residual voltage.
However, phase opposition can also occur in industrial applications if the mains supply is broken very briefly (e.g. for a few milliseconds). In this case the motor will be generating a reducing frequency from its remanence voltage and can be re-energized from the restored mains voltage in phase opposition – albeit with reduced amplitude. The torque peaks can then reach 3 ... 8 times the rated torque.

6 Stepped starting by pole-changing

Pole-changing motors with two or more speeds should always be switched to the lowest possible speed when starting if possible. This will reduce the starting current and heat losses.
The rotor losses during pure flywheel starting are equal in theory to the energy imparted to the accelerated masses after run-up. Thus, after start-up, the total rotor loss will be given by

$$W_{rot} = \frac{J \cdot \varpi^2}{2} = \frac{J \cdot n^2}{182{,}5}$$

The losses can be shown graphically as in Fig. 6.1:
At the moment of switching on, the rotating field Φ almost instantaneously jumps to the synchronous speed of rotation n_{sy}, whereas the rotor is accelerated to this speed over time t_a. The difference between the rotating field speed n_{sy} and that of the rotor n_{rotor} is a measure of the power losses. The triangle above time t_a represents the lost energy V_{rotor} in the rotor.

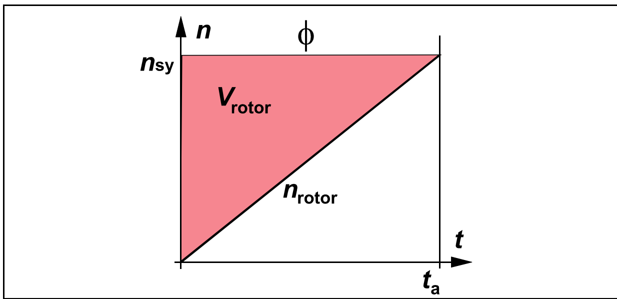

Fig. 6.1 Lost energy in the rotor V_{rotor} for direct-on-line starting with full rotating field speed n_{sy}

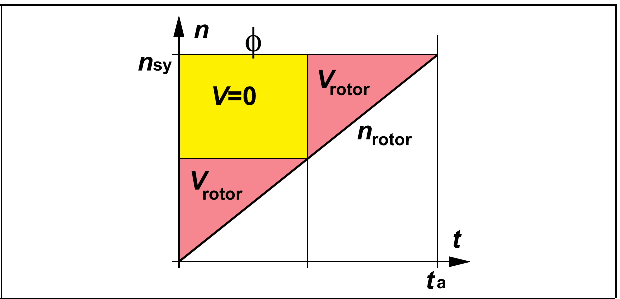

Fig. 6.2 Lost energy in the rotor V_{rotor} with stepped run-up by 1:2 pole-changing (e.g. 4/2 pole), the area V=0 being loss-free

With stepped run-up (e.g. by pole-changing with speed ratio of 1:2 as in Fig. 6.2), the lost energy is reduced to a half compared with direct-on-line starting.
With other pole number ratios, the energy saving will sometimes be considerably less.

Diagram	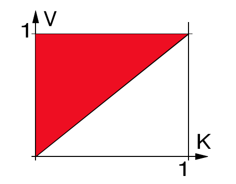	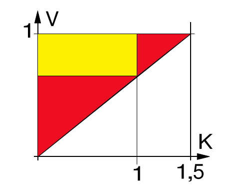	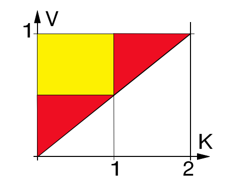	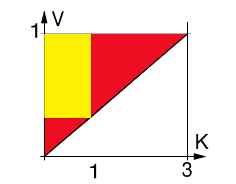
Number of poles	e.g. 4	6/4	8/4, 4/2	6/2
Ratio *K*	1	1:1.5	1:2	1:3
Relative loss *R*	1	0.555	0.5	0.555
Diagram	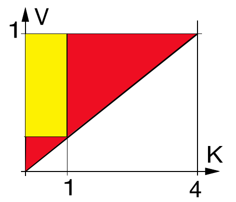	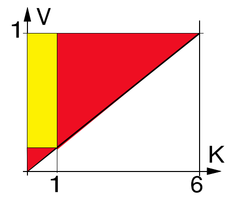	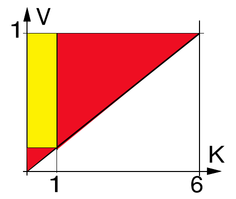	
Number of poles	8/2	12/2	20/2	
Ratio *K*	1:4	1:6	1:10	
Relative loss *R*	0.625	0.72	0.82	

Fig. 6.3 Lost energy (dark areas) and loss saving (light rectangles) with stepped starting by pole-changing with the speed ratio *K*

7 Star-delta starting

In low voltage circuits, the magnitude of the permissible starting current is restricted by the power supply authority. The regulations may vary according to the specific local conditions. Some guidance is given in the following table taken from the “Technical Conditions of Supply” of the Association of German Power Supply Authorities (VDEW – Vereinigung Deutscher Elektrizitätswerke).

	DOL starting	Star-delta starting	Starting via a starter $I_A \leq 2\, I_N$
Single-phase motors at 230 V	up to 1.1 kW	-	-
Three-phase single-cage motors at 400 V	up to 2.2 kW	up to 4 kW	up to 11 kW
Three-phase current-displacement motors at 400 V	up to 4 kW	up to 7.5 kW	up to 11 kW

Table 7.1 Maximum permissible rated motor output for low voltage supplies in accordance with VDEW motor starting regulations

Star/Delta starting is often adopted to comply with these regulations.
The motor is wound for connection to the mains voltage in Δ configuration but is connected to mains supply in star configuration during the starting phase. The voltage across each phase winding will thus only be 1/√3 of the rated voltage. The breakaway torque and starting current are then reduced to one third of the direct-on-line starting values.

$$M_{AY} = \frac{M_{A\Delta}}{3}$$

$$I_{AY} = \frac{I_{A\Delta}}{3}$$

If, for example, a DOL motor has a starting torque of twice the rated torque, the starting torque will be only two thirds the rated torque in the case of star starting. Thus:

$$M_{AY} = \frac{1}{3} \cdot M_{A\Delta} = \frac{2}{3} \cdot M_N$$

That is to say, the motor will not be able to run up in star configuration if the load generates higher torques than (2/3) M_N. ***Star-delta starting is only suitable for starting under no load or against a light load.***

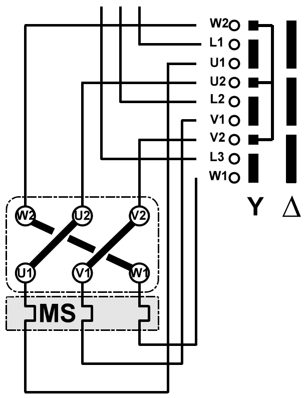

Fig. 7.2
Circuit diagram for star-delta (Y-Δ) starting showing the connection and rating of the motor protection relay for the phase current $I_{ph} = I_N/\sqrt{3}$

When star-delta (Y-Δ) starting is used against a heavy load or full load, the peak starting torque and current will be insufficiently damped, as shown in Fig. 7.3.

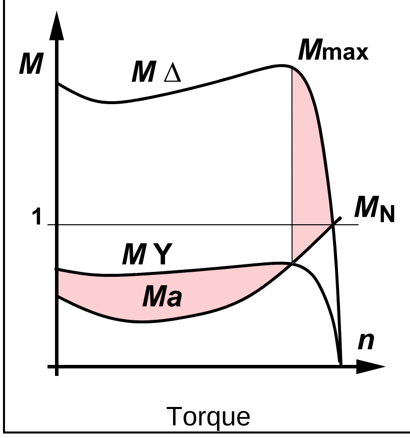

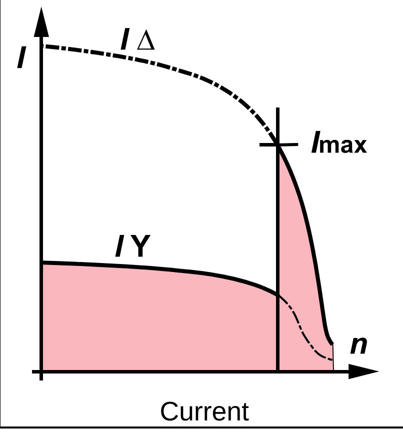

Fig. 7.3
Peak values of torque M_{max} and current I_{max} showing unsuitable switching from star to delta (Y to Δ) due to starting against excessive load

Reinforced star-delta starting is occasionally used because 1/3 run-up torque is not sufficient to overcome partial or full load. This method reduces the torque and current to approximately 50 % the direct-on-line starting values. It requires a relatively expensive winding design (with split phases) and wiring and therefore has very little to do with simple star-delta (Y-Δ) starting except the name (Fig. 7.4).

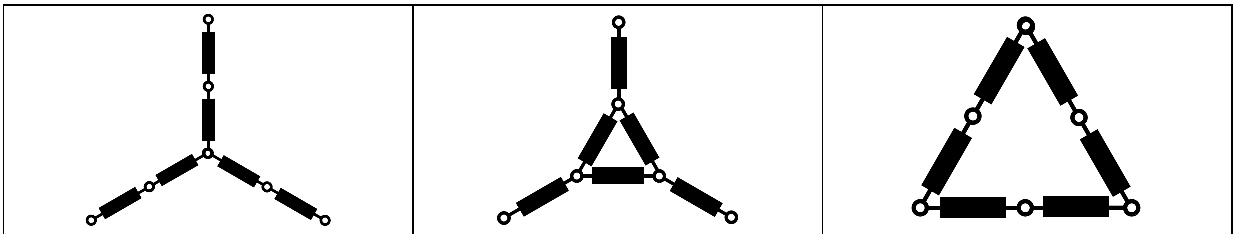

Starting – stage I	Starting – stage II	Running – stage III
M_A/M_{AD} ≈ 30 %	**≈ 40 ... 50 %**	**100 %**
I_A/I_{AD} ≈ 30 %	**≈ 50 %**	**100 %**

Fig. 7.4 Wiring and characteristic values for reinforced star-delta starting

The characteristic values for the breakaway torque and starting current given above compared with direct-on-line starting (index D) refer to a symmetrical split of the phase windings. Asymmetrical splits with correspondingly altered torques and currents have also been designed. These complex methods have generally be superseded by electronic soft starters.

8 Part-winding starting

The star-delta (Y-Δ) starting widely used in Europe to reduce the starting current and breakaway torque is comparatively little used in North America, where ***part-winding starting*** is relatively common. This is defined in NEC 430-3 [2.5] as requiring a stator winding in which two groups are energized in parallel in normal operation. During starting, the parallel connection is overridden, i.e. only one of the groups is energized. This has the effect of a series resistor and reduces the breakaway torque and starting current, although not to the same degree as with star-delta (Y-Δ) starting.
There are a large number of switching variations – a simple example is shown in Fig. 8.1. Here the winding is designed for the rated voltage with two parallel branch (star-star connection); only one of these branches is energized on starting. The connection for this is as follows:

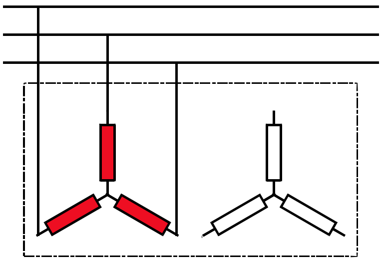 **Start**	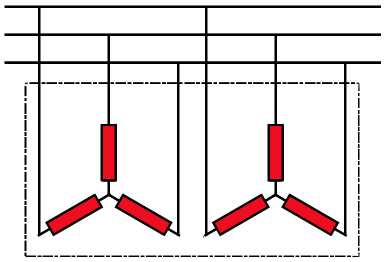 **Run**	Fig. 8.1 Basic circuit diagram for the part-winding starting common in North America Known as the “3-3” method i. e. 3 starting contacts
M_A = 50 %	**M_A = 100 %**	+ 3 running contacts
I_A = 70 %	**I_A = 100 %**	

2/3 of the phases are initially energized in the case of the somewhat complicated “4-2” method.

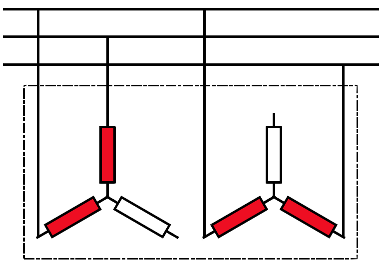 **Start**	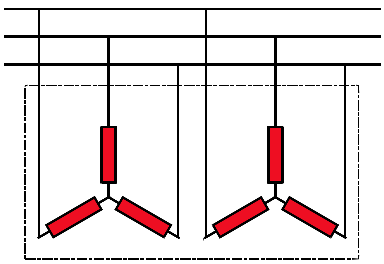 **Run**	Fig. 8.2 Basic circuit diagram for the part-winding starting common in North America Known as the “4-2” method i.e. 4 starting contacts
M_A = 65 %	**M_A = 100 %**	+ 2 running contacts
I_A = 80 %	**I_A = 100 %**	

9 Starting transformer

The breakaway torque of an induction motor is proportional to the square of the voltage applied, whereas the starting current is directly proportional to the voltage applied.

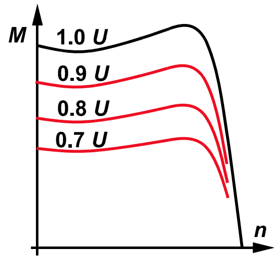

Fig. 9.1
Torque reduction with square-law dependence on the output voltage of a starting transformer

$$M_A \approx U^2$$

$$I_A \approx U$$

In contrast to star-delta (Y-Δ) starting, a variable starting transformer enables the starting cycle to be optimized to the actual load – although at relatively high cost.

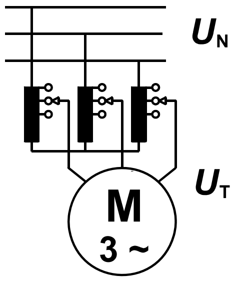

$$\ddot{u} = \frac{U_T}{U_N}$$

$$\frac{M_{AT}}{M_{AN}} = \frac{I_{AT}}{I_{AN}} = \frac{S_{AT}}{S_{AN}} = \ddot{u}^2$$

Fig. 9.2
Characteristic values with Starting transformer

ü	- ratio (<1)
M	- torque
I	- mains current
S	- apparent power
Index	N - without transformer
	T - with transformer
	A - breakaway

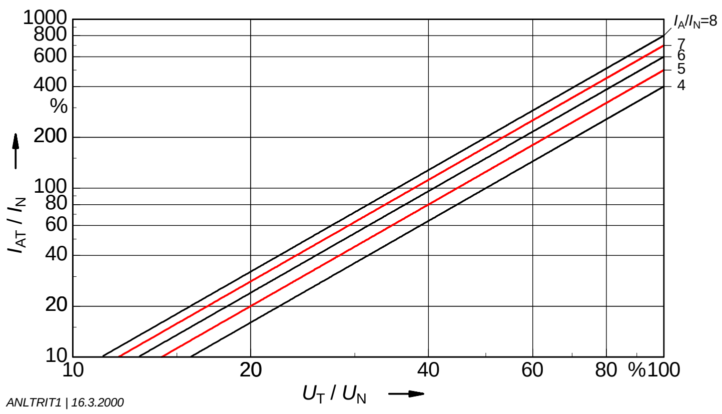

Fig. 9.3
Reduction of the relative starting current drawn from the mains by using a starting transformer

I_A/I_N	Relative starting current drawn from the mains with direct-on-line starting
I_{AT}/I_N	Relative starting current drawn from the main with starting transformer
U_T	Transformer voltage output

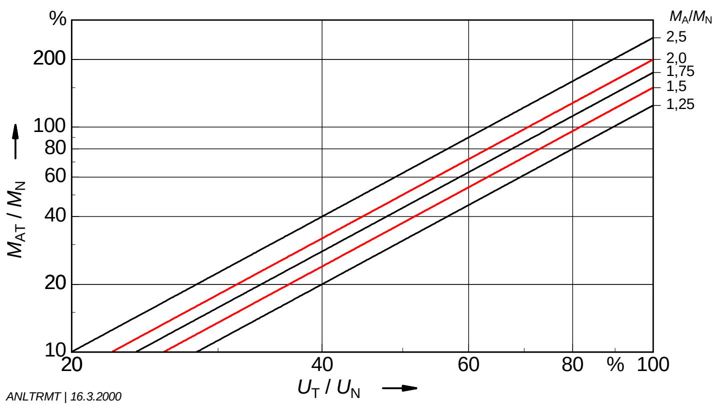

Fig. 9.4
Reduction of the relative breakaway torque by using a starting transformer

M_A/M_N	Relative breakaway torque with direct-on-line starting
M_{AT}/M_N	Relative breakaway torque with starting transformer
U_T	Transformer output voltage

10 Series resistors

A square-law reduction of the run-up torque by lowering the voltage can also be achieved by means of the voltage drop in series resistors.

10.1 Three-phase series resistors

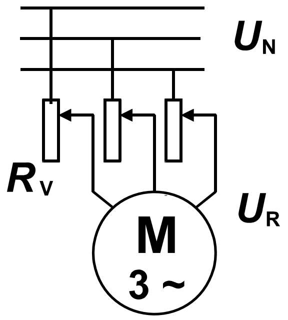

$$\frac{M_{AR}}{M_{AN}} = \left(\frac{U_R}{U_N}\right)^2$$

$$\frac{I_{AR}}{I_{AN}} = \frac{U_R}{U_N}$$

Fig. 10.1.1
Characteristic values with three-phase series resistors

R_V	-	resistance
M	-	torque
I	-	current
U	-	voltage
Index	N -	mains supply
	R -	with resistor
	A -	breakaway

The locked rotor power factor cos φ_A must be taken into account when calculating the series resistance R_V; guide value are given in Fig. 10.1.2.

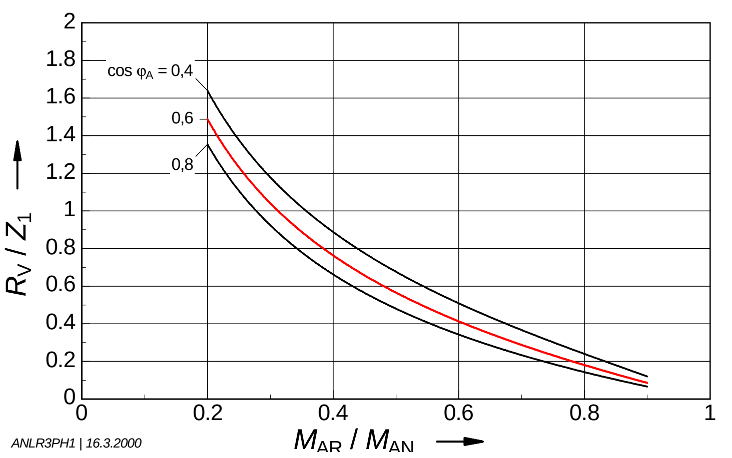

Fig. 10.1.2
Guide values for three-phase series resistance according to the torque reduction required

R_V	series resistance per phase (Ω)
M_{AR}	reduced breakaway torque
M_{AN}	DOL breakaway torque
cos φ_A	locked rotor power factor
Z_1	impedance per phase winding

$$Z_1 = \frac{U_N}{1{,}73 \cdot I_A}$$

10.2 Single-phase series resistance (KUSA resistance)

If it is necessary to reduce the breakaway torque without reducing the starting current accordingly, equipment and circuitry costs can be cut by fitting a series resistor in only one of the three lines. This method is known in German as ***KUSA starting*** (**KU**rzschluss-**SA**nftanlauf, i.e. locked rotor soft starting). The lack of symmetry and the locked rotor power factor make calculations difficult to perform in advance, so that an empirical value is normally used. Because the various motor designs available from manufacturers and the different loading conditions give rise to a relatively large scatter band, it is recommended that the KUSA series resistance be generously rated and fitted with a pick-off so that it can be set to its optimum value for the application on site. A current carrying capacity suitable for S2, S3 or S4 duty is adequate.
After the run-up, the series resistor should be shorted out as shown in wiring diagram 10.2.1. There is a risk of a motor protection relay detecting single-phasing and therefore tripping with comparatively long run-up periods. In this case, phase failure sensitivity must be provided by some other means.

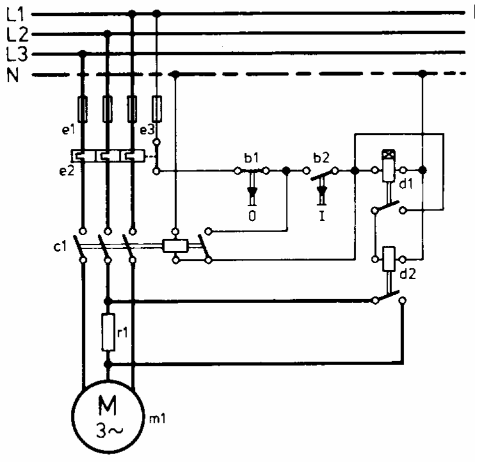

Fig. 10.2.1
Wiring diagram for KUSA starting

c1	-	primary protection
d1	-	timer relay
d2	-	contactor relay
r1	-	KUSA resistor

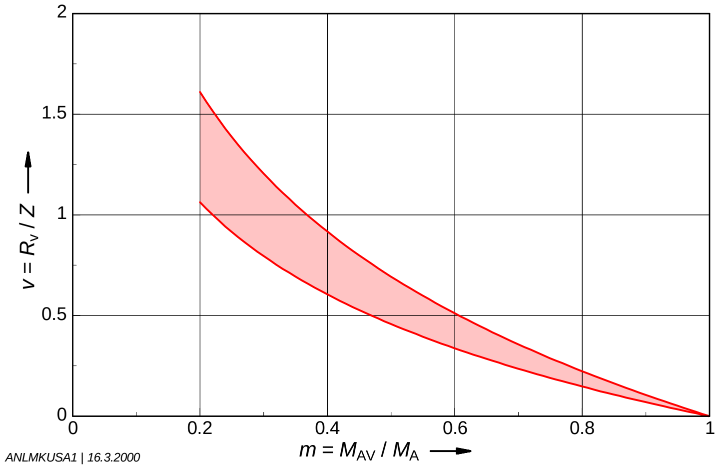

Fig. 10.2.2
Guide values for the KUSA resistor in relation to the torque reduction required

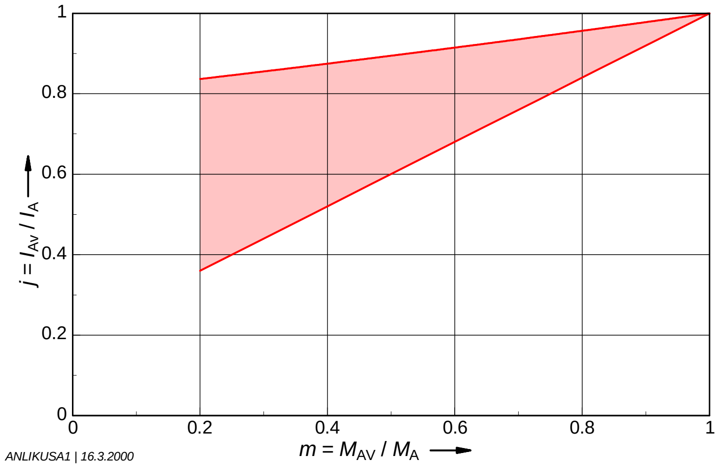

Fig. 10.2.3
Guide values for the starting current consumption in relation to the torque reduction

The following equations are used to plot the graphs above:

$Z = \frac{U \cdot \sqrt{3}}{cA \cdot I_N}$	$R_V = Z \cdot v$	$m = \frac{M_{AV}}{M_A}$	$j = \frac{I_{AV}}{I_A}$

Z	- winding impedance in Ω	R_V	- KUSA series resistance in Ω
U	- mains voltage in V	M_A	- full DOL breakaway torque
I_A	- DOL starting current in A	M_{AV}	- reduced breakaway torque with KUSA
cA	- current ratio I_A/I_N	I_{AV}	- reduced starting current in A

11 Electronic starting circuits

With MCD 3000 series soft starters, the motor voltage (phase chopping) in the three lines is controlled by thyristors connected in anti-parallel as shown in Fig. 11.1. The starting torque and acceleration period can be easily and ***steplessly*** adjusted by setting the limit current. Current transformers in the soft starter measure the motor current and send a feedback signal to the constant current controller.

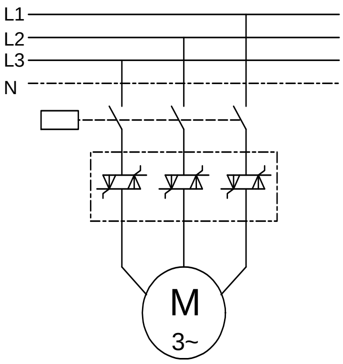

Fig. 11.1
Schematic circuit diagram of an electronic starting circuit with a pair of thyristors connected in anti-parallel in all lines

Unlike other starter circuits (except frequency-controlled starting as described in section 12), the voltage and torque are altered steplessly and transient responses are avoided. The basic differences in the torque and current characteristics compared with direct-on-line starting and with star-delta starting (which is only suitable under no load or against a light load) are shown in Fig. 11.2.

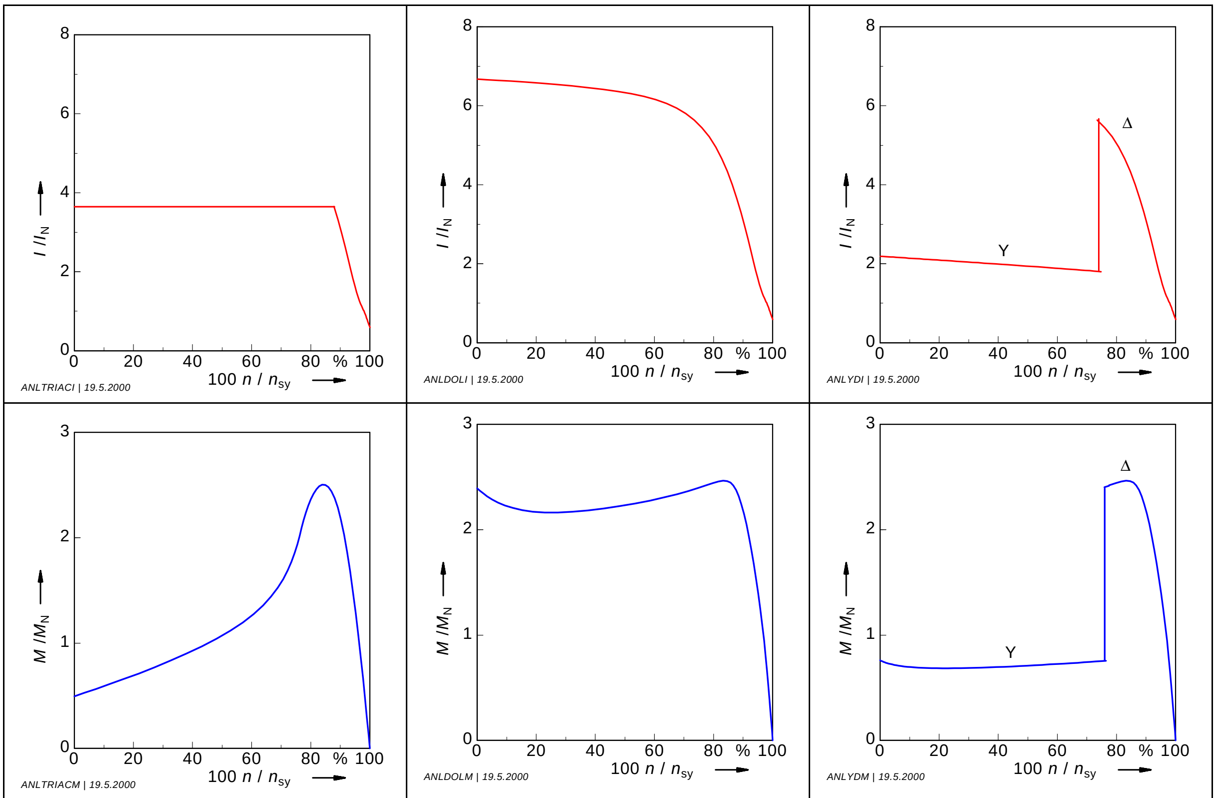

Soft starting	Direct-on-line switching	Star-delta starting

Fig. 11.2 Current *I* and torque *M* for soft starting with electronic device compared with direct-on-line starting and star-delta starting (courtesy of Danfoss Antriebs-und Regeltechnik GmbH)

Soft starters reduce the starting current and the mechanical shock load. This spares the conveyed product and power transmission components, thus increasing service life. They can be easily and infinitely adapted to changing load conditions, unlike star-delta (Y-Δ) starting and the KUSA method. The Danfoss MCD 3000 series also provides D.C. injection braking, the braking torque and operative time of which are infinitely adjustable (see also section 22).
The MCD 3000 soft starter brings benefits to many applications:

Application	**Benefits**
Pumps 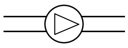	• Minimized hydraulic impact in the pipes under starting and stopping. • Undercurrent protection prevents damage from blocked pipes or low water level. • Automatic reset ensures continuous operation of unmanned pumping stations. • Phase reversal protection prevents damage from contra-rotation of the pump. • Protection against short-term overload prevents damage from waste being drawn into the pump.
Conveyor belts 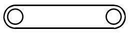	• Controlled soft starting without mechanical shocks (e.g. bottles do not fall over when the belt is started up), minimized belt strain. • Controlled stopping without mechanical shocks. Soft stopping. • Ideal soft starting, even with varying start loads, e.g. in the case of coal conveyor belts starting laden or unladen • Maintenance-free.
Centrifuges 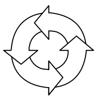	• Uniform application of the torque prevents mechanical stress. • Reduced starting times over star-delta starting. • Reduced stopping times (D.C. braking and soft braking).
Ski lifts 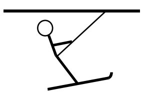	• Jolt-free acceleration increases comfort for riders and prevents the T-bars from swaying etc. • Reduced starting current enables large motors to be started from weak power supplies. • Uniform and gradual acceleration regardless of whether the ski lift is heavily or lightly loaded. • Phase reversal protection prevents reverse operation.
Fans 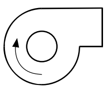	• Reduced starting current allows large fans to be started if the maximum current capacity is restricted. • Phase reversal protection prevents reverse operation.
Mixers 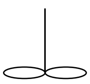	• Gentle rotation upon starting reduces mechanical stress.
Crushers 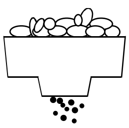	• Maximum starting ability available for starting the machine if it has been stopped without being completely empty. The thermal motor model of the MCD 3000 can be matched to the actual overload capacity of the motor connected and enables the motor to deliver the starting torque for the longest possible duration.

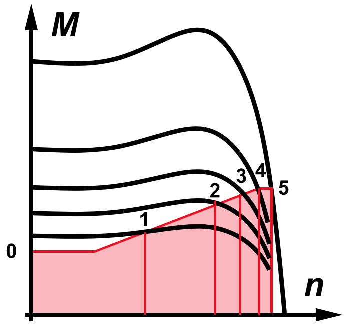 	Fig. 11.3 Run-up ramp for the control of the output voltage on the soft starter giving a slow rise in the torque from 0 to the operating point, 5.

	Fig. 11.4 MCD 3000 series soft starters for motor powers of 4 ... 1300 kW, voltages 200 ... 690 V (Danfoss Antriebs- und Regeltechnik GmbH)

12 Frequency-controlled starting

With all the starting methods described so far, the acceleration period has been increased by reducing the acceleration torque M_a:

$t_a = \frac{\Sigma J \cdot n}{9{,}55 \cdot M_a}$	t_a	-	acceleration period in s
	ΣJ	-	mass moment of inertia in kgm²
	n	-	speed in r/min
	$M_a = M_{mot} - M_L$		acceleration torque in Nm

In each case this is a free and uncontrolled starting process which, for the reasons outlined in section 17, cannot last much longer than about 1 ... 3 seconds. Other more expensive methods, such as controlled-frequency starting, must be used for longer run-up periods. The frequency is ***ramped*** up to a chosen upper value over an adjustable timespan as shown in Fig. 12.1. The rotor speed rises according to the rise in frequency with the degree of slip needed for the particular torque requirement.

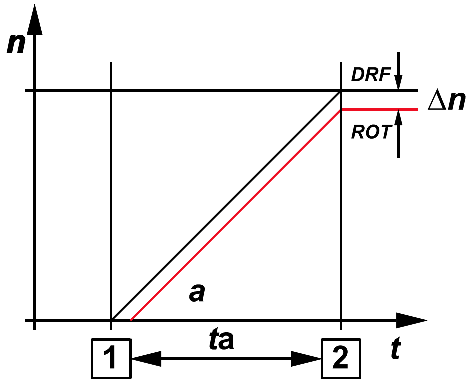

Fig. 12.1
Frequency-controlled starting

DRF	-	rotating field speed
ROT	-	rotor speed
Δn	-	slip speed
t_a	-	acceleration period
a	-	rate of acceleration
(1)	-	start of ramp
(2)	-	end of ramp

The acceleration – represented by the angle *a* – can, within normal practical limits, be set as low as required, that is to say, the process is very soft according to the normal definition for starting. However, if we take a closer look at the transitional behaviour, we can see that the acceleration (angle *a*) changes suddenly at points (1) and (2) in the diagram. In fact, the ***change of acceleration*** can be regarded as a ***jolt***, where:

$$r = \frac{da}{dt}$$

This jolt causes pendulate swinging and other disturbances to sensitive products when they are conveyed. The linear ramp shown in Fig. 12.1 is replaced by an approximation to a more or less ideal sine-shaped ramp to avoid this phenomenon in modern inverter control. Typical applications for this would be any conveyor system for sensitive products, in particular rack drives, turntables and mobile welding robots.
This type of control is also termed ***cosine smoothing*** or ***sine smoothing***.

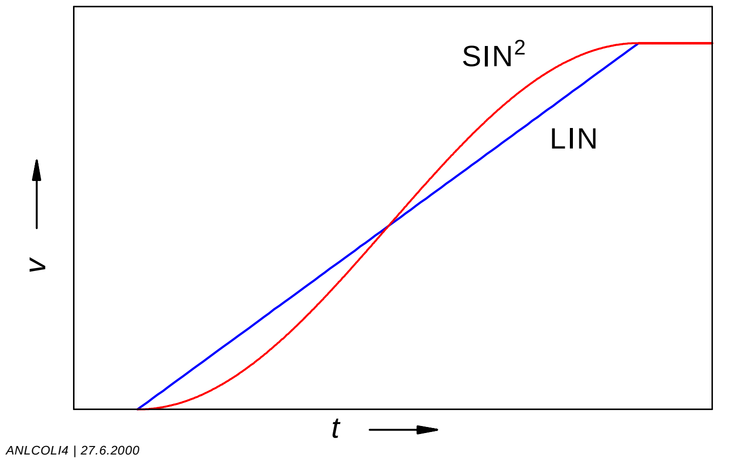

Fig. 12.2
Function of speed v with cosine or sine (SIN²) smoothing of the speed transitions compared with a linear ramp (LIN)

Fig. 12.3

Danfoss VLT series frequency inverter

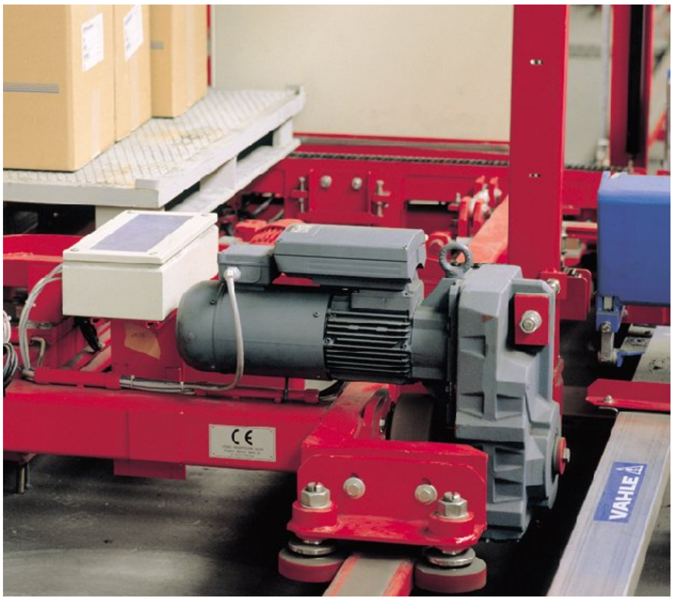

Fig. 12.4

“Eta-K or Eta-Solution”

Shaft-mounted gear unit;
motor with integrated frequency inverter,
Danfoss Bauer K series available for
motor powers up to 7.5 kW

13 Additional rotating mass

It can be seen from the equation for the run-up time that it is also possible to extend the starting period by increasing the mass moments of inertia and by raising the rotor speed.

Benefits:
- ☐ Relatively unaffected by the load
- ☐ No costs associated with circuitry

Disadvantages
- ☐ Non-standard mechanical design
- ☐ Increased thermal loading of the motor during switching duty
- ☐ Increase wear on the mechanical brake during switching duty.

The increase in the mass moment of inertia is expressed by the ***factor of inertia***.

$FI = \dfrac{J_{ext} + J_{rot}}{J_{rot}}$	*FI* - Factor of inertia J_{ext} - External mass moment of inertia J_{rot} - Mass moment of inertia of the rotor

Depending on the constructional design (heavy fan, additional rotating mass) the factor of inertia *FI* will range from 3 to 8. Fig. 13.1 shows some basic motor arrangements with the following characteristics:
- ☐ Heavy fan: little or no change in dimensions
- ☐ Internal mass: extended motor frame
- ☐ External mass: extended second shaft end – observe accident prevention regulations.

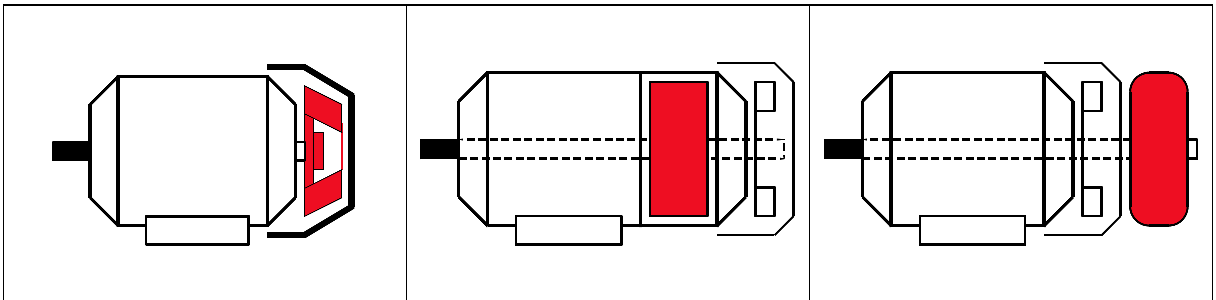

Heavy fan	Additional rotating mass	External rotating mass

Fig. 13.1 Basic design options for an additional rotating mass

The difference in the effect from that of a normal drive can be seen by comparing the following run-up oscillograms. Whereas the normal type (N) runs up very quickly, giving a “hard” start, the special type (G) has a “soft” start for both no load and full-load starting.

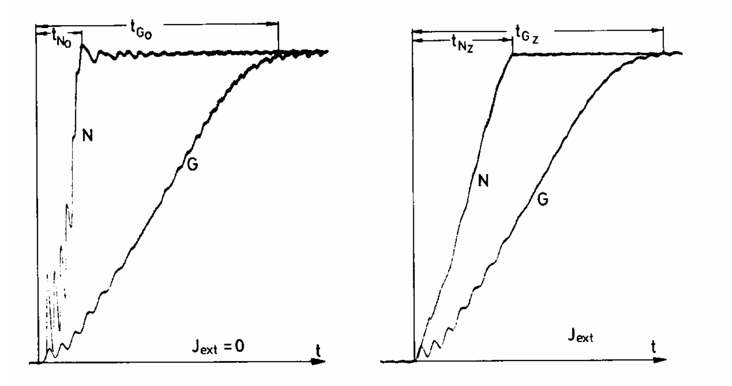

Fig. 13.2
Run-up with and without additional rotating mass
- N - normal type without additional mass
- G - special type with additional mass
- 0 - without external mass (no load starting)
- Z - with external mass (on-load starting)

14 Special rotors with increased slip

Starting slipring motors by means of rotor starters – which are not considered in detail in this discussion – has some definite benefits:

- ☐ The speed can be divided into several steps. A short dwell at part speed allows the load time to "get used" to the speed and stop swinging, for example.
- ☐ The triangular areas with constantly reducing torque provide a soft speed transition comparable to cosine smoothing (section 2.5).
- ☐ The thermal losses occur primarily in the starting resistor, i.e. outside the machine from where they can be easily conducted away.

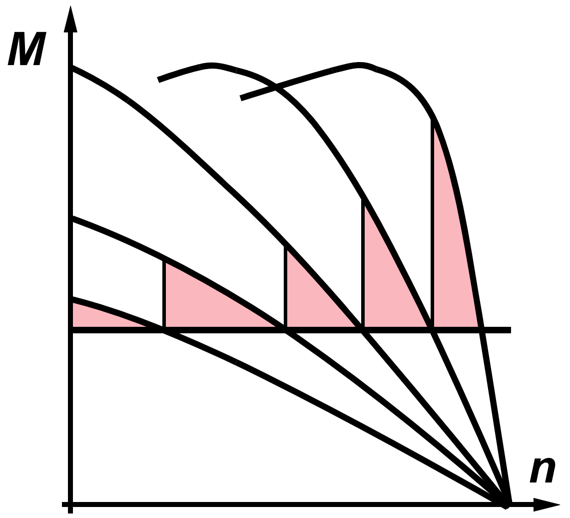

Fig. 14.1
Torque/speed characteristic curve of a slipring motor when started with five speed stages

Induction motors with ***special cage rotors*** combine some of these benefits with the simple principle of the cage rotor. This is clearly shown by the schematic diagrams shown in Fig. 14.2.

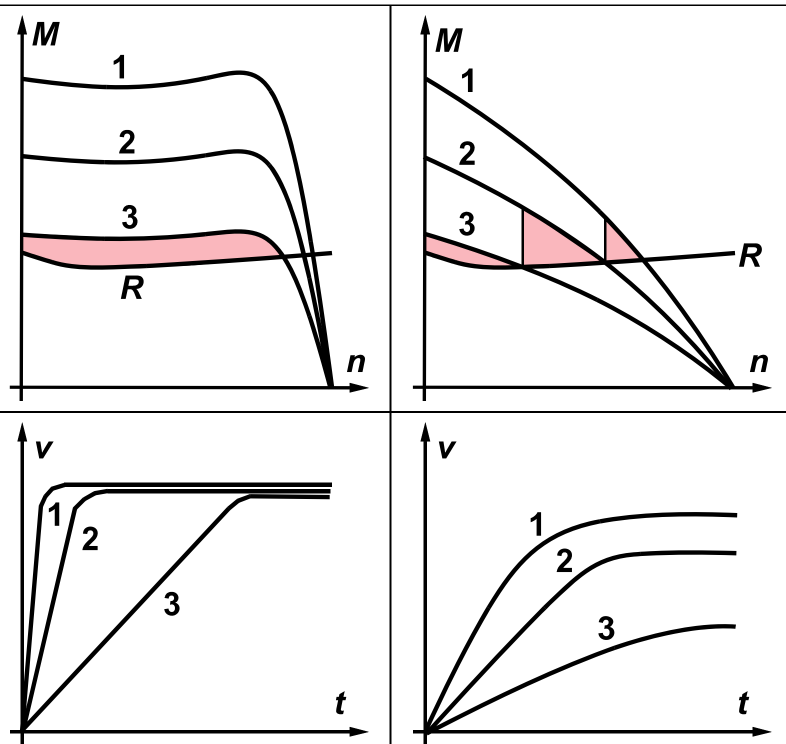

Rectangular characteristic curve	Triangular characteristic curve

Fig. 14.2
Comparison of rectangular and triangular characteristic curves for torque steps (1, 2, 3) down to slightly above the frictional torque *R* showing the effect on the *v/t* graph

The oscillogram in Fig. 14.3 shows the soft transition to the final speed. The "triangular" characteristics are achieved by using a special slot and/or by using high-resistance material in the pressure diecast rotor. The ***travelling gear*** of many small and medium-sized cranes have been equipped with special drives (termed DL drives by Danfoss-Bauer), the outward appearance of which is identical to that of normal cage motors. Because it is not possible to connect into the rotor circuit, steps 1, 2 and 3 as shown in Fig. 14.2 are achieved using star-delta (Y-Δ) starting as described in section 7.

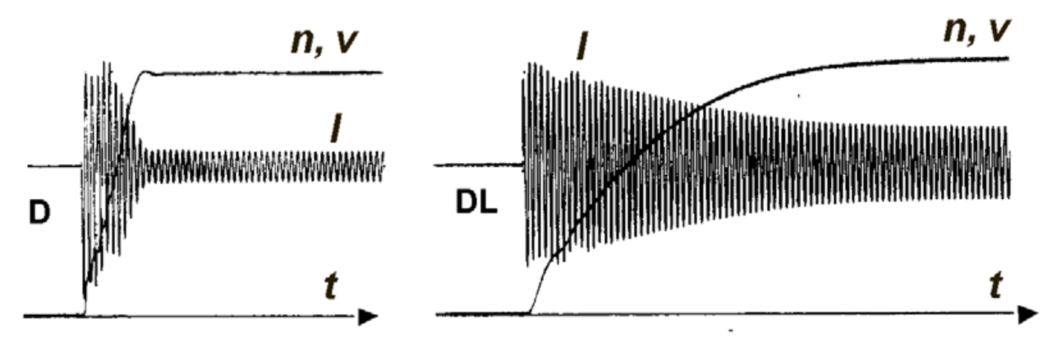

Fig. 14.3 Comparison of current *I*, rotational speed *n* and linear speed *v* plotted against the run-up time *t* of a normal drive (D) and special crane travelling gear (DL)

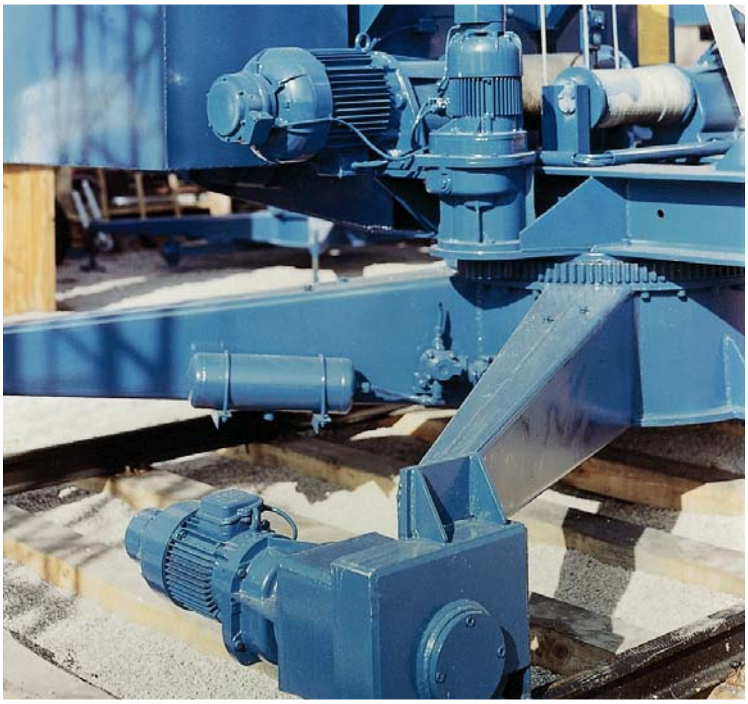

Fig. 14.4
Special DL-type cage motors on the slewing gear and travelling gear of a tower slewing crane

15 Starting clutches

Starting clutches transmit a torque which is initially very low, thus allowing the motor to start quickly under no load. The load itself is only set in motion after a delay. Thanks to automatic processes (such as centrifugal force or turbulence) or electromagnetic control, the torque transmitted by the clutch is slowly increased so that the usually heavy load (e.g. a long conveyor belt) is accelerated gently. This type of clutch is also used because it reduces the thermal load on the drive and on the power supply. In spite of certain differences in the type of construction, the following basic run-up graph will apply to a starting clutch.

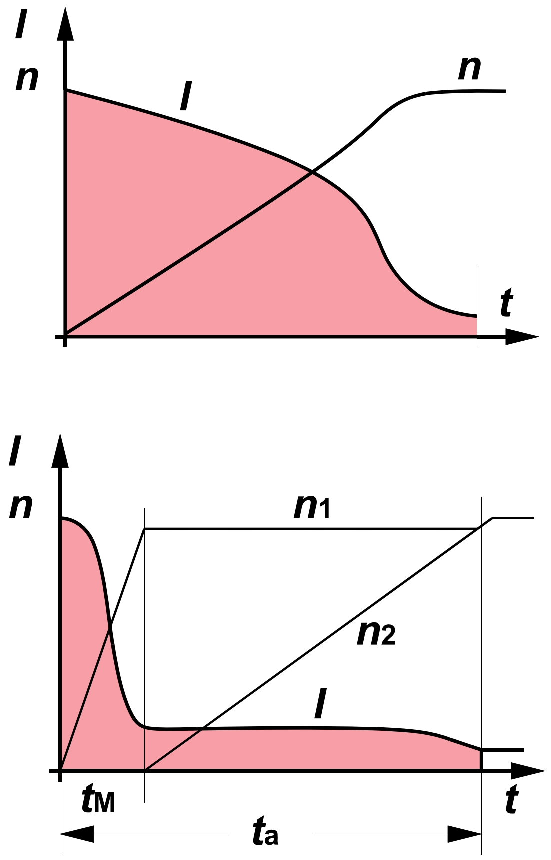

Fig. 15
Characteristic curves of motor speed n_1, operating speed of the driven machinery n_2 and current I with

- direct-on-line starting (above)
- starting clutch (below)

Run-up time with clutch:
t_M - motor
t_a - load

15.1 Centrifugal clutches

These clutches are actuated by the speed of rotation. A slow build-up of the transferable torque proportional to the square of the rotational speed is desirable to obtain a soft start.

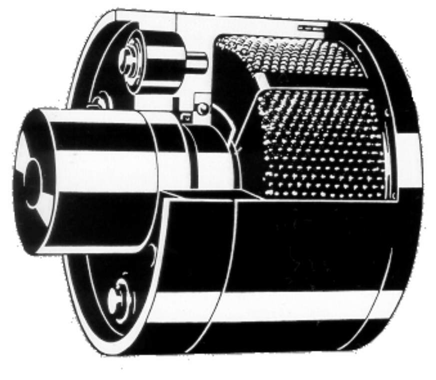

Fig. 15.1
Components of a centrifugal clutch with metal balls

(Type: METALLUK)

15.2 Hydrodynamic couplings

With hydraulic couplings or turbo-couplings, the torque is transmitted without wear by a fluid filling. A delay chamber enables the torque to be increased particularly gently.

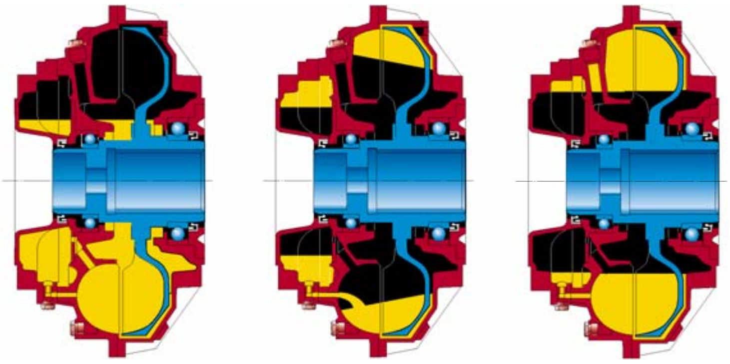

Fig. 15.2
Fill level of a hydrodynamic coupling under various operating states

Left rest
Centre starting
Right running

(Type: VOITH turbo-coupling)

15.3 Induction couplings

This type of coupling is a modification of the polyphase machine. Unlike induction motors, it has two rotating parts, the slip of which drops initially from 100 % to the rated slip of a few percent. The torque characteristic is simple to control by electromagnetic means. Designs are available with and without sliprings.

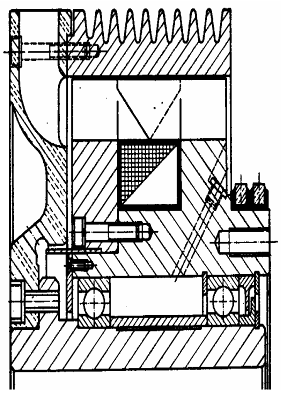

Fig. 15.3
Cutaway of an induction coupling working on the eddy-current principle

(Type: STROMAG)

16 Thermal rating of switching duty

If the switching frequency exceeds a normal value (approximately 60 starting operations/hour as a guide), the additional thermal and mechanical load (depending on the type of power transmission) must be taken into account in the design of the drive.

16.1 Designation of switching duty types

Special abbreviated codes are used in EN 60034-1 to designate the switching duty. Duty type S3 designates no switching duty; it is used in the comparison to make a distinction from duty type S4.

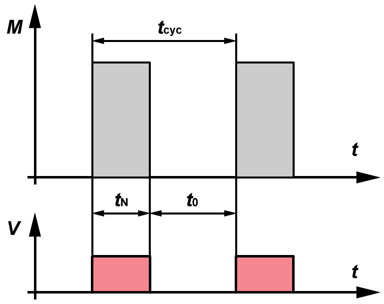 	***M*** Load ***V*** Electrical losses ***t*** Time ***t_{cyc}*** Period of one cycle ***t_N*** Operation at constant load ***t_0*** Time at rest with de-energized windings	**S3** **Duty type S3 - Intermittent periodic duty** A sequence of identical duty cycles, each including a period of operation at constant load and a rest and de-energized period. In this duty, the cycle is such that the starting current does not significantly affect the temperature rise. The designation is S3, supplemented by the cyclic duration factor. For example: S3 25 %
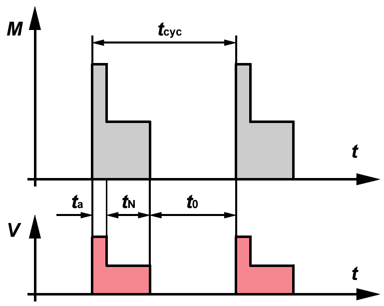 	***M*** Load ***V*** Electrical losses ***t*** Time ***t_{cyc}*** Period of one cycle ***t_N*** Operating hours at constant load ***t_0*** Time at rest with de-energized windings ***t_a*** Run-up time Cyclic duration factor $= (t_a + t_N)/t_{cyc}$	**S4** **Duty type S4 - Intermittent periodic duty with starting** A sequence of identical duty cycles, each cycle including a significant period of starting, a period of operation at constant load and a rest and de-energized period. The corresponding designation is S4, supplemented by the cyclic duration factor, the mass moment of inertia of the motor (J_M) and the mass moment of inertia of the loading machine, (J_{ext}), both in relation to the motor shaft. For example: S4 25 % $J_M = 0.15$ kgm^2 $J_{ext} = 0.7$ kgm^2

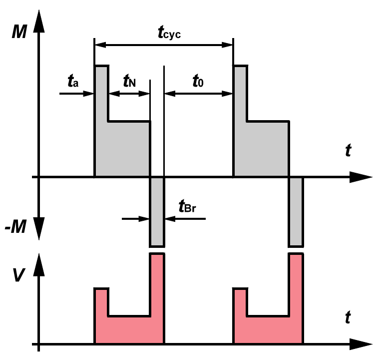	***M*** Load ***V*** Electrical losses ***t*** Time $\boldsymbol{t_{cyc}}$ Period of one cycle $\boldsymbol{t_N}$ Operating hours at constant load $\boldsymbol{t_0}$ Time at rest with de-energized windings $\boldsymbol{t_{Br}}$ Time with electrical braking Cyclic duration factor $= (t_a + t_N + t_{Br})/t_{cyc}$	**S5** **Duty type S5 - Intermittent period duty with electric braking** A sequence of identical duty cycles, each cycle consisting of a period of starting, a period of operation at constant load, a period of rapid electric braking and a rest and de=energized period. The corresponding designation is S4, supplemented by the cyclic duration factor, the mass moment of inertia of the motor (J_M) and the mass moment of inertia of the loading machine, (J_{ext}), both in relation to the motor shaft. For example: S5 25% J_M = 0.15 kgm^2 J_{ext} = 0.7 kgm^2
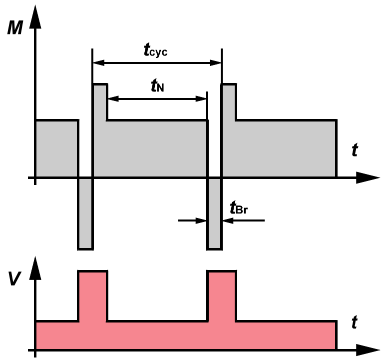	***M*** Load ***V*** Electrical losses ***t*** Time $\boldsymbol{t_{cyc}}$ Period of one cycle $\boldsymbol{t_N}$ Operating hours at constant load $\boldsymbol{t_0}$ Time at rest with de-energized windings $\boldsymbol{t_{Br}}$ Time with electrical braking Cyclic duration factor = 1	**S7** **Duty type S7 - Continuous-operation periodic duty with electric braking** A sequence of identical duty cycles, each cycle consisting of a period of starting, a period of operation at constant load and a period of electric braking. There is no rest and de-energized period. The corresponding designation is S7, supplemented by the mass moment of inertia of the motor (J_M) and the mass moment of inertia of the loading machine, (J_{ext}), both in relation to the motor shaft. For example: S7 J_M = 0.4 kgm^2 J_{ext} = 7.5 kgm^2

16.2 Switching duty with output predominant

While the acceleration coefficient (*B* value) described in section 16.3 is generally used as the type rating of drives used purely for acceleration duty (e.g. roller table drives), the no-load operating frequency is used as the output rating for normal three-phase motors with output power in switching duty. The method of calculation described below is concerned solely with the thermal load on the motor winding; the shock load on the gear unit due to switching duty requires separate consideration.

16.2.1 No-load operating frequency Z_0

The no-load operating frequency is a rating determined for each motor type by testing. It is the number of starting operations per hour of the motor running at no-load without any external moments of inertia at which the winding overtemperature permissible for insulation class F is reached.
The test procedure is comparable to the determination of the *B* value (see section 16.3).
Guide values for Z_0 are given in Fig. 16.2.1.

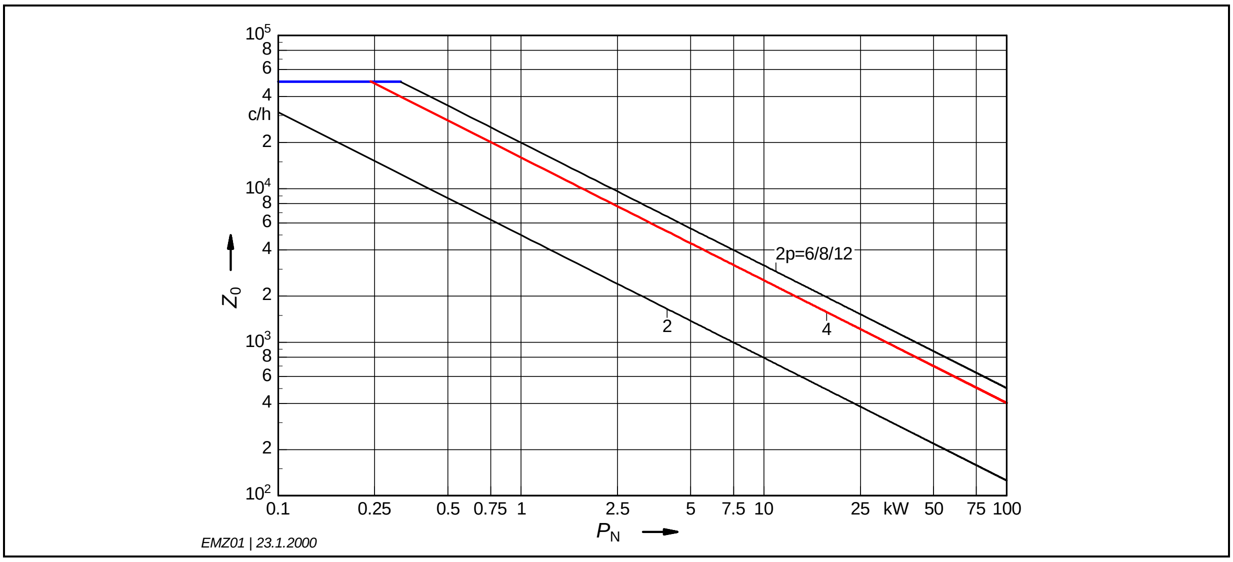

Fig. 16.2.1 Guide values for the thermally permissible no-load operating frequency Z_0 of IP65 three-phase motors, pole numbers 2*p* = 2/4/6/8/12 with class F insulation

16.2.2 Permissible on-load operating frequency Z_{lim}

The no-load operating frequency is reduced to the permissible on-load operating frequency by external loads:

$$Z_{lim} = \frac{Z_0 \cdot K_L}{FI}$$

The effect of the load is determined by the following factors:

16.2.2.1 Factor of inertia *FI*
The factor of inertia is given by the ratio of all moments of inertia (including the rotor) to the moment of inertia of the rotor (where i = gear reduction ratio):

$$FI = \frac{J_{ext1} + J_{rot}}{J_{rot}} = \frac{\frac{J_{ext2}}{i^2} + J_{rot}}{J_{rot}}$$

The run-up time increases proportionally to *FI*:

$$t_a = \frac{J_{rot} \cdot FI \cdot n}{9{,}55 \cdot M_a}$$

The permissible switching frequency is therefore reduced in proportion to *FI*.
The factor of inertia *FI* must be calculated individually for each drive scenario.
Guide values for the rotor moment of inertia J_{rot} can be found in section 26 or in the catalogue data.

16.2.2.2 Load factor K_L

The load factor takes into account the relative utilization P/P_N and the cyclic duration factor *ED* of the motor in operation between switching operations.
The utilization factor has a square law effect on the permissible switching frequency. The effect of the cyclic duration factor varies. If there is no-load or little utilization, the *ED* acts to relieve the load due to the longer cooling periods, whereas it acts to increase the load at nominal load or heavy utilization due to the load losses.
Values for the load factor K_L are given in Fig. 16.2.2.2. These apply in the case of class F insulation.

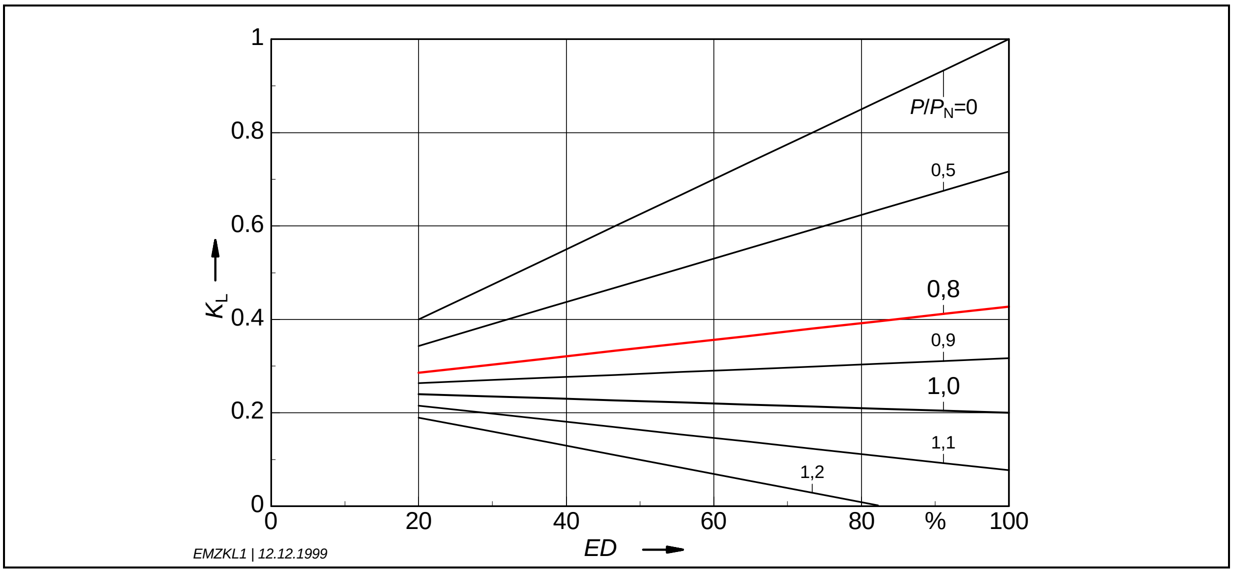

Fig. 16.2.2.2 Load factor K_L for switching duty as a function of the cyclic duration factor *ED* and the relative motor loading P/P_N

16.2.3 Thermally-equivalent switching frequency Z_{th}

The various thermal effects of the different switching operations are determined by factors of the type of switching concerned.

$$Z_{th} = K_A \cdot Z_A + K_G \cdot Z_G + K_R \cdot Z_R + K_B \cdot Z_B + K_M \cdot Z_A$$

The following factors will apply according to the switching operation:

16.2.3.1 Starting factor K_A

The run-up time becomes longer as the load torque M_L increases:

$$t_a = \frac{J \cdot n}{9{,}55 \cdot M_a} = \frac{J \cdot n}{9{,}55 \cdot (M_A - M_L)}$$

Starting is therefore made more onerous thermally by the load torque.
K_A = 1 in the case of starting where there is no load torque

This effect of the breakaway torque M_A and load torque M_L on this factor is given by the following equation:

$$K_A = \frac{M_A}{M_A - M_L}$$

Because M_A and M_L are usually quoted as relative values, the following equations are used:

$$K_A = \frac{\frac{M_A}{M_N}}{\frac{M_A}{M_N} - \frac{M_L}{M_N}} = \frac{1}{1 - \frac{M_L}{M_A}}$$

Average values for the factor K_A are given in Fig. 16.2.3.1.

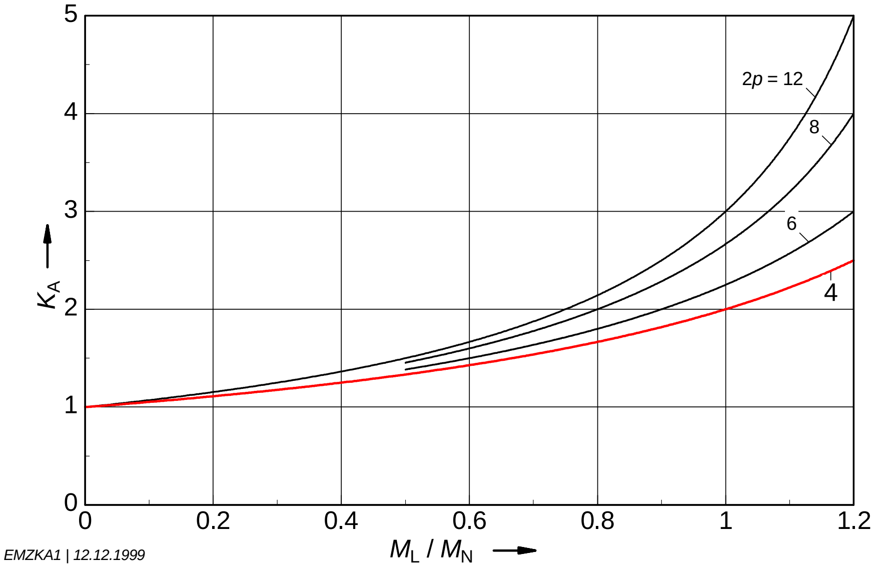

Fig. 16.2.3.1 Starting factor K_A for switching duty as a function of the relative load torque M_L/M_N during the switching operation and for pole numbers 2*p*

16.2.3.2 Plugging factor K_G and reversing factor K_R

Theoretically, one plugging operation as discussed in section 20 has the same thermal effect as three starting operations, and one reversing operation is equivalent to four starting operations. The influence of current displacement reduces these theoretical values to the following practical factors:

Motor rating	P_N	≤ 1.5	≤ 7.5	≤ 22	≤ 50 kW
Plugging	K_G	2	1.8	1.6	1.4
Reversing	K_R	3	2.8	2.6	2.4

16.2.3.3 D.C. injection braking factor K_B

D.C. injection braking imposes a thermal load equivalent to about 1.6 times that of a motor start, i.e.:

K_B = 1.6

16.2.3.4 Mechanical braking factor K_M

When the motor is energized, there is a delay in the mechanical brakes' release response which increases the run-up time of the motor. This additional loading is difficult to measure since it is influenced by a number of parameters.
Where the brake is not pre-released, the following applies:

$$K_M = \frac{1{,}3 \cdot t_{A1}}{t_a}$$

In the case of overexcitation of the brake:

$$K_M = \frac{0{,}65 \cdot t_{A1}}{t_a}$$

The actual run-up time under load is used as the value for t_a.
The response time t_A of the brakes under normal excitation is given in the tables in the Appendix.
This value is also to be used for overexcitation in the equation above.

16.2.4 Type test

The condition that the permissible on-load operating frequency must be equal to or greater that the thermally equivalent frequency applies to the type test, i.e.

$$Z_{lim} \geq Z_{th}$$

16.2.5 Summary of terms used:

Z_0 - no-load operating frequency in c/h
Z_{lim} - permissible on-load operating frequency in c/h
Z_{th} - thermally equivalent switching frequency in c/h
Z_A - number of starting operations in c/h
Z_G - number of plugging operations in c/h
Z_R - number of reversing operations in c/h
Z_B - number of D.C. injection braking operations in c/h
FI - factor of inertia
J_{ext} - external mass moment of inertia in kgm^2
J_{rot} - rotor mass moment of inertia in kgm^2
n - speed in r/min
t_a - run-up time in s
t_{A1} - brake response time in s
M_a - acceleration torque in Nm
M_A - breakaway torque in Nm
M_L - load torque in Nm
P - power consumption in kW
P_N - rated motor output kW
ED - cyclic duration factor in %
K_L - load factor
K_A - switching type factor for starting
K_G - switching type factor for plugging
K_R - switching type factor for reversing
K_B - switching type factor for D.C. injection braking
K_M - switching type factor for mechanical braking
i - gear reduction ratio

16.3 Switching duty with acceleration predominant

Relatively high electrical losses will occur with every acceleration (run-up) and deceleration (electrical braking) operation. These are proportional to the starting or braking time which, in turn, are proportional to the driven masses.
The ***acceleration coefficient*** is a measure of the acceleration work required per hour in switching duty and hence provides some indication of the temperature rise on the motor.

$B = \Sigma J \cdot Z$	B J Z	- acceleration coefficient (B value) in kgm^2/h - total mass moment of inertia (mr^2) in kgm^2 - number of starts per hour

The temperature rise due to switching duty is additional to the basic temperature rise due to normal rated operation (without repeated starting) $\Delta\vartheta_N$ and is directly proportional to the B value.

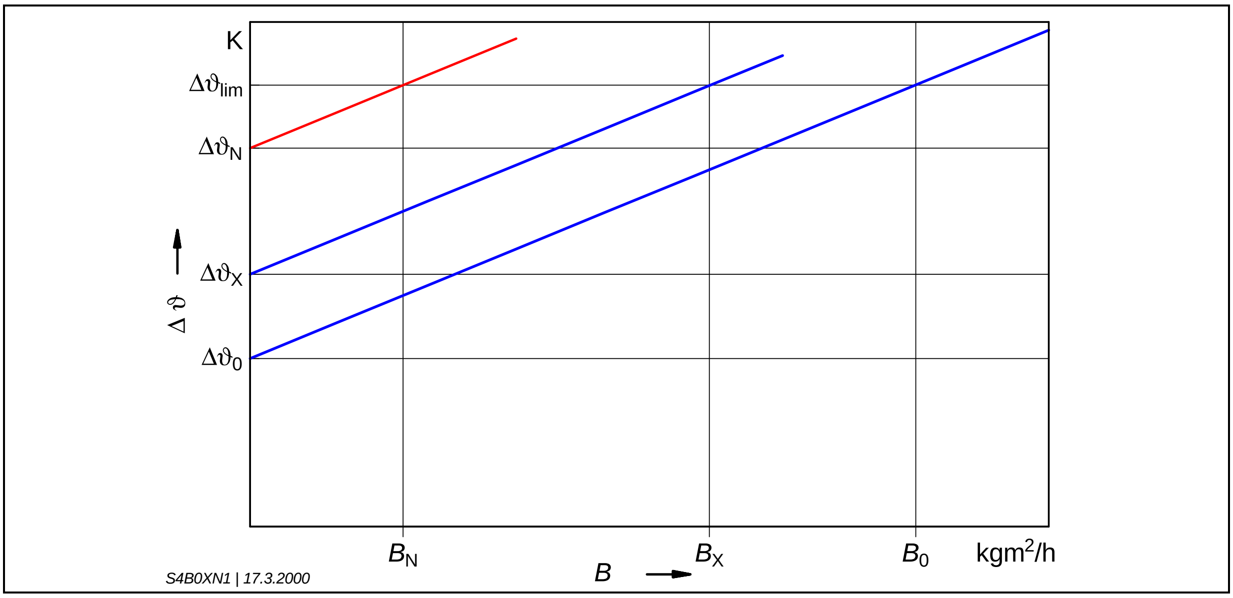

Fig. 16.3.1 Acceleration coefficient B for different loads
(N - rated load, X - partial load, 0 - no-load)

If a motor is operated at its rated load and undergoes a temperature rise ($\Delta\vartheta_N$) close to the maximum rated overtemperature ($\Delta\vartheta_{lim}$), it will be able to provide very little additional starting energy (B_N).
However, at partial loading (X) or no-load (0), the motor can be assumed to subjected to a correspondingly higher switching frequency without exceeding the permissible overtemperature for its insulation class.
Within normal practical limits, the temperature rise for a particular B value remains the same irrespective of whether the motor is loaded with a large mass moment of inertia for a low switching frequency or with a small mass moment of inertia for a high switching frequency (see Fig. 16.3.2). However, the mechanical shock loading on the power transmission components will increase with the mass of the moving parts [2.9].

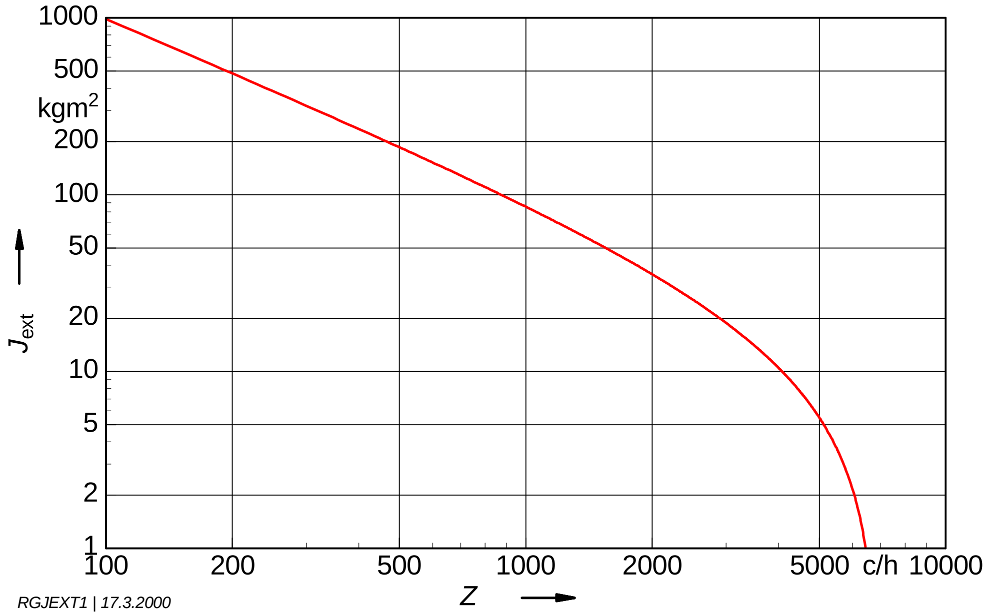

Fig. 16.3.2 Permissible external mass moment of inertia J_{ext} at different switching frequencies Z, in relation to the output shaft of an 8-pole roller table geared motor with a rated torque of 1250 Nm, a speed of 75 r/min and a B value of 1000 kgm^2/h

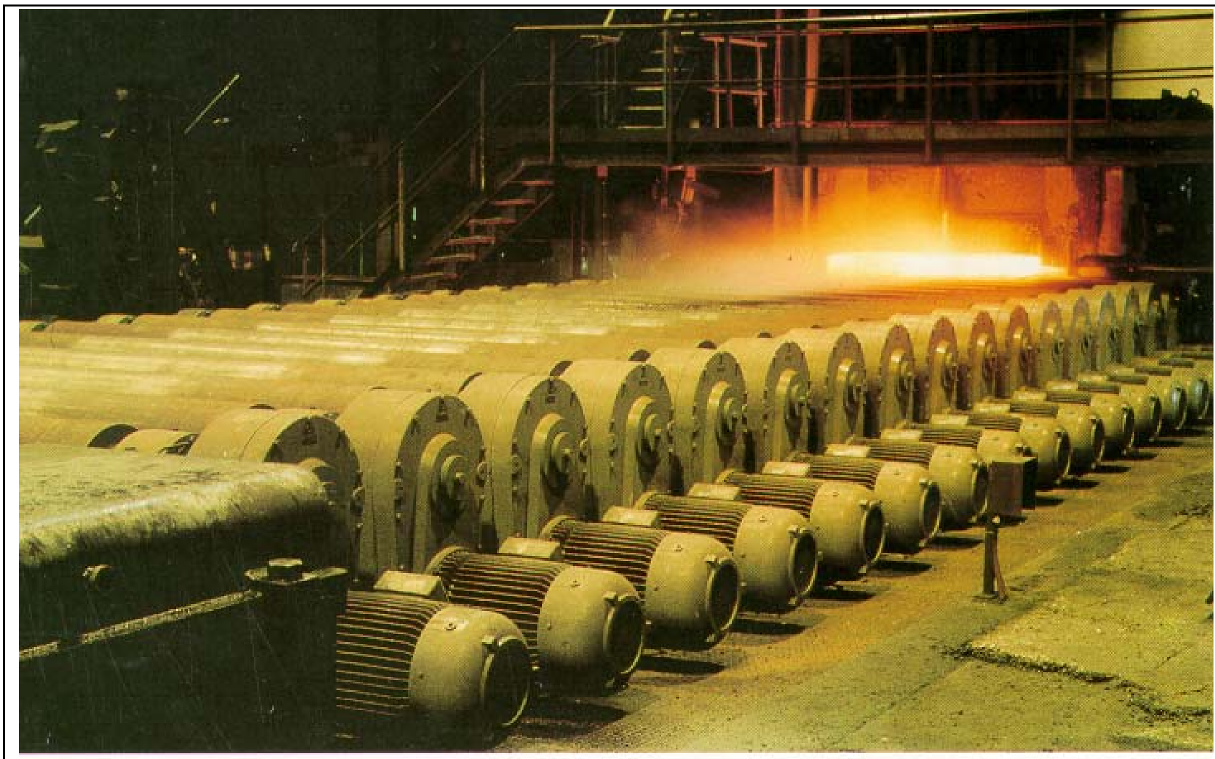

Fig. 16.3.3 Application example of roller table geared motors with a work-load consisting predominantly of acceleration on a rolling table

17 Determination of the run-up time

Extending the run-up time t_a by reducing the acceleration torque M_a has some technical limitations, as shown by the following sample calculations for a standard 90L frame size motor:

P_N = 1.5 kW	M_A/M_N = 1.8	FI	= 1.5
n = 1405 r/min	M_K/M_N = 2.2	J_{rot}	= 0.0035 kgm²
		M_N	= 10 Nm

$$M_{Hmean} = \frac{(1{,}8 + 2{,}2)}{2} \cdot 10 = 20 \text{ Nm}$$

$$M_a = M_{Hmean} - M_N = 20 - 10 = 10 \text{ Nm}$$

$$t_a = \frac{0{,}0035 \cdot 1{,}5 \cdot 1405}{9{,}55 \cdot 10} = 0{,}074 \text{ s}$$

The run-up time should be about 1 second for a “soft start”; the acceleration torque therefore needs to be reduced to

$$M_a = \frac{0{,}0035 \cdot 1{,}5 \cdot 1405}{9{,}55 \cdot 1} = 0{,}772 \approx 0{,}8 \text{ Nm}$$

The average run-up torque developed by the motor would then amount to
$M_{Hmean} = M_N + M_a = 10 + 0{,}8 = 10{,}8$ Nm

A proportional representation of the corresponding characteristic curves shows that this solution would be impractical. The excess torque (heavily shaded area) is so small that the slightest sluggishness (e.g. due to cold or fouling) would result in the drive no longer being able to run up to speed.

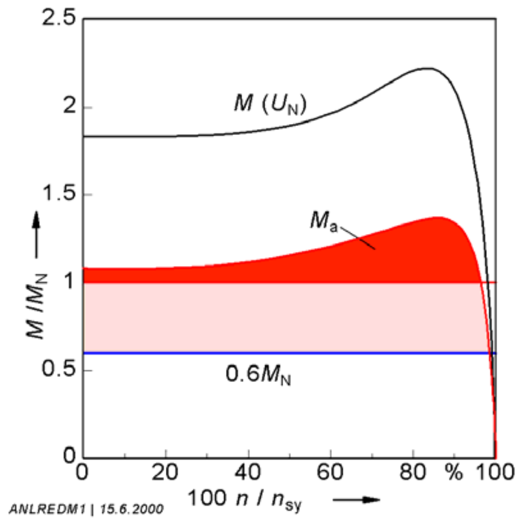

Fig. 17.1
Limits of possible changes to the run-up time by reduction of the calculated acceleration torque M_a

However, we can assume that the actual load on run-up will be less than the rated torque, e.g.
$M_L = 0{,}6 \cdot M_N = 0{,}6 \cdot 10 = 6$ Nm
The lightly shaded area in the diagram thus denotes the actual acceleration torque
$M_a = M_{Hmean} - M_L = 10{,}8 - 6 = 4{,}8$ Nm
giving an actual run-up time of

$$t_a = \frac{0{,}0035 \cdot 1{,}5 \cdot 1405}{9{,}55 \cdot 4{,}8} = 0{,}16 \text{ s}$$

Instead of about 1 second, the drive will then take barely 0.2 s to run up to speed – which is certainly not a soft start.

In the run-up times calculated in the above example, the equations used have assumed that the acceleration torque M_a is virtually constant. This assumption is valid if the motor and load characteristics are as shown in Fig. 3.6, but if the characteristic curves are as plotted in Fig. 17.2, the equation will yield relatively inexact values. If the functions, and hence the mathematical relationships between the torque and the speed for the characteristic curves of the motor and load, are known, a mathematical solution could be considered. Since this function is not usually available, at least for the motor characteristic curve and usually also for the load characteristic curve, it is necessary to adopt a method of approximation. The degree of error can be reduced by dividing the speed range into steps. Three such steps will generally be sufficient; for greater accuracy or for very irregular characteristic curves, the same principle can be used with up to ten steps.

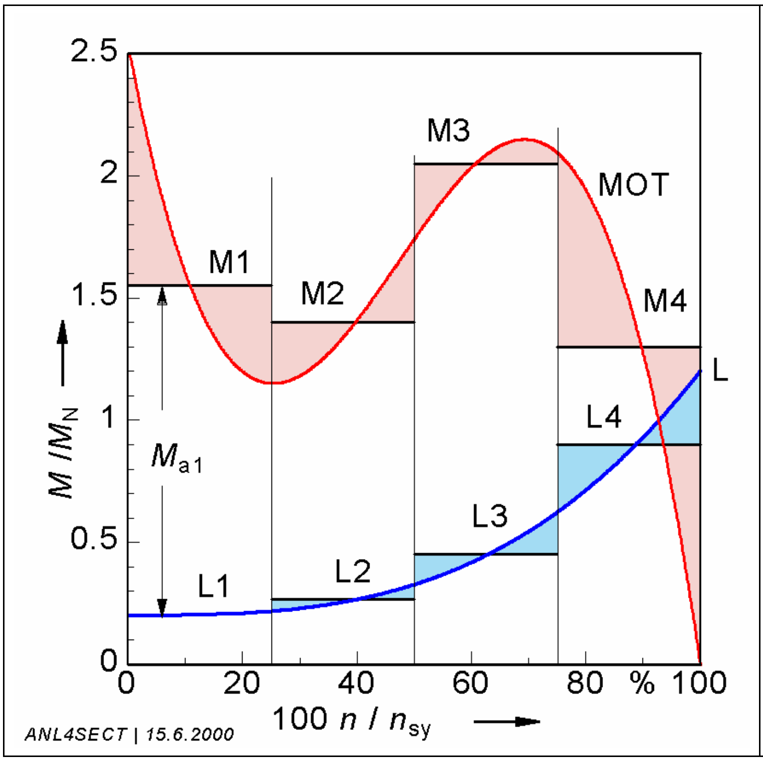

Fig. 17.2
Calculation of the run-up time for irregular torque characteristic curves of motor (MOT) and load (L) by subdividing
into four steps 1, 2, 3, 4

An ***arithmetic mean*** is found for each
step of the motor torque M_1
of the load torque L_1
of the acceleration torque $M_{a1} = M_1 - L_1$

and the run-up time is calculated for each step. Thus:

$$t_{a1} = \frac{\Sigma J \cdot n_1}{9{,}55 \cdot M_{a1}}$$

The total run-up time for z steps is then:

$$\Sigma t_a = t_{a1} + t_{a2} + ... + t_{az}$$

To assess the error rate, the run-up time t_a for the example shown in Fig. 17.2 was calculated by three methods:

- ☐ by taking the average value of the entire characteristic curve: 100 %
- ☐ by the stepwise method using four steps: approx. 105 %
- ☐ by the stepwise method using ten steps: approx. 110 %

The effort involved in the stepwise method is generally not justified, considering the large errors possible in the specification of the mass moments of inertia and particularly with respect to the effective load torque.

A simple method of calculation giving only minor errors can be used for the relatively frequent case of a load characteristic curve where the torque rises as a square of the speed (fans, pumps):

$t_a = \frac{J_{rot} \cdot FI \cdot n}{9{,}55 \cdot M_N \cdot (a - \frac{b}{3})}$	t_a	-	Run-up time in s
	J_{rot}	-	Mass moment of inertia of the rotor in kgm²
	FI	-	Factor of inertia
	n	-	Rotor speed in r/min
	M_N	-	Rated torque of the motor in Nm
	a	=	M_H/M_N
	b	=	M_L/M_N

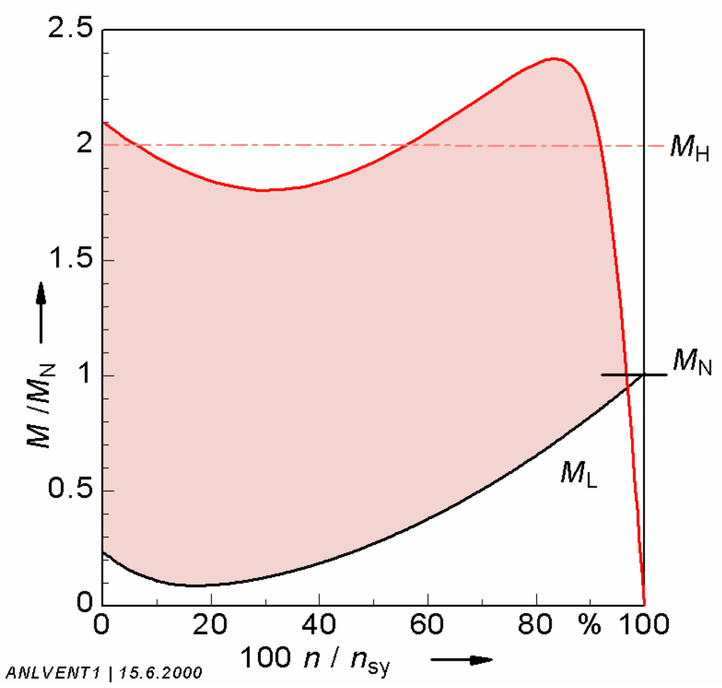

Fig. 17.3
Parameters for calculating the run-up time where the torque rises as a square of the speed (fans, pumps)

M_H - average run-up torque
M_N - rated torque
M_L - load torque

18 Classification of starting behaviour

Some standardized systems that have been adopted in practice for the classification of the starting behaviour of cage motors are given below.

18.1 Starting behaviour in accordance with IEC 60034-12

The work of IEC TC2/WG 8 has led to IEC 60034-12, “Rotating electrical machines; Starting performance of single-speed three-phase cage induction motors for voltages up to and including 690 V, 50 Hz”. Limits for the starting torques and the apparent starting current related to the rated output have been determined in accordance with the American NEMA standards [2.3]:

Design N
Motors with normal starting characteristics for direct-on-line starting; 2, 4, 6 and 8-pole; 50 and 60 Hz
Design NY
Motors with normal starting characteristics for star-delta starting (values 25 % of N)
Design H
Motors with high starting torque for direct-on-line starting 4, 6 and 8-pole; 60 Hz
Design HY
Motors with high starting torque for star-delta starting (values 25 % of H)

The requirements for design N are met by all standard IP 65 motors manufactured by Danfoss Bauer. The requirements for design H are met by standard 4-pole models from 7.5 kW and by 6-pole models from 4.4 kW. The limit value for the relative apparent locked rotor input S_1 in kVA/kW is met by all standard models.

P_N (kW)	>0.4 ≤ 6.3	>6.3 ≤ 25	>25 ≤ 100
S_1 (kVA/kW)	13	12	11

Table 18.1.1 Limit value for the relative apparent locked rotor power S_1 of three-phase induction motors with rated outputs P_N = 0.4 ... 100 kW in accordance with IEC 60034-12

As far as the starting conditions and starting sequence are concerned, the standard requires that standard N-design motors be capable of starting twice in succession from cold or once from operating temperature against a relatively high external moment of inertia and with a load torque that increases as a square of the speed.
The external moments of inertia are given in the standard as absolute values; a conversion to the relative value *FI* (see section 29) will provide the guide values shown in Fig. 18.1.2.

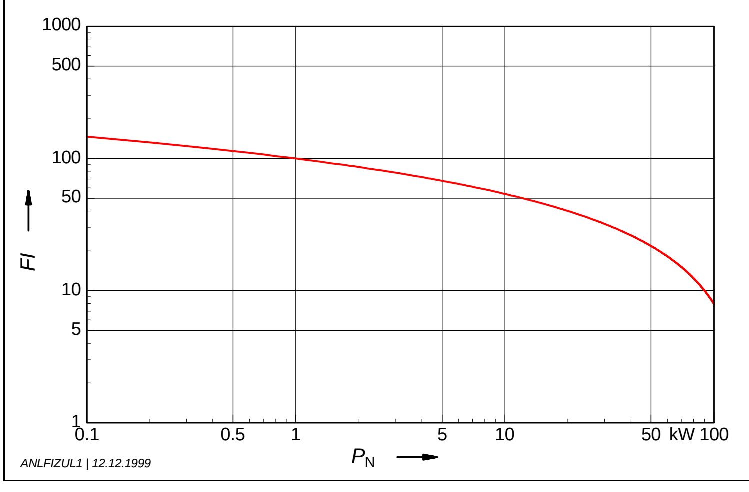

Fig. 18.1.2
Guide values for the relative external moment of inertia *FI* under the starting conditions for standard N-design three-phase motors in accordance with IEC 60034-12

These requirements are met by standard IP65 motors, although it is not necessarily realistic to apply them to geared motors. They yield theoretical run-up times of about 5 seconds irrespective of the rated output; this is hardly borne out by practice for small rated outputs.
All the above consideration on the subject of standardized starting behaviour are based on the thermal properties of the motor. The mechanical effects – due, for instance, to shock loading of the extremely high external moment of inertia – must be considered separately.

18.2 NEMA code letters

The power supply arrangements in North America make it necessary to take into account the additional loading ("inrush") when switching on. NEMA MG1-10.37 calls for the ***apparent locked rotor power*** P_A (kVA) to be related to the output (HP), i.e. the ratio P_A/P_N given as kVA/HP whereas the starting current ratio I_A/I_N is used as the characteristic value in Europe [2.4].

This characteristic value is specified as a code letter in accordance with the following table:

Code letter	kVA/HP	**Code letter**	kVA/HP
A	< 3.15	**K**	≥ 8.0 ... < 9.0
B	≥ 3.15 ... < 3.55	**L**	≥ 9.0 ... < 10
C	≥ 3.55 ... < 4.0	**M**	≥ 10 ... < 11.2
D	≥ 4.0 ... < 4.5	**N**	≥ 11.2 ... < 12.5
E	≥ 4.5 ... < 5.0	**P**	≥ 12.5 ... < 14
F	≥ 5.0 ... < 5.6	**R**	≥ 14 ... < 16
G	≥ 5.6 ... < 6.3	**S**	≥ 16 ... < 18
H	≥ 6.3 ... < 7.1	**T**	≥ 18 ... < 20
J	≥ 7.1 ... < 8.0	**U**	≥ 20 ... < 22.4
		V	≥ 22.4

Table 18.2.1 Code letters in accordance with NEMA MG1-10.37

The following applies to special designs:

- ☐ pole-changing: highest code letter
- ☐ dual volötage motors: highest code letter if they differ
- ☐ 50/60 Hz frequency: code letter for 60 Hz
- ☐ star-delta (Y-Δ) starting: code letter for star starting step
- ☐ Part-winding starting: code letter for direct-on-line starting on full winding

Fig. 18.2.2 shows the scatter band of the code letter for common 4-pole standard motors – it cannot and should not be used as a substitute for individual classification.

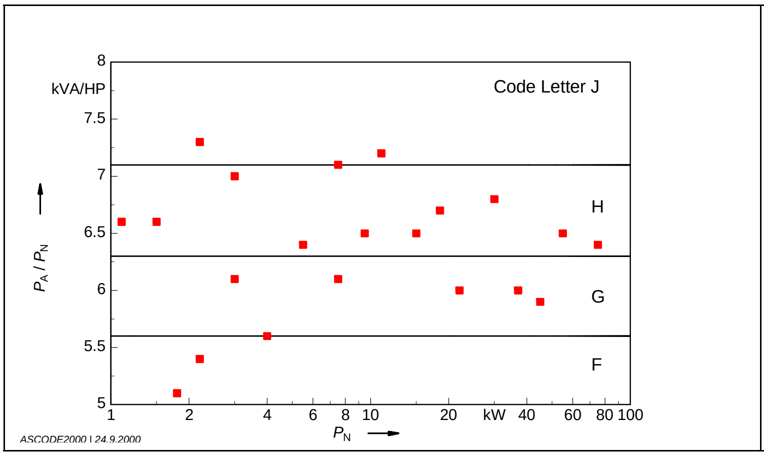

Fig. 18.2.2
Scatter band of the code letter for common 4-pole standard motors

Plotted against the rated output in kW

Code letter specified for corresponding output in HP

18.3 NEMA classification according to the torque characteristics

NEMA provides a choice of four variants according to the basic shape of the torque characteristic curve plotted against the speed and to the level of the relative inrush current. These designs are denoted ***A, B, C, D and E***. Design A has the same torque characteristics as B but with a higher inrush current.

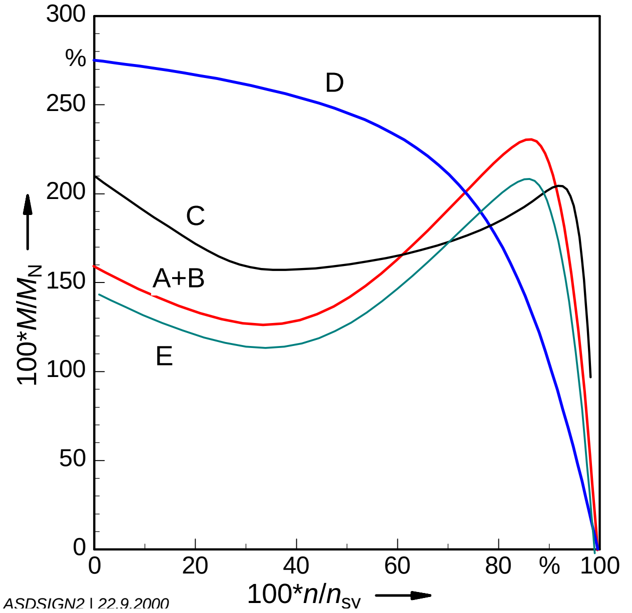

Fig. 18.3 Basic torque characteristics for Design A, B, C, D and E in accordance with NEMA MG10

The startingy torque, pull-out torque and atarting current limits are tabulated in NEMA MG1. ***Design B*** is mostly used for normal applications, although the standard limits the slip to 5 %, irrespective of the frame size. This seems technically unnecessary and barely achievable for small machines.
Design D (soft characteristics without any definite pull-out torque) is preferred for applications requiring a high peak torque (presses, shears, lifting gear).
According to NEMA MG1-10.37, the design letter must be given on the rating plate.

18.4 Starting classes

The torque characteristic curves of individual models can be divided into “starting classes” (AK) to assess the starting performance of standard three-phase induction motors. The starting class denotes the load torque against which the drive can safely run up.

Starting class	Load torque
AK 10	100 % rated torque
AK 13	130 % rated torque
AK 16	160 % rated torque

Additional letters – e.g. AK 16A – indicate the shape of the torque characteristic curve taking account of definite values of starting torque, pull-up torque and pull-out torque as well as the rated-load slip. In general the rated-load slip increases in alphabetical order of the suffix letter.

The scatter band adopted (Figs 18.4.1 and 18.4.2) is relatively wide due to the collation of a large number of models but should still make adequate assessment possible for standard applications.

The following standardized tolerances are used:

- ☐ starting torque: -15 % to +25 %
- ☐ pull-out torque: -10 %
- ☐ rated-load slip: +20 %

It should also be noted that the torque characteristic curve is that for the rated voltage and that the torque will vary proportionally to the square of the actual applied mains voltage. At 5 % undervoltage, the characteristic curve will already be approximately 10 % lower. Figs 18.4.1 and 18.4.2 show examples of AK 16A and AK 13D. The corresponding characteristic curves for standard models are available in individual cases.

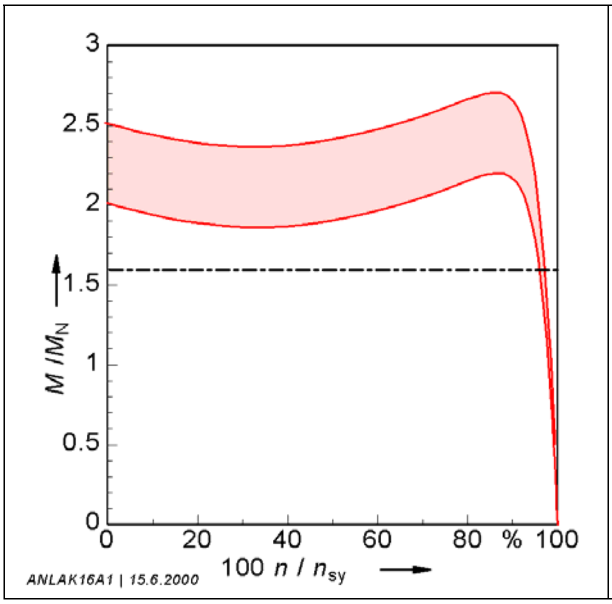

Fig. 18.4.1
Torque characteristic curve for starting class AK 16A

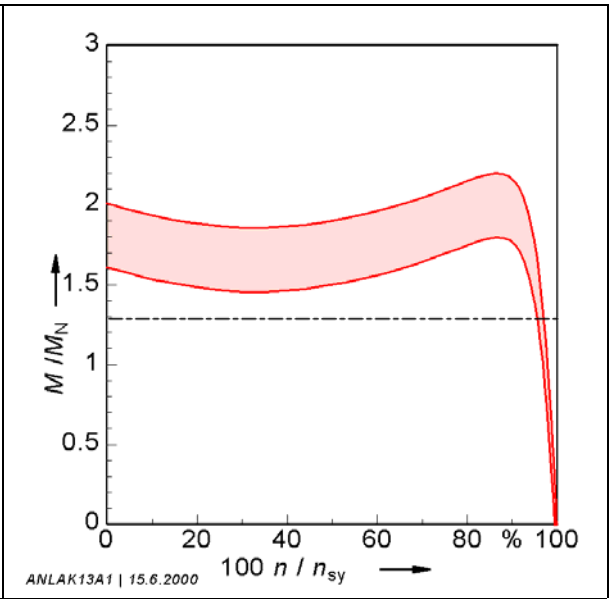

Fig. 18.4.2
Torque characteristic curve for starting class AK 13D

This term draws attention to three important properties of this method of braking:

- ☐ The process involves the braking effect of an induced conductor in the magnetic field, i.e. the process functions ***without physical contact or wear***.
- ☐ The braking effect is ***dynamic*** and therefore is operative only while the machine is rotating. There is no braking effect (***i.e. no clamping brake***) while the machine is at rest.
- ☐ The motor winding is subjected to additional ***thermal loading*** by the braking.

Depending on the braking process, different parts of the torque/speed characteristic curve of a three-phase asynchronous motor come into play.

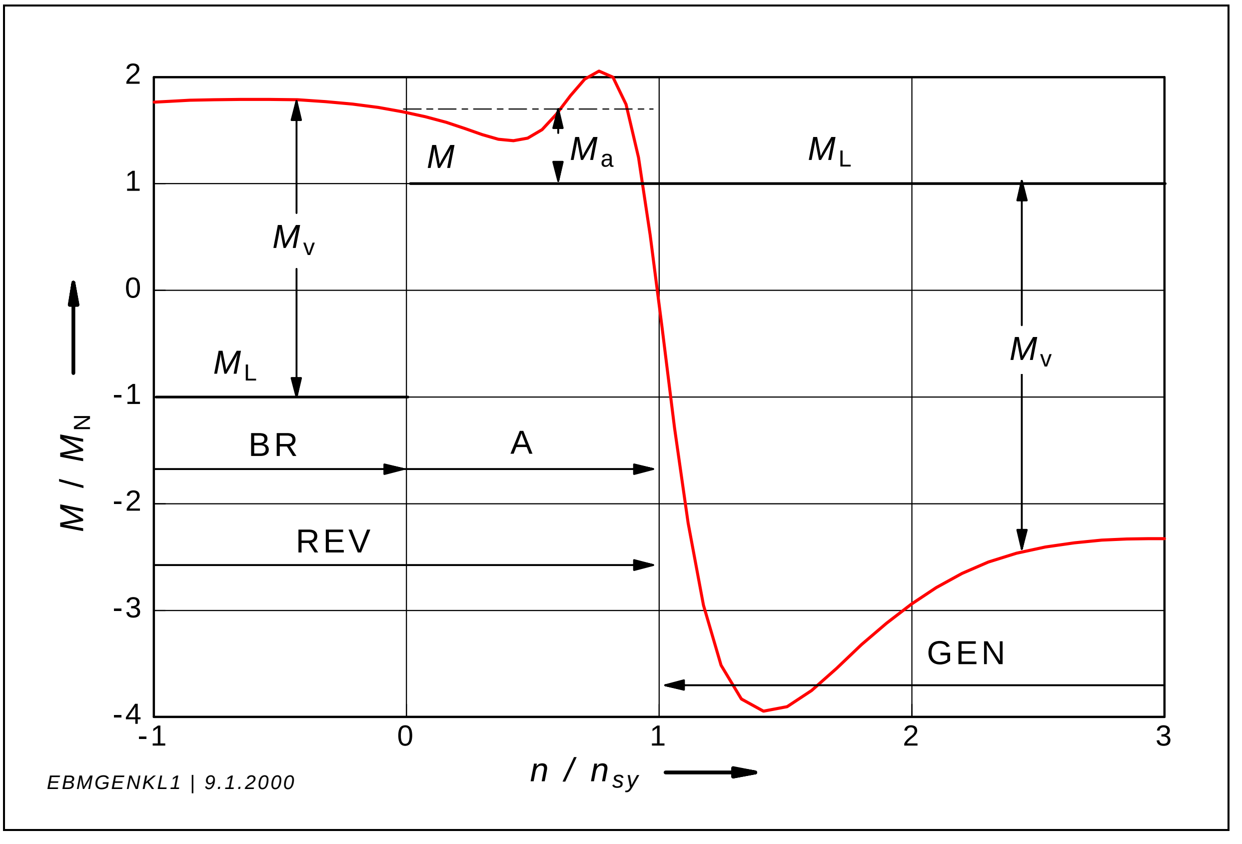

Fig. III Starting, braking and reversing with cage motors

A	-	starting
BR	-	plugging (reverse-field braking)
REV	-	reversing
GEN	-	regenerative braking
M	-	motor torque
M_L	-	load torque
M_a	-	acceleration torque
M_v	-	deceleration torque

19 Hyper-synchronous regenerative braking

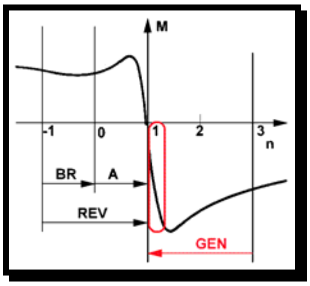

When a loaded hoist is descending, the motor will be driven at hyper-synchronous speed – although this is not perceptible to the operator – and will thus be delivering power back to the mains as an asynchronous generator.
The “regenerative torque characteristic curve” when working in this hyper-synchronous range will be almost a mirror image of the normal speed of rotation n_{sy}: However, the “regenerative breakdown torque” will be significantly greater than the breakdown torque when motoring. Although the shock load of changing from a higher to a lower speed can cause faults (see section 23), in the lowering mode the high breakdown torque provides a safety factor since a load raised by a motor cannot “break through” the “braking generator” – even with a two-wire connection (that is to say, even if the breakdown torque were drastically reduced to 50 % of that of a three-phase connection), the braking torque would be sufficient to lower the load safely without undue rise in speed.

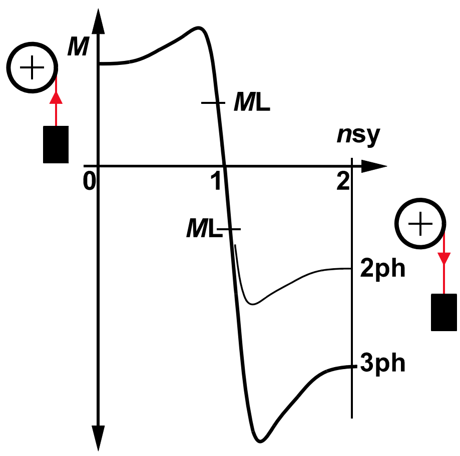

Fig. 19.1
Lowering a load (M_L) in hyper-synchronous generating mode with three-phase connection (3ph) and two-phase connection (“phase failure” 2ph)

Fig. 19.2
Hoist drive in the automotive industry, driven by a geared motor.

Shaft-mounted bevel gear

When descending, the motor is drive at hyper-synchronous speed, generating power back to the mains

20 Reversing (changing the direction from full speed)

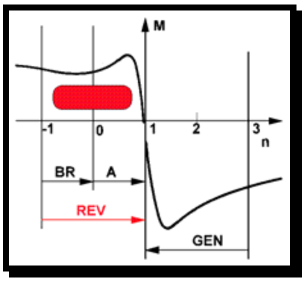

To reverse a motor, the phase lines connected to the supply for “clockwise” rotation are changed over to “anti-clockwise” rotation without a break. The field, now rotating in the anti-clockwise sense, first of all brakes the clockwise rotating mass moment of inertia until it comes to rest and then accelerates it up to speed in the anti-clockwise direction.
By “plugging” the motor in this way, the surge causes approximately four times the lost energy which would occur if the motor were switched off from clockwise rotation, allowed to coast to rest and then switched on for acceleration in the anti-clockwise direction.

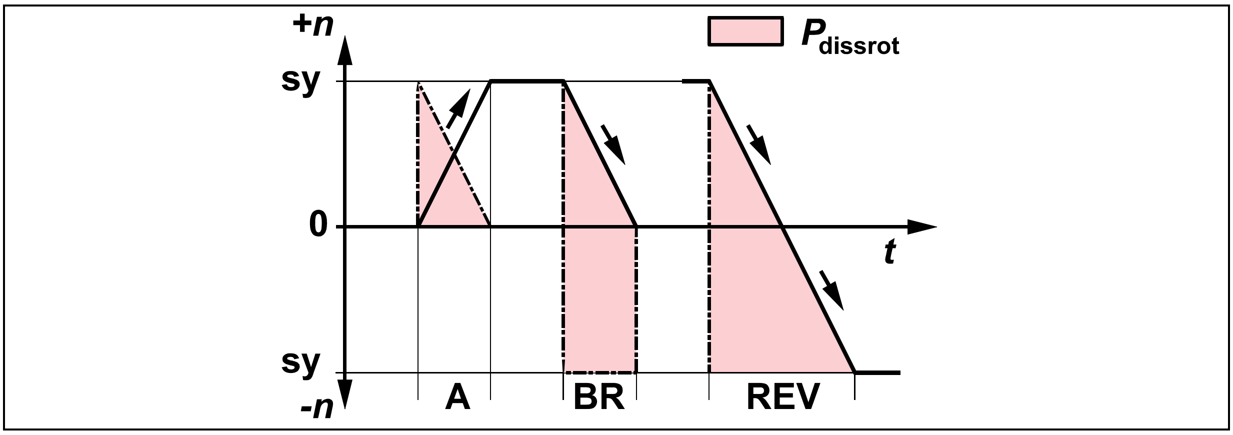

Fig. 20.1 Schematic diagram illustrating the following terms: starting (A), plugging (BR) and reversing (REV) and the respective rotor losses $P_{diss_{rot}}$

Reversing from full speed is a typical operation for roller table motors. The rate of acceleration which can be transmitted by the friction between the rollers and the workpiece is limited (see Figs 2.1 and 20.2) so that a reversal procedure often takes several seconds. It can be very important therefore to make full use of the limit imposed by the coefficient of friction to perform the reversing operation in the shortest possible time and thus achieve the best possible rate. A quasi-rectangular characteristic curve as shown in Fig. 20.2 will permit significantly shorter reversing times than the triangular characteristic curve shown in Fig. 20.3 often recommended for roller tables drives.

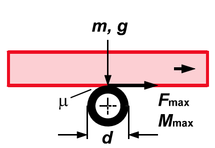

Fig. 20.2 Maximum torque that can be transmitted by friction on a roller table drive

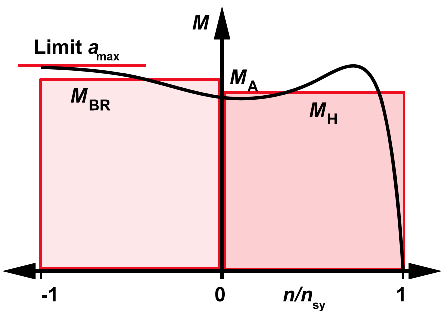

Fig. 20.3 Rectangular characteristic curve with optimum use of the frictional limit for braking (M_{BR}) and run-up (M_H)

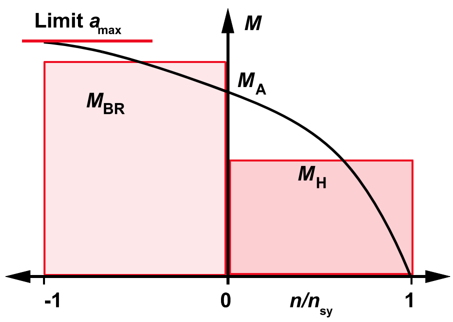

Fig. 20.4 Triangular characteristic curve with poor use of the frictional limit for braking (M_{BR}) and run-up (M_H)

21 Plugging (reverse-field braking)

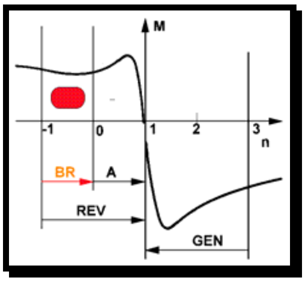

In plugging operation (reverse-field braking), the mass moments of inertia of the drive are decelerated to a stop in the same way as in the first part of a reversing operation. As the speed change passes through zero, the “plugging contactor” is opened by a braking monitor (zero speed switch) to prevent the driving motor from re-starting in the reverse direction.
Although plugging would appear to be simple both in its effect and in its circuitry, in practice there are two important limitations:

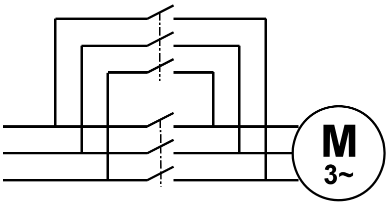

Fig. 21.1

Basic circuit diagram for plugging

- ☐ The mechanical shock load can be unacceptably high, particularly where the transmission components have some lost motion or backlash (such as chain drives and claw couplings) for the conveyance of goods and equipment.

- ☐ The difficulty of opening the “plugging contactor” at exactly zero speed becomes greater as the braking time is shortened. Timers cannot register the effect of different loads and mass moments of inertia and speed of rotation detectors will involve increased costs.

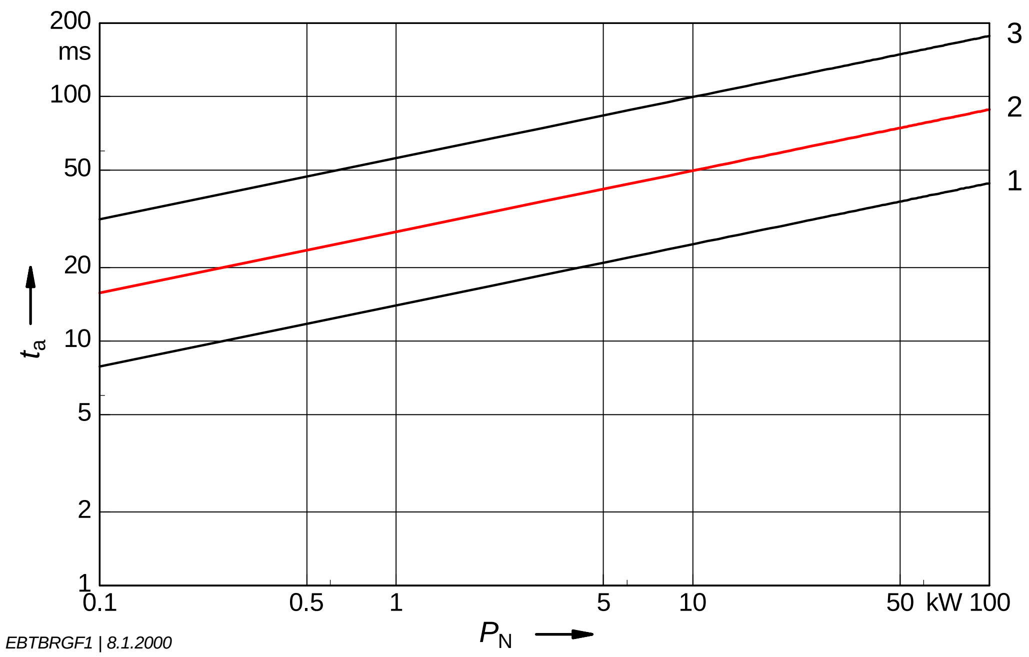

Fig. 21.2 Guide values for the plugging times for 4-pole three-phase cage motors, showing the effect of the factor of inertia *FI* (relative external inertia) and M_L (load torque)

1 - *FI* = 1, $M_L = 1$ Load torque = friction assists braking
2 - *FI* = 1, $M_L = 0$
3 - *FI* = 2, $M_L = 0$

There are, however, areas of application where plugging is very popular. It is frequently used, for instance, for roller table drives since this method requires no additional equipment costs.

Because the friction between the rollers and the workpiece forms a limit to the maximum deceleration which can be transmitted, the braking times usually lie within a range which can be visually monitored. The operator can therefore manually "counter" the plugging contactor by switching it off so that the braking process does not go beyond zero speed.
It is relatively unusual to find systems which stop the plugging process automatically in roller table applications since, under these arduous types of duty, such refinements may cause other problems.

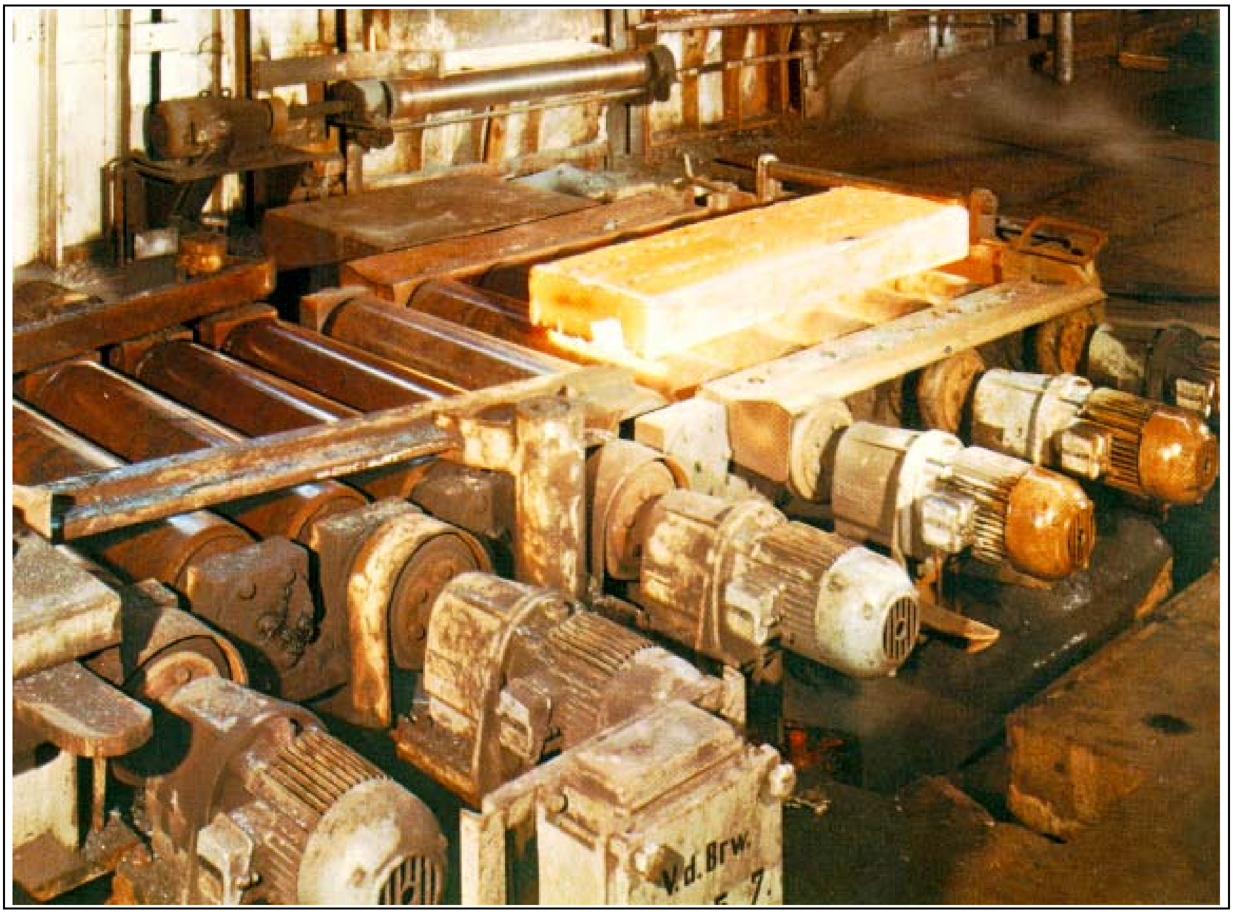

Fig. 21.3 Example of a roller table application suitable for plugging

22 D.C. injection braking

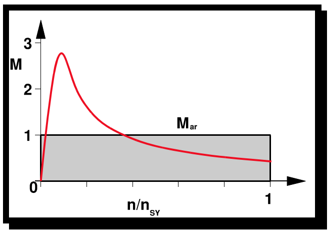

If the three-phase winding of the stator is fed with direct current, a stationary magnetic field Φ will be set up in the stator bore causing a voltage to be induced in the bars of the cage rotor as long as the rotor is in motion (Fig. 22.0).

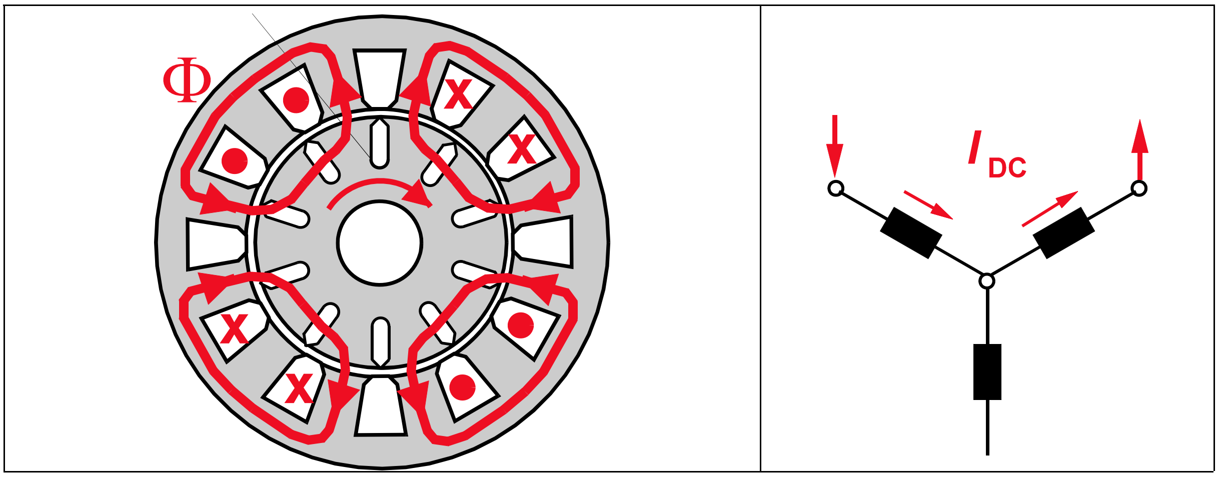

Fig. 22.0
Field developed by D.C. supply to a 4-pole three-phase stator winding in star connection

22.1 Principle of D.C. injection braking

Since the electrical resistance of the rotor cage is very low, even small induced voltages can create a high rotor current. This current will produce a strong braking effect on the bars and hence on the rotor.

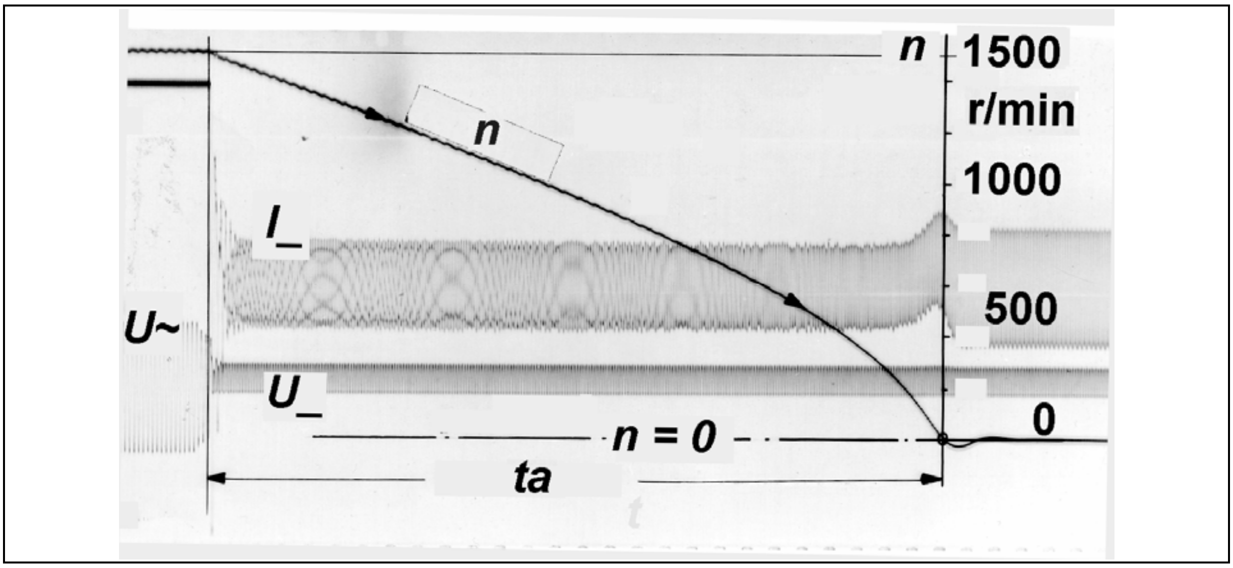

Fig. 22.1.1 Oscillogram of D.C. injection braking with steep deceleration of the speed *n* at the end of the braking time t_a

As the speed falls, the frequency of the induced voltage falls and with it the inductive impedance. The ohmic resistance of the rotor gradually becomes dominant and so increases the braking effect as the speed comes down. The braking torque generated falls away steeply just before standstill and finally ceases when there is no further movement.
Direct current injection braking is therefore not suitable for actually holding a load at rest. On the other hand, the initially gentle but increasingly powerful effect of this method of braking makes it virtually ideal for almost any retardation process (Figs 22.1.1 and 22.1.2).

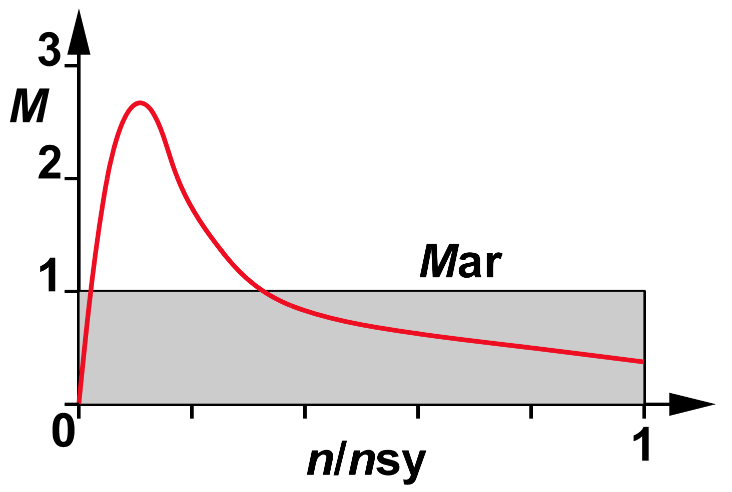

Fig. 22.1.2
Effectiveness of D.C. injection braking during retardation of speed from $n \rightarrow 0$

M	Instantaneous braking torque
M_{ar}	Average value of the braking torque

22.2 Connection of the stator winding

The most effective retardation is obtained by connecting the D.C. supply to two phases in the case of motors in star configuration or by connecting the D.C. supply to two of the three-phase terminals in the case of motors in delta (Δ) configuration.
Other possible methods of supply produce a lower retardation effect.

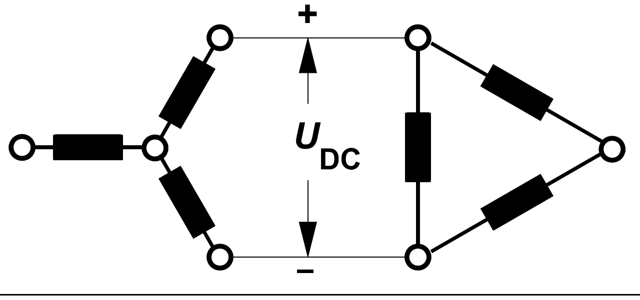

Fig. 22.2.1
Stator winding configurations for connection to D.C. voltage U_{DC}

22.3 Rating the D.C. source

The mean value shown in Fig. 22.1.2 for the braking torque can be used to obtain a quantitative comparison when rating the D.C. source. However, this is not suitable for calculating the braking time and braking travel. The stepwise method described in section 23.3 must be used for this calculation.

The average braking torque is approximately equal to the rated motor torque when the braking current I_{DC} is approximately 200 ... 250 % of the rated motor current I_N, i.e. when

$$I_{DC} \approx 2.5 \cdot I_N$$

The D.C. voltage to be applied should be sufficient to cause this braking current to flow for a given winding resistance.

The D.C. voltage U_{DC} required for standard models with windings designed for 400 V in either star or delta (Y or Δ) connection can be obtained from the curves shown in Fig. 22.3.1 depending on the rated motor output P_N. Due to the difference in winding designs according to the number of poles, the curves encompass a relatively wide scatter band, the upper values of which produce harder braking while the lower values result in softer braking. If the braking effect is found to be too harsh in practice, it can be softened by lowering the voltage, e.g. by inserting a series resistor in the D.C. circuit.
Rectifier in single-phase bridge configuration are the most suitable means of transforming the A.C. mains into D.C. current. Silicon diodes must be protected against the inductive voltage spikes expected.

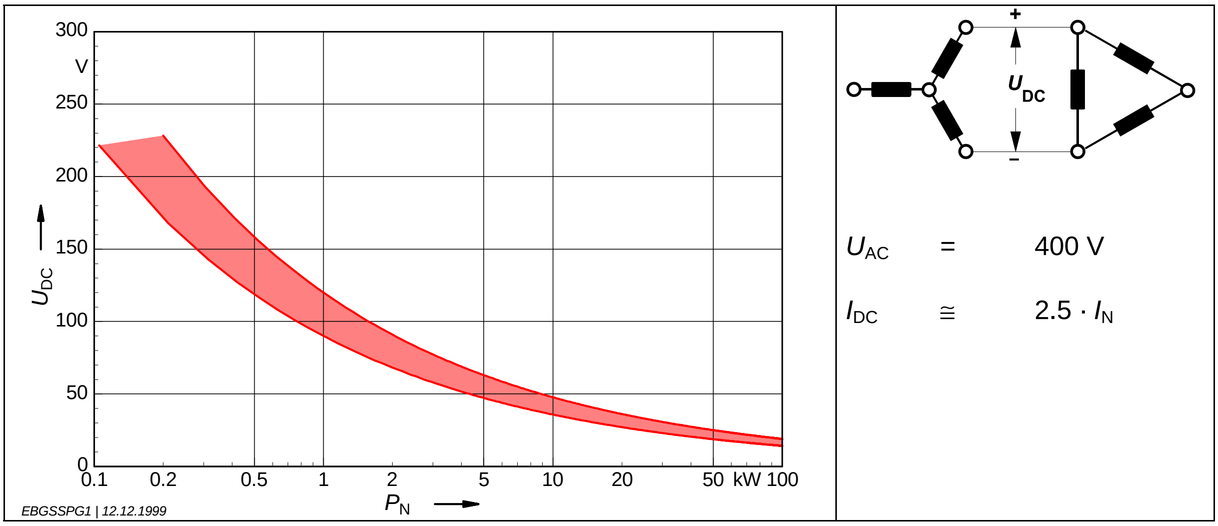

Fig. 22.3.1 Guide values for braking by D.C. injection braking

Since the D.C. voltage U_{DC} required is generally lower than the rated voltage or the A.C. supply control voltage, a transformer will also be required. The secondary voltage U_{sec} of this transformer must be 25 % higher than the D.C. voltage required since the arithmetic mean of the pulsating D.C. voltage on a single-phase bridge circuit is lower that the effective value of the A.C. voltage by a factor of 0.8. The rated current of the rectifier must be chosen such that it can provide the necessary D.C. braking current I_{DC} under S3 intermittent periodic duty with a 5 % cyclic duration factor. The rated output of the transformer under S3 at 5% cyclic duration factor will be given approximately by:

$$P_{Tr} = U_{DC} \cdot I_{DC} \cdot 1.5 \text{ (VA)}$$

22.4 Control circuit diagram

The circuit is designed such that the D.C. voltage is applied to two terminals of the motor winding after the motor is disconnected from the three-phase supply. To protect the rectifier against inductive voltages generated by the motor, the switchover from A.C. feed to D.C. feed is only made via a voltage relay when the residual voltage has decayed to approximately on third of the operating voltage. A timer relay switches the D.C. off after completion of the injection braking (1 ... 3 s) to prevent impermissible heating of the windings.

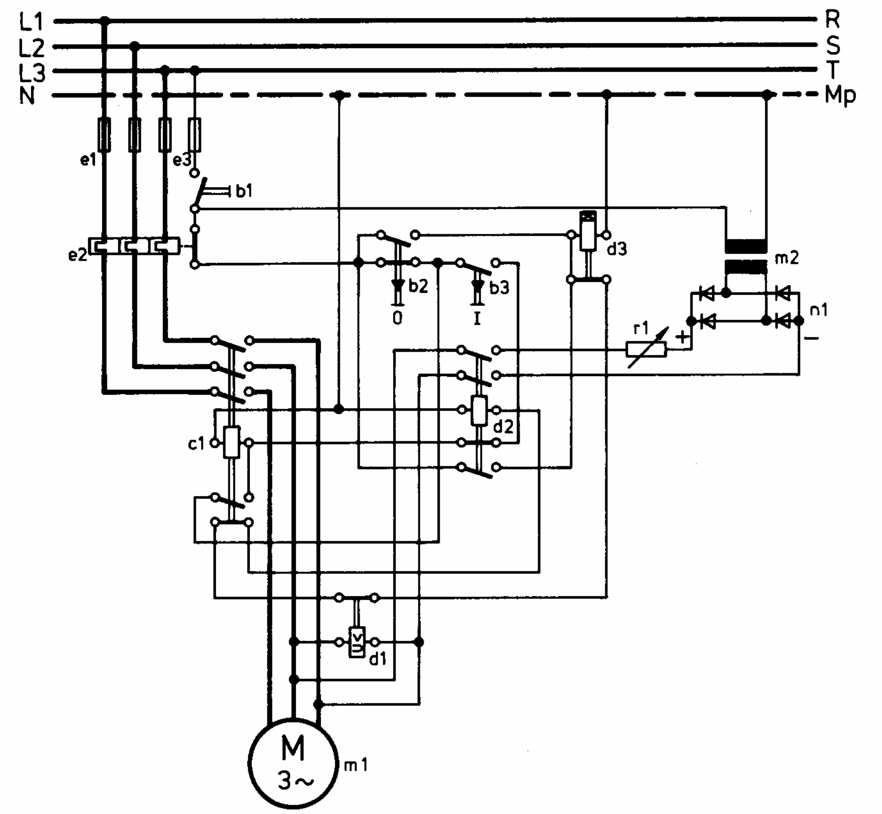

Fig. 22.4 Circuit diagram for D.C. injection braking

22.5 Electronic D.C. braking unit

The previous sections intentionally restricted the discussion to “conventional” methods of A.C./D.C. conversion and control to explain the principles of operation. There are many “D.C. braking units” available on the market. These use electronic components to provide a compact and flexible solution incorporating safety features (e.g. to prevent overlap between the D.C. and A.C. feeds or the loss of the D.C. supply) and, in some cases, an optional soft start feature.

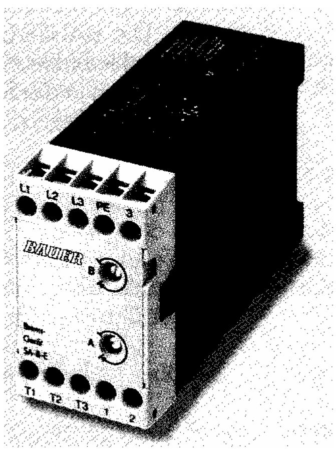

Fig. 22.5 D.C. braking unit with electronic components for the conversion, adjustment and disconnection of the D.C. voltage

23 Pole-changing

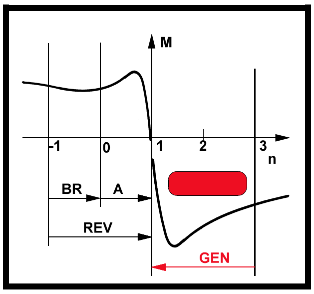

Pole-changing cage motors with speed ratios of 1:2, 1:3, 1:4, 1:6 or 1:10 are frequently used for inching. A ***single*** winding in ***Dahlander connection*** is all that is required for a speed ratio of 1:2. All other speed ratios need two separate stator windings, which of course involves lengthier manufacturing processes (Fig. 23.0.1) and consequently higher costs (Fig. 23.0.2). Nevertheless, they are in many cases less expensive than motors with stepless speed control, such as D.C. or inverter-fed motors.

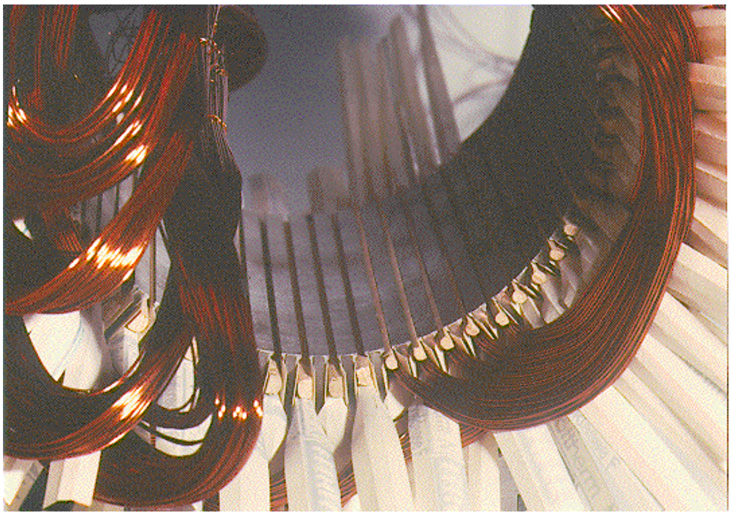

Fig. 23.0.1
Manual formation of two separate windings on a pole-changing motor

The 20-pole winding is fully installed in the slot ground section;

the 2-pole winding is partly installed in the slot opening section

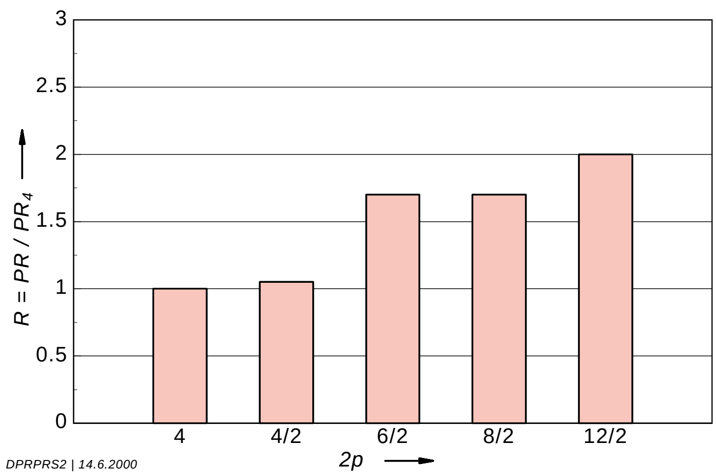

Fig. 23.0.2

Guide values for the costs of pole-changing geared motors with speed ratios of
1:2 (4/2-pole), 1:3 (6/2-pole),
1:4 (8/2-pole), 1:6 (12/2-pole)
and 1:10 (20/2-pole) compared to a geared motor with a fixed speed (4-pole)
Higher speed of approximately 100 r/min – based on the same maximum power

23.1 Production and characteristics of the braking torques

Regenerative braking will always occur if the instantaneous speed *n* of the rotor is greater than the synchronous speed of the stator's rotating field. This occurs, for example, where pole-changing three-phase motors are switched from a lower number of poles to a higher number of poles. This causes regenerative braking torques, the characteristics of which depend on the pole number or speed ratio and on the type of motor. More specifically, they will depend on the ohmic resistance and reactance in the rotor circuit.
The following factors are critical for three-phase cage motors:
- ☐ shape of the cage bars
- ☐ shape of the end rings
- ☐ material used for the cage bars and the end rings.

Figs 23.1.1 and 23.2.2 show the shape of the torque characteristic curve in motoring and generating mode. The regenerative braking torques are considerably greater than the motoring torques.
Brief noises may be heard in regenerative braking; these are above the operating sound of the three-phase machine.

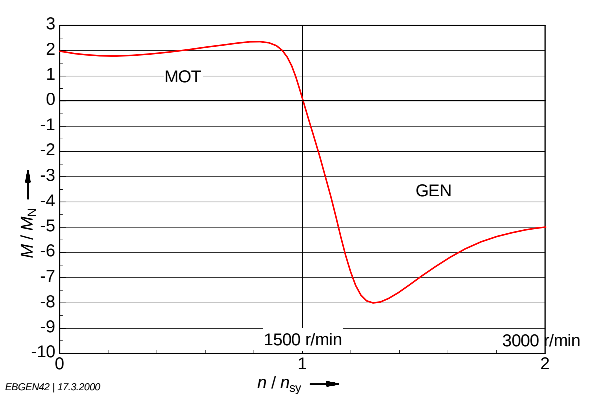

Fig. 23.1.1
Shape of the torque characteristic curve when switching from the lower to the higher pole number with a speed ratio of 2:1.

The motoring breakdown torque to regenerative breakdown torque ratio is approximately 1:4 in this case

23.2 Damping the braking torques

With regard to the effect of retardation on conveyed products by such pole-changing switching it is advisable in some instances and sometimes even essential to reduce the rate of deceleration. This can be achieved simply by suitable modification of the existing contactor control (Fig. 23.2.1).

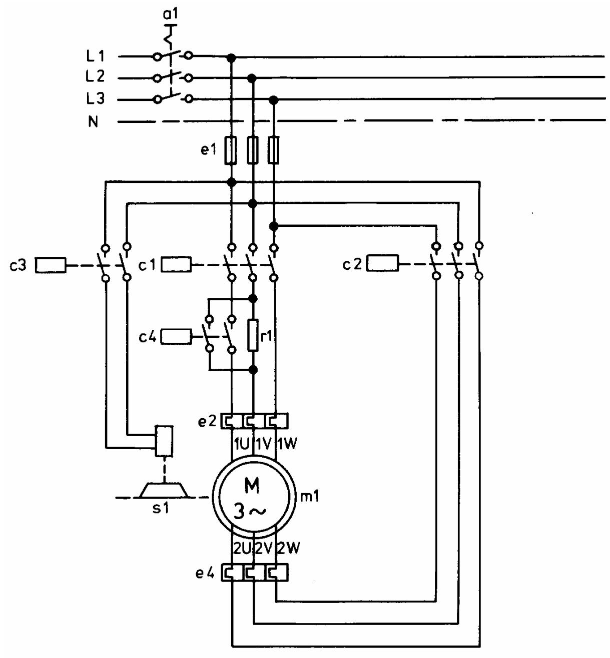

Fig. 23.2.1 Circuit diagram for retrofitting a contactor to reduce the regenerative braking torques

When the motor is switched for two-phase regenerative braking, with or without a series resistor, it must be ensured that single-phasing is effective only during the regenerative braking period. As soon as the regenerative braking period has ended, the motor must be reconnected to the three-phase lines L1, L2 and L3, otherwise part of the winding may become thermally overloaded (see section 5.2.4).
Reducing the decelerating torque will reduce the mechanical load on the gearing and downstream transmission elements. The respective braking torques are shown in Fig. 23.2.2.

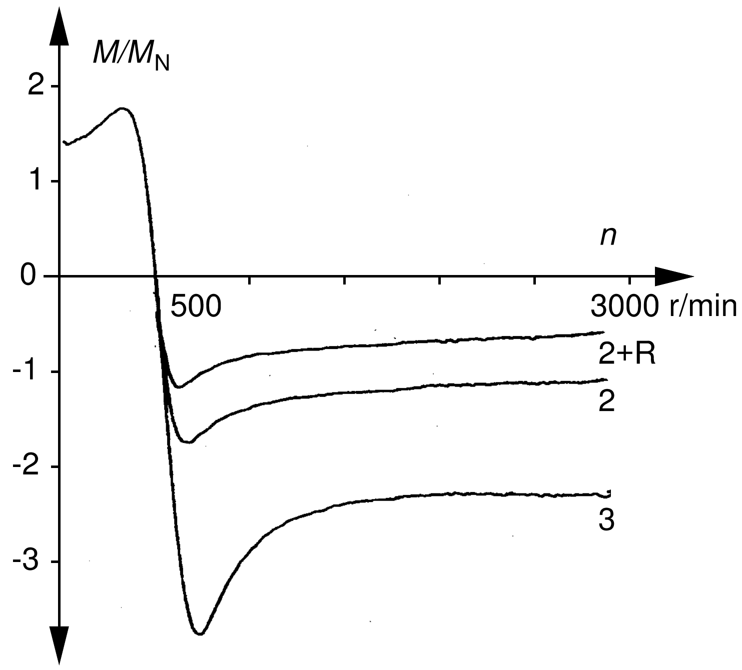

Fig. 23.2.2 Torque curves produced by switching a two-speed three-phase induction motor with different circuits to the lower speed at a speed ratio of 6:1

Curve 3: three-phase regenerative braking
Curve 2: two-phase regenerative braking
Curve 2+R: two-phase regenerative braking with an additional series resistor in one supply line

Other possible ways of reducing the braking effect:

- ☐ for three-phase motors with a separate winding, the extra winding can, in certain limited cases, be adapted for use solely for regenerative braking. In this case the frictional conditions, flywheel masses and speeds must be known precisely. This winding can then be designed for the application concerned and with this method no alterations to the control circuit are required.
- ☐ Regenerative braking is achieved by phase chopping whereby, during the retardation period, the voltage for the required rate of deceleration can be pre-set. This enables soft and time-controlled regenerative braking to be obtained.
- ☐ The conventional method of control shown in Fig. 23.2.1 can be replaced by an “electronic soft control inverter” as shown in 23.5.

23.3 Calculation of the braking time and braking travel

The torque characteristic curves shown in Figs 23.1.1 and 23.2.2 cannot be applied to any design at will. The shape of the curve, which often has a very pronounced “regenerative breakdown torque”, makes calculation of the braking time very complicated because the use of an arithmetic mean gives inaccurate results.
The very imprecise method using the mean is compared with the time-consuming stepwise method in Fig 23.3.1.

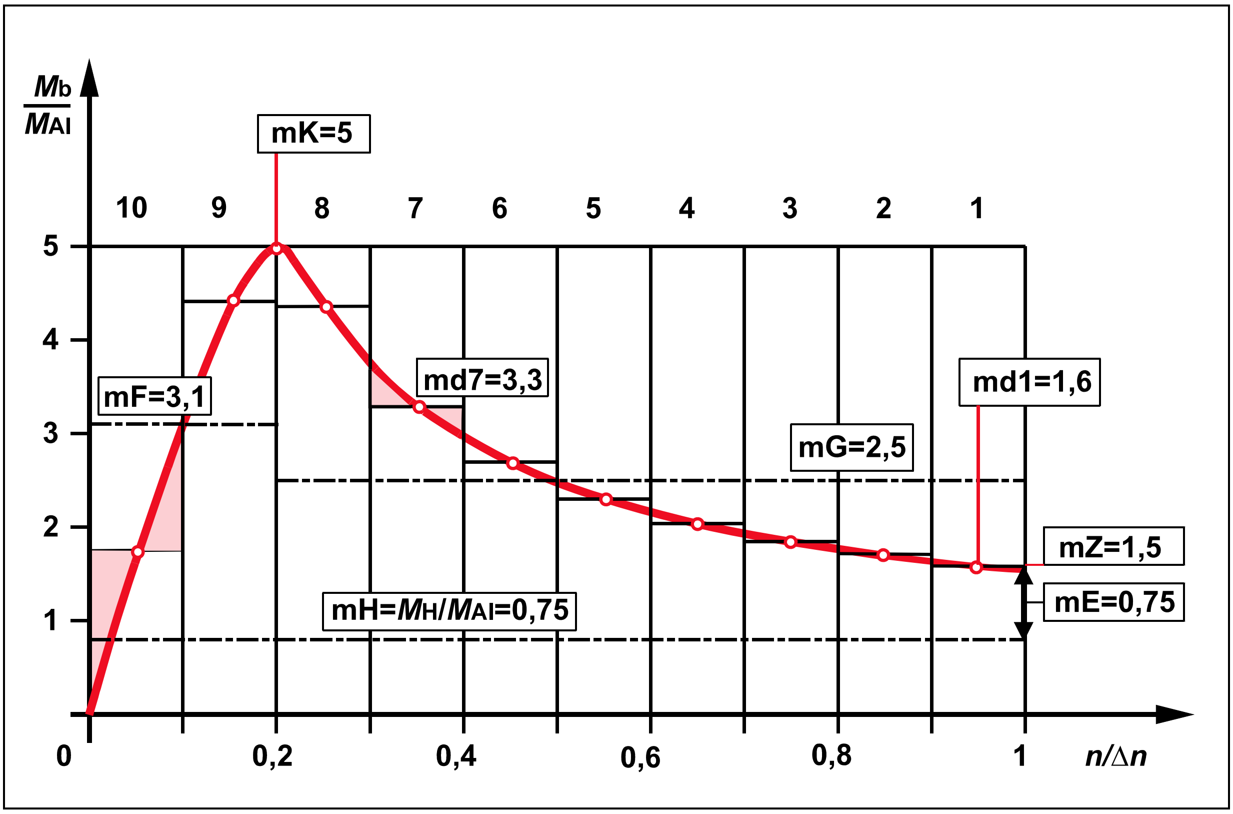

Fig. 23.3.1 Diagram explaining the calculation of the braking time and braking travel for regenerative braking using the averaging method and the stepwise method

M_b/M_{Al} - relative regenerative braking torque
M_{Al} - breakdown torque at low speed
Δn - speed difference n_{syII} - n_{syI}
mK - relative regenerative breakdown torque
mH - relative load torque (lifting torque)
mG - arithmetic mean of the regenerative braking torque in the range $n/\Delta n$ = 1 ... 0.2
mF - arithmetic mean of the regenerative braking torque in the range $n/\Delta n$ = 0.2 ... 0
md - arithmetic mean of the regenerative braking torque in the respective speed step (e.g. md1 in step 1 through $n/\Delta n$ = 0.1)

Calculation using the arithmetic mean values mG and mF results in braking times that are too short and, in particular, braking travel that is much too short. This applies especially if the relative regenerative braking torque mZ is only slightly higher than the relative lifting torque mH in the high speed range ($n/\Delta n \rightarrow 1$), i.e. if the difference available for deceleration is very small.

The following applies for pole-changing regardless of the effort required to calculate the braking time and braking travel: the times and travel are those for ***slowing*** from the running speed to the positioning speed t_a. There then follows varying period (t_{pos}) at the ***positioning speed*** (Fig. 23.3.2) and finally the mechanical braking period (t_b).

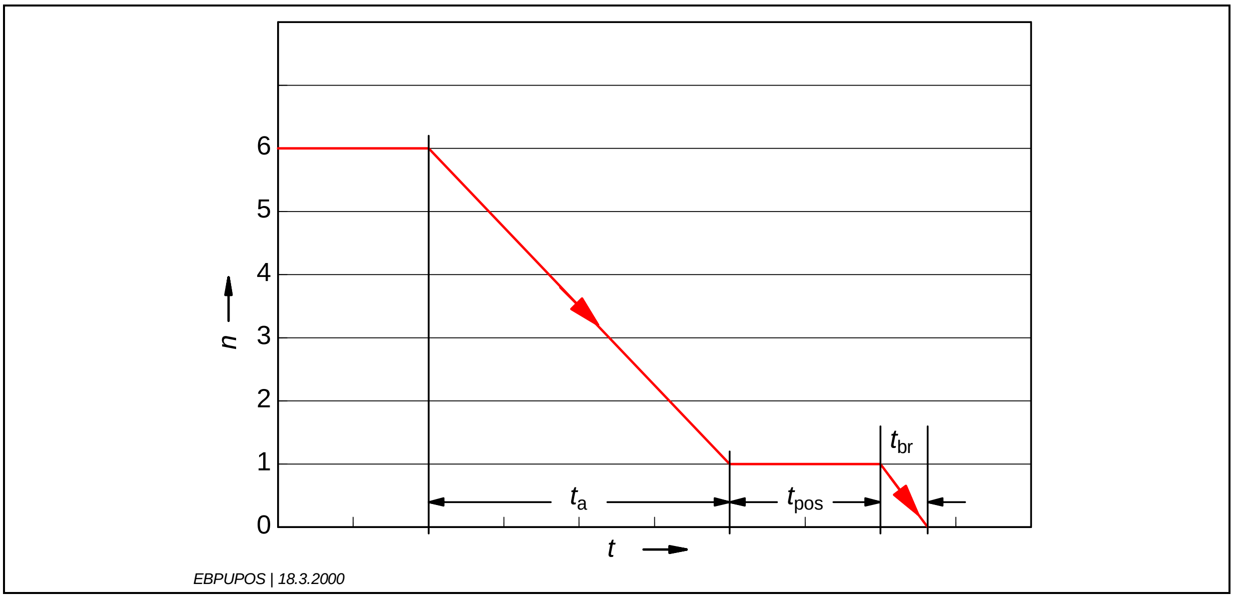

Fig. 23.3.2 Speed reduction by 6:1 pole-changing from the running speed (n = 6) to the positioning speed (n = 1)

An initial calculation of the stopping times and stopping distances is only possible if the regenerative torque characteristic curve is known. However, the following approximate guide values are given. These assume that the mean regenerative braking torque is about twice the rated motor torque. The guide values should only be used to help you decide whether or not to perform a more detailed calculation.

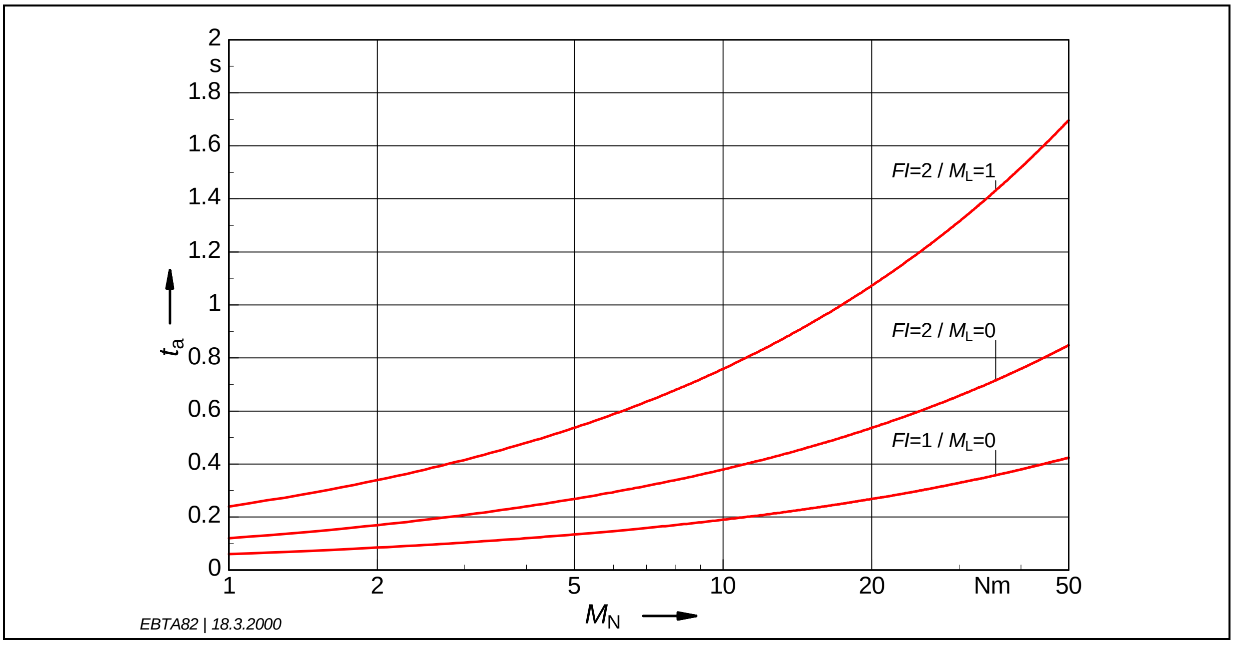

Fig. 23.3.3 Guide values for the stopping times t_a of 8/2-pole positioning motors with rated torques M_N = 1 ... 100 Nm

FI = 1/M_L = 0 : no external rotating masses, no load torque

FI = 2/M_L = 0 : external rotating masses correspond to the rotor mass, no load torque

FI = 2/M_L = 1 : external rotating masses correspond to the rotor mass, load torque with descending load = rated motor torque

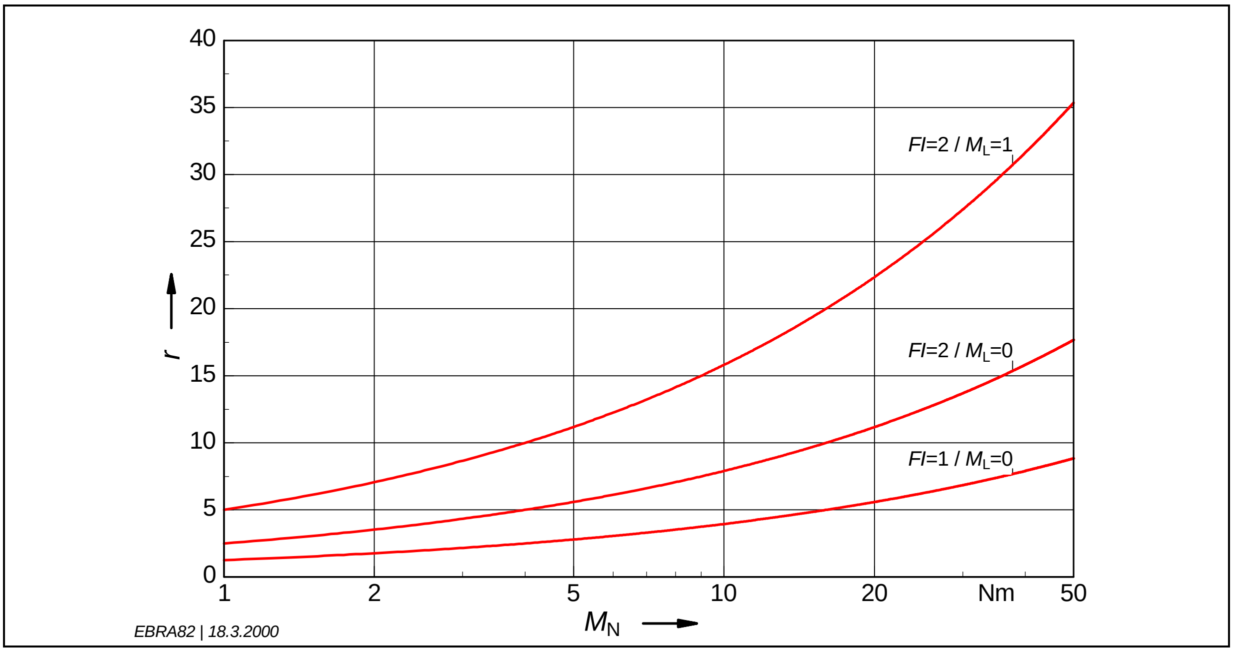

Fig. 23.3.4 Guide values for number of rotations φ to standstill of 8/2-pole positioning motors with rated torques M_N = 1 ... 100 Nm

FI = 1/M_L = 0 : no external rotating masses, no load torque

FI = 2/M_L = 0 : external rotating masses correspond to the rotor mass, no load torque

FI = 2/M_L = 1 : external rotating masses correspond to the rotor mass, load torque with descending load = rated motor torque

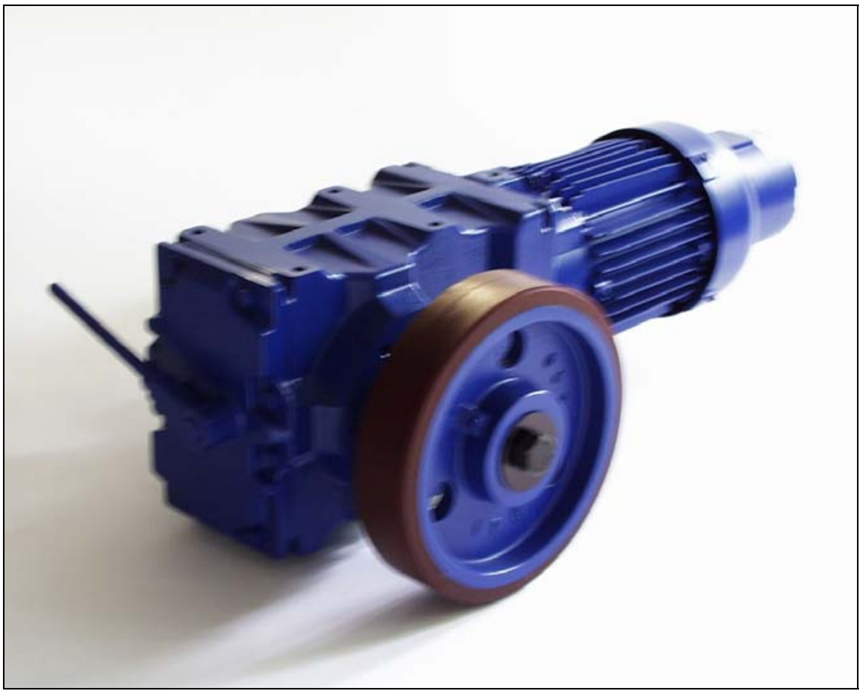

Fig. 23.3.5 Danfoss Bauer series B 2000 electric monorail drive (EHB) with 1:4 pole-changing bevel-geared motor

23.4 Recommended deceleration principles

The time taken to change from the high speed to the low speed is unimportant for many applications for instance, when changing a fan drive in the evening from day duty to night duty. Instead of an instantaneous changeover from speed II to speed I, the drive can be switched off and allowed to spin down to the lower speed I.
The load on the power transmission components – shafts, couplings and gears – can be reduced significantly by selecting the optimum switch-over time as shown in Fig. 23.4. Since the mass moments of inertia and loading do not change in this type of duty, the optimum switch-over point can be determined by trial and set with a timer relay.
At the optimum switch-over point, the drive will first spin down free by the amount Δ*n*I and will then be accelerated by the torque *M*I which is slightly lower than the motor's starting torque M_A.
If switch-over occurs too soon after the coasting time ΔnII, the regenerative braking torque *M*II will be imposed which, in this example, is about 400 % of motoring the breakdown torque.

The diagram represents a drive intended for high-inertia loads only without any significant load torque; these conditions could, in principle, be applied to a fan drive.

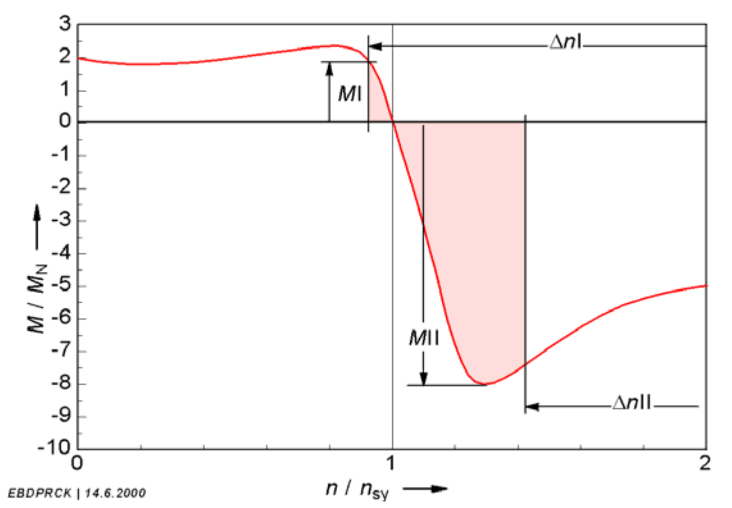

Fig. 23.4
Comparative example of switching a pole-changing drive in the ratio of 1:2 from speed stage II to speed stage I.

Optimum coasting Δ*n*I
results in a peak torque *M*I

Unsatisfactory coasting Δ*n*II
results in a peak torque *M*II

23.5 SPR electronic soft deceleration

This device unites the conventional contactor control functions for two phase reverse braking, including the connection of the third phase cable in good time, shortly before the synchronous positioning speed is reached. The switching command for the electronic, contactless switch is determined from motor performance characteristics, meaning that it automatically adapts to the relationship between current load torque and mass inertial torque. A timer relay and load-dependent adjustment are not necessary. The SPR device needs neither its own power supply nor control signals; it is simply necessary to loop two of the three supply leads through to the low-speed winding (Fig. 23.5.1).

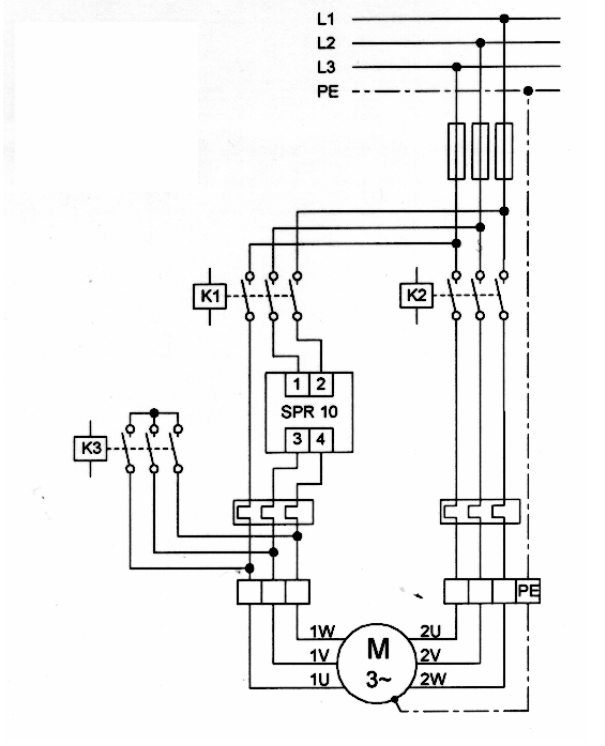

Figure 23.5.1
Circuit diagram of the SPR electronic soft power reversal for pole-changing motors

K1	Low speed range contactor
K2	High speed range contactor
K3	YY circuit contactor at high speed, together with K2 (not required when there are 2 separate Y/Y windings)

The effects of the circuit on the torque characteristic can be seen in figure 23.5.2: The regenerative braking torque (GEN) is dampened over its entire range (2 phase) to values which roughly correspond to the motoring starting torque of a three wire connection (3 phase). Shortly before the transition to the motor (MOT), the device's logic circuit reconnects the third conductor, so that the motor can develop its full torque (3 phase), which is primarily necessary for crane operation. The optimum changeover instant "window" F is quite tight: If changeover is too soon, a high breakdown torque ($M_{K3\ phase}$) occurs in the generator phase; if changeover is too late, the torque (2 phase) developed in motoring (MOT) is too low. The optimum instant is determined by the device, independently of the current load relationships, according to an evaluation of the motor's ratings.

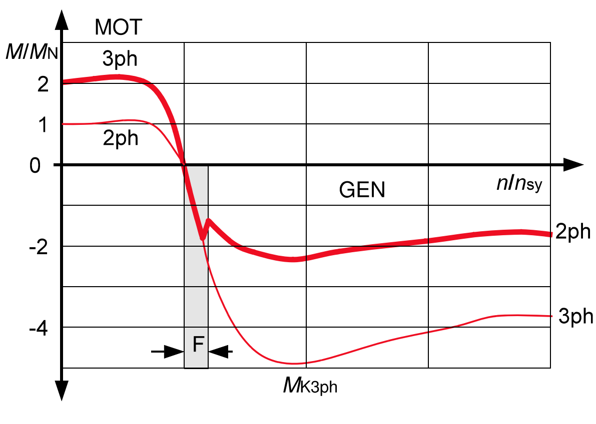

Figure 23.5.2
Torque characteristic change in the motoring (MOT) and generator (GEN) phases of three-wire (3 phase) and two-wire (2 phase) circuits, during 8/2 pole motor reverse braking using a soft power reversal SPR

The device automatically makes the changeover to normal operation in period "F"

The electronic soft power reversal SPR prevents the torque pulse during the changeover from the working to the positioning speed, and makes it possible also to use the robust, pole-changing cage motor for moving moderately fragile transport property.

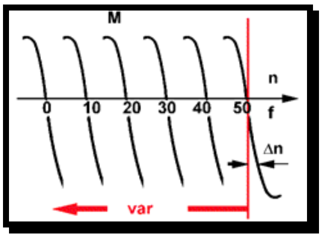

The hyper-synchronous regenerative braking described in section 19 can also be used for retardation to speeds $n \rightarrow 0$ if the frequency is reduced to $f \rightarrow 0$. Frequency inverters make this possible. The regenerated energy flows into the inverter. The blocking diodes in the input rectifier of the frequency inverter normally prevent power flowing back into the mains. To prevent undue charging of the intermediate link capacitor, which would force it to a dangerously high voltage, this regenerated energy must be dissipated by the brake-chopper through an auxiliary resistor where it will be converted to heat.
Recent developments also permit energy to be fed back to the mains thanks to their special design.
In specifying the brake-chopper it is necessary to check:
- ☐ maximum braking duty
- ☐ average braking duty
- ☐ equivalent continuous load on the basis of the duty cycle.

It is recommended that there be contact between the motor supplier and the inverter supplier.
The braking sequence is represented qualitatively in Fig. 24.1. In the period t_L from the time 0 to (1), the motor runs with an asynchronous rotor speed *ROT* which is slower than the rotating field speed *DRF* by the slip speed. Deceleration starts at time (1); the frequency, and hence the rotating field speed, follows a pre-set ramp down to zero under inverter control. The rotor speed and that of the driven masses – depending on the retardation effect of the load torque – initially remains at virtually its normal full value. This is therefore above the rotating field speed. Due to its hyper-synchronous speed Δn, the motor will develop a regenerative braking torque that will slow down the rotor over the braking time t_a. At time (2), the frequency and speed of rotation of the stator field reach zero and the retardation effect then corresponds to D.C. braking. The rotor now runs on to time (4) uncontrolled, unless it is stopped at (3) by a mechanical brake (clamping brake). The diagram assumes that the ramp will have been calculated beforehand to produce the required stopping time t_a and that the value of the parameters used will correspond to the actual conditions.

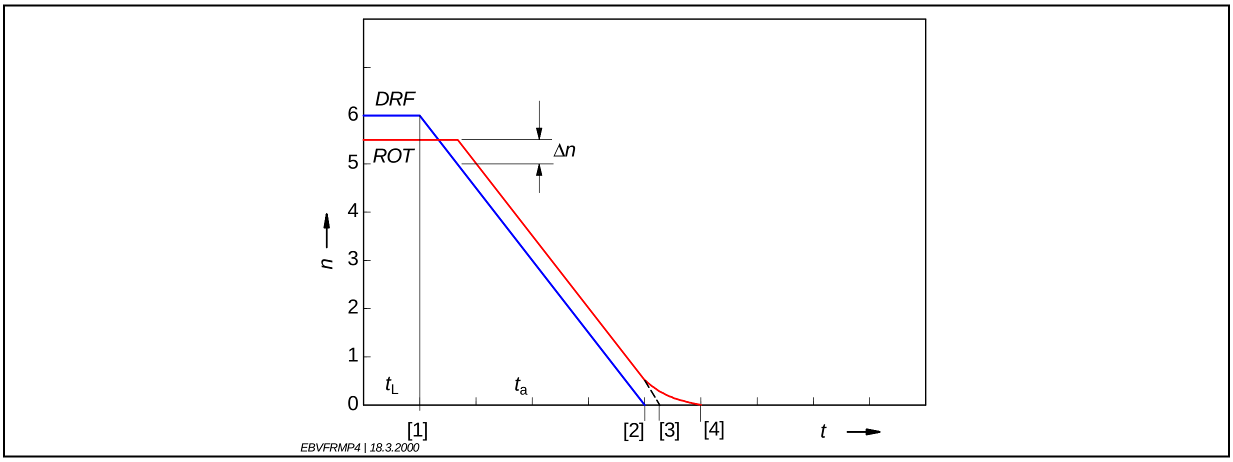

Fig. 24.1 Schematic diagram of frequency-controlled regenerative braking from speed *n* over time *t*

DRF	- Rotating field speed	(1)	- Start of ramp
ROT	- Rotor speed	(2)	- End of ramp
Δn	- Slip speed	(3)	- Application of mechanical clamping brake
t_L	- Running time	(4)	- Free-wheeling deceleration
t_a	- Braking time	(5)	- Intermittent deceleration

Fig. 24.2 compares how the braking process may develop in test operation.
The rotor speed is retarded at a much slower rate than would be expected by the ramp selected. The “fault” would be indicated by the inverter or noticed by running a practical test.

The following are possible causes of a delayed rate of deceleration:

Calculation errors:

- ☐ The mass moments of inertia are greater than had been assumed
- ☐ The additional retardation effect of the load torque is less than had been assumed.

Inverter errors:

- ☐ The deceleration torque M_a developed by the motor is insufficient due to the lack of a brake-chopper or the current limiter being set too low or the inverter being too small; this results in intermittent braking as represented by (5).
- ☐ The brake-chopper is not adequate, the inverter operates "intermittently";
  mechanical braking (3) or free-wheeling deceleration (4) results according to the design of the control system;
  the speed characteristics are governed by the drive characteristics (braking torque, load torque, *FI*).

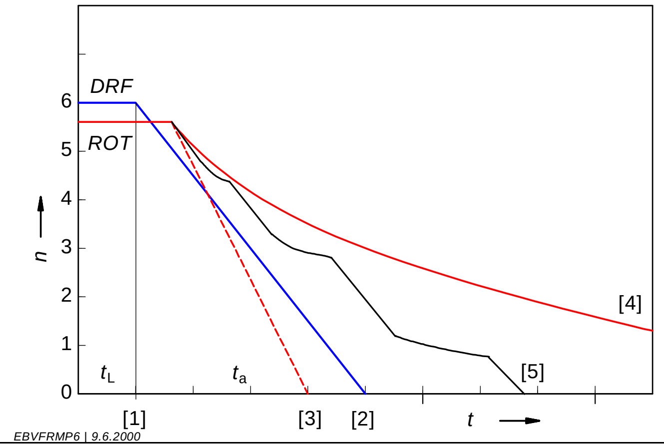

Fig. 24.2
Schematic diagram of frequency-controlled regenerative braking with inadequate retardation effect; key and text as for Fig. 24.1

There are significantly lower losses associated with frequency-controlled braking than with other electrodynamic braking methods. The reasons can be demonstrated in principle by the example of direct-on-line starting:
Where the motor is started using the mains supply, the rotating field speed *DRF* jumps almost instantaneously to the synchronous speed n_{sy} whereas the rotor is only accelerated to its asynchronous speed after a starting time determined by the load and mass moments of inertia. The initially high slip speed between *DRF* and *ROT* causes the relatively high energy loss W_{rot} from the rotor (Fig. 24.3).
With frequency-controlled starting, by contrast, the rotating field speed *DRF* is only in advance of the rotor speed *ROT* by the slip speed at which a sufficient acceleration torque can be generated. The hatched area corresponds to the lost energy W_{rot} in the rotor – it is significantly lower for frequency-controlled starting than for direct-on-line starting from the mains supply (Fig. 24.4).
These considerations also apply to regenerative braking.

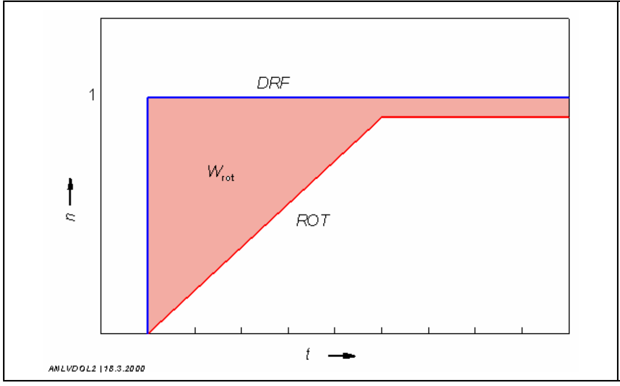

Fig. 24.3
Schematic diagram of the lost energy in the rotor W_{rot} for DOL starting from the mains supply

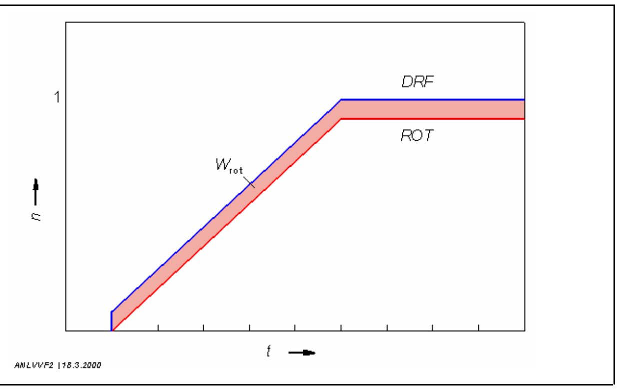

Fig. 24.4
Schematic diagram of the lost energy in the rotor W_{rot} for frequency-controlled starting

25 Thermal rating of electrodynamic methods of braking

The braking methods described have different thermal effects on the motor. If the frequency and duration of individual braking processes are so high that the heat balance of the motor is seriously affected, it will be necessary to specify the duty type in accordance with EN 60064-1.
The thermal rating in particular instances must be decided by the motor manufacturer; some guide values are given below. ***Reversing*** processes are compared with a ***starting*** process.

25.1 Hyper-synchronous regenerative braking

Since the level of efficiency of an induction motor is better in generating mode than in motoring mode, the rated output quoted of the motor can also be used in generating mode.

25.2 Reversing

Factor K_R for the thermal rating of a reversing operation compared to that of a starting operation:

P_N (kW)	≤ 1.5	≤ 7.5	≤ 22	≤ 50
K_R	3	2.8	2.6	2.4

25.3 Plugging (reverse-field braking)

Factor K_G for the thermal rating of a reversing operation compared to that of a starting operation:

P_N (kW)	≤ 1.5	≤ 7.5	≤ 22	≤ 50
K_G	2	1.8	1.6	1.4

25.4 D.C. injection braking

Factor K_B for the thermal rating of a braking operation compared to that of a starting operation:

$K_B = 1.6$

25.5 Pole-changing

Factor K_{PU} for the thermal rating of a speed-reduction operation compared to that of a starting operation:

$K_{PU} \approx 1$

The value here is somewhat high; it can be corrected downwards in some instances on the basis of measurements or experience.

25.6 Frequency control

The drive works as a generator; it is not loaded thermally to any greater extent than when running as a motor with corresponding output. The braking energy is absorbed by the chopper which should be rated as described in section 24. Full details are given in section 24.

IV CALCULATION OF THE MASS MOMENT OF INERTIA

The mass moment of inertia is an important parameter when calculating the starting and braking performance. This section addresses the most important rules for assessing this variable.

26 Rotor mass moment of inertia

26.1 Fixed-speed motors

The rotor mass moment of inertia is often a dominant factor and can be obtained from the manufacturers' catalogues for commercial motors. Guide values are shown in Fig. 26.1.

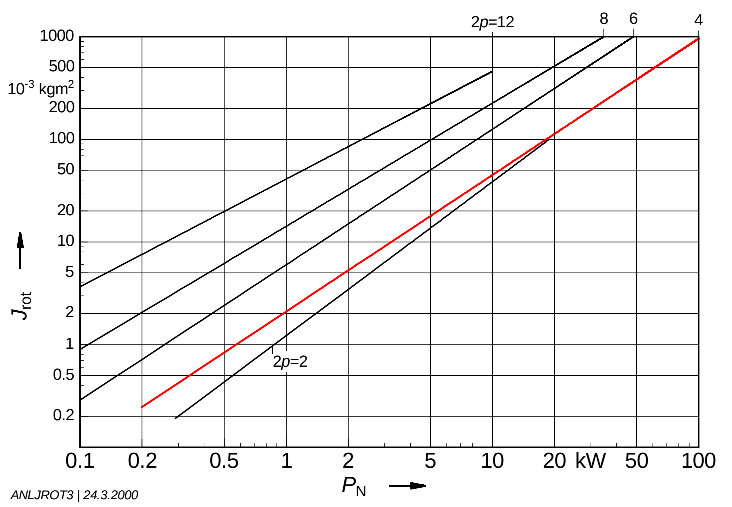

Fig. 26.1
Guide values for the rotor mass moment of inertia J_{rot} of standard motors in the power range P_N = 0.1 ... 100 kW and pole numbers $2p$ = 2 ... 12

The graph can only provide a rough idea and it should be noted that even manufacturers' specifications regarding these values have tolerances of ± 10 % in accordance IEC 60034-1, Table 8.

26.2 Pole-changing motors

With pole-changing motors, the mass moments of inertia will be very dependent on their respective design. The following graph can therefore give only approximate guide values.

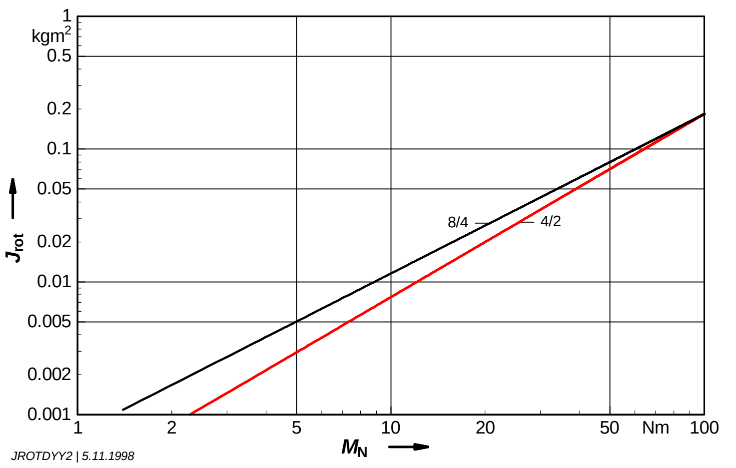

Fig. 26.2

Guide values for the rotor mass moment of inertia J_{rot} of pole-changing cage motors with a rated output P_N in the upper speed range;

Dahlander connection for speeds 1:2
$2p$ = 8/4 or 4/2

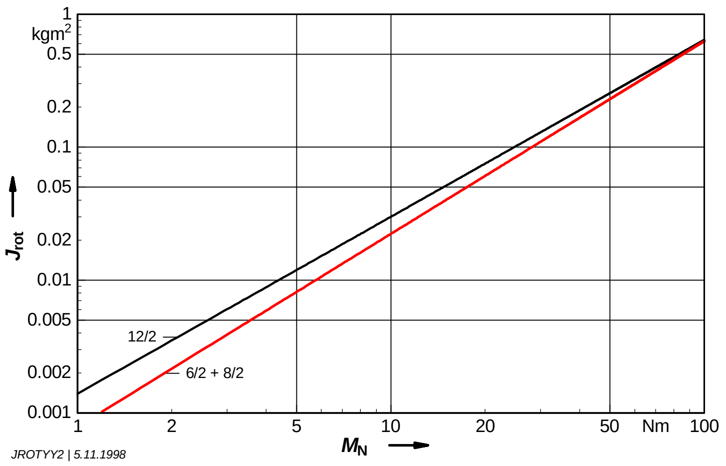

Fig. 26.3

Guide values for the rotor mass moment of inertia J_{rot} of pole-changing cage motors with a rated output P_N in the upper speed range;

Separate winding for speeds 1:3, 1:4 or 1:6 $2p$ = 6/2, 8/2 or 12/2

26.3 Cylindrical steel bodies

The mass moment of inertia for cylindrical solid or hollow steel bodies in standard dimensions can be calculated according to Fig. 26.3 in relation to a length of 0.1 m**.**

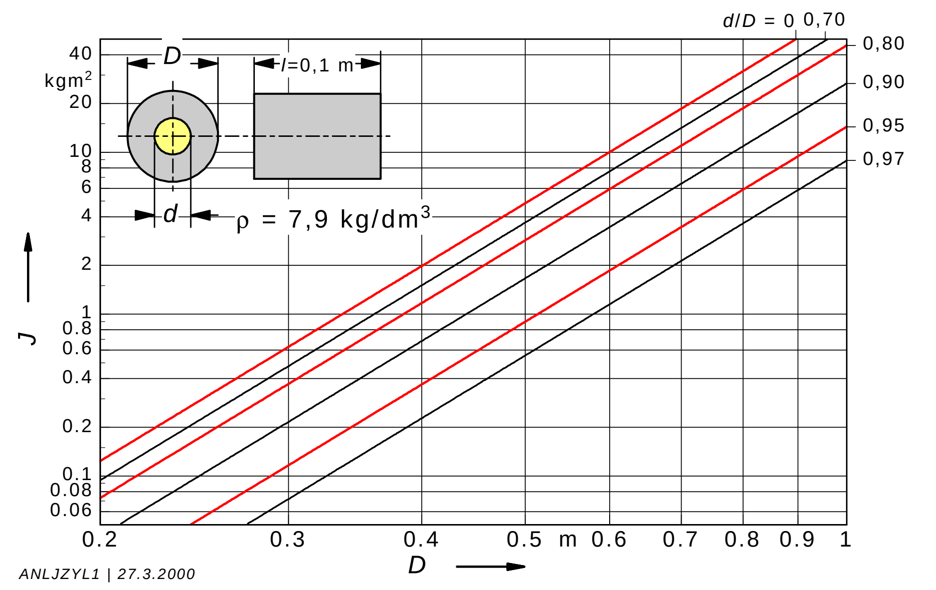

Fig. 26.3 Graph for the calculation of the mass moment of inertia J or solid or hollow steel in relation to a length of 0.1 m

27 Homogeneous bodies with simple geometric shapes

Body with mass *m* (kg)	Mass moment of inertia *J* about the *x*-axis	Mass moment of inertia *J* about the *y*-axis
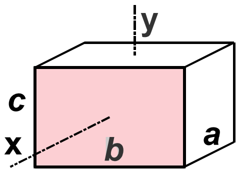	$J_x = m\frac{b^2 + c^2}{12}$	$J_y = m\frac{a^2 + b^2}{12}$
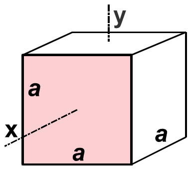	$J_x = m\frac{a^2}{6}$	$J_y = m\frac{a^2}{6}$
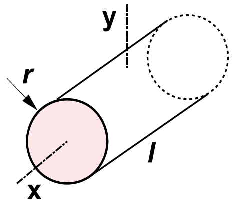	$J_x = m\frac{r^2}{2}$	$J_y = m\frac{3r^2 + l^2}{12}$
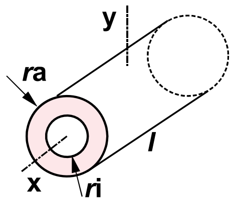	$J_x = m\frac{r_a^2 + r_i^2}{2}$	$J_y = m\frac{1}{4}\left(r_a^2 + r_i^2 + \frac{l^2}{3}\right)$
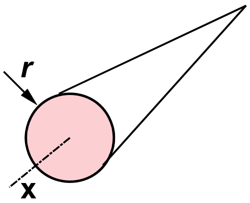	$J_x = m\frac{3r^2}{10}$	
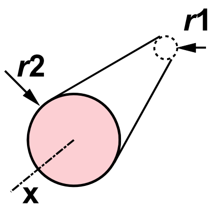	$J_x = \frac{3m}{10}\cdot\frac{r_2^5 - r_1^5}{r_2^3 - r_1^3}$	
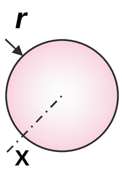	$J_x = m\frac{2r^2}{5}$	
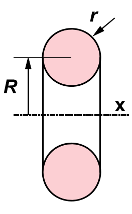	$J_x = m\left(R^2 + \frac{3}{4}r^2\right)$	

28 Experimental determination of the mass moment of inertia

The calculation of the mass moment of inertia is often not simple with complex geometric shapes and different densities. For this reason it is often determined experimentally. If the rotating body is available as a separate part, the method described in section 28.1 can be used. Where the machine has already been fully assembled, the bar pendulum test described in section 28.2 or the run-down test given in section 28.3 are possible methods.

28.1 Torsional pendulum

The rotating body (e.g. a rotor) is suspended from two or three parallel filaments and is rotated from rest, resulting in rotational oscillation about its vertical axis. The period is then measured – e.g. as $T = T_n/n$ for n oscillations.

$J_{rot} = \frac{m \cdot g \cdot r^2 \cdot T^2}{4 \cdot \pi^2 \cdot l}$	m	-	mass = weight in kg
	g	-	acceleration due to gravity (9.81 m/s²)
	r	-	radius in m
	T	-	time for one cycle in s
	l	-	filament length in m

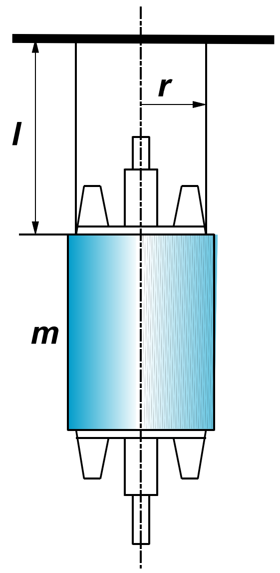

Fig. 28.1
Principle of the torsional pendulum test to determine the mass moment of inertia of a rotor

28.2 Bar pendulum

The machine with the unknown mass moment of inertia is coupled to a machine with a known mass moment of inertia. The entire system is then set in rotational oscillation by a bar pendulum and the period is determined (preferably by timing several cycles).

$J_x = m \cdot g \cdot e \cdot \frac{T^2}{4 \cdot \pi^2} - J_{mot} - J_P$	J_x	-	mass moment of inertia to be determined in kgm²
	J_{mot}	-	known mass moment of inertia in kgm²
	J_P	-	mass moment of inertia of the pendulum in kgm² $J_P = m_P \cdot e^2$
	m	-	mass (weight) of the pendulum in kg
	g	-	acceleration due to gravity (9.81 m/s²)
	e	-	distance from the pendulum's centre of gravity to
	the		axis of rotation in m
	T	-	oscillation period in s

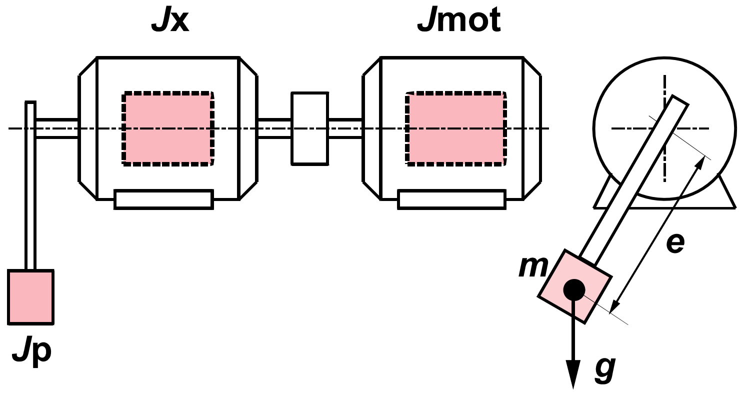

Fig. 28.2
Principle of the bar pendulum test to determine the mass moment of inertia of a rotor

28.3 Run-down test

This test assumes a relatively accurate knowledge of the no load friction losses V_{Rbg} of the drive; these will have been as part of the type test by the “summation-of-losses” method. Provided this value is known and the driven machinery can be uncoupled, a run-down curve can be plotted (speed as a function of time) using an oscillograph or – in the case of long run-down times – the curve can be plotted incrementally. Errors can be reduced if the speed can be increased by raising the frequency. The tangent shown in Fig. 28.3 should preferably not contact the curve at n = 0. The following equation is used to calculate the mass moment of inertia:

$J_x = \frac{91250 \cdot T_a \cdot V_{Rbg}}{n_a^2}$	J_x - mass moment of inertia to be determined in kgm² T_a - imaginary run-down time tangential section in s V_{Rbg} - friction losses in kW n_a - speed at the point of contact of the tangent in r/min

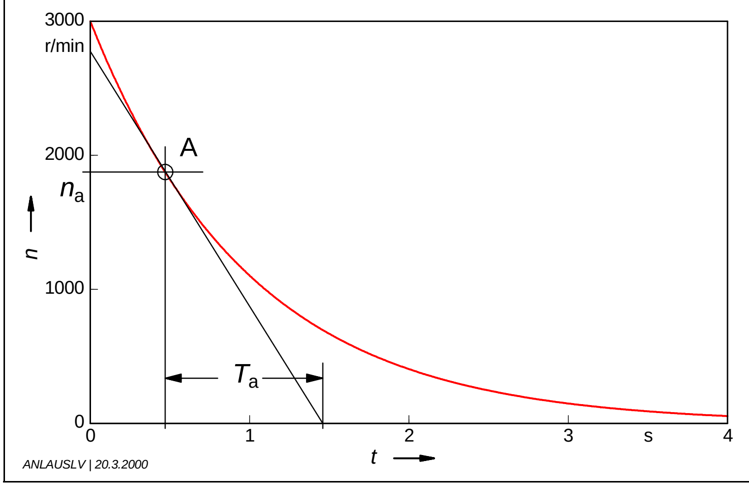

Fig. 28.3
Run-down test to determine the mass moment of inertia of an assembled machine
A - arbitrary point of contact of the tangent

29 Factor of inertia *FI*

The factor of inertia *FI* is the relationship between all masses driven by the motor converted to the motor speed, including the motor rotor's moment of inertia, to the moment of inertia of the motor rotor itself, hence:

$$FI = \frac{J_{\text{total}}}{J_{\text{rotor}}} = \frac{J_{\text{extern}} + J_{\text{rotor}}}{J_{\text{rotor}}}$$

Fig. 29 Geared motor in V1 mounting driving a cooling tower fan
Fan impeller diameter up to 3.4 m
Typical factors of inertia *FI* up to 30

30 Division of the torque according to the mass fractions

The acceleration torque developed by the motor is distributed linearly amongst the masses. The rule is primarily significant for the ***loading of series-connected power transmission components*** e.g. the gear unit.

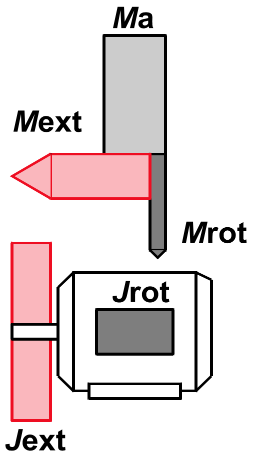

Fig. 30.1
Torque depends on mass

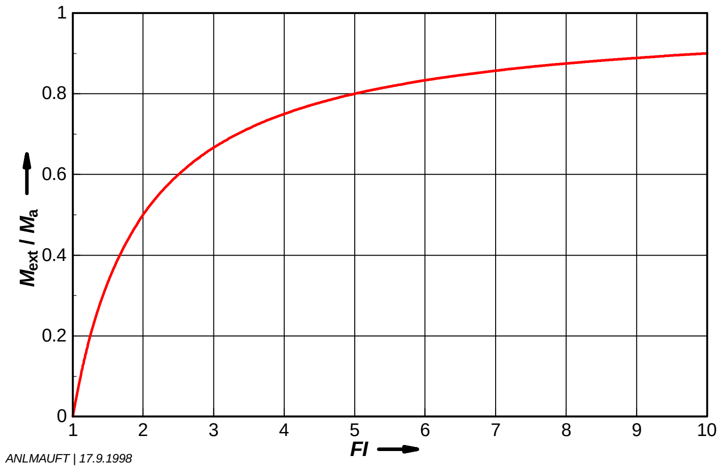

Fig. 30.2
External component of the torque

The proportion of the acceleration torque flowing out of the system is shown in Fig. 30.2; this is calculated from

$$\frac{M_{ext}}{M_a} = \frac{J_{ext}}{\Sigma J} = \frac{J_{rot} \cdot (FI - 1)}{J_{rot} \cdot FI} = \frac{FI - 1}{FI}$$

This examination makes it clear why the factor of inertia *FI* has a fundamental function in ***shock classification*** determination. The shock classification determines the ***service factor*** for choice of a gear unit. The following factors are decisive in the determination of the service factors for Danfoss Bauer gear units:

Shock classification	**I**	**II**	**III**
Factor of inertia	$FI \leq 1.3$	$1.3 < FI \leq 4$	$FI > 4$
Gear loading as a proportion of M_a as a proportion of M_N (approx.)	 $\leq 0.23\ M_a$ $\leq 0.5\ M_N$	 0.23 ... 0.75 M_a 0.5 ... 1.5 M_N	 $> 0.75\ M_a$ $> 1.5\ M_N$

31 Conversion of moving masses

The mass fractions of the power transmission components and of the driven machinery have to be converted to the speed of the rotor shaft according to their rotational or linear speed.

31.1 Rotation

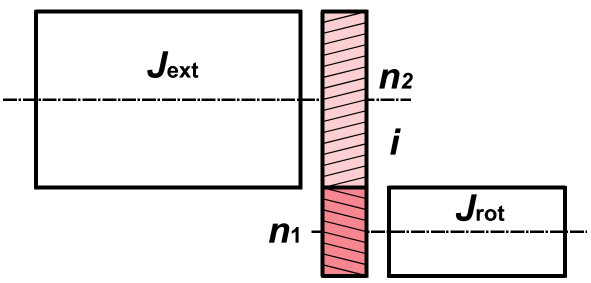

Fig. 31.1
Diagram of the conversion of a rotating mass to the speed of the rotor shaft

$$\Sigma J = J_{ext1} + J_{rot}$$

$$= \frac{J_{ext}}{\left(\frac{n_1}{n_2}\right)^2} + J_{rot} = \frac{J_{ext}}{i^2} + J_{rot}$$

31.2 Translation

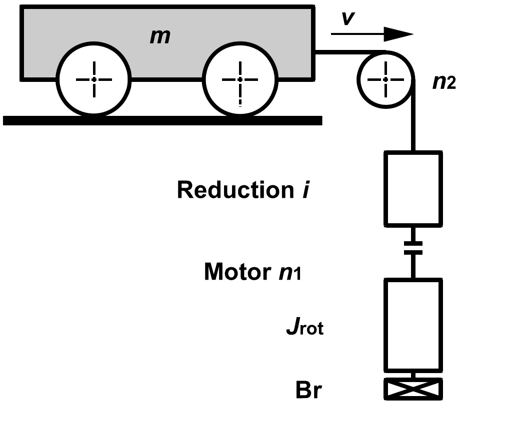

Fig. 31.2
Diagram of the conversion of a linearly moving mass to the speed of the rotor shaft

$$\Sigma J = J_{ext1} + J_{rot}$$

$$= 91{,}2 \cdot m \cdot \frac{v^2}{n_1^2} + J_{rot}$$

J	-	mass moment of inertia in kgm²
m	-	weight in kg
v	-	linear speed in m/s
n	-	rotational speed in r/min
i	-	gear reduction ratio

31.3 Linear motion as a tangent to the circle

The term "flywheel effect GD^2" previous common in the Technical Measurement System has not been adopted in the SI. The different units and the ***different definition must therefore be heeded in calculation that use the mass moment of inertia*** ***mr^2*****.**

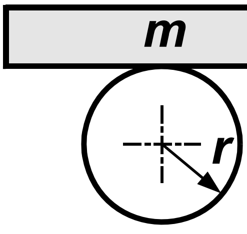

$$J = m \cdot r^2 = \frac{m \cdot d^2}{4}$$

m	-	mass in kg
d	-	diameter in m
r	-	radius in m

Fig. 31.3
Motion linear to the circle

Definition of mr^2 and GD^2

Fig. 31.4

Large portal crane as an example where linearly moving masses form the dominant loading component on the crane's travelling gear.

V MECHANICAL BRAKING

32 General

The number and relative proportion of electric motors assembled with a mechanical brake built onto or integrated into them to form a "brake motor" is growing steadily. This development is linked to the demand for rational and automatic manufacturing processes. Even the shortest times lost waiting for a motor and its driven machinery to run down are no longer acceptable in today's highly mechanized work processes which run to tightly fixed cycles. There is a demand for precise positioning of tools, workpieces and conveyed goods on mechanized production lines that is unaffected by external influences.

Mechanical brakes reduce principally the ***overtravel times*** and ***overtravel distances*** experienced with unbraked free-wheeling deceleration. It is therefore understandable that mechanical brakes have traditionally enjoyed great popularity for use with all types of ***hoists***.

In fact, a whole range of "electrical" or "dynamic" braking methods are available for pure injection braking, all of which are based on the retardation effect of a current-carrying or induced conductor in a magnetic field. This principle means that they are not exposed to mechanical friction, hence they are wear-free.

In spite of this clear benefit associated with maintenance-free electrical braking methods, the number of mechanical brakes in use indicate that they are still preferred.

This can be explained initially by technical and practical considerations. Electrical braking works "dynamically" only, i.e. when the motor is running down, and not "statically" when the motor is at rest. Furthermore, because they generally rely on an electricity supply system as the power source or power recipient, they are not generally recognized as "safety brakes" in terms of accident prevention regulations.

However, the explanation usually comes from different quarters. Whereas a "normal" electric motor configured for electrical braking can be turned into a "braked motor" by implementing special design, installation and control measures, i.e. through additional expenditure, the installation and connection to the mains of a motor built specifically as a brake motor are entirely "normal".

Designers and electrical engineers designing new driven machinery pass the problem of braking onto the supplier of the electric motor due to a justifiable tendency to simplify matters and to cut costs.

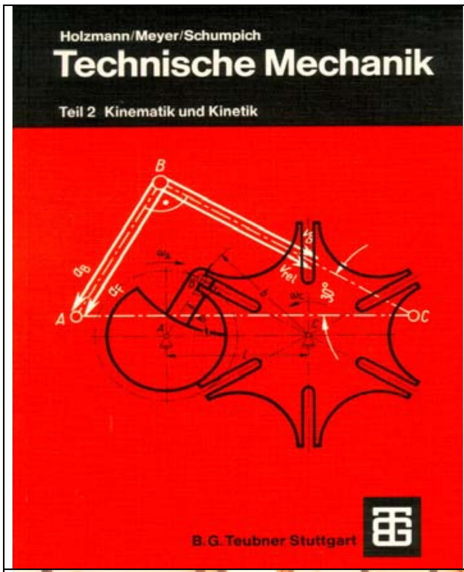

Fig. 32.1
Maltese cross on the title page of a well-known textbook on mechanics

Example mechanical solution for an indexing table

Fig. 32.2
Rotating table in a SCHENCK transport system operated by Lufthansa driven by a geared brake motor – example of the modern solution using an electrical drive

Fig. 32.3
Geared brake motors on the lifting gear, slewing gear and travelling gear of a tower slewing crane

Possible applications of geared brake motors

33 Braking systems

Mechanical brakes can be classified according their constructional elements which, simplified, operate on three main principles:

- ☐ Friction
- ☐ Braking force
- ☐ Releasing force

33.1 Classification of braking systems

The schematic diagram in Fig. 33.1 shows the main constructional elements of mechanical brakes. Many combinations are possible from the basic elements shown; these combinations are also found in practice.

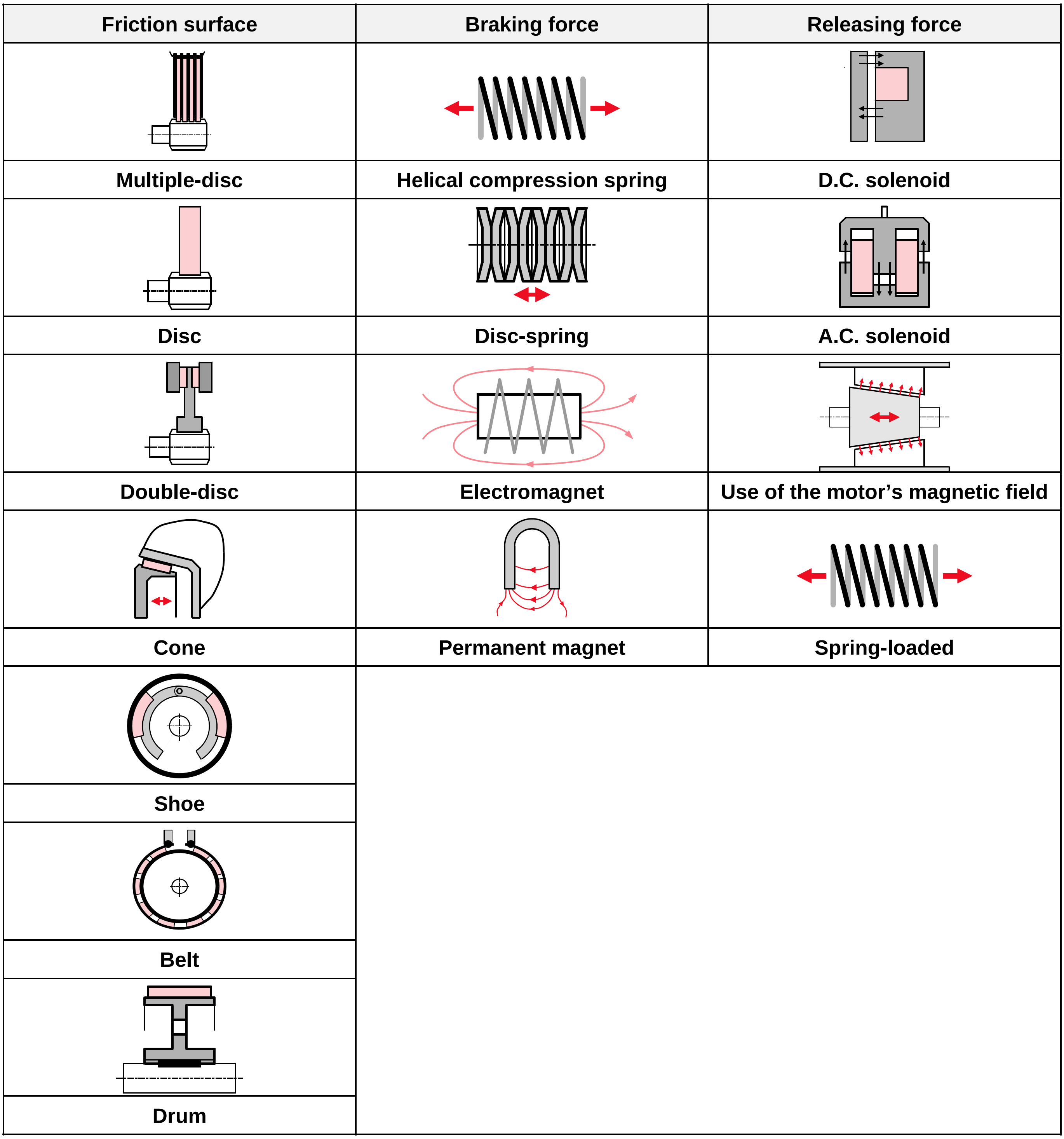

Fig. 33.1 Classification of braking systems

33.2 Spring-loaded brake or magnetic brake

If the braking force is generated by one or more springs, the brake is termed a spring-loaded brake.
Because this type of system will also result in a braking effect in the event of an inadvertent power loss, it is recognized as a ***safety brake*** for the purpose of accident prevention regulations. The technical regulations for elevators governing the type of elevator in question in terms of the rating and design of the brake must also be heeded. If, on the other hand, the braking force is supplied by an electromagnet that relies on mains electricity for its operation, this is termed a magnetic brake. This cannot, in general, be regarded as a safety brake. Since the spring-loaded brake requires an electromagnet to release the brake, the terms "spring-loaded brake" and "magnetic brake" are commonly used interchangeably.

34 Built-on or built-in

The design solutions for brake motors also vary greatly in terms of the choice of mounting arrangements. On the one hand, the braking systems of brake motors are so fully integrated with the drive motor as to form a ***constructional unit*** such that they can scarcely be distinguished from normal motors in their outward appearance. The brake is integrated into components of the motor to form a unit and must therefore be termed a ***built-in brake***.

Fig. 34.1 Geared motors with a "built-in brake" or a built-on brake on the end shield" cannot be distinguished in their outward appearance

With other solutions, the brake is designed and fitted as a ***totally separate unit*** and mounted onto the reinforced fan cowl or onto the end shield of the motor in the form of a ***built-on brake***.

Fig. 34.2 Geared motor with "built-on brake" on the fan cowl

Including the brake in the overall design of the motor so that both share the same casing would seem sensible from an economic and structural point of view. Furthermore, the possibility of exploiting the magnetic field present in the motor to release the brake rather than provide the brake with its own magnetic system would seem attractive. This basic principle opens up a whole range of solutions with interesting technologies. Besides, these solutions are often more cost-effective thanks to the structural fusion of the motor and brake. However, this fusion also depends on the functions of the motor and brake being fully dependent on each other. Maintenance work and repairs on the brake nearly always require intervention in the motor involving the complete shutdown of the drive; damage to the brake often results inevitably in serious consequential damage to the motor. ***All mechanical brakes work on the principle of friction; it is therefore inevitable that they are subject to constant wear and have generally shorter maintenance periods and service lives than the virtually wear-free electric motor***.

Brake motors with built-on brakes are generally less aesthetically attractive than "motors with integrated brakes"; the separate encapsulation of the braking system in its own casing, together with the fact that a separate magnetic system must be provided, calls for greater expenditure. It is true that full separation of the functions makes maintenance, repair and stocking of reserve wear parts simpler. It will even be possible with some applications to overhaul the brake without halting operations or to run the motor temporarily without the brake. This principle also applies to solutions where the brake is designed to be "self-sufficient" and is mounted under the fan cowl onto the motor's end shield.
The built-on brake therefore represents a dependable component for all applications that demand high reliability and the shortest possible downtimes.
Further benefits of the built-on principle are described in detail in section 46. Various examples of the built-on principle and their technical benefits and drawbacks are given in the sequence of figures 34.3 below.

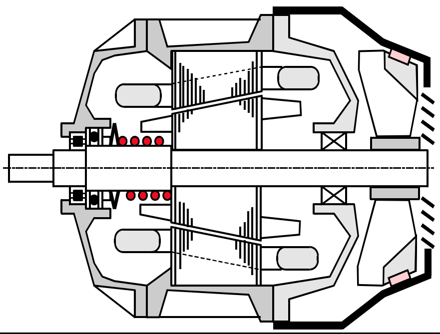	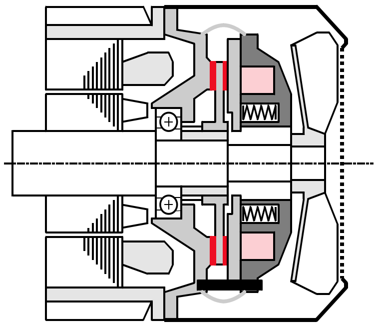	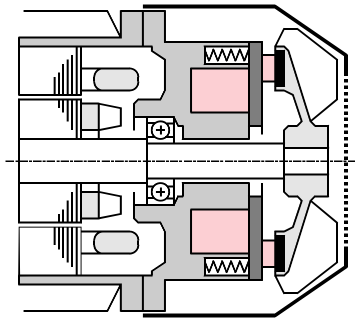
Fig. 34.3.1 Built-in brake with cone rotor **Benefits:** Exploitation of the motor's magnetic field, compact design **Drawbacks:** Axial rotor movement,large inertial forces, function of motor and brake fully integrated	Fig. 34.3.2 Built-in brake with D.C. solenoid **Benefits:** Short overall length **Drawbacks:** Fixed motor/brake assignment, function of motor and brake largely integrated, impaired access to the friction lining	Fig. 34.3.3 Built-in brake with D.C. solenoid **Benefits:** Short overall length, easy access to the friction lining **Drawbacks:** Fixed motor/brake assignment, function of motor and brake largely integrated
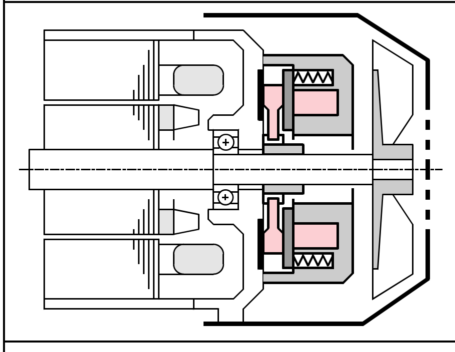	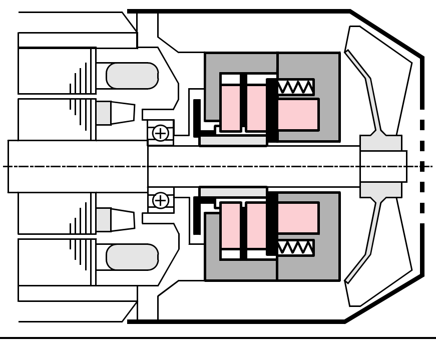	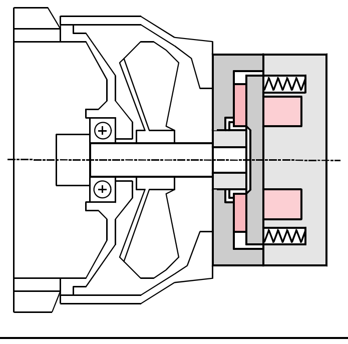
Fig. 34.3.4 Built-on brake on the end shield **Benefits:** Partial separation of the function of motor and brake, relatively short overall length **Drawbacks:** Fan and fan cowl must be removed to access the friction lining	Fig. 34.3.5 Built-on brake on the end shield **Benefits:** Total separation of the function and encapsulation of motor and brake **Drawbacks:** Fan and fan cowl must be removed to access the friction lining; sufficient clearance required to disassemble the fan cowl	Fig. 34.3.6 Built-on brake on the fan cowl **Benefits:** Total separation of the function and encapsulation of motor and brake, motor can be operated in emergency mode, brake can be easily replaced **Drawbacks:** Slightly more space required – see Fig. 34.4

The increased axial space required for a built-on brake (Figs 34.2 and 34.3.6) over a built-in brake (Fig. 34.3.3) looks worse than it actually is.
Fig. 34.4 shows the length increase over the corresponding design without a brake based on a comparison between Danfoss Bauer built-on brakes and units designed as built-in brakes as shown in Fig. 34.3.3.

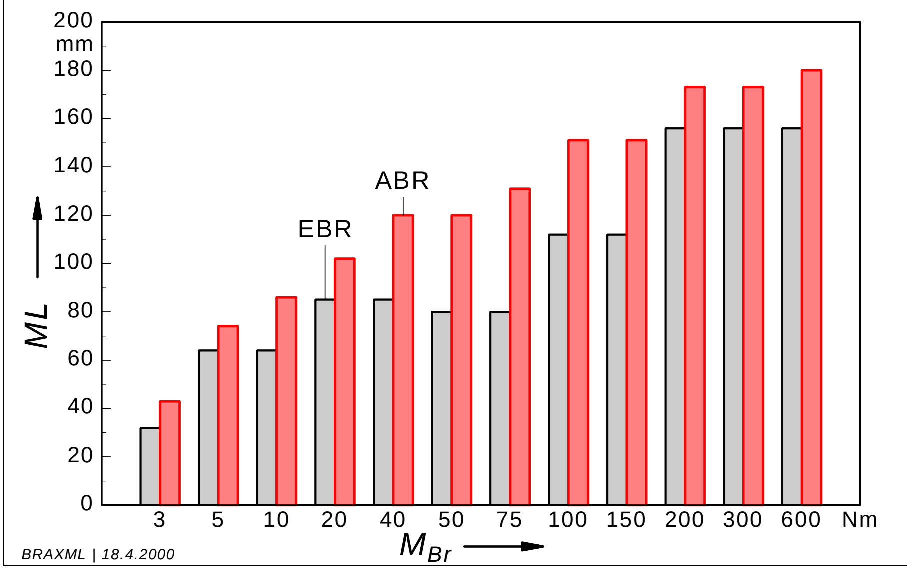

Fig. 34.4
Length increases (ML) over the corresponding motor without a brake for
built-in brakes (EBR)
and
built-on brakes (ABR)
as a function of the nominal braking torque (M_{BR}) of the brake

35 Example designs

The following collection comprising ten examples includes designs that are no longer offered. However, the designs shown have been supplied in very large numbers of units and are still in use. These tried and tested brakes have been included since this book is also aimed at the ***users*** of Danfoss Bauer drives.

35.1 Series E003B single-disc spring-loaded brake with D.C. solenoid release, mounted onto the end shield

The solenoid casing (5) contains the encapsulated coil. The thrust plate (2) is pressed axially against the brake disc (4) by the springs (3). The brake disc is supported in the peripheral direction by the bolts (10). When energized, the thrust plate is attracted by the solenoid casing against the force of the springs. The brake disc (4) can move axially from its position on the driver (1) which is secured onto the extended shaft end of the electric motor.
The electromagnet is sufficiently dimensioned to be able to accommodate an increased air gap provided the degree of wear remains within normal limits. There is no means to make adjustments. The braking torque can be adjusted in steps by the number of springs.
The spring-loaded brake can also be designed with manual release (HL) upon request so that the brakes can be released manually in the event of a power loss. A second shaft end (2. WE) enables manual turning in such circumstances. The brake is mounted externally onto the motor's end shield but can be broken down into three main parts.
The fan cowl and fan must be removed before the friction disc can be replaced; a disassembly clearance in the axial direction roughly equivalent to the length of the fan cowl must be provided for this.

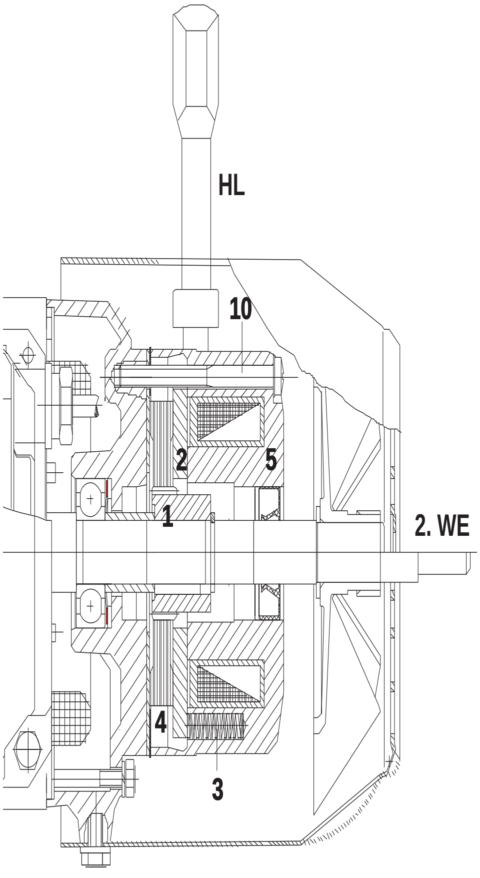

Fig. 35.1 Single-disc spring-loaded brake with D.C. solenoid release
Type series E003B

35.2 Series Z008A double-disc spring-loaded brake with D.C. solenoid release, mounted onto the end shield

The brake is secured externally to the motor's end shield by the mounting bolts (A); the brake is held together by the internal securing bolts (B) and can be held as a complete component in stock.
The fan cowl and fan must be removed before the friction disc can be replaced; a disassembly clearance roughly equivalent to the length of the fan cowl is provided for this in the axial direction.

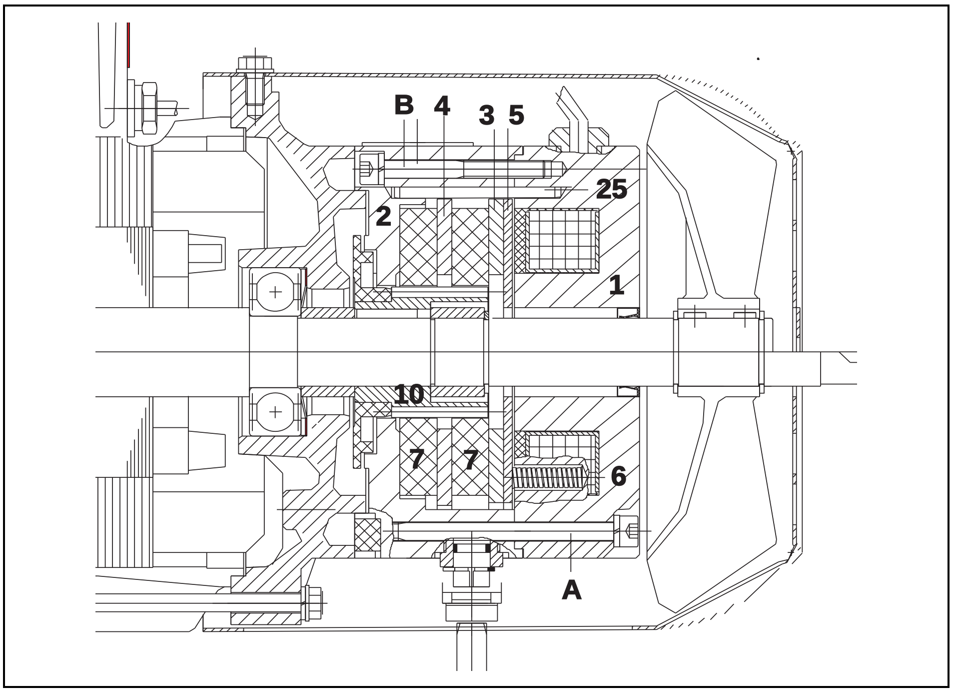

Fig. 35.2.1 Double-disc spring-loaded brake with D.C. solenoid release Type series Z008A

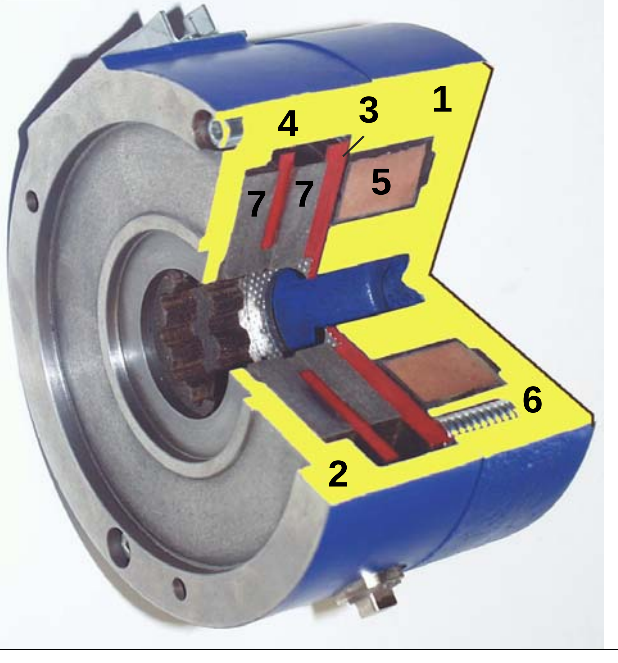

Fig. 35.2.2 Perspective view of a double-disc brake

1	Solenoid casing	5	Solenoid
2	Centering flange	6	Springs
3	Brake plate	7	Brake discs
4	Friction plate	10	Driver

35.3 Series E 025A single-disc spring-loaded brake mounted onto the fan cowl

The solenoid casing (1) contains the encapsulated coil. The casing is permanently bonded to the centering flange (2). The coated magnetic disc (5) and the brake plate (3) are pressed axially onto the brake disc (7) by the springs (6). The springs are supported in the peripheral direction by the spiral roll pins (25). When energized, the magnetic disc and brake plate are attracted by the solenoid casing against the force of the springs. The brake disc (7) and the friction plate (4) can move axially from their position on the driver (10) which is secured onto the extended shaft end of the electric motor.

There is no means to make corrections. The braking torque can be adjusted in steps by the number of springs.

Manual release (HL) and a second shaft end (2. WE) are options that are available upon request.

The brake is secured externally to the motor's fan cowl by the mounting bolts (A); the brake is held together by the internal securing bolts (B) and can be held as a complete component in stock.

The fan cowl and fan does not have to be removed to replace the friction disc; additional axial disassembly clearance is not necessary.

The built-in rectifier and the terminals are housed in the motor terminal box on the version shown here; the connection is provided by an easily accessible external cable.

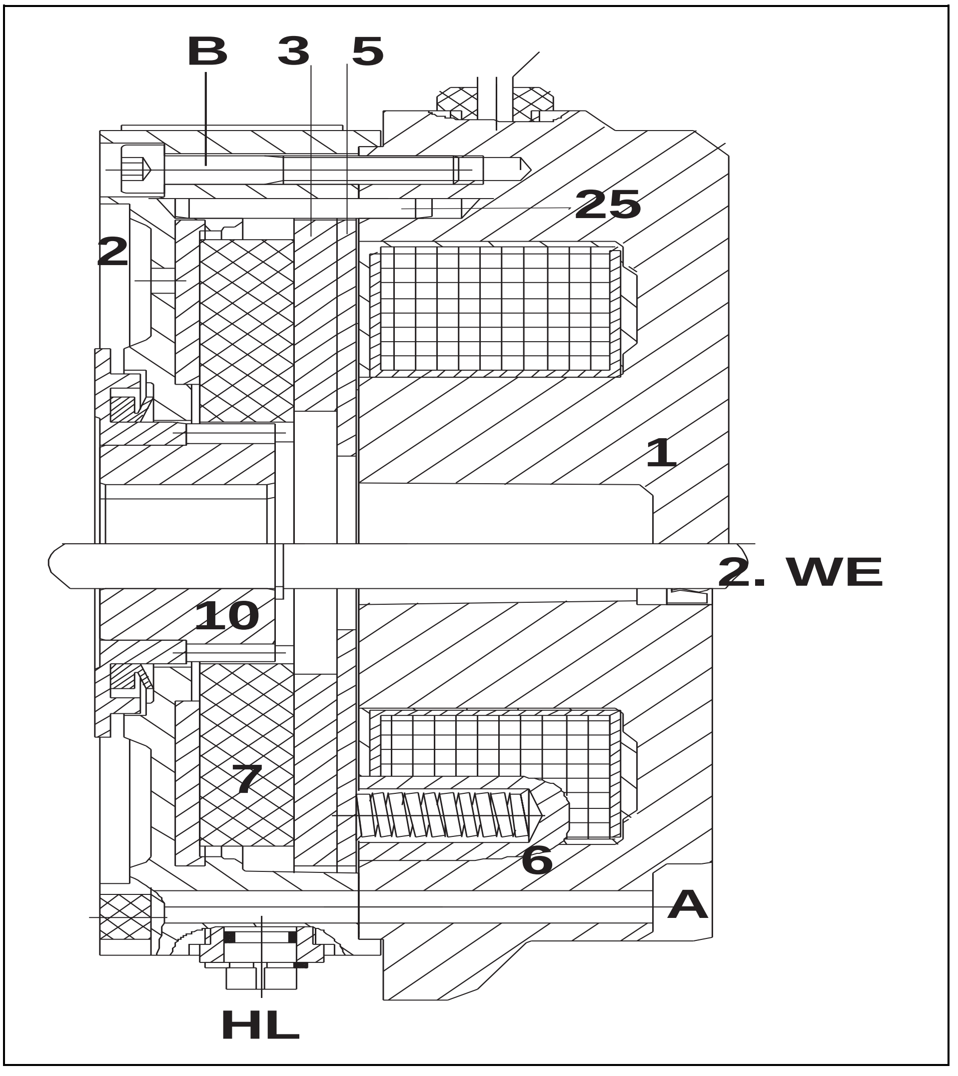

Fig. 35.3 Single-disc spring-loaded brake with D.C. solenoid release
Type series E025A; connected via a cable on the motor terminal box

35.4 Series Z025A double-disc spring-loaded brake with D.C. solenoid release, mounted onto the fan cowl

The solenoid casing (1) contains the encapsulated coil. The casing is permanently bonded to the centering flange (2). The coated magnetic disc (5) and the brake plate (3) are pressed axially onto the brake discs (7) and friction plate (4) by the springs (6). The springs are supported in the peripheral direction by the spiral roll pins (25). When energized, the magnetic disc and brake plate are attracted by the solenoid casing against the force of the springs. The brake discs (7) and the friction plate (4) can move axially from their position on the driver (10) which is secured onto the extended shaft end of the electric motor. Manual release (HL) and a second shaft end (2. WE) are options that are available upon request. The electromagnet is sufficiently dimensioned to be able to accommodate an increased air gap provided the degree of wear remains within normal limits.

There is no means to make corrections. The braking torque can be adjusted in steps by the number of springs.

The brake is secured externally to the motor's fan cowl by the mounting bolts (A); the brake is held together by the internal securing bolts (B) and can be held as a complete component in stock.

The fan cowl and fan does not have to be removed to replace the friction disc; additional axial disassembly clearance is not necessary.

The built-in rectifier and the terminals are housed in the built-on terminal box (KK) on the version shown here; the external connection is routed directly to this terminal box.

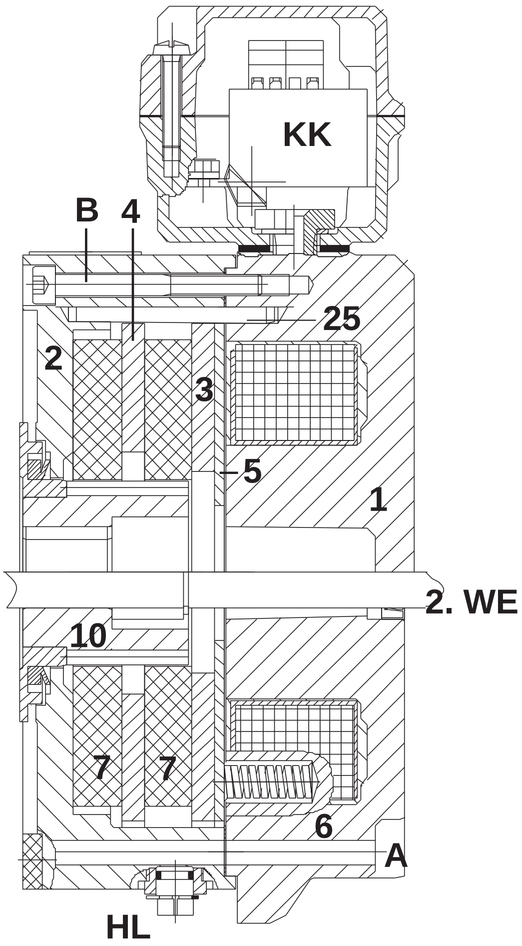

Fig. 35.4 Double-disc spring-loaded brake with D.C. solenoid release
Type series Z025A; connected to the brake terminal box

35.5 Series ABR single-disc spring-loaded brake with D.C. solenoid release, mounted onto the fan cowl

This design contains the same active braking components as the series GBR design, however it has been greatly simplified by, for example, not including a dedicated terminal box and therefore represents greater cost-effectiveness for the same working capacity.

The solenoid casing (1) contains the encapsulated coil; an anti-locking plate is riveted in place (4). The casing is permanently bonded to the centering flange (2). The thrust plate (3) is pressed axially onto the brake disc (8) by the springs (5). The brake disc is supported in the peripheral direction by two cylindrical pins (12). When energized, the thrust plate is attracted by the solenoid casing against the force of the springs. The brake disc can move axially from its position on the driver (7) which is secured onto the second shaft end of the electric motor.

The brake is secured externally to the motor's fan cowl by the mounting bolts; the brake is held together by the internal securing bolts (13) and can be held as a complete component in stock.

There is no means to make corrections. The braking torque can be adjusted in steps by the number of springs.

The fan cowl and fan do not have to be removed to replace the friction disc; additional axial clearance is not necessary.

The built-in rectifier and the terminals are housed in the motor terminal box.

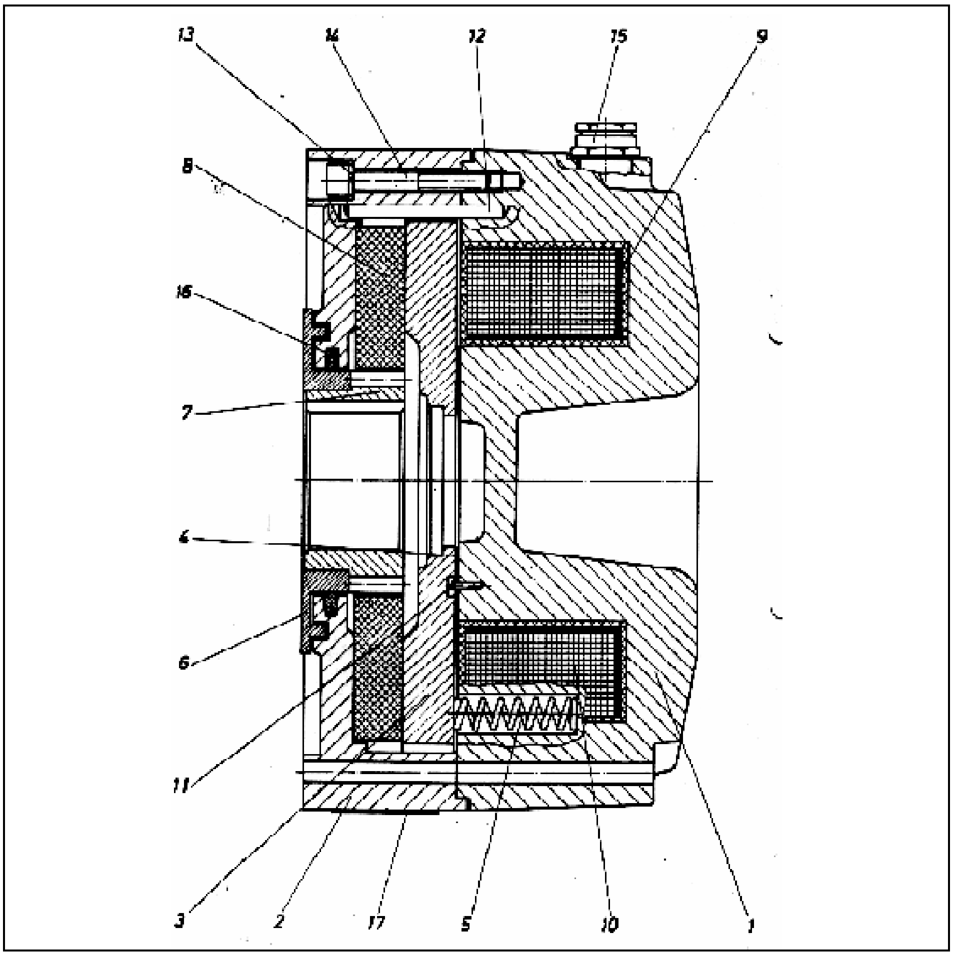

Fig. 35.5 Single-disc spring-loaded brake with D.C. solenoid release
Type series ABR

35.6 Series FBR single-disc spring-loaded brake with A.C. solenoid release, mounted onto the fan cowl

The brake pressure of the set of disc springs (35) is transmitted to the brake disc (9) by the clamping bolt (11) and the clamping disc (2). The braking force developed by friction on the two lateral plane surfaces of the brake disc provides a braking torque via the rectangular driver (8) sitting on the second shaft end of the motor rotor. When the brake is released, the A.C. solenoid (43) attracts its armature and the roller yoke (4) and the chamfered lever (5) moves the clamping bolt (11) axially against the pressure of the spring set (35) and thus releases the clamping disc (2) and the friction disc (9).
The fan cowl and fan do not have to be removed to replace the friction disc; additional axial clearance is not necessary.
The solenoid release does not require a rectifier; it is connected in parallel to the motor terminals or to the control voltage.

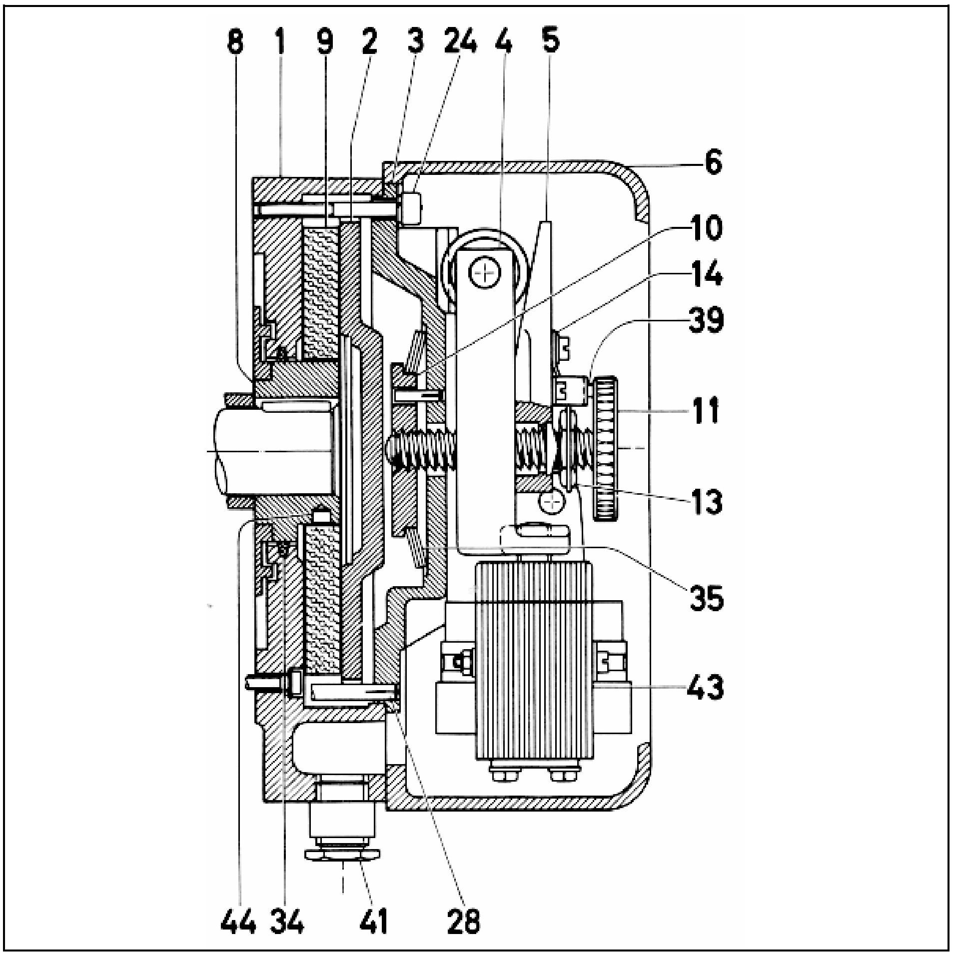

Fig. 35.6 Single-disc spring-loaded brake with A.C. solenoid release
Type series FBR

35.7 Cone spring-loaded brake released by the motor's magnetic field, integrated into the motor

A magnetically permeable cup (1) is attracted axially by the leakage field from the end of the normal electric motor. The cup is riveted in place by three pins (2) offset on the periphery; these can move axially in the end shield (3) and in turn bear the brake cone (4) outside the motor frame. Under braking, the spring (5) presses the brake cone (4) and its friction lining (6) into the internal cone of the fan impeller (7).
The fan impeller (7) and be adjusted axially by a ring nut (8), thus adjusting the degree of wear on the friction lining (6).

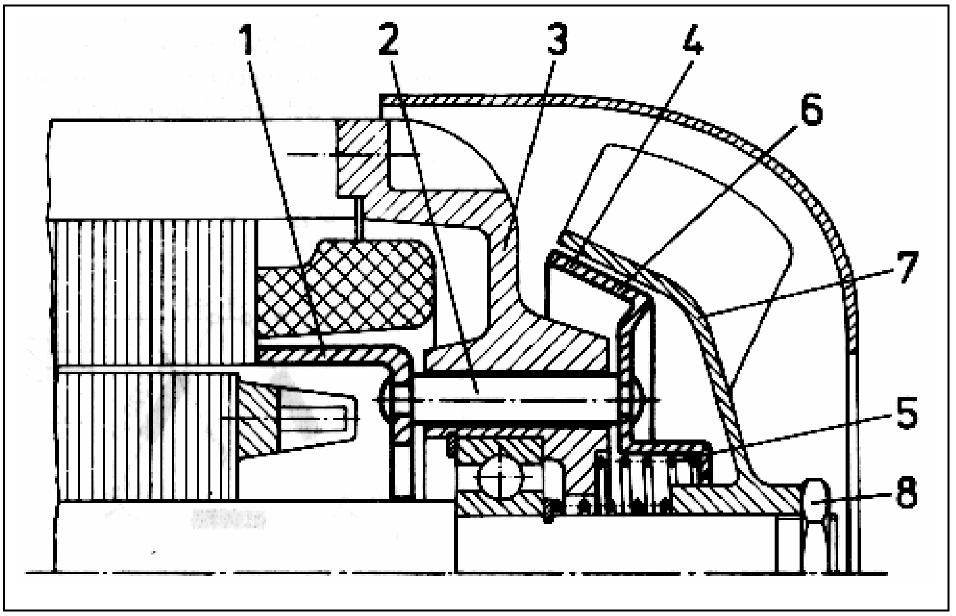

Fig. 35.7 Cone spring-loaded brake released by the leakage field of the electric motor

35.8 Series 75 (BINDER) shoe spring-loaded brake with A.C. solenoid release mounted on the fan cowl

The brake drum (1) is bell-shaped and secured by a keyway and key onto the extended shaft end of the rotor. The two limbs (3) of the internal shoe brake are mounted on a pin (2) so that they can swivel. They bear the friction shoes (4) made of high-grade friction material on their outer diameter; the limbs themselves are made from electrical sheet, thereby forming the magnetic circuit for the solenoid release (5). Under braking, the spring (6) presses the two friction shoes against the inside of the brake drum. When the brake is released, the A.C. solenoid (5) attracts the two limbs (3) and thus releases the brake drum.

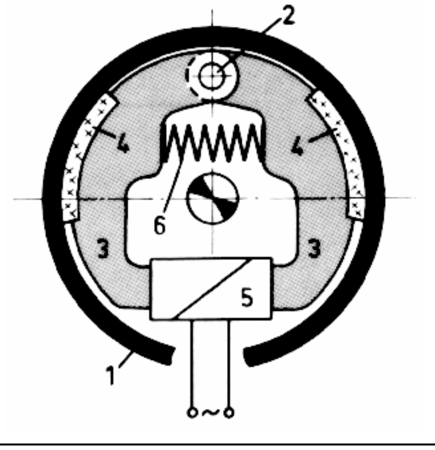

Fig. 35.8 Principle of a shoe spring-loaded brake with A.C. solenoid release; type series 75 (BINDER)

35.9 Series 71/72 (BINDER) multiple-disc spring-loaded brake with D.C. solenoid release, mounted onto the fan cowl

The solenoid casing (1.1) of the multiple-disc brake contains the encapsulated coil (1.2) and is bonded to the toothed ring (5) and mating flange (16) by bolts (8). The armature (4.1), mounted on bushes (7) between the solenoid casing and toothed ring, is released when the coil is de-energized. The springs (11) press on the disc set via the collar pins (4.2). When the coil is energized, the armature is magnetically attracted against the spring pressure, thereby releasing the discs, i.e. the brake is released.

The disc set comprises externally-toothed steel plates (19) – which are prevented from rotating by the toothed ring (5), the bolts (8) and the mating flange (6), although they can be displaced axially – and the internally toothed friction plates (18). The plates are arranged alternately. The number of steel plates is always one more than the number of friction plates in the set. The friction plates are made of a special material and their teeth engage with those of the driver (20). The driver is mounted on the rotor shaft. If these perfectly plane steel and friction plates are pressed together by the spring force via the armature, a braking torque is produced and transmitted through the mating flange, toothed ring, steel plates and friction plates. No outward pressure at all is produced in the axial direction.

Additional split springs (19.1) and disc springs (23) are fitted to damp vibrations on larger brakes.

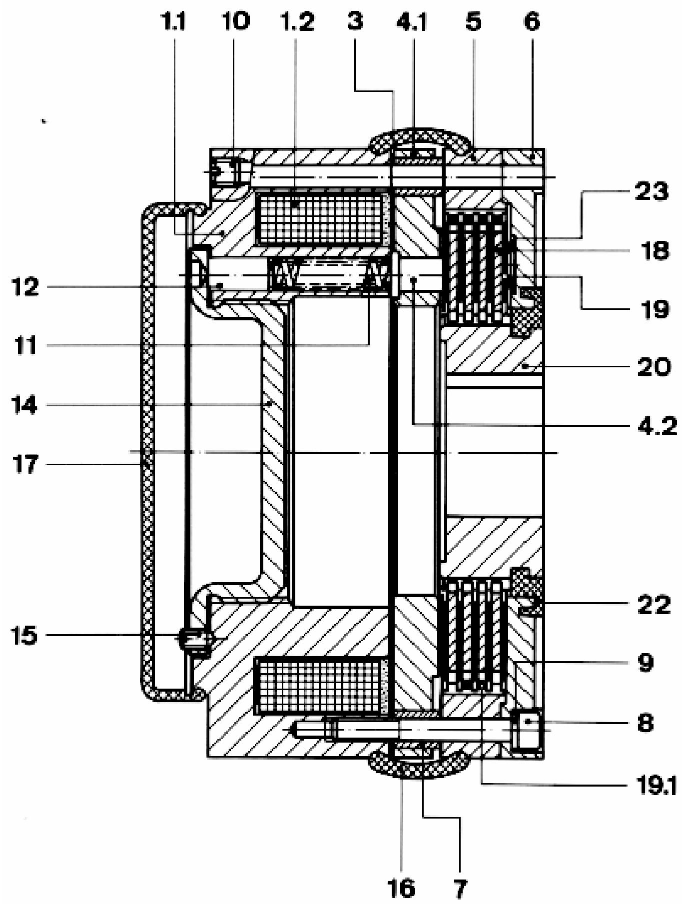

Fig. 35.9 Multiple-disc spring-loaded brake with D.C. solenoid release; type series 71/72 (BINDER)

35.10 Series 73 (BINDER) single-disc spring-loaded brake with three-phase solenoid release

The magnetic system (1) with its yoke and coils is mounted on the hexagon bolts (6). It forms the fixed part of the brake together with the armature (2) and the ring (3). The ring (3) and magnetic system (1) are held apart by the springs (5). The friction disc (4) is axially movable on the driver (10) and together they form the rotating part of the brake via a keyed rotary connection. When the brake is released, the magnetic system (1) attracts the armature (2), thus releasing the friction disc (4). Under braking, the springs (8) press the armature (2) against the friction disc (4) and the end shield (11).
The two auxiliary bolts (7) are removed once the unit is attached.
The three-phase magnetic system can be connected to the motor terminals.
The fan cowl and fan must be removed before the friction disc can be replaced; a disassembly clearance roughly equivalent to the length of the fan cowl is provided for this in the axial direction.

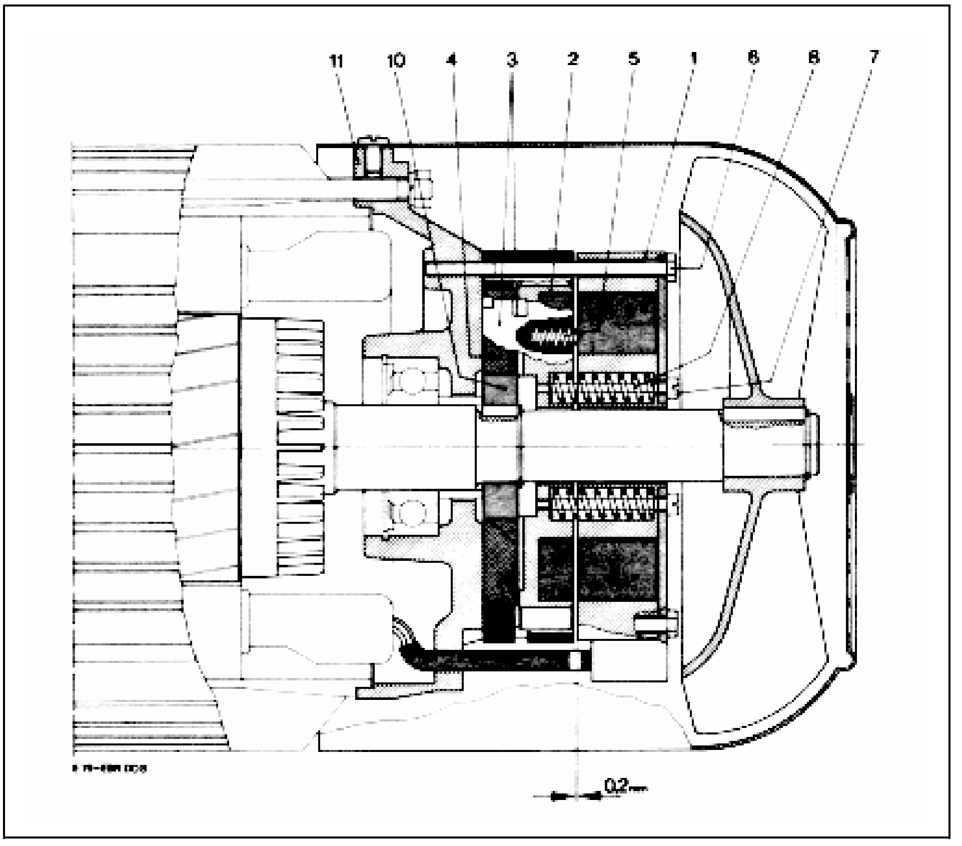

Fig. 35.10 Single-disc spring-loaded brake with three-phase solenoid release, mounted on the end shield; type series 73 (BINDER)

36 Electrical supply to the solenoid

Whereas the decision to use D.C. or A.C. to energize the solenoid release will have been made with the choice of the braking system, one will be free to choose the level of voltage and circuit configuration to a certain degree. The following sections provides a few basic notes on this subject.

36.1 One rated voltage in star or delta connection

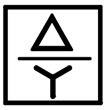

The simplest solution is to select the same supply voltage as the voltage for the associated electric motor so that the solenoid release coil can simply be connected ***in parallel across two of the motor terminals***. The connection diagram also applies to star-delta (Y-Δ) starting. The switching delay between the star and delta switch positions must be kept as short as possible so that the brake is not applied.

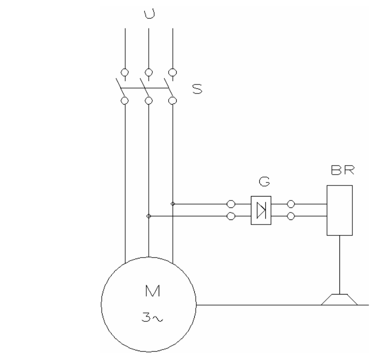

Fig. 36.1.1
Motor (M) with brake (BR) and rectifier (G) for the same rated voltage (U) and a joint switch (S)

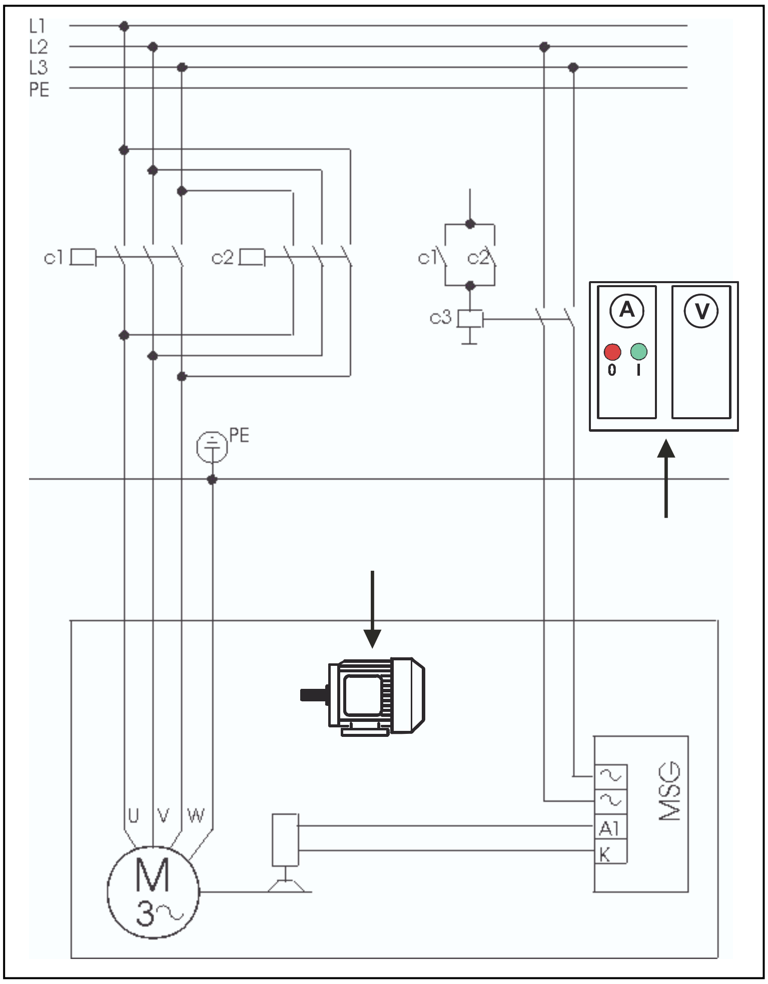

Fig. 36.1.2 Example of the complete connection diagram for a single-speed three-phase motor with separate brake actuation (Danfoss Bauer wiring diagram A 311.1000-18)

36.2 Dual voltage winding in the ratio 1:1.73

Δ/Y

The solenoid release coil is connected in parallel across two terminals of a phase winding and always carries the ***phase voltage*** as shown in Fig. 36.2 regardless of the mains voltage. In star connection, the motor winding acts as an autotransformer; the minor neutral point offset due to the small coil current has practically no effect on the characteristics of the motor.

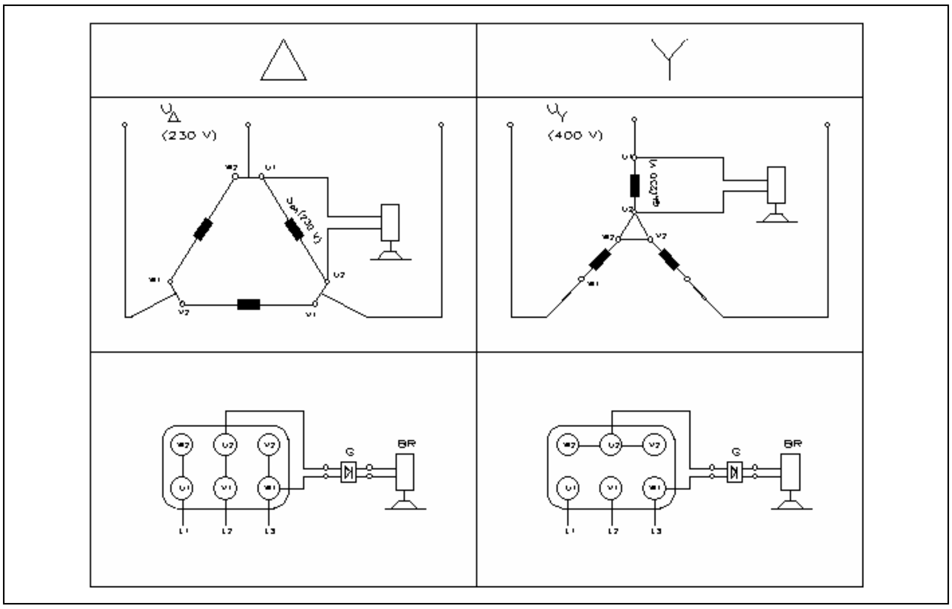

Fig. 36.2 Connection of the A.C. input in parallel across a phase winding on dual voltage motors in delta and star connection

36.3 Dual voltage winding in the ratio 1:2

ΔΔ/Δ

The solenoid release coil is connected in parallel across half of a phase winding and always carries ***half*** the higher "phase voltage" in both connection types regardless of the mains voltage. The motor winding acts as an autotransformer; the minor neutral point offset due to the small coil current has practically no effect on the characteristics of the motor.

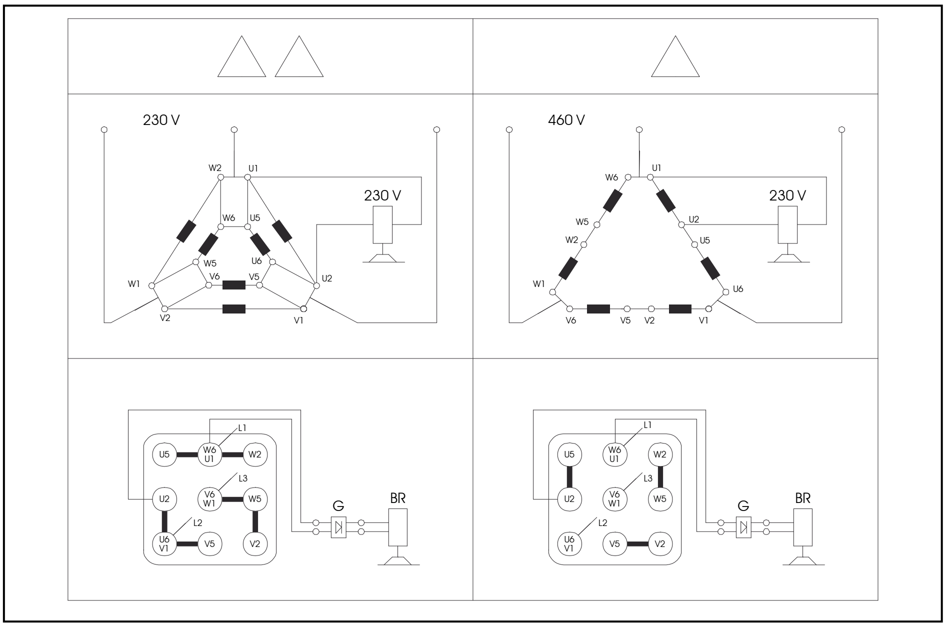

Fig. 36.3 Connection of the A.C. input in parallel across half a phase winding on dual voltage motors in double delta/delta connection

36.4 Pole-changing: Dahlander connection or two separate windings

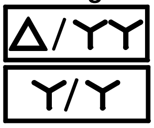

In many cases it is advisable to connect the rectifier input to the ***control voltage*** rather than to the motor terminal board. This applies especially to motors with an abnormal rated voltage, with a pole-changing winding, with frequency control or with starting devices.
The brake should now be connected to the pole-changing switch using special ***auxiliary contacts*** and not to the motor terminal board.

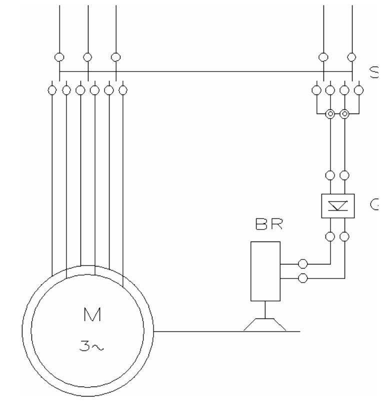

Fig. 36.4.1
Connection of the A.C. input (G) for a brake (BR) on pole-changing motors

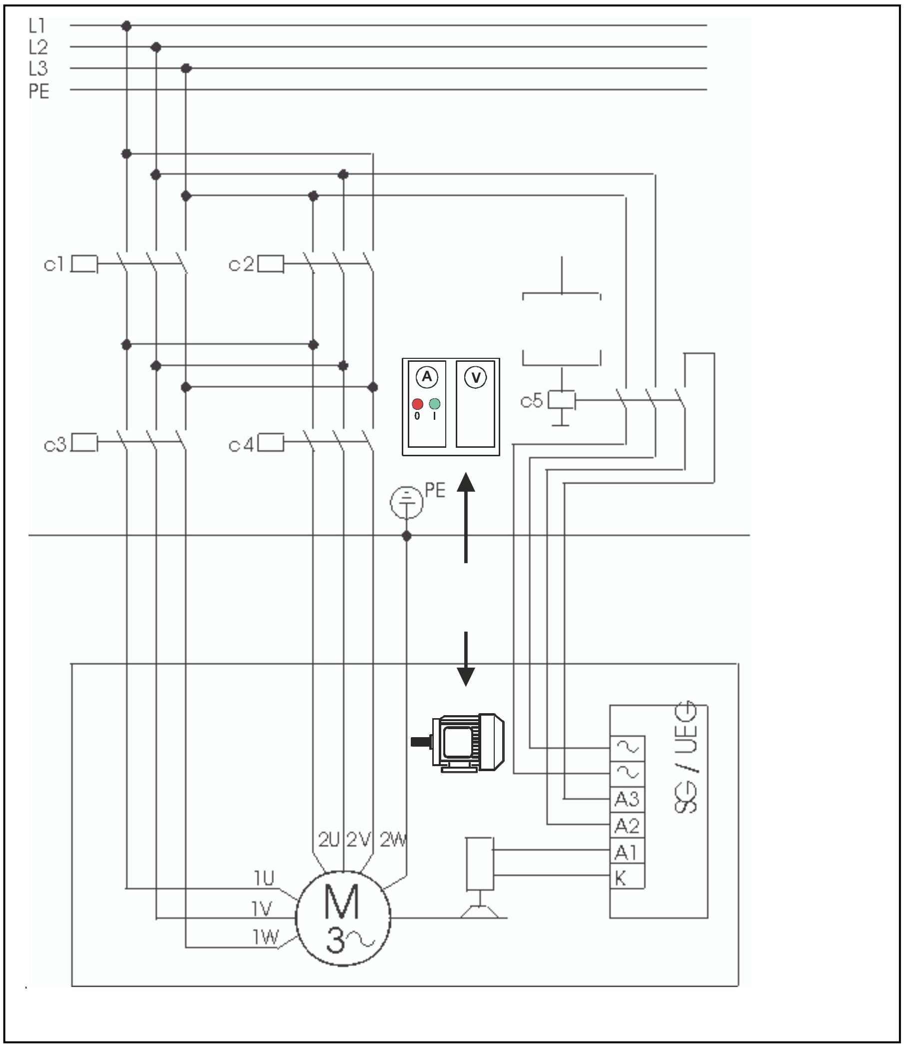

Fig. 36.4.2 Example of the complete connection diagram for a pole-changing three-phase motor with separate brake actuation; with a brake in the solenoid circuit on the A.C. side; (Danfoss Bauer wiring diagram A 311.1000-07)

36.5 Starting devices to reduce the terminal voltage

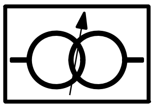

Where primary starters, starting transformers, soft starters etc. are used, the circuit configuration must be designed such that the brake receives the ***full rated voltage*** in the very first starter position.

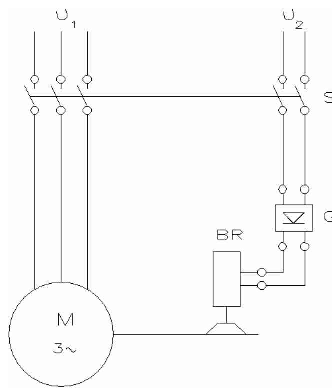

Fig. 36.5
Connection of the A.C. input (G) of a brake (BR) to the control mains U_2

The motor receives the reduced voltage U_1 in the starting step

36.6 Operation from an inverter with variable frequency

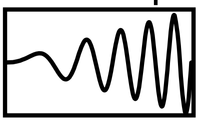

The brake must be connected to the ***control mains*** if an inverter is used.

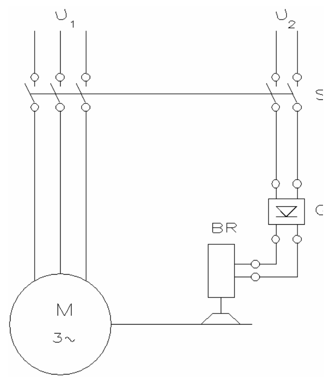

Fig. 36.6.1
Connection of the A.C. input (G) of a brake (BR) to the control mains U_2

The brake is supplied with a constant voltage and frequency regardless of the motor

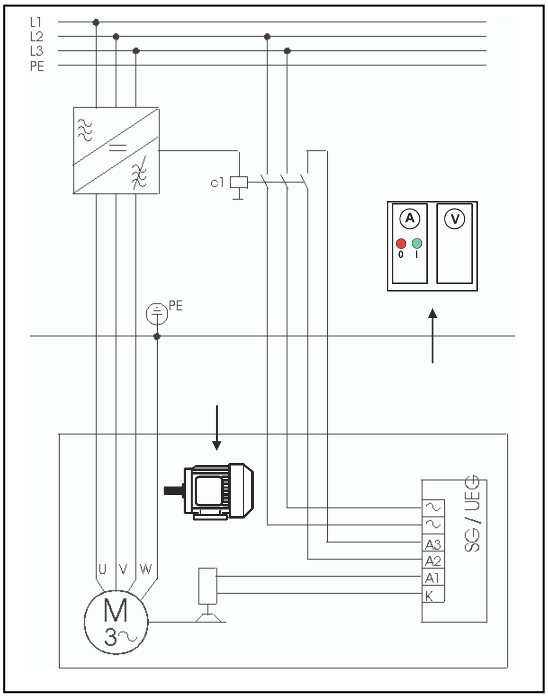

Fig. 36.6.2
Example of the complete connection diagram for an inverter-fed three-phase motor with separate brake actuation; with a brake in the solenoid circuit on the A.C. side (Danfoss Bauer wiring diagram A 311.1000-08)

36.7 Sample cases and their preferred solutions

The following tables contain tried and tested suggestions and circuit configurations.

36.7.1 Motors with a fixed rated voltage

Motor design	Connection	Solenoid release fed with		
		Motor voltage (e.g. 400 V)	Main star voltage (e.g. 230 V)	Control voltage (e.g. 230 V)
		U2 = U1	U2 = U1/1.73	U2 < U1
Fixed speed	Δ / Y	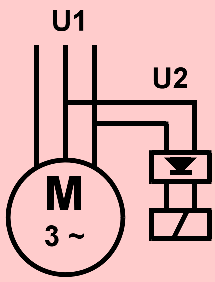	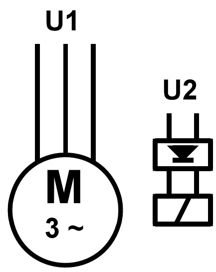	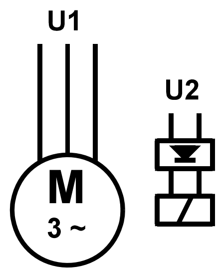
Dahlander connection	Δ/YY	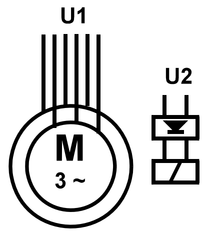	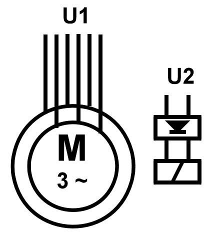	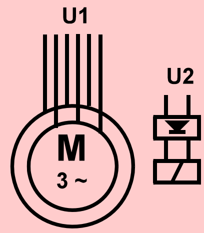
Separate windings	Y/Y	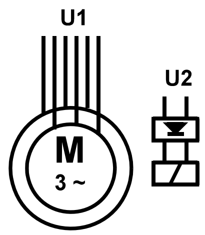	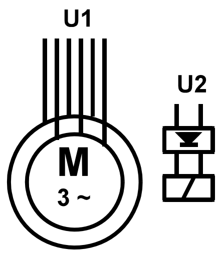	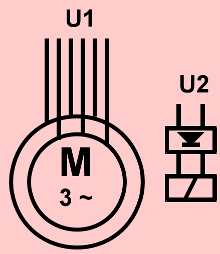

= preferred solution

36.7.2 Motors with dual or variable rated voltages (e.g. 220/380 V)

Motor design	Connection	Solenoid release fed with		
		Phase voltage (e.g. 220 V)	Phase voltage (e.g. 220 V)	Control voltage (e.g. 230 V)
		U2 = U1	U2 = U1/1.73	U2 < U1
Switchable for two voltages, 1:1.73	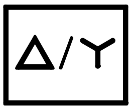	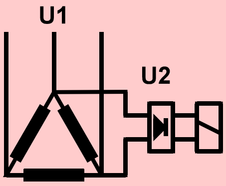	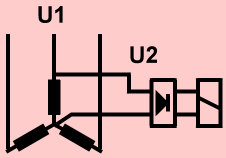	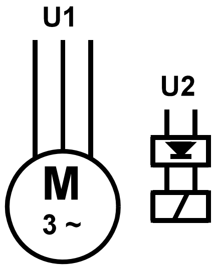
Switchable for two voltages, 1:2		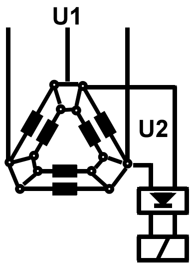	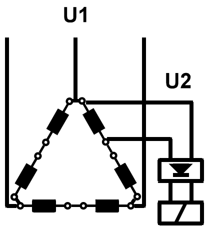	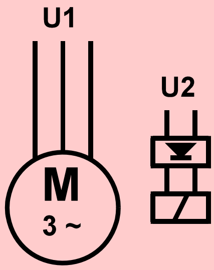
		Main voltage (e.g. 380 V)	Phase voltage (e.g. 220 V)	Control voltage (e.g. 230 V)
		U2 = U1	U2 = U1/1.73	U2 < U1
Soft starting by voltage reduction	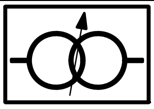	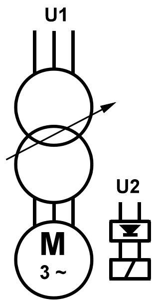	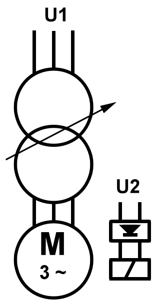	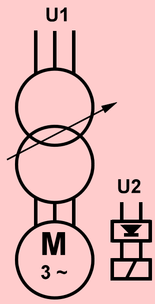
Inverter duty with variable frequency	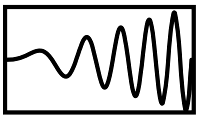	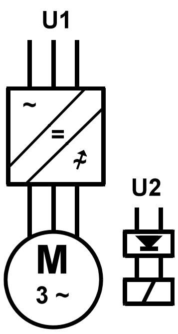	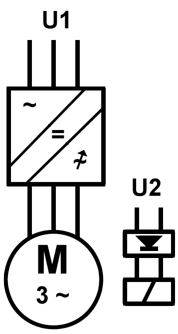	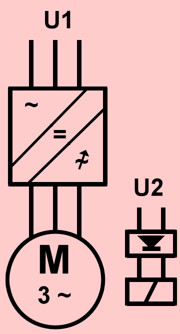

= preferred solution

36.8 Rated voltage of D.C. solenoids

The following main points must be borne in mind when choosing the coil voltage for D.C. solenoids:

36.8.1 Voltage spikes caused by self-inductance

When a solenoid is switched on, a ***cutoff voltage spike*** is generated from the energy of the magnetic field, the magnitude of which is determined by the cutoff speed.

$$e = \frac{d\Phi}{dt}$$

The oscillogram Fig. 36.8.1.1 shows a cutoff process of this type.

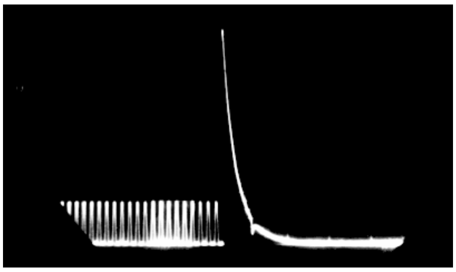

Fig. 36.8.1.1
Oscillogram of the cutoff voltage spike of a D.C. solenoid release

At worst, induction spikes of up to ***20 times the rated voltage*** may be experienced when the power is switched off. It is therefore recommended that as low a rated voltage as possible be selected for the solenoid (e.g. 24 V) so that the voltage spike (e.g. 480 V) remains within the breakdown strength of normal insulating materials. The voltage spikes may become dangerously high (e.g. 3600 V) at higher coil voltages (e.g. 180 V) and must be reduced by special protective circuitry with resistors, capacitors, suppresser diodes, zener diodes or varistors.

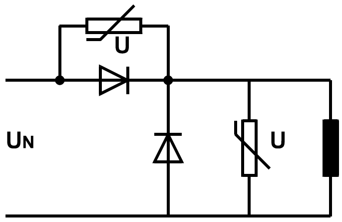

Fig. 36.8.1.2
Half-wave rectification with free-wheeling diode and protective circuitry provided by voltage-dependent resistors (varistors)

As this self-inductance voltage acts in the direction of the current previously flowing in accordance with Lenz's law, i.e. in the forward direction of the diodes, it does not pose a danger to the diodes, unlike voltage spikes on the A.C. side. Nor does the current increase resulting from the voltage rise pose a thermal danger to the diodes since its duration is extremely short. The Joule heat would only be of concern if the switching frequency were extremely high.

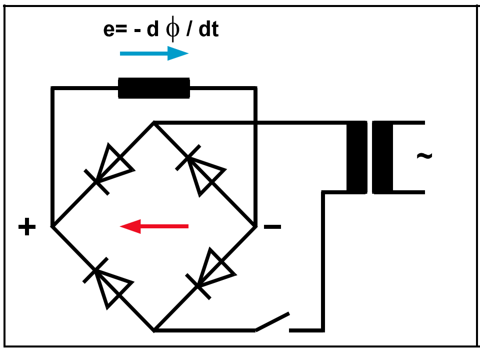

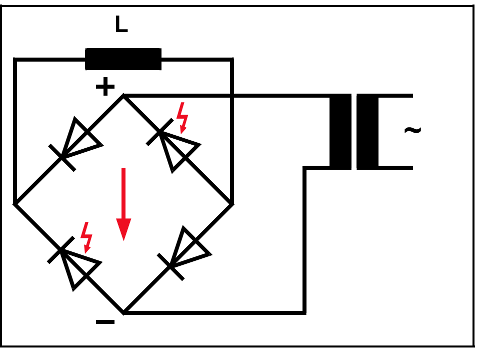

Fig. 36.8.1.3
Direction of a cutoff voltage spike in the solenoid circuit

Fig. 36.8.1.4
Direction of a voltage spike on the mains side

36.8.2 Standardized rated D.C. voltages

IEC 38, "IEC standard voltages", standardizes rated values for D.C. voltages of 24 V, 36 V, 110 V, 220 V.
Because these values are often available as the control voltage, the coils of D.C. solenoid releases are wound to be used with one of these rated voltages. The relatively low ***rated voltage of 24 V*** is preferred in view of the cutoff voltage spikes discussed in section 36.8.1.

36.8.3 Circuit configuration of diodes

If the required D.C. voltage is not available from a control mains, it must be provided by special rectifiers so that the D.C. solenoid releases can be supplied. Transformers are sometimes necessary to allow adaptation to the particular A.C. mains voltage available.
The following circuit arrangement are particularly common.

36.8.3.1 Single-phase bridge circuit with diodes and a transformer

It is possible to exploit ***both half-waves*** of the alternating current by using four bridge-connected diodes, thereby achieving a relatively high arithmetic mean D.C. value of 80 % of the effective alternating current value for a tenable ripple of approximately 48 %.
Given a coil voltage *U_* of 24 V, the secondary side of the transformer must therefore be rated for 24/0.8 = 30 V.

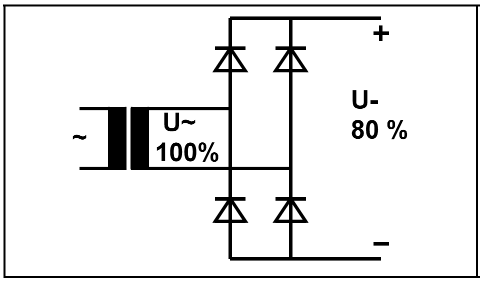

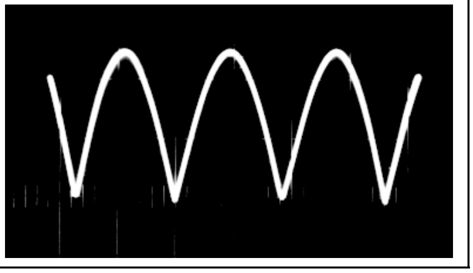

Fig. 36.8.3.1.1
Single-phase bridge circuit with diodes and a transformer

Fig. 36.8.3.1.2
Oscillogram of no load D.C. voltage of a single-phase bridge circuit

36.8.3.2 Half-wave circuit with a free-wheeling circuit

The half-wave rectifier circuit connects only ***one half-wave***, e.g. only the positive half-wave, to the solenoid connected while the other half-wave – the negative half-wave in this example – is fully suppressed. The solenoid is an ohmic-inductive load. The magnetic current continues to flow through the ***free-wheeling circuit*** while the rectifier diode is blocked. A pulsating current flow is associated with the half-waves applied to the coil, the ripple of which depends on the ratio of inductance to resistance in the coil. The design of the solenoid for half-wave rectification allows for rapid excitation of the solenoid circuit in special applications by means of brief full-wave rectification.

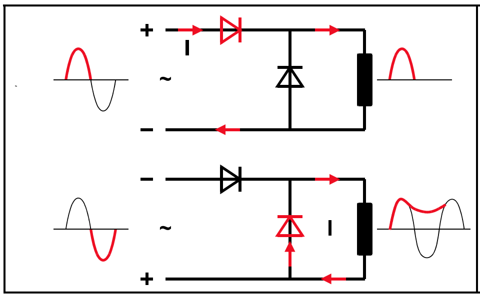

Fig. 36.8.3.1
Circuit configuration and principle of operation of the half-wave circuit with a free-wheeling circuit

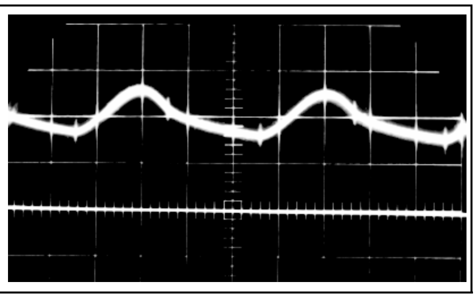

Fig. 36.8.3.2.2
Oscillogram of the current in a coil fed from a half-wave circuit with a free-wheeling circuit

The arithmetic mean D.C. value in this circuit configuration is approximately 45 % of the effective alternating current value due to half-wave rectification. A coil voltage of 105 V DC is thus obtained from direct connection to 230 V AC; the coil must be rated for 180 V at 400 V.

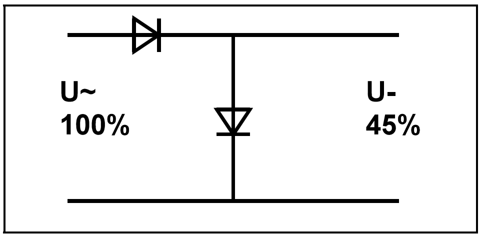

Fig. 36.8.3.2.3
Relative magnitude of the D.C. voltage associated with the half-wave circuit with a free-wheeling circuit

36.9 Plug-in connection option

The benefits of the "built-on brake" principle in terms of shorter downtimes for servicing are particularly great in conjunction with the "plug-in connection" option. The brake can be replaced in the shortest possible time without the need for connection work.

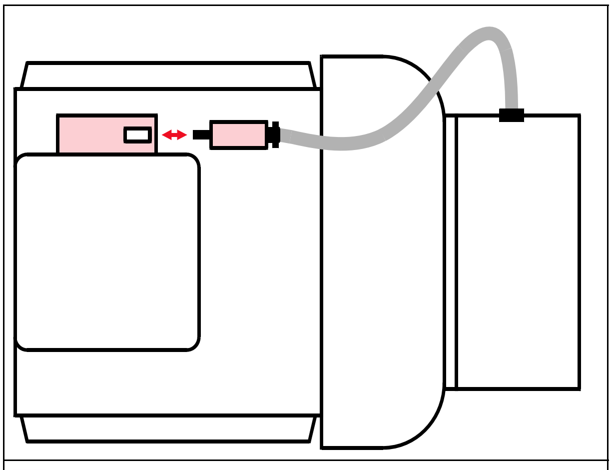

Fig. 36.9.1
Principle of a built-on brake with the plug-in connection option for replacing the brake in the shortest possible time; no skilled electricians required

Fig. 36.9.2
Motor and built-on brake with the plug-in connection option

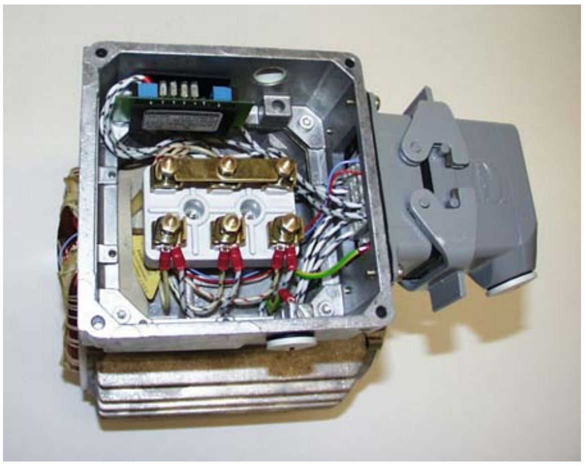

Fig. 39.9.3
Terminal compartment with factory-built wiring

37 Brake release response time

Due to ***mechanical and electrical inertia***, response delays occur at each switching operation, that is to say when a mechanical brake is released and applied. Although the mechanical response times cannot be reduced in a certain design principle, that portion of the response times caused by magnetism can be decreased by switching technology. This applies in particular to brakes with D.C. solenoids, the field of which builds up and decays as an exponential function and which therefore have especially long response times compared to those of brakes with A.C. solenoids.

37.1 Brake release using A.C. solenoids

A.C. solenoids are characterized by particularly ***rapid reaction*** so special switching measures to shorten the response time are generally not required.
The oscillogram in Fig. 37.1.1 shows the switch-on procedure of a three-phase induction motor with built-on single-disc spring-loaded brake and A.C. solenoid release.

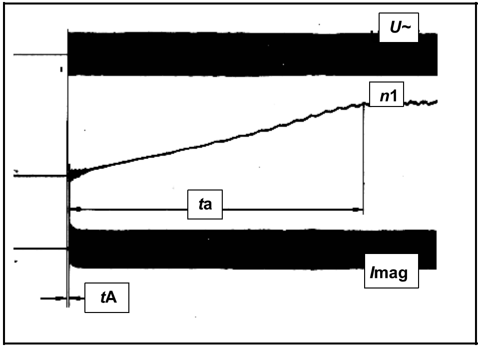

Fig. 37.1.1
Oscillogram of the switch-on procedure using an A.C. solenoid release
U - mains voltage
n_1 - speed
t_a - run-up time
I_{magn} - current in the solenoid release
t_A - response time

Guide values for the brake release response times of spring-loaded brakes with rated braking torques of 1 ... 100 Nm with A.C. solenoids are given in Fig. 37.1.2.

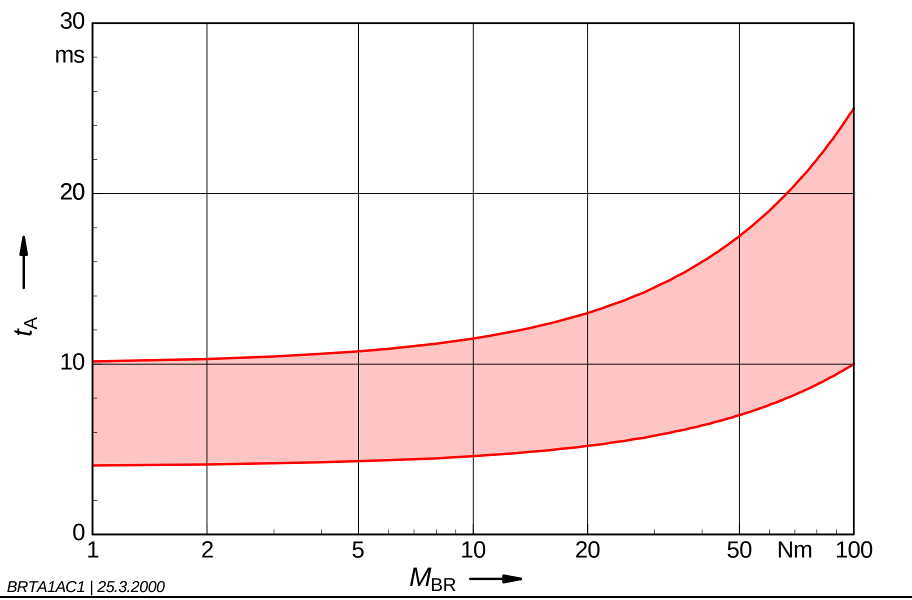

Fig. 37.1.2 Guide values for the brake release response times t_A when releasing spring-loaded brakes with nominal brake torques M_{Br} 1 ... 100 Nm

37.2 Brake release using D.C. solenoids

The time characteristics of the coil current when switched on and switched off follows a known exponential function, the slope of which is determined by the ***time constant***:

$$T = \frac{L}{R}$$

T	- time constant
L	- circuit inductance
R	- ohmic resistance of the circuit

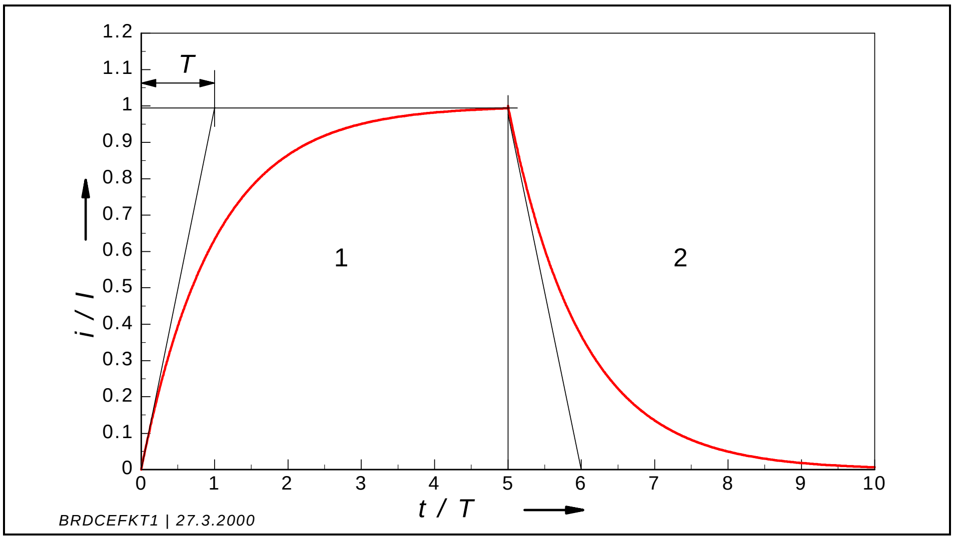

Fig. 37.2.1 Theoretical current characteristics when switching on (1) and switching off (2) a D.C. solenoid

The significance of the time constant becomes more pronounced as the size of the brake increases and all measures to reduce the response time must ultimately be aimed towards ***changing the time constant***.
The oscillogram in Fig. 37.2.2 shows the switch-on procedure of a three-phase induction motor with a built-on multiple-disc spring-loaded brake and D.C. solenoid. During the response time t_A, which becomes more and more pronounced as the size of the brake increases, the drive is locked or rotates against the applied brake, thus placing an ***additional*** load on the mains, motor and brake.

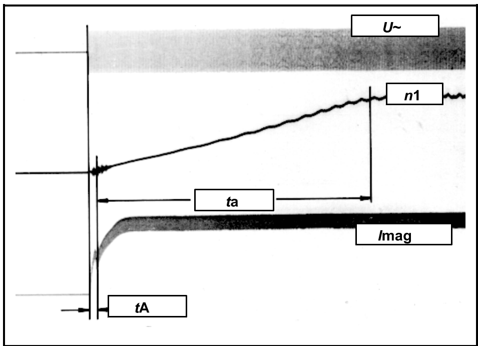

Fig. 37.2.2
Oscillogram of the switch-on procedure using a D.C. solenoid release

Guide values for the duration of the brake release response time are given in Fig. 37.2.3.

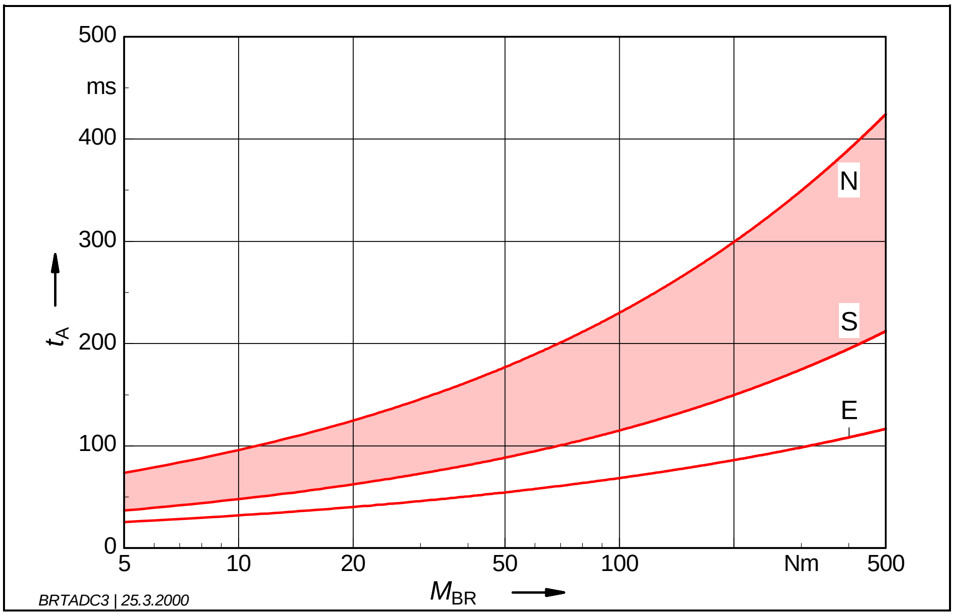

Fig. 37.2.3 Guide values for the release response time t_A of spring-loaded brakes with D.C. solenoids and a braking torque M_{BR}
S - switching brakes with reduced braking torque
N - standard brakes with full braking torque
E - overexcitation for reduced response time

It is possible to shorten the response time electrically by reducing the time constant *L/R* as explained in section 37.2.1. Since a specific inductance *L* is also required for a given solenoid design, the ohmic resistance *R* must be increased using an additional ***series resistor*** to improve the time constant.
The voltage applied must also be increased to the same extent to achieve the full coil current required. This makes it possible to reduce the response time by half, for example by using "high-speed excitation" with a series resistor rated at 200 % of the intrinsic resistance, i.e. three times the rated voltage.

"Overexcitation" can also be used in place of or in addition to high-speed excitation.
The coil is connected to a multiple ***overvoltage*** for a limited period when it is switched on. The excessive current causes a correspondingly amplified magnetic force which accelerates the release process. The response time can be reduced to approximately 20 %, for example, by multiple overexcitation.

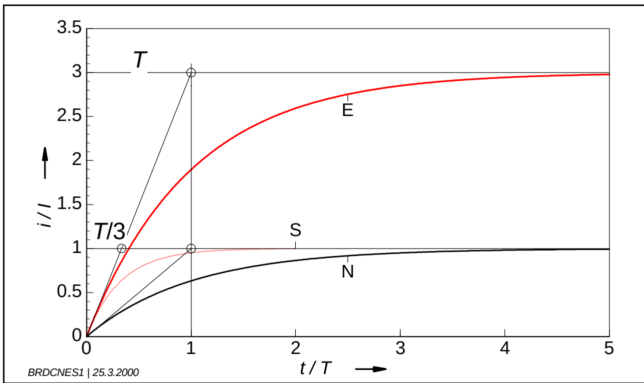

Fig. 37.2.4. Comparison of the current increase for switch-on procedures using normal excitation (N), high-speed excitation (S) and overexcitation (E)

The schematic diagram in Fig. 37.2.5 shows the increase in the solenoid current I_1 in the case of overexcitation with twice the rated voltage compared with the current for normal excitation I_2. The rated voltage is restored once the overexcitation period t_{sup} permanently set at 300 ms on the MSG rectifier has elapsed. The response time for overexcitation t_{A1} in this case is approximately less than half that for the normal response time t_{A2}.

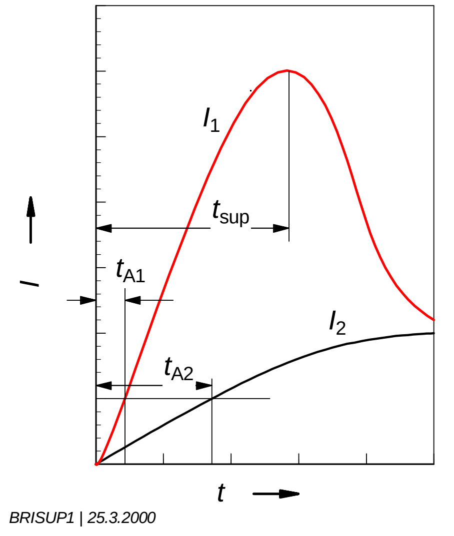

Fig. 37.2.5
Solenoid current I_{mag} and response time t_A for overexcitation 1 and normal excitation 2 with switch-over after the overexcitation period t_{sup}

Time delay and ***contactless*** switch-over are provided electronically on modern overexcitation inverters. The overexcitation function is integrated into the electronic brake on the D.C. side on the new Danfoss Bauer MSG rectifier (section 38.2). The electronic circuitry is to replace the control technology solution using a microswitch common in the past (Fig. 37.2.6).

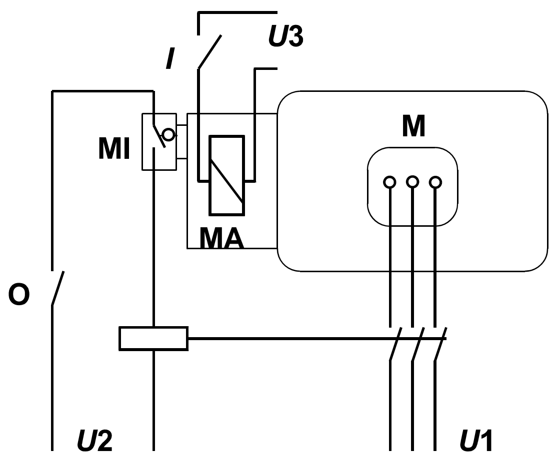

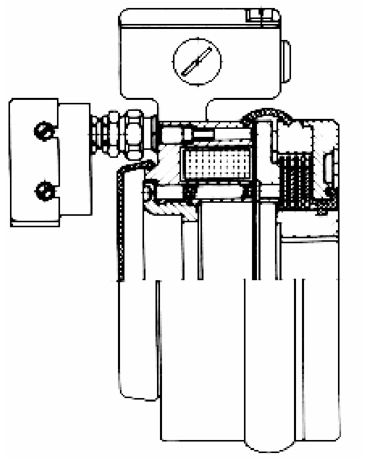

Fig. 37.2.6
Circuit engineering elimination of the response time by the use of a brake with a built-on microswitch (MI)

Fig. 37.2.7
Multiple-disc spring-loaded brake with built-on microswitch
(manufactured by BINDER)

37.3 Lost energy with long release time

The response time when ***releasing*** a brake is not generally regarded as harmful since the starting cycle commences when the motor starts to move as far as the onlooker is concerned. In fact, the processes occurring around "time 0" can cause considerable loading on the motor and brake.

37.3.1 Basic differences in the starting cycle

Superficially, the brake release and motor start appear as synchronous processes as shown in Fig. 37.3.1.

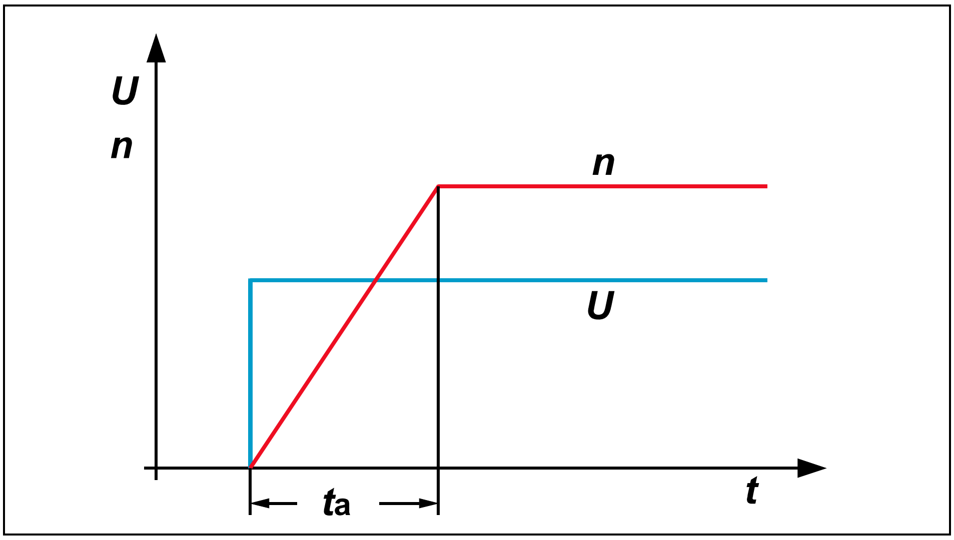

Fig. 37.3.1 Simplified portrayal of simultaneous brake release (voltage U) and motor start (speed n) over the run-up time t_a

If we take a closer look at the processes occurring around "time 0", two variants become evident:

37.3.1.1 Motor is locked

$\boldsymbol{M_A < (M_L + M_{Br})}$

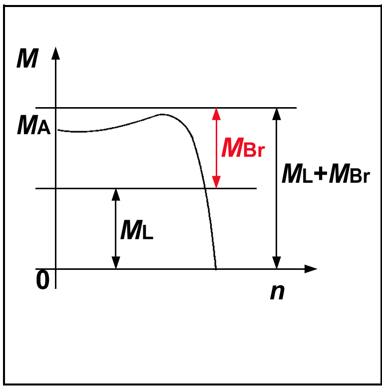

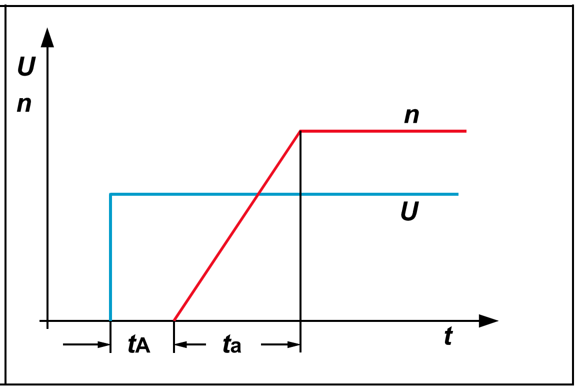

Fig. 37.3.1.1.1
Motor locked
M_A - breakaway torque
M_L - load torque
M_{Br} - braking torque

Fig. 37.3.1.1.2
Starting is delayed by the response time t_A of the brake

Additional loading:
Motor carries the starting current during the response time t_A and is subjected to additional thermal loading.

37.3.1.2 Brake is overcome

$M_A > (M_L + M_{Br})$

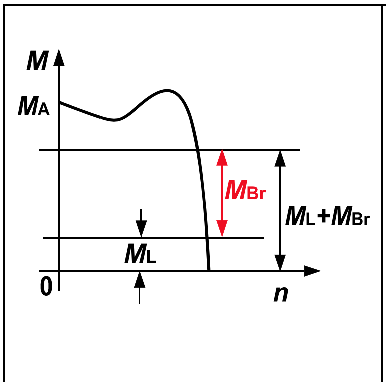 	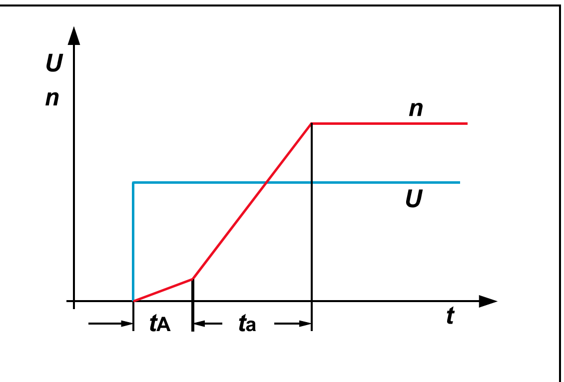
Fig. 37.3.1.2.1 Motor overcomes the brake M_A - breakaway torque M_L - load torque M_{Br} - braking torque	Fig. 37.3.1.2.2 Starting is successful when the motor is switched on by the brake is overcome during the response time t_A

Additional loading:
The brake is also thermally loaded during starting and suffers abrasive wear.

37.4 Thermal relief of the motor

The reduction in the brake release response time can relieve a considerable load from the motor and brake, above all for medium-size and large brakes which have particularly marked response times.
Fig. 37.4.1 shows that the locking times are relatively high in comparison to the normal starting time t_a and so can have a considerable effect on the ***balance of losses***.

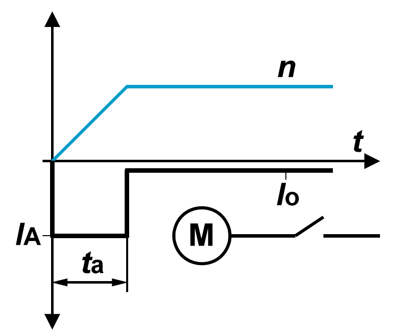	**1** Without brake; run-up time t_a
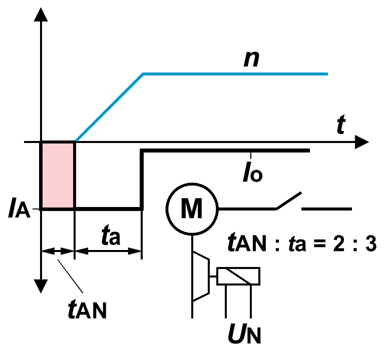	**2** Brake with normal excitation; locking time t_{AN}
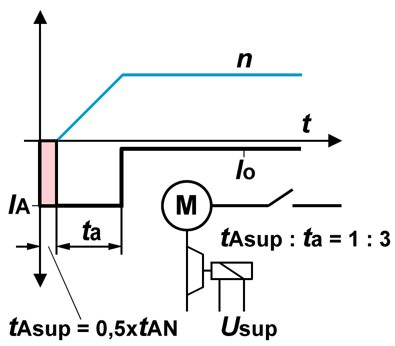	**3** Brake with overexcitation; locking time t_{Asup}

Fig. 37.4.1 Comparison of locking times when releasing the brake

If the motor locks as described in section 37.3.1.1, it will be subjected to additional thermal loading. The permissible switching frequency is reduced. Various methods are employed to quantify this process. One manufacturer's catalogue specifies the thermally permissible no load operating frequency for the motor determined by testing under normal excitation and with overexcitation. Fig. 37.4.2 provides and example of the quantified effect of reducing the response times. The value Z_0 for the no load operating frequency of three-phase motors operated with brakes that are released "rapidly" (E) or "normally" (N) are compared. Although this method of calculation is not adopted by Danfoss Bauer, it is cited here to clarify the physical effect of overexcitation on the thermal loading capacity of a motor.

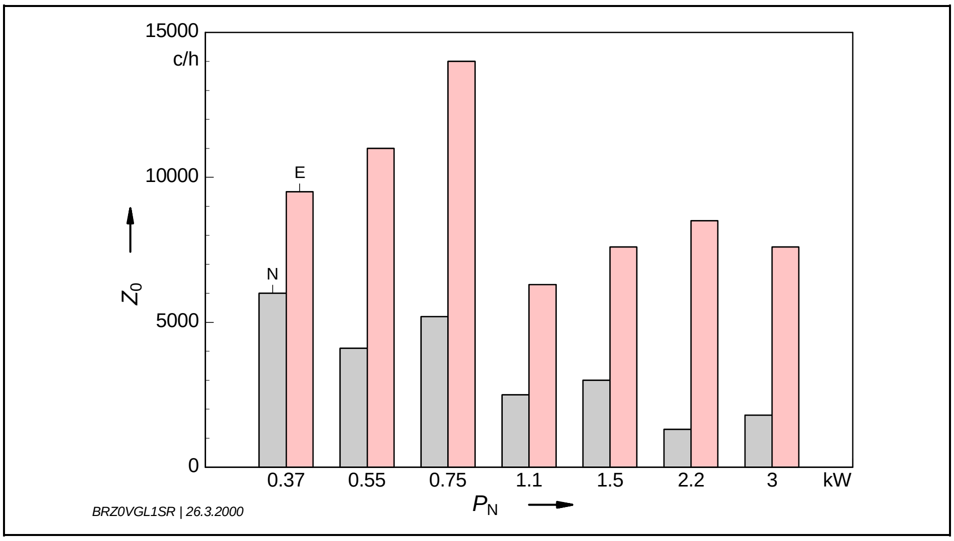

Fig. 37.4.2 Comparison of the thermally permissible no load operating frequency Z_0 of 4-pole three-phase motors with a rated output of P_N according to the catalogue data of one manufacturer
N - brake released by normal excitation
E - brake released by overexcitation

Danfoss Bauer's calculation method assesses the excitation of the using a factor K_M in the equation for the "thermally equivalent switching frequency".
This method of calculation takes into account the influence of the excitation type on the ***switch-on*** procedures only, and not on the ***switch-over*** procedures which do not involve the brake.
Where the relationship between the response time and run-up time is normal, the thermal effect of normal excitation to overexcitation is assessed in the approximate ratio of 1:2.
In the BAA method of calculation for the "thermally permissible switching frequency of three-phase motors" the thermal loading loading is evaluated. In an example given based on pole-changing motor, the motor locking caused by the normally-released brake accounts for 48 % of the thermal load on the motor winding. This value could be reduced in this example to 31 % by the use of overexcitation.
The actual switching operations are "weighted" in this calculation using a calculation factor according to their thermal effect.

38 Brake application response time

Since the "holding force" of a magnet – i.e. the force required to hold a brake ***open*** – is relatively low, the magnetic field must decay to a large extent and, consequently, for a long time until the spring force is sufficient to allow the brake to be applied. For this reason, the response times for brake application are very pronounced, particularly for larger brakes, and must be reduced for demanding applications by circuit engineering.

38.1 Brake application with A.C. solenoids

The solenoid used for the braking process as shown by the oscillogram in Fig. 38.1.1 is connected to two motor terminals. The motor's remanence induces a ***slowly decaying*** voltage which initially allows the solenoid current to continue to flow. The response time is relatively long.

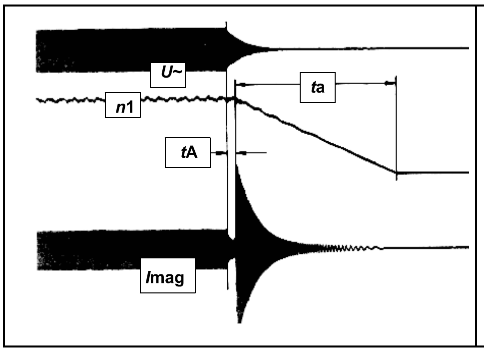

Fig. 38.1.1
Oscillogram of the cutoff process using an A.C. solenoid without a break in the solenoid circuit
U - mains voltage
n_1 - speed
t_a - braking time
I_{magn} - current in the solenoid
t_A - response time

The solenoid current can be broken immediately thanks to the solenoid circuit being switched separately and the response time can be reduced as shown in the oscillogram in Fig. 38.1.2.

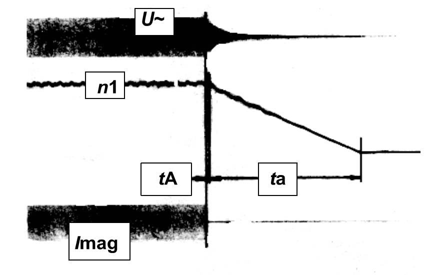

Fig. 38.1.2
Oscillogram of the cutoff process using an A.C. solenoid with a break in the solenoid circuit
U - mains voltage
n_1 - speed
t_a - braking time
I_{magn} - current in the solenoid
t_A - response time

Guide values for the brake application response times of spring-loaded brakes with nominal braking torques 1 ... 100 Nm with A.C. solenoids can be obtained from Fig. 38.1.3.

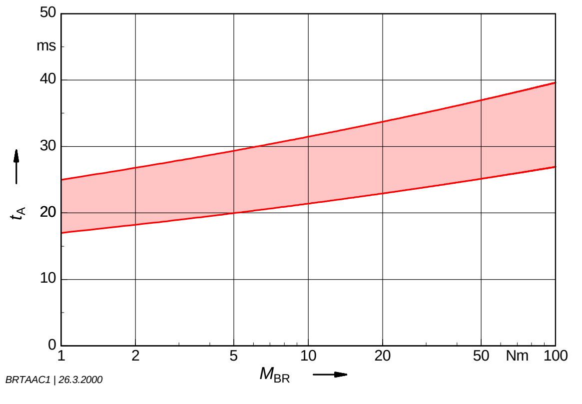

Fig. 38.1.3
Guide values for the brake application response times (t_A) of spring-loaded brakes with A.C. solenoid and a break in the solenoid circuit
Nominal braking torques (M_{Br}) 1 ... 100 Nm

38.2 Brake application with D.C. solenoids

The current decay process results in a relatively long response time as shown in the oscillogram in Fig. 38.2.1 because the "holding amperage" of the D.C. solenoid is very low.

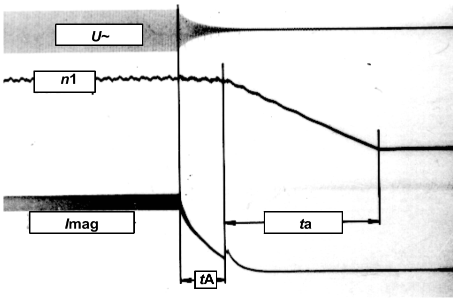

Fig. 38.2.1
Oscillogram of the cutoff process using a D.C. solenoid without a break in the solenoid circuit
U - mains voltage
n_1 - speed
t_a - braking time
I_{magn} - current in the solenoid
t_A - response time

The coil current must be broken together with the power circuit to reduce the response time. Although the direct currents being switched are not very high, careful attention must be paid to the switching capacity of the contacts in conventional solutions that use contactors as an electric arc is produced when direct current is switched off and the contacts could be corroded.
As many auxiliary contacts as possible should be connected in series or, better still, the main contacts of a D.C. or A.C. contactor should be used.

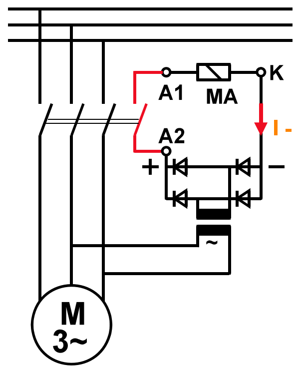

Fig. 38.2.2
Circuit diagram of the D.C. circuit for the solenoid MA

Circuit diagram 38.2.2 shows the basic circuit and oscillogram 38.2.3 shows the effect of the ***D.C.-circuit break*** on the response time.
The guide values for the overtravel time and the overtravel distance given in subsections 13 and 14 represent the response time with a D.C.-circuit break.
The D.C. break function is integrated into the new Danfoss Bauer MSG rectifier, together with the overexcitation function (section 37.2). The break is contactless and is pereformed electronically. Brake application by means of a D.C. circuit break is triggered by either

- the supply voltage being cut off (intentionally or unintentionally)
- the current in a main conductor falling below a prescribed limit.

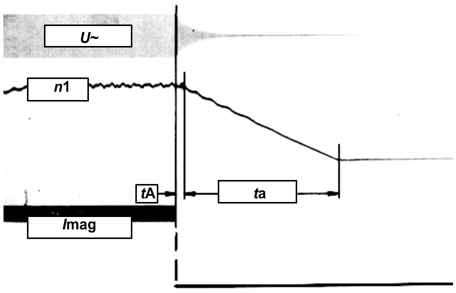

Fig. 38.2.3
Oscillogram of the cutoff process using a D.C. solenoid with a break in the solenoid circuit
U - mains voltage
n_1 - speed
t_a - braking time
I_{magn} - current in the solenoid
t_A - response time

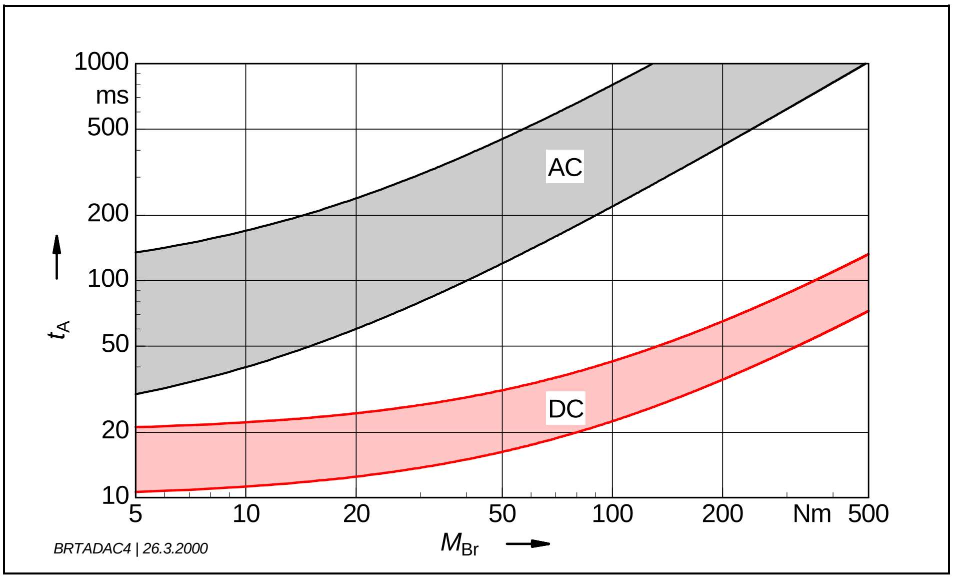

Fig. 38.2.4 Guide values for the brake application response time t_A of spring-loaded brakes with a D.C. solenoid, braking torque M_{Br}

AC - A.C. cutoff

DC - D.C. cutoff

39 Mass moment of inertia of the friction discs

The mass moment of inertia of the rotating brake components (friction disc and driver) is generally ***negligible***, as can be seen from Table 39.1 and Fig. 39.6.2.

Size	.003B	.005A	.008A	.010A	.025A	.050A	.075A	.100A	.150A	
Type E...	0.01	0.1	0.1	0.185	0.7	1.6	1.6	4.25	4.25	10^{-3} kgm²
Type Z...	–	0.2	0.2	0.37	1.4	3.2	3.5	8.5	8.5	10^{-3} kgm²

Table 39.1 Mass moment of inertia of the rotating components of spring-loaded brakes, type series E ... (single-disc brakes) and Z ... (double-disc brakes)

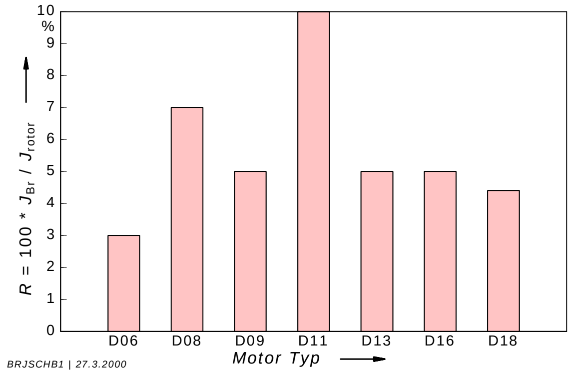

Fig. 39.2
Relationship between the mass moment of inertia of friction discs and motor rotors for typical type series D06 to D18 motors and their standard brakes

40 Selection according to the braking torque

Brake motors are constructed and offered in catalogues in frame sizes to meet demand – the brakes are designed for optimum ***braking torque***, i.e. they offer the they highest possible rated torque.
The ***working capacity***, i.e. the ability to perform retardation work, is often a by-product that is determined by test and experience.
This procedure is justified if the brake is used as a ***holding brake***, as is usually the case. In other words, if the retardation work is performed by a pole-changing three-phase motor and the brake is required predominantly to hold a load. If, however, the brake is used frequently for retardation during operation, the working capacity must be calculated according to the ***braking energy and service life*** (section 41) – it may be necessary to avoid using the full braking torque.

40.1 Required braking torque

The braking torque required can be calculated to determine the correct brake size, provided all data and requirements are known.

$$M_{\mathrm{Br}} = M_{\mathrm{a}} \pm M_{\mathrm{L}}$$

M_{Br} - rated torque of the brake in Nm
M_{a} - deceleration torque in Nm
M_{L} - braking or driving load torque in Nm

$$M_{\mathrm{a}} = \frac{J \cdot n}{9{,}55 \cdot t_{\mathrm{a}}}$$

J - mass moments of inertia in kgm²
n - speed in r/min
t_{a} - delay time in s.

Assumptions about the motor and braking time:
P_{N} = 7.5 kW n_1 = 1500 r/min J_{rot} = 0.029 kgm²
M_{N} = 50 Nm t_{a} = 1 s M_{L} = 0

Relationship between the size/weight and the motor for a spring-loaded brake

calculated using the equation above:
M_{a} = 4.6 Nm;
brake selected: 5 Nm

determined by the following rule:
$M_{\mathrm{Br}} \geq 0.8 \cdot 50 = 40$; brake selected: 50 Nm

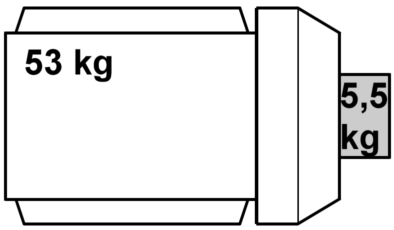

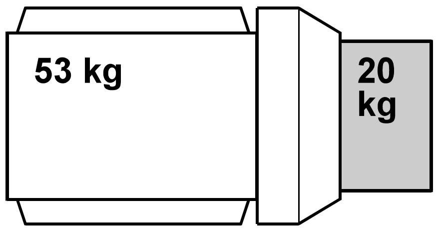

The braking torque can also be calculated by the following rule of thumb, from which the starting energy, overtravel time and overtravel distance can be determined. If the calculated values are within the limits demanded, the brake can be kept at its present size.
It is recommended that the braking torque selected is not significantly lower or higher (minimum factor of 0.5, maximum factor of 2) than that calculated by this rule of thumb, even if the calculated values for starting energy, overtravel time and overtravel distance permit or demand this.

If the brake selected is too small, it will be subjected to increased wear and its service life will be reduced; if the brake selected is too large, too great a load may be placed on the drive's mechanical power transmission components.

40.2 Run-out braking

Rule for calculating the brake size:

Braking torque at least 80 % of the drive's rated torque.

The rated torque is calculated as follows:

$$M = \frac{9550 \cdot P}{n}$$

M - rated torque of the motor in Nm
P - rated output of the motor in kW
n - speed in r/min

A braking torque at the lower limit of the rating rule (M_{Br} = 0.8 M_N) is assumed in the calculation of the following graphs.
Fig. 40.2.1 shows that guide values for the overtravel times of approximately 50 ms ... 1 s can be expected if this rule is used under standard operating conditions for 4-pole three-phase motors with rated outputs of 1 ... 100 kW. These values are acceptable for most applications.
In fact, $M_{BR} > M_N$ and $FI < 2$ will generally apply since the rated braking torques are stepped; the actual values are therefore lower than the values shown in the graphs.

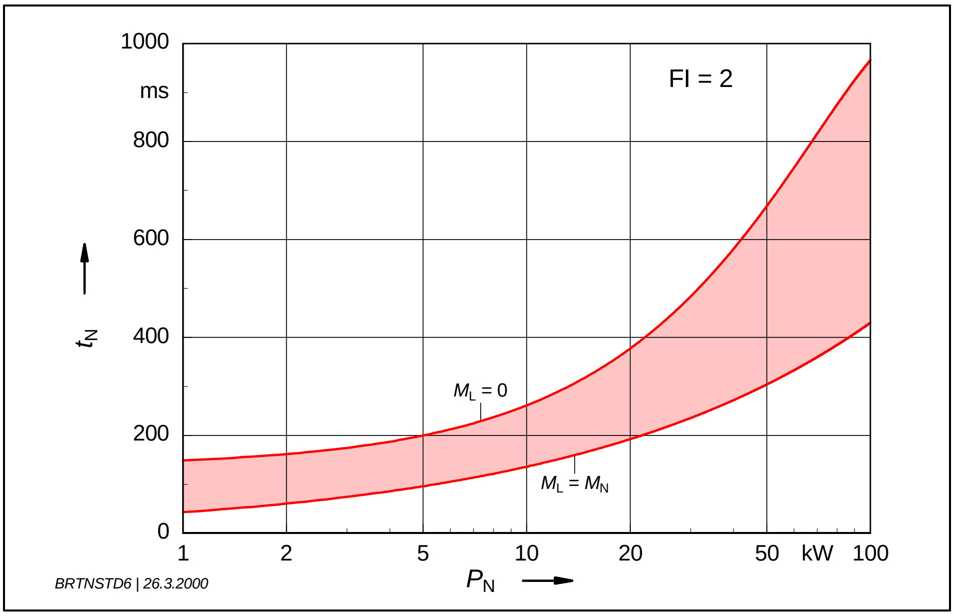

Fig. 40.2.1 Guide values for the overtravel time t_N of 4-pole three-phase motors with a rated output P_N for run-out braking with a factor of inertia FI = 2

$M_L = 0$: without the assistance of a load torque
$M_L = M_N$: with the assistance of a load torque = rated torque

The overtravel angle on the rotor of these motors is approximately 360 ... 5,000 angular degrees under the same conditions, which corresponds to approximately 1 ... 14 revolutions (Fig. 40.2.2).
This overtravel distance is reduced at the drive station by the reduction gearing that is usually fitted downstream.

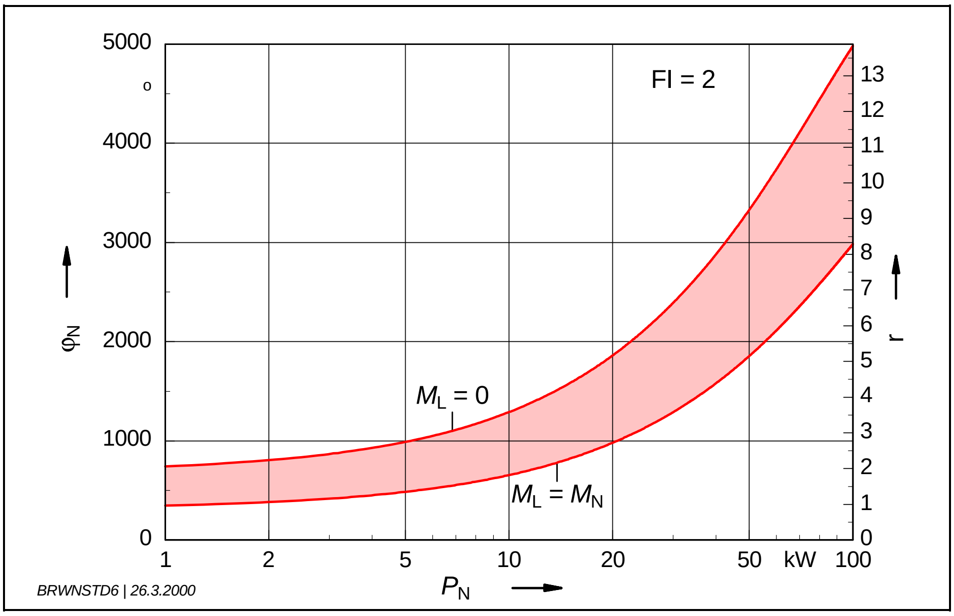

Fig. 40.2.2 Guide values for the overtravel angle φ_N of 4-pole three-phase motors with a rated output P_N for run-out braking with a factor of inertia *FI* = 2

$M_L = 0$: without the assistance of a load torque
$M_L = M_N$: with the assistance of a load torque = rated torque

40.3 Lifting duty

Rule for calculating the brake size

Braking torque equal to double the drive's rated torque

The equation given in section 40.2 is used to calculate the rated torque.

The drive motor operates as a generator in lowering duty and provides a uniform downwards movement thanks to its retardation effect. If one disregards the transmission losses, the drive must be braked with the full rated torque at full load. If a mechanical brake were applied with the rated torque after the motor were switched off, the downwards movement would continue without retardation.
An ***additional*** braking torque is therefore required to brake to a standstill. Approximately 100 % of a brake rated for 200 % of rated torque is consumed “statically” and the remained can be used “dynamically” to provide retardation.
A braking torque at the lower limit of the rating rule ($M_{Br} = 2\ M_N$) is assumed in the calculation of the following graphs.

Fig. 40.3.1 shows that guide values for the overtravel times of approximately 120 ms ... 800 s can be expected if this rule is used for the ***lowering duty*** of 4-pole three-phase motors with rated outputs of 1 ... 100 kW. These values are acceptable for most applications.
In fact, $M_{BR} > 2\ M_N$ will generally apply since the rated braking torques are stepped; the actual values are therefore lower than the values shown in the graphs.

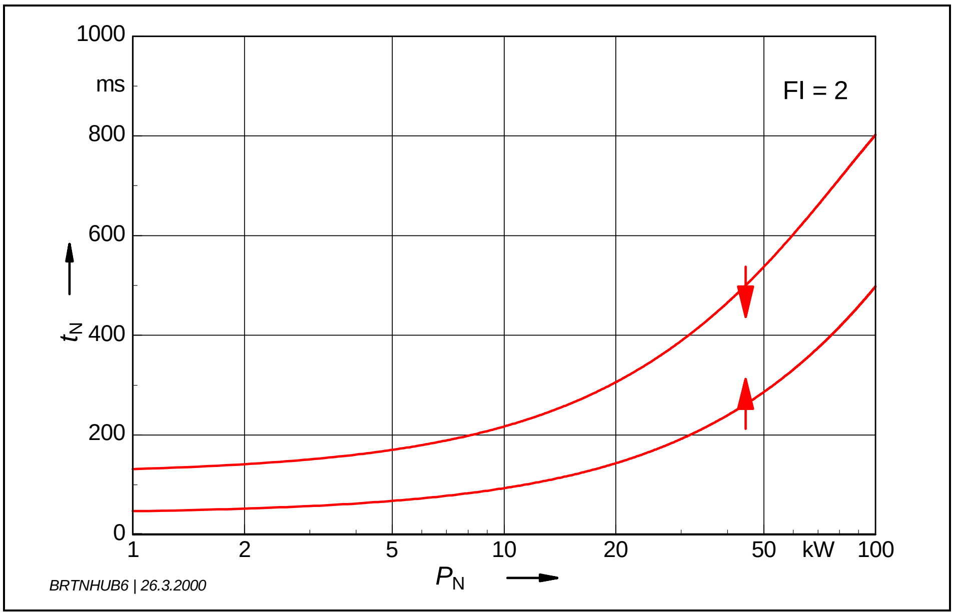

Fig. 40.3.1 Guide values for the overtravel time t_N of 4-pole three-phase motors with a rated output P_N with a factor of inertia *FI* = 2
⇓ Lowering duty, load is driving
⇑ Lifting duty, load is braking

The overtravel angle on the rotor of these motors is approximately 500 ... 5,000 angular degrees under the same conditions, which corresponds to approximately 1.5 ... 11 revolutions (Fig. 40.3.2).
This overtravel distance is reduced at the drive station by the reduction gearing that is usually fitted downstream.

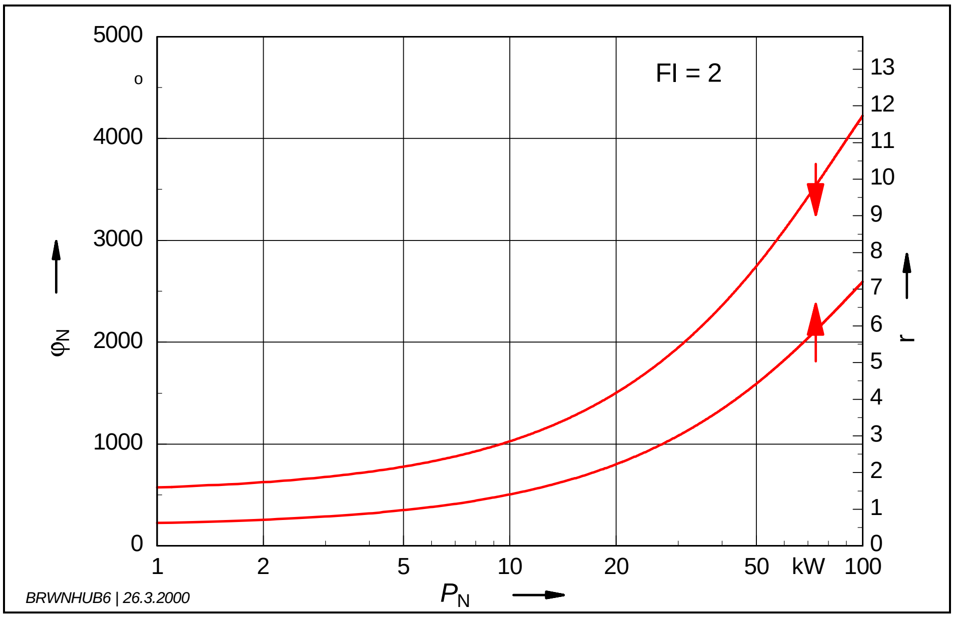

Fig. 40.3.2 Guide values for the overtravel angle φ_N of 4-pole three-phase motors with a rated output P_N with a factor of inertia *FI* = 2
⇓ Lowering duty, load is driving
⇑ Lifting duty, load is braking

41 Selection according to the braking energy

In addition to the braking torque, particular attention must be given to the ***thermal loading*** and ***wear caused by switching*** in the selection of a mechanical brake. Consideration is usually only given to the switching frequency in this context. However, this rating cannot describe the actual loading on its own. Thermal loading is rather a product of the switching energy, i.e. the kinetic energy in play whenever the brake is applied, and the average number of switching operations per hour, i.e. the switching frequency. The actual loading should not exceed the limits of a brake's thermal capacity, i.e. its ***working capacity***. The friction elements have a limited ***switching energy service life***.

The international unit of measurement for work or energy (W in equation) is either J or Nm or Ws. 1 J = 1 Nm = 1 Ws.

The unit J (joule) is preferred in this book and in documentation produced by Danfoss Bauer GmbH to prevent confusion with the unit of torque (Nm).

The following sections are preceded by an example to make the subjective evaluation of the standard energy capabilities for the braking of drive motors easier. This should serve to clarify the amount of energy (= wear or destructive work) stored in the rotating mass of a medium-size electric motor and the amount of energy that mechanical brakes must absorb over many millions of switching operations.

Assumptions:	Standard 4-pole motor	P_N	=	11 kW
	Idling speed	n_0	=	1500 r/min
	Mass moment of inertia	J_{rot}	=	0.057 kgm²

Kinetic energy of the rotating rotor mass

$$W_{rot} = \frac{J_{rot} \cdot \omega^2}{2} = \frac{J_{rot} \cdot n^2}{182{,}5} = \frac{0{,}057 \cdot 1500^2}{182{,}5} = 703 \text{ J}$$

$$\omega = \frac{\pi \cdot n}{30}$$

Potential energy

To illustrate, this energy can be converted into a mass which has potential energy through being raised to a height of 1 m:

$$W_{rot} = W_{pot} = m \cdot g \cdot h$$

$$m = \frac{W_{rot}}{g \cdot h} = \frac{703 \text{ J}}{9{,}81 \frac{\text{m}}{\text{s}^2} \cdot 1 \text{ m}} = 71{,}6 \frac{\text{N} \cdot \text{s}^2}{\text{m}} = 71{,}6 \text{ kg}$$

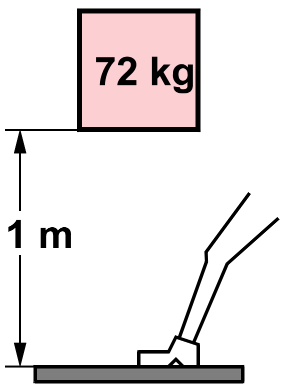

Conversion of the "working capacity" in the rotor of a 11 kW, 1500 r/min three-phase motor into an equivalent "potential energy" for the subjective rating of the "working capacity" of spring-loaded brakes

41.1 Switching energy per braking operation

The kinetic energy of the moving masses is converted into heat by friction. This is calculated as

$$W_{rot} = \frac{J \cdot \omega^2}{2}$$

or using the variables commonly adopted in practice

$$W_{rot} = \frac{J \cdot n^2}{182{,}5}$$

W_{rot} - work (energy) in Nm = Ws = J
J - mass moment of inertia in kgm^2
n - speed in r/min

If an extremely large mass moment of inertia is braked from a high speed, ***heat accumulates*** on the friction surfaces and impairs the brake. For this reason, the ***working capacity per individual braking operation*** as stated in the manufacturer's specifications for the particular brake size must be heeded.
The effect of the switching frequency on the permissible switching energy per switching operation is discussed on a general basis in VDI code of practice 2241 Sheet 1. Fig. 41.1.1 shows this in a simplified, relative form based on the equations specified in this code of practice.
Line 1 represents constant total work as a product of the working capacity per switching operation multiplied by the switching frequency.
In fact, line 2 provides the only usable values: for ***one*** switching operation per hour, i.e. only 16 % of the theoretically possible value.

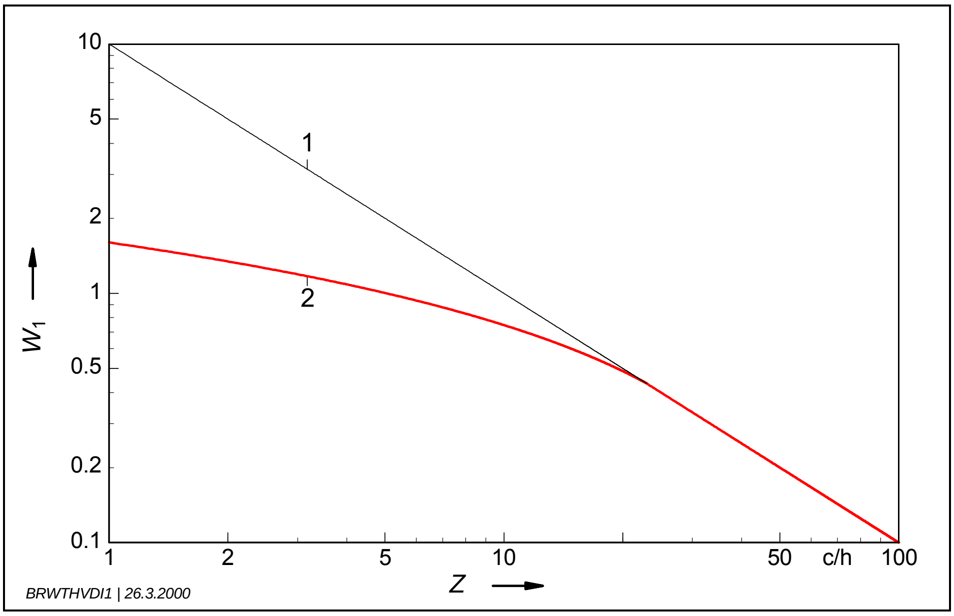

Fig. 41.1.1 Consumption of the working capacity per switching operation at a low switching frequency per hour
Relative representation based on VDI 2241 Sheet 1
1 - theoretically usable 2 - actually usable

The determination by calculation or experiment of a limit value for a single switching operation is not at all simple – manufacturers' catalogue specifications differ as a result (Fig. 41.1.2 in accordance with [5.4]).

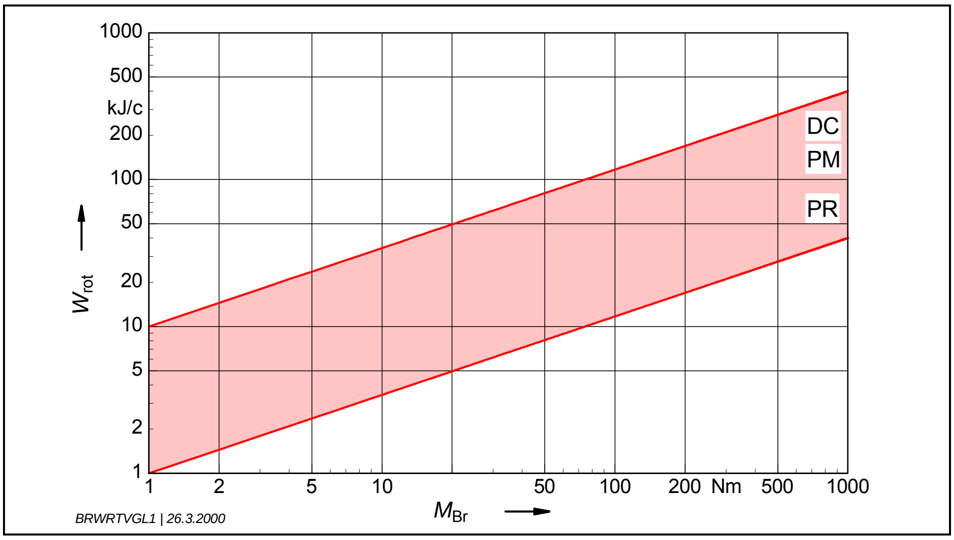

Fig. 41.1.2 Scatter band of the catalogue data for the limit value W_{rot} of a single braking operation

DC - with a D.C. solenoid release
PM - with a permanent magnet
PR - pole friction brakes

However, subsequent calculation for 4-pole standard motors with standard brakes demonstrate that extremely high external rotating masses (expressed as *FI* = factor of inertia which describes the mass ratio compared to the rotor mass) must be present to endanger the brake during a single braking operation. Fig. 41.1.3 shows the limit values *FI* plotted against the rated output of 4-pole three-phase motors.

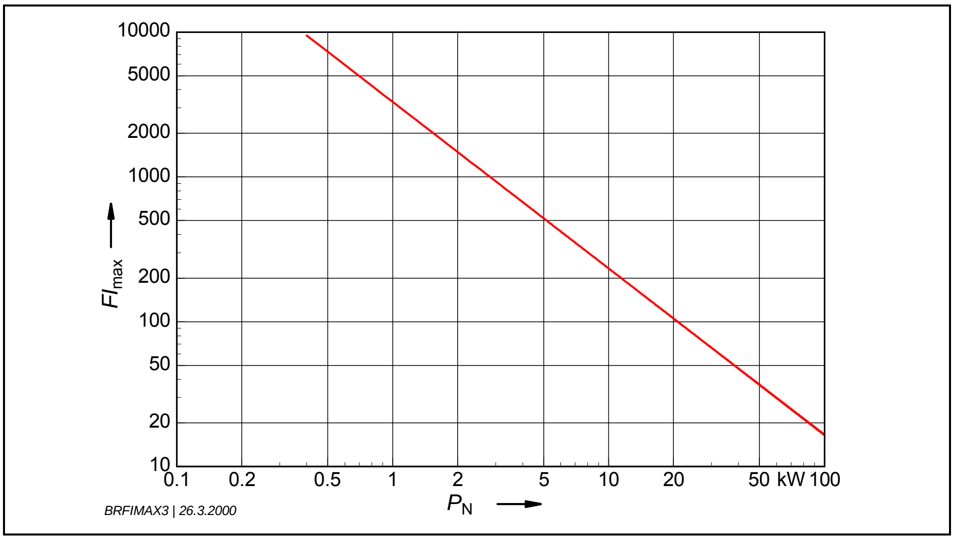

Fig. 41.1.3 *FI* limit value FI_{max} for a single braking operation with a standard brake on 4-pole three-phase motors with a rated output P_N

The following rule is obtained from this graph:
Recalculation of the thermal loading is not necessary for standard applications in the case of a single braking operation.

41.2 Thermally permissible switching energy

The level of heating rises in the case of a uniform sequence of braking operations, i.e. a known average switching frequency per hour, until it reaches an equilibrium between generation and dissipation. The permissible temperature should be such that neither the coil nor the friction lining is thermally overloaded, taking into account the ambient temperature.

The thermal loading for pure injection braking is calculated as follows:

$$W_{th} = W \cdot Z$$

W_{th} - thermally permissible switching energy per hour
W - switching energy per switching operation at $FI \leq 2$
Z - number of braking operations per hour

The highest average value occurring over ***several hours*** must be used for Z since we are dealing here with a ***thermal limit***.
If a proportion of the braking torque is required statically for the load in the case of lifting duty as described in section 9.2, the slip period and consequently the thermal loading will be higher. The following will then apply:

$$W_H = \frac{M_{Br}}{M_{Br} - M_L} \cdot W_{th}$$

$$W_H = f_W \cdot W_{th}$$

W_H - thermally permissible switching energy per hour for lifting duty
W_{th} - thermal permissible switching energy per hour
M_{Br} - braking torque of the brake
M_L - static torque of the load
f_W - $M_{Br} / (M_{Br} - M_L)$

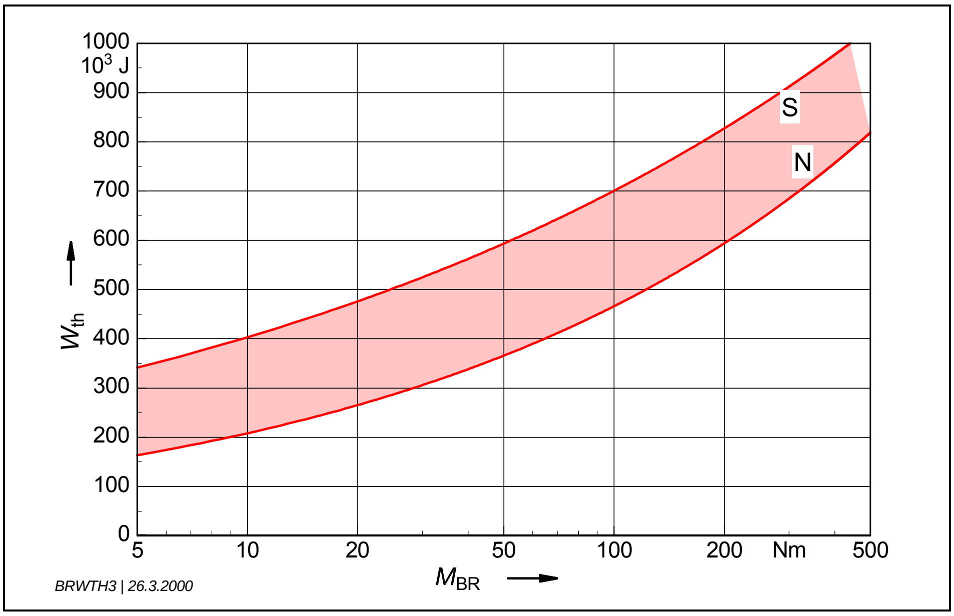

Fig. 41.2.1 Guide values for the thermally permissible switching energy W_{th} of Danfoss Bauer series 2000 spring-loaded brakes
N - Standard brakes
S - Switching brakes

A recalculation for standard 4-pole motor with standard brakes yields interesting results:
The thermally permissible switching frequency limit of standard brakes is greater than the corresponding limit value for the motor up to a rated output of approximately 5.5 kW – this relationship is reversed for larger outputs (see Fig. 41.2.2).

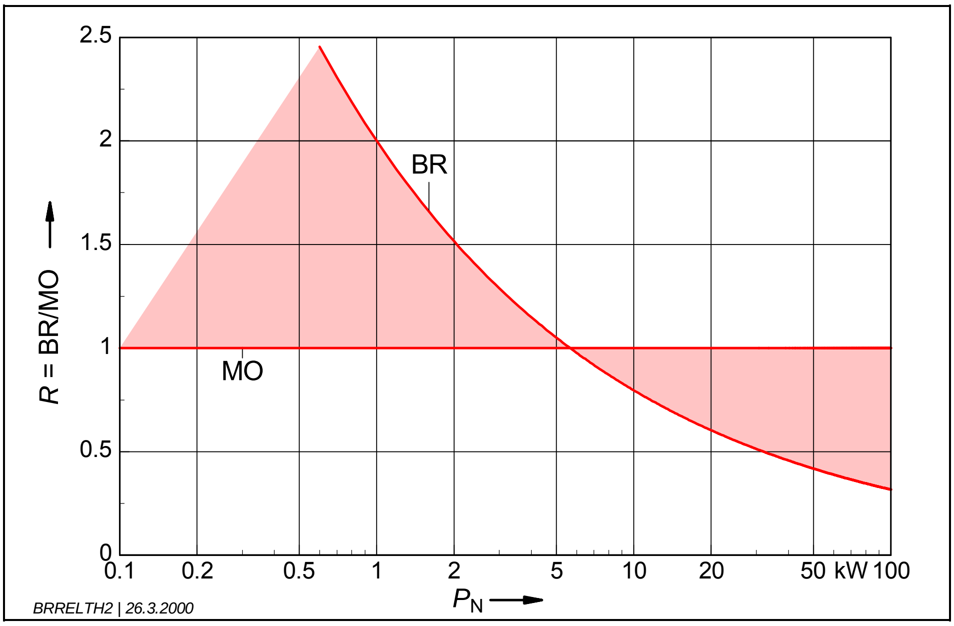

Fig. 41.2.2 Relationship *R* between the thermally permissible switching frequency limit of 4-pole motors (MO) with a rated output P_N and their standard brakes (BR) (motor = set at 1)

The following rules can be established from the graph:

- ***the thermal recalculation for the motor is sufficient for rated outputs up to approximately 5.5 kW – the standard brake will not be jeopardized.***
- ***The thermal utilization of the brake must be recalculated above a rated output of approximately 5.5 kW. The standard brake should be replaced with a switching brake of a type with a higher switching capacity once the limit value has been reached.***

41.3 Reduction of the mechanical switching energy by electrical switching measures

Without attempting to provide a general rule, Fig. 41.2.2 shows that the permissible switching frequency of the brakes for small and medium motor outputs is so high that it is practically never usable and that the switching frequency limit of the motors is generally lower. However the brake suited to the particular torque permits a relatively low number of switching operations for rated outputs at the upper end of the range shown; moving up to the next size of brake does not significantly increase this number. The task in such cases is to ***reduce*** the ***switching energy*** to such an extent that the working capacity of the brake is not overtaxed. According to the equation given in section 41.1, it is possible to reduce the speed under certain drive conditions – e.g. by pole-changing.
The degree to which the brake is spared is considerable since the loading decreases in proportion to the ***square*** of the speed as shown in Fig. 41.3.1.

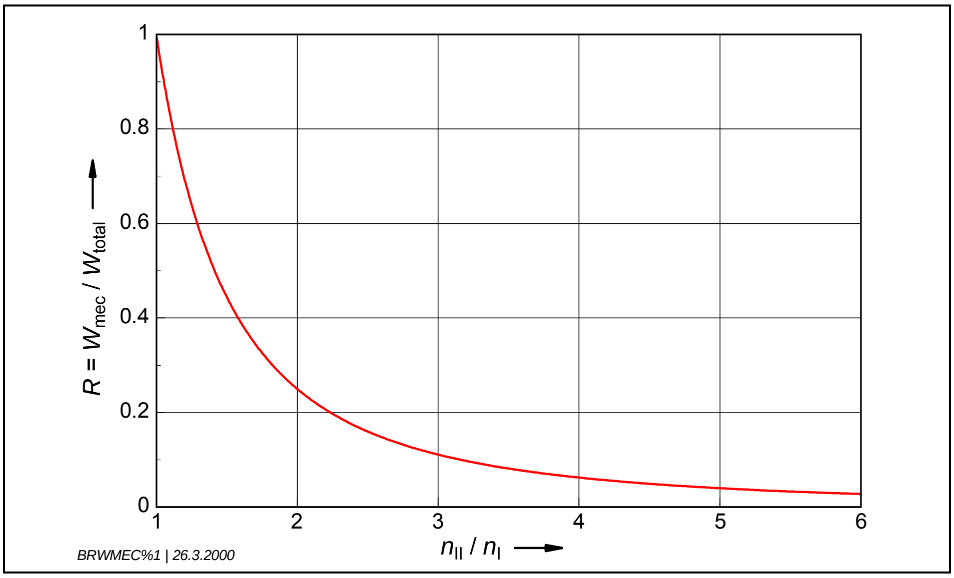

Fig. 41.3.1 Mechanical residual switching energy with electrical speed change operations from a high speed n_{II} to a low speed n_{I}

Fig. 41.3.2 shows the torque characteristics of a pole-changing three-phase induction motor in the ratio of 1:2 for hyper-synchronous braking.

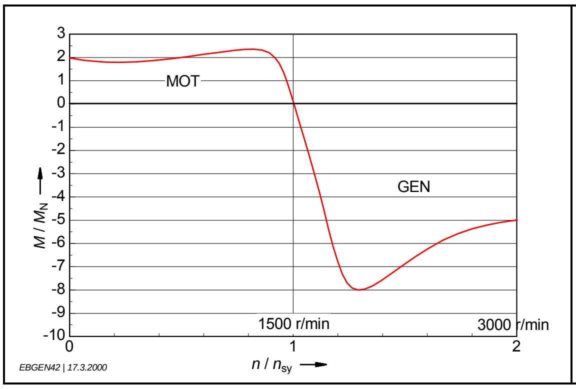

Fig. 41.3.2
Characteristics of the regenerative braking torque for a speed-reduction operation on a pole-changing motor in Dahlander delta/double-star connection from the high speed to the low speed

With this ***combination of electrical and mechanical braking*** it must be checked whether the relatively high regenerative braking torques can be transferred by the drive system without causing damage. Furthermore, it should be borne in mind that the relief on the brakes naturally comes at the expense of increased thermal loading on the motor (see also [5.3]).

41.4 Switching energy per friction element

The friction elements (friction disc, friction plates) are worn due to the total friction energy on brakes with a high switching frequency. This causes the working air gap to increase slowly. The amount of relief on the compression springs and the resulting reduction in the braking torque are negligible. The magnetic field is weakened with a limit air gap – in the order of 1 ... 2 mm, for example – to such an extent that the magnet's power of attraction will no longer be sufficient to ensure that the brake is released if the air gap increases any more. This process does not impair safety as the brake will continue to be braked, only it will no longer be possible to release the brake. Depending on the type of design, the air gap will have to be adjusted or the brake disc replaced to restore the air gap to its original size – e.g. approximately 0.25 mm.

If one terms the switching energy up to the point where the limit air gap is reached as W_L, the ***service life of the friction element*** is calculated as follows:

$$Z_L = \frac{W_L}{W}$$

$$t_L = \frac{Z_L}{Z}$$

Z_L - number of braking operations until the limit air gap is reached
W_L - working capacity per friction element in Nm = Ws = J
W - switching energy per switching operation in Nm = Ws = J
t_L - service life of the friction element in operating hours (h)
Z - average number of braking operations per hour (c/h)

The ***average value*** for Z that is decisive in terms of ***wear*** must be used to calculate the ***entire operating life*** since we are dealing here with wear.
It is recommended that you have the limit value thus calculated/checked by the manufacturer who will be able to take actual operating conditions into account. This applies for the thermally permissible switching frequency of the motor and the mechanically permissible switching frequency of a gear unit.
Fig. 41.4.1 should serve to point out that specifications of the "service life" of brakes vary a great deal from manufacturer to manufacturer.

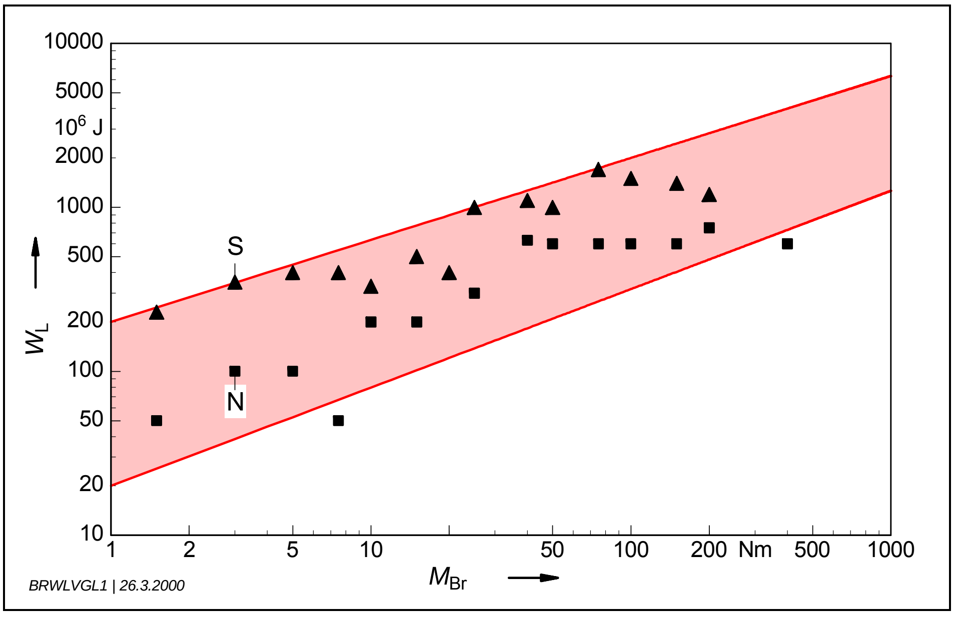

Fig. 41.4.1 Catalogue specification of six different manufacturers for the working capacity W_L of mechanical brake compared with Danfoss Bauer series 2000 brakes
■ - standard brakes N
▲ - switching brakes S

Guide values for the working capacity of Danfoss Bauer series 2000 spring-loaded brakes are given in Fig. 41.4.2.

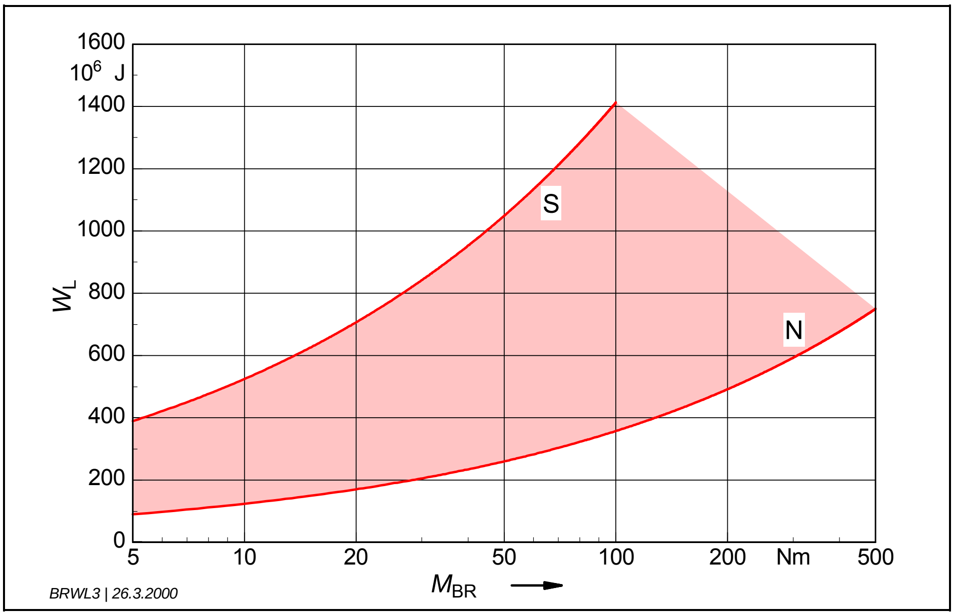

Fig. 41.4.2 Guide values for the permissible braking energy W_L until the friction linings must be changed for Danfoss Bauer series 2000 spring-loaded brakes
N - standard brakes
S - switching brakes

Recalculation using the values of the actual brake employed is recommended in each case (see Appendix).
Guide values for the permissible switching frequency can be obtained from Fig. 41.4.3 for certain marginal conditions (e.g. service life expectancy t_L = 4000 h, factor of inertia *FI* = 1).

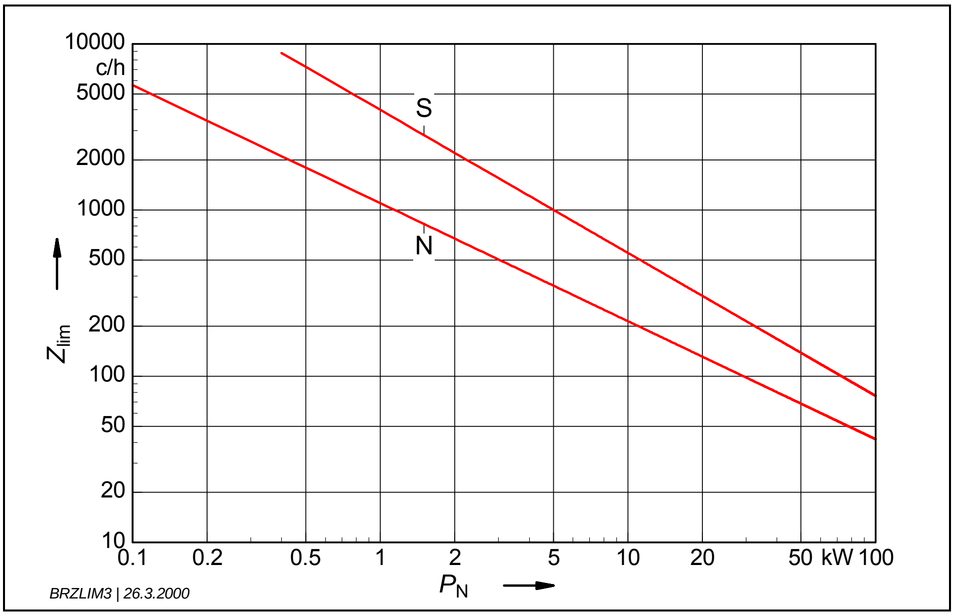

Fig. 41.4.3 Guide values for the permissible switching frequency Z_{lim} of 4-pole IP65 motors with a friction lining service life expectancy of approx. 4000 h
N - standard brakes with ideal braking torque
S - switching brakes with maximum working capacity

41.5 Reduced number of springs

The braking torque and working capacity can be ideally matched to the prevailing operating conditions by reducing the number of compression springs.

Fig. 41.5.1
Brake with a max. of 4 springs

Type series
E003B

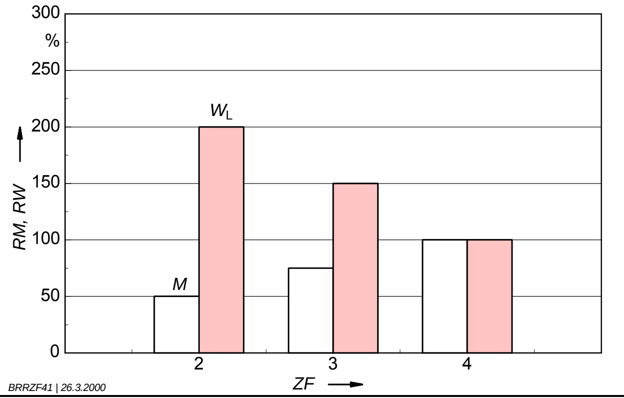

Fig. 41.5.2
Brakes with a max. of 5 springs

Type series
E008B Z008

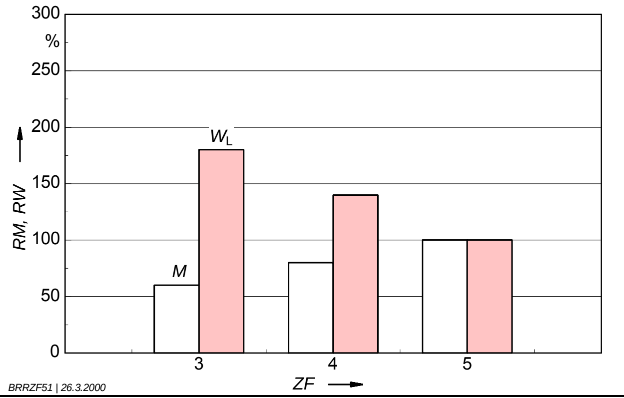

Fig. 41.5.3
Brakes with a max. of 6 springs

Type series
E005 Z005
E010 Z010
E015 Z015
E025 Z025

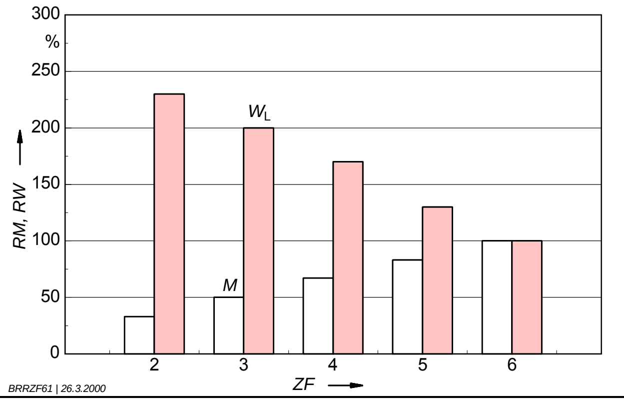

Fig. 41.5.4
Brakes with a max. of 8 springs

Type series
E050 Z050
E075 Z075
E100 Z100
E150 Z150

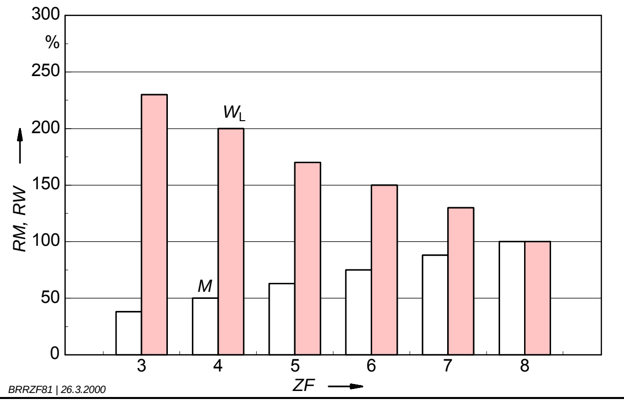

ZF - number of compression springs
RM - relative braking torque
RW - relative permissible starting energy until replacement is necessary

42 Wear

Mechanical brakes, by their very nature, are subject to wear.
How much wear is "normal" – and how does wear affect the function of the brake?
Most manufacturers specify a "working capacity" for their brakes, after which the friction elements must either be ***adjusted*** or ***replaced***. Since the work performed per braking operation is determined to a large extent by the moment of inertia ($W = J\omega^2/2$), the service life can only be expressed in number of switching operations, provided that the moments of inertia (masses and linear speeds) are known. The method of calculation is explained in section 10. The features that characterize the end of the service life and the measures required to restore the brake to its original condition are of interest in terms of maintenance. The magnetic resistance in the solenoid circuit will increase if the air gap a shown in Fig. 42.1 increases significantly due to wear on the friction disc. The magnetic flux decreases and the releasing force decreases in proportion to the square of the magnetic flux. The brake will be ***sluggish to release*** and finally it will not release at all.

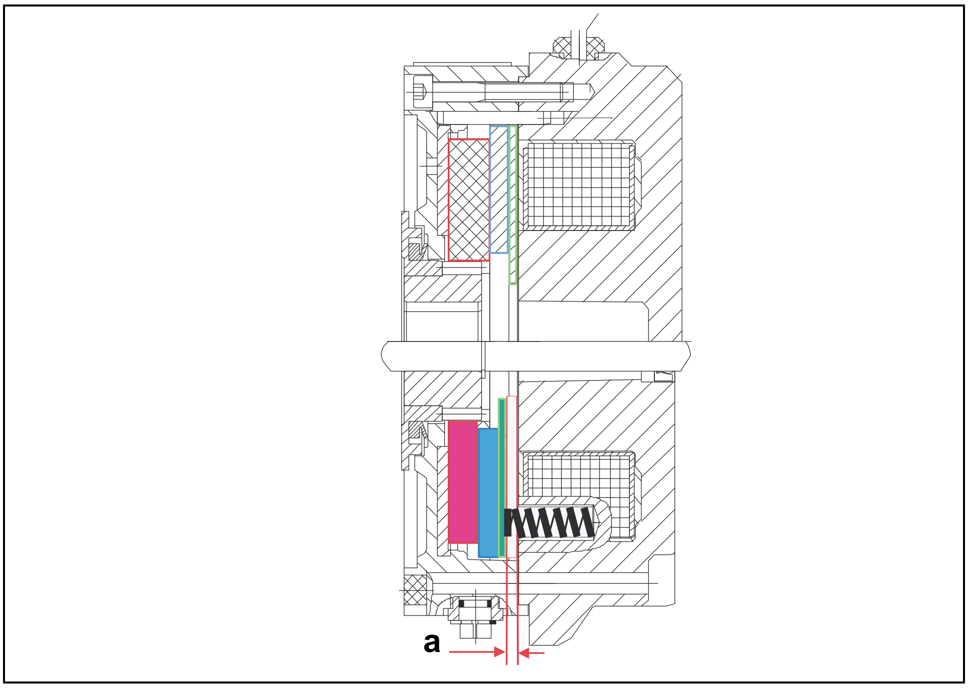

Fig. 42.1 Section through a single-disc spring-loaded brake with D.C. solenoid release
Top: new condition Bottom: increased working air gap

Adjustment measures to compensate for wear have not been considered for the example in Fig. 42.1. The air gap on this brake may be between 1.5 ... 2 mm depending on the brake size. The friction disc is relatively easy to change once the brake has been dismantled– with ***built-on brakes***, this can be carried out in the workshop if time is not an issue and a ***replacement brake*** is available.
Since the springs (F) are ***pre-tensioned***, the release in tension corresponding to the degree of wear (Δs) will cause a slight decline in the braking torque ΔM of approximately 10 ... 15 % (Fig. 42.2). The brake's function as a safety brake is therefore not impaired by wear and most applications do not require "adjustment" to compensate for the braking torque.
A clear distinction should be drawn between the terms "adjustment" (to compensate for wear) and "setting" (to alter the braking torque).

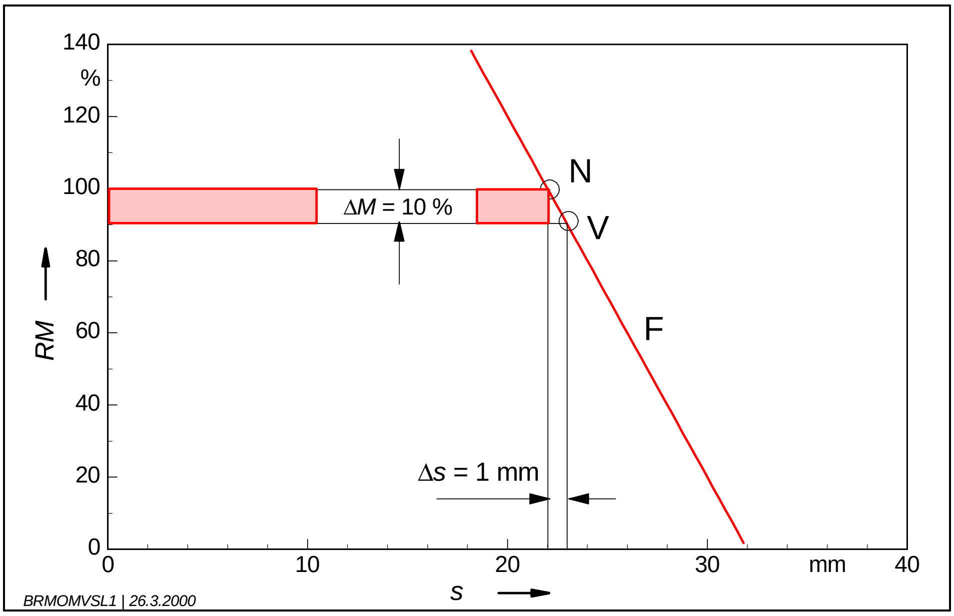

Fig. 42.2 Reduction of the braking torque Δ*M* due to a decline in the spring force (F) from the new condition (N) to the wear point (V) as a result of wear Δ*s*

Fig. 42.3 shows the principle of a multiple-disc brake with an adjustment facility to compensate for wear. If the overall thickness *b* of the friction elements (1) decreases by the amount of wear Δ*b* and the distance between the armature plate (2) and the solenoid casing (3) increases, the magnet has to overcome the increased air gap (*a* + Δ*b*). To compensate for wear, the “adjustable thrust plate” (4) should be adjusted as necessary on the outside diameter using its thread.
This is an example of different possible design solutions, from “automatic self-adjustment” to mini locking mechanism to precision-machined pins. The effectiveness of these interesting design solutions must be assessed by their performance in practice under the influence of corrosion, temperature and fouling. In any case, the brake must be partially dismantled to operate the wear adjustment mechanism in the example shown and it may be necessary to make the thread accessible on the major diameter.

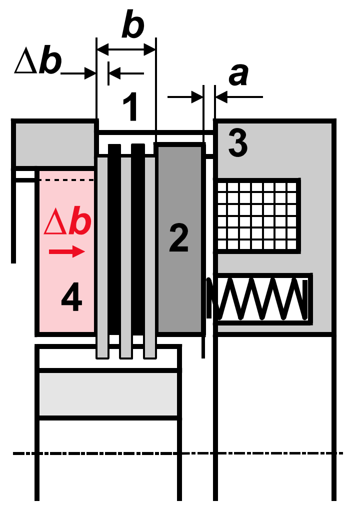

Fig. 42.3
Example of a multiple-disc spring-loaded brake with adjustment facility to compensate for the increased working air gap *a* caused by wear Δ*b* (in accordance with VDI 2241 Sheet 1)

43 Braking time

The pure braking time from the start of the mechanical braking operation to rest is determined by the ***rate of deceleration***. This is given by

$$\alpha = \frac{M_a}{J}$$

α	-	angular deceleration
M_a	-	deceleration torque
J	-	mass moment of inertia

43.1 Deceleration

Fig. 43.1 shows a simplified representation of the braking torque of a disc brake recorded using an x-y plotter against the speed. It shows a practically constant braking torque from the start to the end of the braking operation, i.e. over the entire speed range. We can therefore expect a practically constant rate of deceleration.

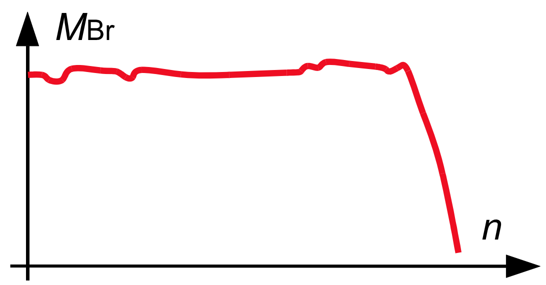

Fig. 43.1
Braking torque (M_{Br}) during the braking process, recorded with an *x-y* plotter against the speed (*n*)

If we accept the above assumptions, the deceleration time or braking time is calculated as

$$t_a = \frac{\omega}{\alpha}$$

t_a	-	deceleration time
ω	-	angular velocity
α	-	angular deceleration

This gives us the main basis of comparison in standard units

$$t_a = \frac{J \cdot n}{9{,}55 \cdot M_a}$$

t_a	-	deceleration time in s
J	-	mass moment of inertia in kgm^2
n	-	speed in r/min
M_a	-	deceleration torque in Nm

It must be ascertained whether the load torque assists or counters the braking, particularly with ***lifting duty***, but also with other drive applications. The following applies:

$$M_a = M_{Br} \pm M_L$$

M_a	-	deceleration torque
M_{Br}	-	nominal torque of the friction brake
M_L	-	braking (+) or driving (–) load torque

Figs 43.2 and 43.3 shows the different retardation effects for raising and lowering a load.

43.2 Lifting duty

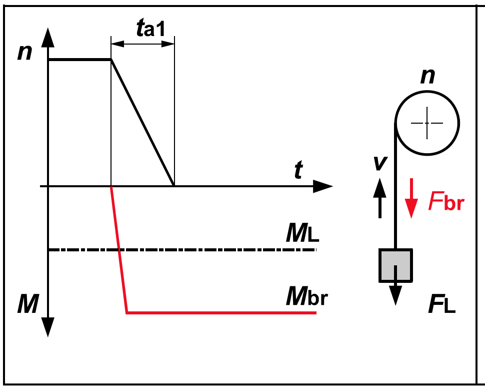

Fig. 43.2
Braking operation for raising a load

The load torque M_L and braking torque M_{Br} have a retarding effect, resulting in a deceleration torque when lifting

$$M_a = M_{Br} + M_L$$

The braking time for lifting duty is given by

$$t_a = \frac{J \cdot n}{9{,}55\left(M_{Br} + M_L\right)}$$

43.3 Lowering duty

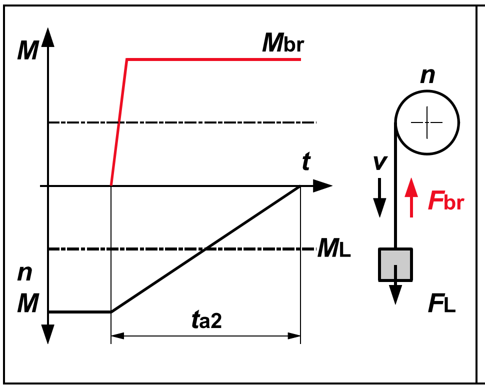

Fig. 43.3
Braking operation for lowering a load

The load torque M_L has an accelerating effect, the braking torque M_{Br} has retarding effect, resulting in a deceleration torque when lowering

$$M_a = M_{Br} - M_L$$

The braking time for lowering duty is given by

$$t_a = \frac{J \cdot n}{9{,}55\left(M_{Br} - M_L\right)}$$

ta - braking time in s
J - mass moment of inertia in kgm²
n - speed in r/min
M - torque in Nm

44 Overtravel time

The total overtravel following the "stop" command until the motor comes to rest comprises two main components, each of which has its own tolerance.

44.1 Response time

The response time as described in section 38 is not affected by the loading conditions and is practically constant. This component can be relatively large. It can be ***eliminated*** relatively easily by bringing the "off" command forward where the control system functions according to travel or time. The inherent delay in switchgear must be taken into account where there is an extreme requirement on stopping accuracy. According to the specifications of one competent switchgear manufacturer, A.C.-operated contactors have a tolerance of approximately 10 ms in their mechanical switch-off times. The scatter band for arcing times is of roughly the same magnitude. Consequently, deviations of 10 ... 15 ms in the switch-off time of a contactor cannot be avoided.
These guide values apply to the small control contactors commonly used in the brake circuit. The opening delay may be even greater if the auxiliary contacts of the mains contactor are used. Final values can be obtained from the switchgear manufacturer's documentation.
Particular attention must be paid to the ***selection of the control unit*** if particularly short or tightly toleranced response times are required.

44.2 Braking time

The equation for calculating the braking time is given in section 43.

44.3 Overtravel time

$$t_N = t_A + t_a$$

t_N - overtravel time
t_A - response time
t_a - braking time

Fig. 44.3 shows an example application where the shortest possible and most tightly toleranced overtravel time is required. The "off" command for the dosing augers is given by the scales. Any excess feed speed results in overfilling and lost product.

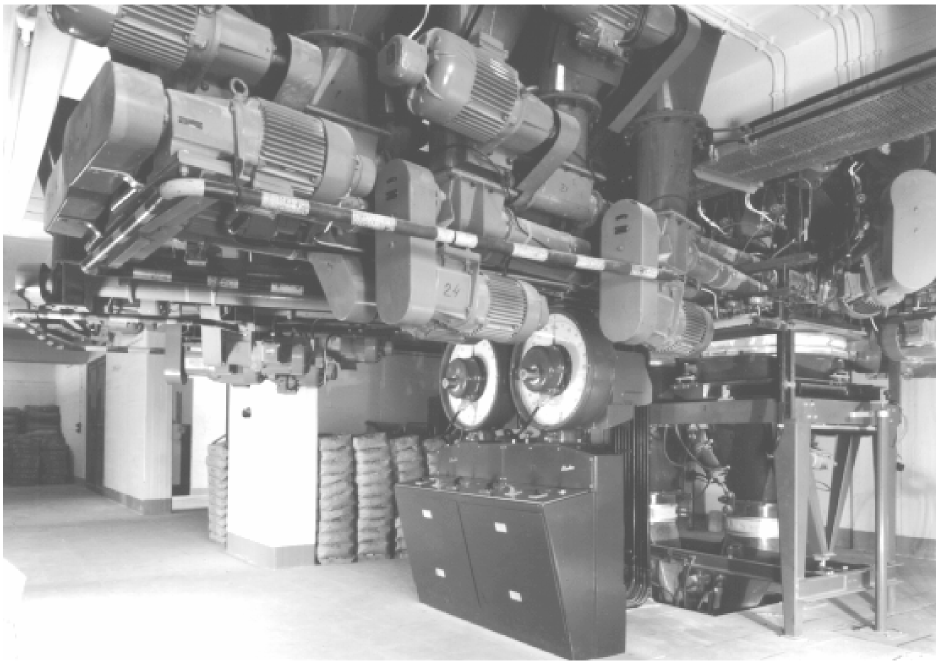

Fig. 44.3 Metering screws for filling and fine feed; friction brakes with a short overtravel time prevent unwanted overfilling

45 Overtravel distance

The total overtravel distance following the "stop" command before the motor comes to rest comprises two main components, each of which has its own tolerance:

- Overtravel during the brake application ***response time*** (see section 38). This component may be very pronounced, particularly with larger brakes and if special circuitry is not fitted. The travel component is particularly large since the ***full*** linear speed is present over this period and even ***increases*** in the case of lowering duty.
- Overtravel during the ***braking time*** (see section 43). If deceleration is uniform, as is assumed for mechanical brake, ***half*** the linear speed is expected as an average through this period.

45.1 Translation

The overtravel distance for linear motion is calculated as follows:

$$s_N = t_A \cdot v + \frac{t_a \cdot v}{2}$$

s_N - overtravel distance in m
t_A - response time in s (in accordance with section 38)
t_a - braking time in s (in accordance with section 43)
v - linear speed in m/s at the start of braking

Fig. 45.1 provides guide values for the overtravel distance of driven machinery (conveyor system) with a linear speed of 0.1 m/s using a 4-pole three-phase motor with a standard brake.

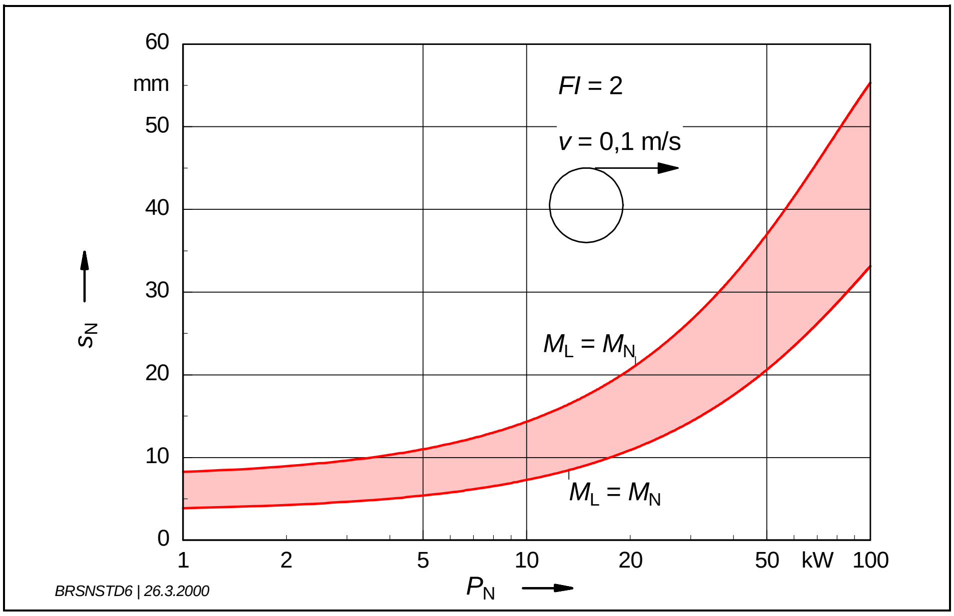

Fig. 45.1 Guide values for the overtravel distance when braking from v = 0.1 m/s using a 4-pole three-phase motor with a standard brake; FI = 2

A different solution must be sought if calculations indicate that the limit value for the overtravel distance will be attained or exceeded once the tolerance has been taken into account (section 47). An increase in the braking torque is not an indication of success the braking travel component of the total travel is relatively low since the overtravel also increases during the response time in the case of larger brakes with higher braking torques.

In Fig. 45.2 contains a graph showing how a ***reduction in the linear speed*** – e.g. by pole-changing or by frequency adjustment– can ***significantly improve positioning***.

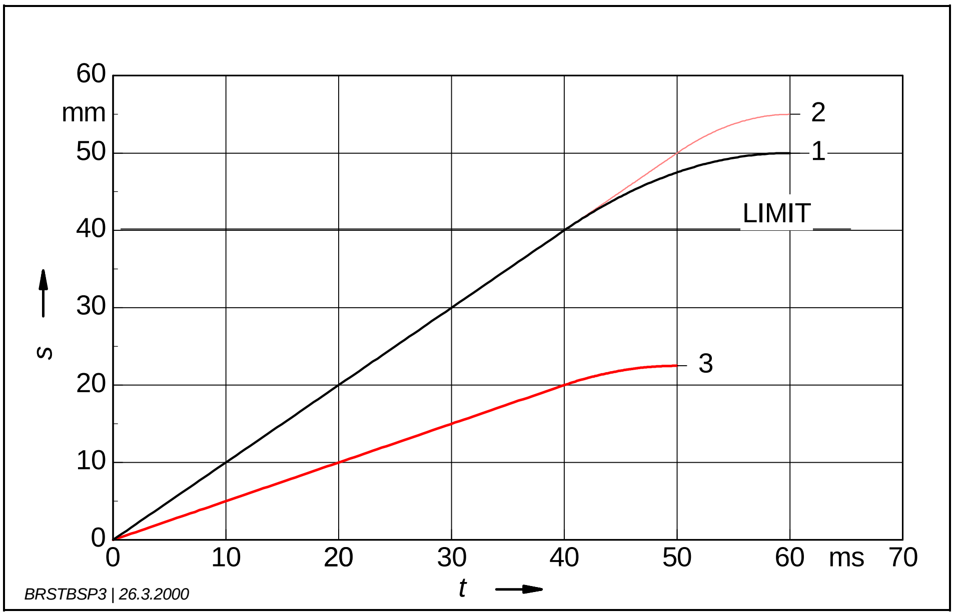

Fig. 45.2 Travel/time graph for a braking operation from v = 1 m/s

Solution 1:	M_{Br} = 100 %	t_A = 40 ms	t_a = 20 ms	v = 1 m/s
Solution 2:	M_{Br} = 200 %	t_A = 50 ms	t_a = 10 ms	v = 1 m/s
Solution 3:	M_{Br} = 100 %	t_A = 40 ms	t_a = 10 ms	v = 0.5 m/s

45.2 Rotation

The overtravel distance for rotary motion is calculated as follows:

$$\varphi_{N1} = 6 \cdot n_1 \cdot t_A + 3 \cdot n_1 \cdot t_a = 3 \cdot n_1 \cdot (2 \cdot t_A + t_a)$$

$$\varphi_{N2} = \frac{\varphi_{N1}}{i} = \varphi_{N1} \cdot \frac{n_2}{n_1}$$

φ_{N1} - overtravel distance of the rotor shaft in °
φ_{N2} - overtravel distance of the output shaft in °
n_1 - speed of the rotor shaft in r/min
n_2 - speed of the output shaft in r/min
i - gear reduction ratio
t_A - response time in s (section 38)
t_a - braking time in s (section 43)

Guide values for the overtravel distance of 4-pole three-phase motor with standard brakes for run-out braking or with enlarged brakes for lifting duty as in section 45.1.

46 Benefits of a modular system

Section 34 discussed in detail the benefits of the “built-on brake” principle for the ***user***. However, a modular principle also offers the ***designer*** of a machine or system the benefit of being able to choose freely from several brake variants, each of which is tailor-made for a specific application, rather than being restricted to one built-in brake. This should become clear from the example of a D09-size motor (corresponds to a standard shaft height of 90).
The diagram in Fig. 46.1 is to scale and shows that six different brake sizes can be mounted. The size and weight – compared to the motor – give an indication of the relationships between working capacity and price.

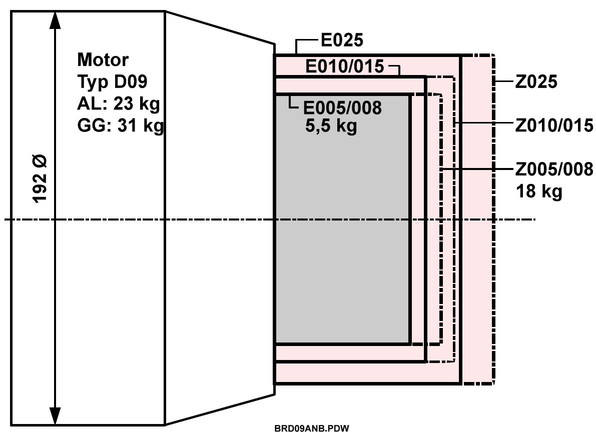

Fig. 46.1
Relationship between the size and weight of the D09 (AH 90) motor and its six mountable brakes

Forty variants are actually possible according to Table 46.3 since the brake torque can be reduced in relation to the rated torque on each of the six brakes; each variant can be supplied as part of the modular system for the D09 motor. This table is an extract from the Danfoss Bauer’s full spring-loaded brake manufacturing and options program (see appendix A1).

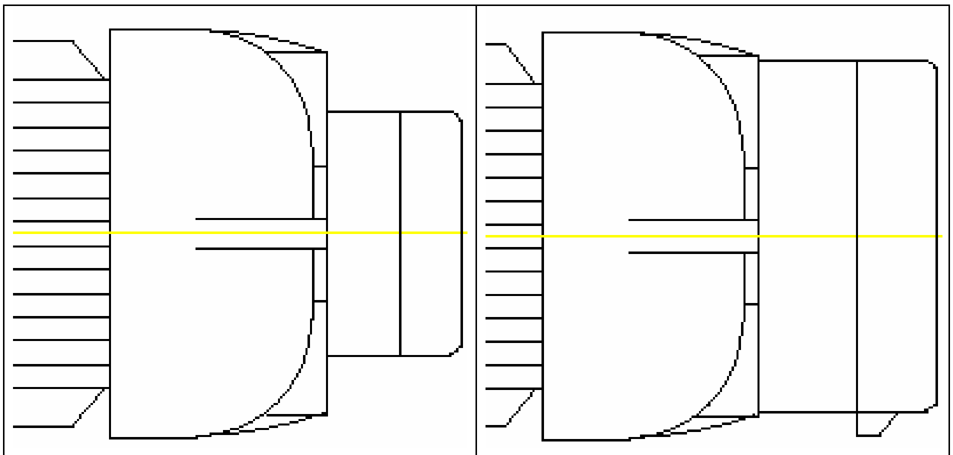

E 005 brake; 1.5 ... 5 Nm	Z 025 brake; 25 ... 50 Nm

Fig. 46.2 Comparison of the smallest and largest built-on brake on a D09 motor

MOT	BR type	M_{BR}	P_{el}	W_{max}	W_{th}	W_L	t_A	t_{AC}	t_{DC}	*ZF*
		Nm	W	10^3 J	10^3 J	10^6 J	ms	ms	ms	
D09	E..005A2	1.5	25	50	250	230	15	140	22	2
D09	E..005A4	2.5	25	50	250	200	35	110	15	3
D09	E..005A6	3	25	50	250	170	45	100	15	4
D09	E..005A8	4	25	50	250	130	50	100	15	5
D09	E..005A9	5	25	50	250	100	60	100	15	6
D09	E..008A6	4.5	25	50	250	90	60	70	10	3
D09	E..008A8	6	25	50	250	70	70	45	7	4
D09	E..008A9	7.5	25	50	250	50	80	45	7	5
D09	E..010A4	5	45	50	350	400	90	200	10	3
D09	E..010A6	6.5	45	50	350	330	90	200	10	4
D09	E..010A8	8	45	50	350	270	90	200	10	5
D09	E..010A9	10	45	50	350	200	90	200	10	6
D09	E..015A4	7.5	45	50	350	400	90	200	10	3
D09	E..015A6	10	45	50	350	330	90	200	10	4
D09	E..015A8	12	45	50	350	270	90	200	10	5
D09	E..015A9	15	45	50	350	200	90	200	10	6
D09	E..025A4	12.5	70	75	450	600	100	400	20	3
D09	E..025A6	16	70	75	450	500	100	400	20	4
D09	E..025A8	20	70	75	450	400	100	400	20	5
D09	E..025A9	25	70	75	450	300	100	400	20	6
D09	Z..005A2	25	3.3	50	250	350	15	140	22	2
D09	Z..005A4	25	5	50	250	300	35	110	15	3
D09	Z..005A6	25	6.5	50	250	250	45	100	15	4
D09	Z..005A8	25	8	50	250	200	50	100	15	5
D09	Z..005A9	25	10	50	250	150	60	100	15	6
D09	Z..008A6	9	25	50	250	180	60	70	10	3
D09	Z..008A8	12	25	50	250	140	70	45	7	4
D09	Z..008A9	15	25	50	250	100	80	45	7	5
D09	Z..010A4	12.5	45	50	350	600	90	200	15	3
D09	Z..010A6	16	45	50	350	500	90	200	15	4
D09	Z..010A8	20	45	50	350	400	90	200	15	5
D09	Z..010A9	25	45	50	350	300	90	200	15	6
D09	Z..015A4	15	45	50	350	400	90	200	15	3
D09	Z..015A6	20	45	50	350	330	90	200	15	4
D09	Z..015A8	25	45	50	350	270	90	200	15	5
D09	Z..015A9	30	45	50	350	200	90	200	15	6
D09	Z..025A4	25	70	75	450	800	100	400	20	3
D09	Z..025A6	32	70	75	450	670	100	400	20	4
D09	Z..025A8	40	70	75	450	530	100	400	20	5
D09	Z..025A9	50	70	75	450	400	100	400	20	6

Table 46.3 **Spring-loaded brakes mountable on a D09-size motor**

MOT - motor size
BR type - brake type
P_{el} - power consumption of the solenoid in W
M_{BR} - braking torque in Nm
W_{max} - permissible switching energy for a single braking operation in 10^3 J
W_{th} - thermally permissible switching energy per hour in 10^3 J
W_L - permissible switching energy before the friction disc(s) must be replaced in 10^6 J
t_A - brake release response time in ms
t_{AC} - brake application response time with A.C.-side break in ms
t_{DC} - brake application response time with D.C.-side break in ms
ZF - number of compression springs
[grey box] - preferred brake type

One may wonder whether the extraordinarily large range of nominal braking torques available, i.e. 1.5 ... 50 Nm, for the D09 motor frame size is even ***technically wise***. Fig. 46.4 provides the answer:
The rated torques of 4-pole motors in the D09 frame size designed for S1 continuous running duty S1 in the 7.5 ... 15 Nm range are marked CAT (S1, 2p = 4) in the chart. A rated motor torque of 20 Nm is achieved with special designs for S2 short-time duty or S3/S6 intermittent periodic duty. In addition, a brake rated at 40 Nm is required for lifting duty – marked SPEC (S2 HUB) in the chart.
The lower end of the range required is marked by a positioning motor with a speed ratio of 1:6 (12/2 pole-changing). The smallest listed motor power is 0.063/0.4 kW with an associated rated torque of 1.29/1.36 Nm. The braking torque should not be greater than about 1.5 Nm to give soft run-out braking.

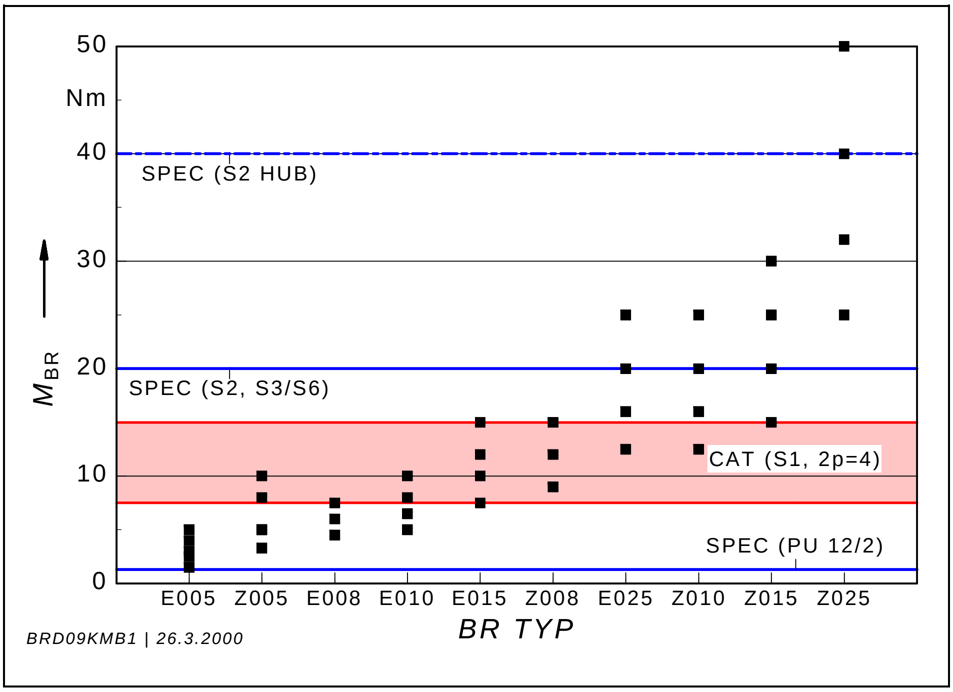

Fig. 46.4 Mountable brake for D09 motors
Brakes (BR TYP) and braking torque (M_{Br}) offered
Requirements caused by the design width of the motor

CAT (S1, 2p=4) - 4-pole catalogue types for S1 duty type
SPEC (S2, S3/S6) - special types for S2, S3 and S6 duty types
SPEC (S2 HUB) - special types for S2, S3, S6, and lifting duty types
SPEC (PU 12/2) - special 12/2-pole-changing type

47 Working capacity of large brakes

If the size of a spring-loaded brake is only determined according to the nominal braking torque required, the recalculation for the standard power range of geared motors of approximately 0.1 to 100 kW highlights an interesting trend. While there is generally no problem achieving an acceptable brake service life on drives with relatively low rated outputs (below approximately 10 kW), even at high switching frequencies (e.g. several hundred switching operations per hour), caution is called for with ***larger rated outputs***.
Fig. 47.1 shows the relative permissible switching frequency of brakes with nominal torques determined using the equation given in section 40.2. The switching frequency has been calculated to produce the same lifetime or service life for the brake discs. If one sets the permissible switching frequency of a brake motor with a rated output of 1.1 kW operating under such conditions at 1, approximately five times this switching frequency is permissible for a 0.1 kW motor. By contrast, a motor with a rated output of 100 kW would permit only about 4 % of the switching frequency of the 1.1 kW motor. This large difference can be explained by various physical influences superimposed on top of one another. For instance, the mass moment of inertia of rotors on three-phase induction motors increases super-proportionally in relation to the rated output.

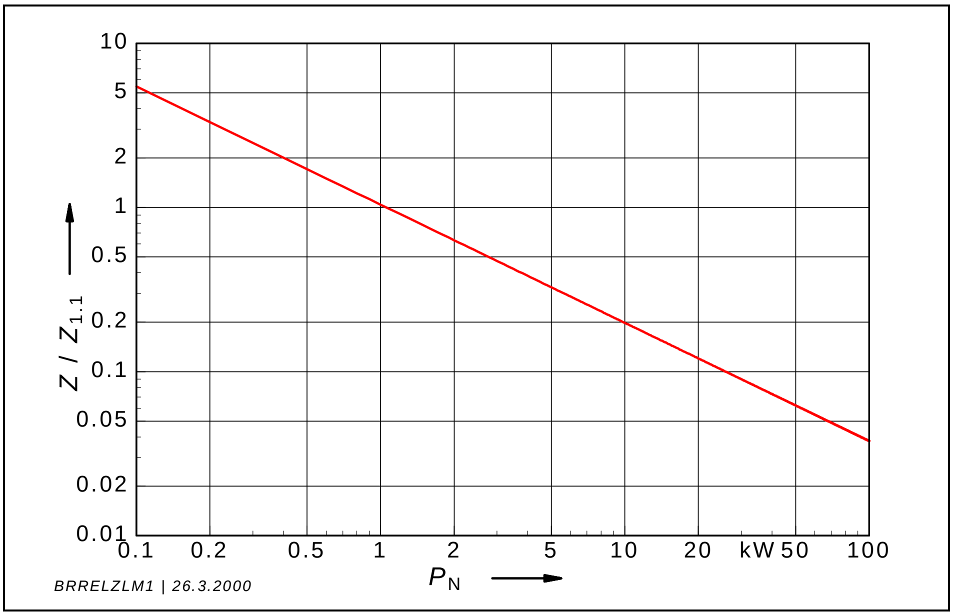

Fig. 47.1 Relatively permissible switching frequency of standard brakes on motors with a rated output of P_N for the same calculated service life

If one forms a "per-unit rotor mass moment of inertia", i.e. a value representing kgm^2/kW, Fig. 47.2 demonstrates that the 100 kW motor requires seven times the rotor mass of that required by the 1.1 kW "unit" motor to generate a 1 kW rated output. This relatively large mass must be accelerated and decelerated during switching duty and limits the permissible switching frequency. The ***work-causing mass*** of the drive ***increases super-proportionally***, whereas the "working capacity" of a series of spring-loaded brakes falls far short of increasing in proportion to their nominal torque (i.e. to the rated output of the assigned motor).

Fig. 41.4.2 highlights that a brake rated for 100 Nm has only about three times the working capacity of a brake rated for 10 Nm. This is due to the fact that the friction area (i.e. that wear volume available) in a brake series increases far less than the nominal torque of the brake.

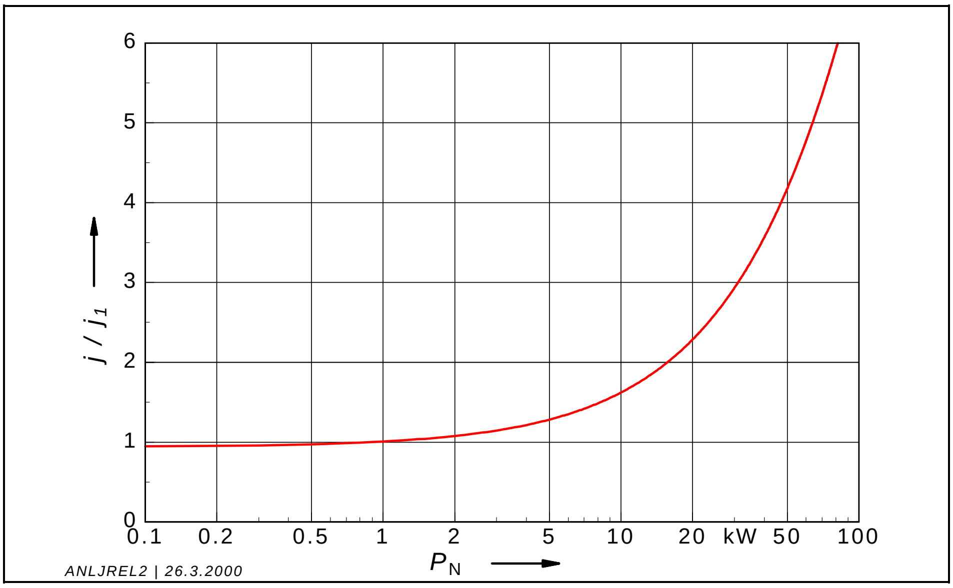

Fig. 47.2 Per-unit rotor mass moment of inertia

Fig. 47.3 shows this relationship once more in the form of per-unit variables, i.e. using a surface/braking torque value (cm^2/Nm), in relation to the 10 Nm "unit" brake. According to this graph, the wear volume available per torque unit decreased to approximately one third if the nominal torque of the brake within the type series increases from 10 to 100 Nm.

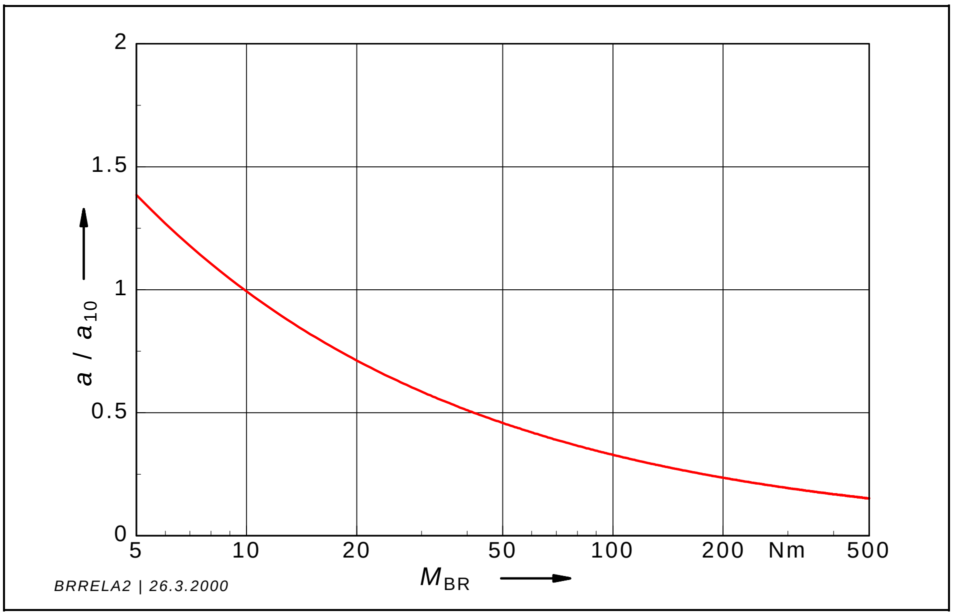

Fig. 47.3 Per-unit friction area of disc brakes compared to a brake with a nominal toque M_{BR} = 10 Nm

These observations demonstrate that careful recalculation is called for, especially ***with large drive unit*** and that the electrical ***speed-reduction devices*** discussed in section 41.3 can prove particularly important. A further cost-effective and reliable solution is possible if the maximum available braking torque of a particular frame size is not exploited to the full or where a single-disc brake is expanded to form a ***double-disc brake*** with double the working capacity for half the spring pressure, i.e. a constant working capacity.

VI POSITIONING

48 General remarks on positioning

If one compares the scopes of supply of geared brake motors designed for classic applications of “lifting drives” with the large number of motors used, for example, in materials handling for “positioning”, the significance of this latter field of application will become clear. This section deals therefore with the basic principles and with common solutions.
The development of electric drives shows a clear trend towards more frequent switching and to greater precision in the positioning of the load. Previously, motors were designed for continuous operation and the conveyed material or the driven tools were controlled by mechanical systems which provided stepwise movement. Nowadays, braked motors can be ***accurately positioned by a combination of braking and pulse control.***
This development is particularly in evidence with servo drives and stepper motors, such as are required in present-day robotics. However, positioning drives are also used in the peripherals of these “robots”.
Starting, braking and positioning – these are important aspects of the duties required of electric drives in the context of automation and rationalization.

Where very high speeds and extremely accurate stopping positions are required, motors with ***steplessly adjustable speeds*** are used. For example, D.C. shunt motors with a controllable armature voltage or three-phase inverter motors where the frequency is varied by a static inverter.
The speed can be "reduced" to the positioning speed by a setpoint generator.
The cost of this modern solution is justified if one bears the overall cost in mind.

A declining field of application remains for the conventional solution using a pole-changing three-phase motor with ***fixed speed stages*** in a maximum ratio of 10:1, controlled by conventional switchgear components.
Switching from the high speed to the low speed is a consequence of regenerative braking, whereby the positioning speed is achieved within very tight tolerances without incurring any controller or regulator costs. The switch-over times and travel distances are extremely short, which is highly beneficial in terms of rationalization. However, a transport process which is completely jolt-free and has a slower rate of deceleration is often necessary where sensitive products are to be moved – see section 2.
Mechanical braking and stopping from the positioning speed is provided by an auxiliary spring-loaded mechanical brake. This also works as a safety brake, securing the load in a stationary position in the event of a power loss.
Since the movements in transportation and robotics occur at relatively low speeds – usually at less than about 1.5 m/s – correspondingly low speeds are required of the drive unit. Such low speeds cannot generally be provided by standard three-phase motors. Reduction gearing must therefore be connected after the electric motor. This is integrated into the motor to simplify the mounting process and to save space to form a single unit – the geared motor.
Pole-changing positioning geared motors and inverter-fed geared motors are used in materials handling and robotics systems.
Figs 48.1 to 48.3 show three of many possible applications.

Fig. 48.1
Vertical conveyor for car bodies
Pole-changing motor in the ratio 1:6; with spring-loaded brake and (covered) square shaft end for setting up; reserve drive ready

(Manufacturer:
STOTZ KRÄMER GmbH)

Fig. 48.2
Electric monorail (EHB) with 1:4 pole-changing geared motors

(Manufacturer:
TRANSLIFT WHYLEN)

Fig. 48.3
Palleting machine for cement sacks
Bevel-geared motor with controlled synchronization of the four drive units; pole-changing 1:6

(Manufacturer: BEUMER)

49 Tolerances

The overtravel consistency is often demonstrated at exhibitions and trade fairs by having magnetic or optical pulses from a perforated disc rotating with the rotor read by an electronic counter. The tolerance generally remains in the range of a few per thousand over the period of observation. One should pose the critical question of why there should be any significant deviations at all under the constant conditions of the short period of observation. The warm-up condition and temperature of the friction linings together with all other marginal conditions should not cause any deviations. However, any alteration in the overtravel tolerance over the ***course of the brake's service life*** may be decisive for the function of a drive system – i.e. under the highly changeable conditions of roughness, wear, temperature, humidity etc.
If one takes all influences into account, a ***tolerance for braking torque and braking travel of approximately ±25 %*** must be expected to allow for an adequate safety margin.
This relatively large tolerances can be better understood if one considers the parameters acting on the mating friction surfaces (see section 49.2).

49.1 Drive

The following well-known equation is used to calculate the synchronous speed of a three-phase induction motor:

$$n_{sy} = \frac{60 \cdot f}{p}$$

n_{sy} - synchronous speed in r/min
f - frequency in Hz
p - number of pole pairs

As the frequency of public mains supplies hardly deviates from a setpoint value of 50 Hz, the synchronous speed is also practically constant. The actual speed alters as a function of the load-dependent slip: The actual speed is lower than the synchronous speed in motoring mode and higher than the synchronous speed in generating mode.
Fig. 49.1 shows the torque-speed characteristic curve with the values relevant to this discussion.

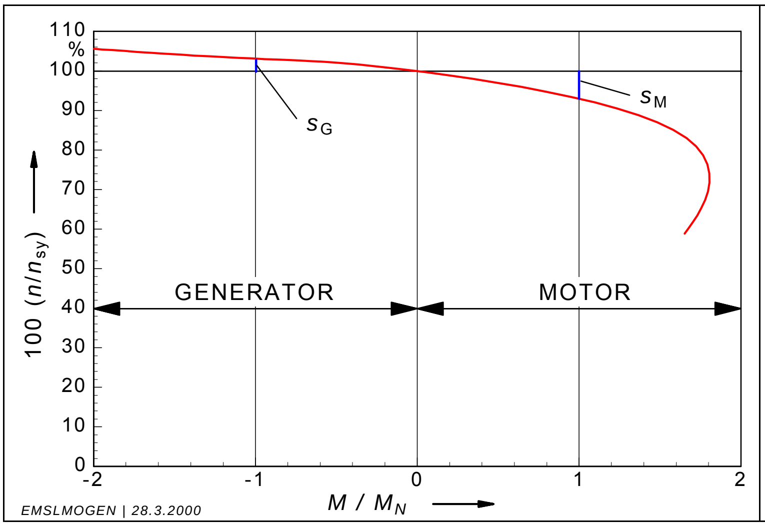

Fig. 49.1
Torque-speed characteristic curve in motoring and generating mode
s_G - slip as a generator
s_M - slip as a motor
each at the rated torque

The magnitude of the rated-load slip depends on the size and number of poles of a motor; Fig. 49.2 gives guide values for positioning motors.
If one assumes the same degree of slip in generating mode as in motoring mode – it is actually slightly lower – the maximum speed deviation is approximately +2 to +30 % once load fluctuations (no load – rated load) and torque alteration (driving – driven) have been taken into account.

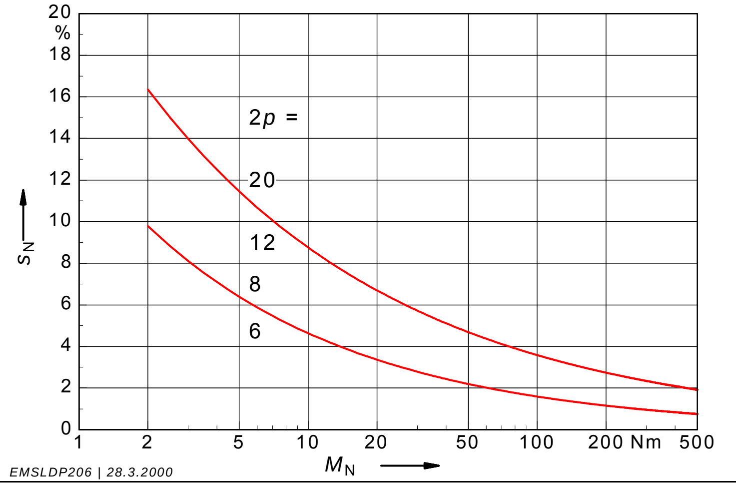

Fig. 49.2
Guide values for the rated-load slip s_N of positioning motors with various rated torques M_N and numbers of poles 2*p*

49.2 Mechanical brake

According to publication [5.6], the braking torque is dependent on:

- ☐ Temperature
- ☐ Material properties such as strength, heat conductivity, specific heat, coefficient of thermal expansion, density
- ☐ Slip velocity
- ☐ Pressure
- ☐ Duration of the loading as a loading frequency (switching frequency), interval duration
- ☐ Surface condition such as surface quality, hardness
- ☐ Stress
- ☐ Chemical and electrostatic influences such as mass attraction, cold welding, molecular interaction
- ☐ Environmental influences such as moisture, fouling
- ☐ Braking system (with or without intrinsic reinforcement).

Studies [5.5] have shown that the coefficient of friction can fluctuate between 0.3 and 0.45, i.e. by more than 30 %, depending on the material, roughness and slip velocity (see Fig. 49.2).

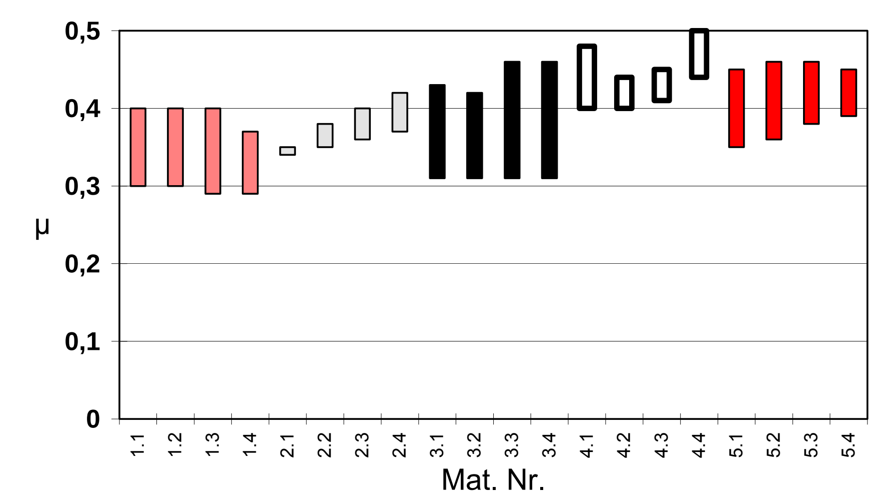

Fig. 49.2
Fluctuation in the coefficient of friction μ for five different materials (1.x ... 5.x) and four degrees of roughness *Rz* (x.1 ... x.4)

49.3 Control system

With ***travel-dependent control systems***, the pulses from the sensors or other monitoring devices permanently mounted at a predefined point in the route are detected and processed by the control system. This means that the control function is always precise and initiated at the same point.
A travel-dependent control system should always be used with positioning drives where stopping accuracy is required.

The tolerance will then only depend on the tolerance of the components used as described in sections 49.3.1 to 49.3.2.

With ***time-dependent control systems***, the pulses are processed by timers (e.g. timer relays) using control technology. Individual time sections for the sequence of manufacture are calculated from the *VT* graph specified and relayed to the timers. Since the timers themselves have tolerances, the control function may not always occur at the same point.

If the time sections are processed sequentially, the stopping variation may be too great.

The tolerances caused by the control system cannot be ignored where very high demands are placed on the positioning accuracy.

49.3.1 Response times of contactors

Two different forms of actuation are used for contactors:

- □ Mainly A.C.-operated contactors are used in conventional control systems. Medium-size contactors have a closing response time of approximately 10 ... 20 ms (scatter band of about 10 ms). The opening response time is approximately 5 ... 14 ms (scatter band of about 9 ms).

- □ D.C.-operated contactors are often used in conjunction with PLCs (programmable logic controllers).
  The closing response time of medium-size contactors is approximately 40 ... 55 ms (scatter band of about 15 ms) and approximately 6 ... 10 ms for closing (scatter band of about 4 ms).

An arcing time of approximately 5 ... 10 ms must also be expected with both methods of actuation. The total switch-off time can be obtained by adding the opening response time to the arcing time. The guide values cited apply to contactors designed for motors with a rated output of approximately 5.5 kW. Final values can be obtained from the switchgear manufacturer's data sheets.

49.3.2 Proximity switches

Contactless capacitive or inductive proximity switches are subject to tolerances that could have consequences for the ***device's operation***; for example, the on-off differential, the reproducibility together with the sensitivity of the proximity switch to temperature and voltage. Furthermore, the susceptibility of capacitive proximity switches to humidity must also be borne in mind.
System-related tolerances depend on the precision of a system. For example, accurate positioning may be impossible with a roller conveyor due to warped approach guides or differences in the distances between the active surface of the proximity switch and the approach guide. Fig. 49.3.2 shows this problem in a simplified form.

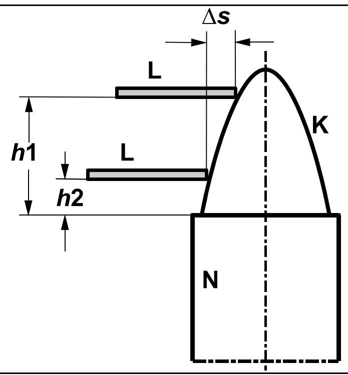	Fig. 49.3.2 Effect of different distances h_1 and h_2 of the approach guide (L) on the point of contact with the response contour (K) of a proximity switch (N); this results in a difference Δ_s in the response point

49.3.3 Timer relays

The tolerances of a timer relay depend on temperature and voltage. Manufacturers specify different tolerances so the values for a given product must be taken from the technical data sheets in each case. The repeat accuracy of a set value is specified with a tolerance of ± 0.5 % to ± 1 % by most manufacturers.

49.4 PLCs (programmable logic controllers)

If a programmable logic controller is used to control a machine, ***additional variance*** must be expected if the control system is not designed for short control periods.
The scatter band depends on a variety of influences:

- ☐ The point in the user program at which the address counter finds itself at the time of the control pulse.
- ☐ The number of commands in the user program, i.e. the length of the cycle timed.

The cycle time is therefore an important variable in the assessment of the positioning accuracy. Cycle times of approximately 30 to 70 ms used to be standard on compact devices with a maximum memory capacity of 1 K = 1024 commands. Modern devices take only about 1 ... 2 µs per command, i.e, 1024 commands result in a cycle time of only about 1 ... 2 ms.
This technical development and its consequences may be demonstrated by a concrete example: A PLC with a user program containing 860 commands controls a sidetracking carriage with a travelling speed of 10 m/min. This produces a travel section with different variances once the processing times have been taken into account.
Fig. 49.4 plots three possibilities. The virtually constant switch-on and switch-off delays of the PLC are taken as roughly 6 ms for the calculation of the travel.

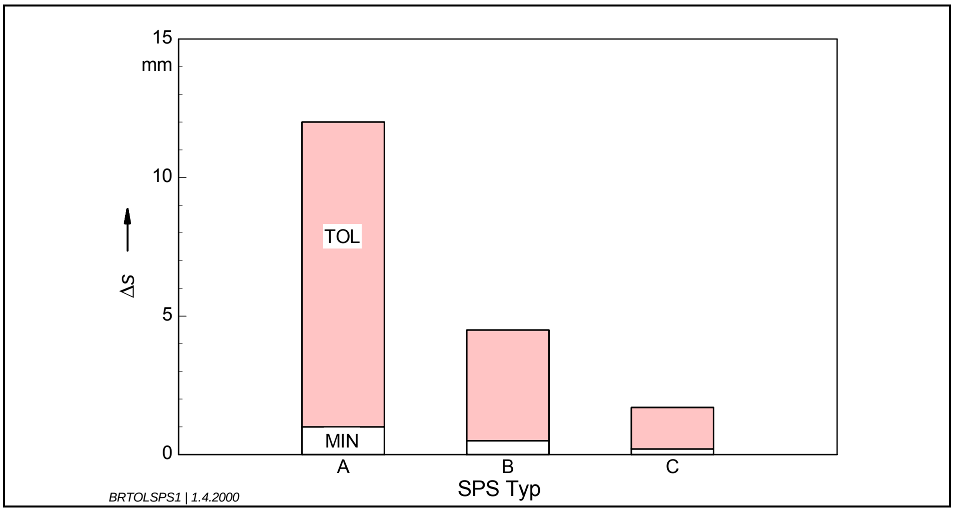

Fig. 49.4
Travel tolerances Δ*s* caused by PLCs with different processing times for an example program containing 860 commands
TOL - tolerance in braking travel
MIN - smallest braking travel
A - compact PLC with a processing speed of 75 ms/1 K
B - PLC with a processing time of 20 ms
C - PLC with a processing time of 2 ms

The reaction time of a PLC is the time delay between the binary change at the input and the reaction at the corresponding output. This comprises the processing time for the number of commands and the switch-on/switch-off delay.

The following may be stated in conclusion:
By using programmable logic controllers (PLCs), additional times (governed by the cycle time and reaction time) of approximately 5 ... 30 ms may be associated with relatively "fast" devices; these may amount to 75 ms for "slow" models. Particular attention must be paid to the selection of the control unit if particularly short or tightly toleranced response times are required.

50 Gear backlash

The influence of backlash must also be taken into account where there is an extreme requirement on positioning accuracy. A minimum backlash must be present to be sure to prevent the possibility of the gearing locking, i.e. the tooth flanks seizing and the bearings being extremely overloaded. The magnitude of this rotational backlash in the pitch circle is 0.1 ... 0.2 mm regardless of the machining quality and, as far as the orders of magnitude dealt with here are concerned, also largely regardless of the pitch circle diameter or modulus. A ***backlash S = 0.15 mm*** is assumed for the following discussions.

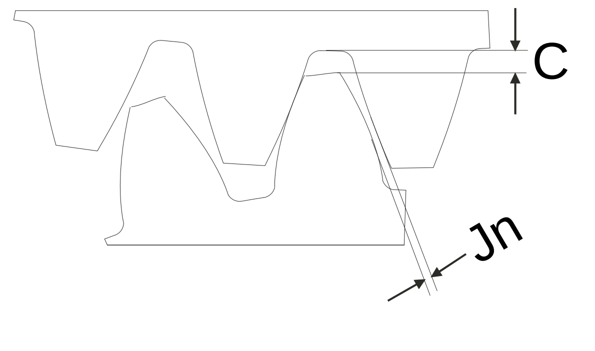

Fig. 50
Definition of crest clearance *C*
and backlash j_n
in accordance with DIN 3960 ($S = j_n$)

50.1 Guide values for standard gear units

The minimum values for the meshing backlash j_N are specified in Fig. 50.1.1 for high-quality gearing It becomes clear that the backlash increase is far below a linear function (LIN) when plotted against the shaft-centre distance *AA*. This means that far greater torsional offset within the backlash can be expected on relatively small gear units than on larger gear units.

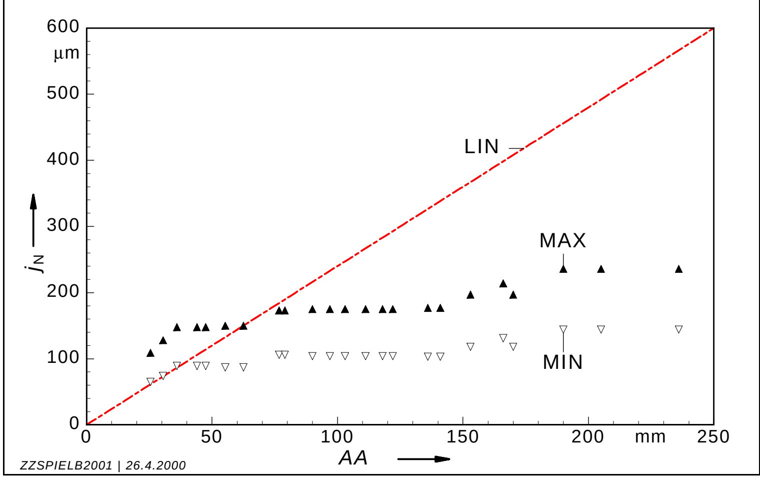

Fig. 50.1.1
Standardized minimum values for backlash j_N as a function of the shaft-centre distance *AA*

It is beneficial to express the pitch circle radii of the pinion and gearwheel (*r*1 and *r*2) as a function of the shaft-centre distance (*A*) and of the reduction ratio (*i*) to obtain a comprehensive calculation (Fig. 50.1.2).

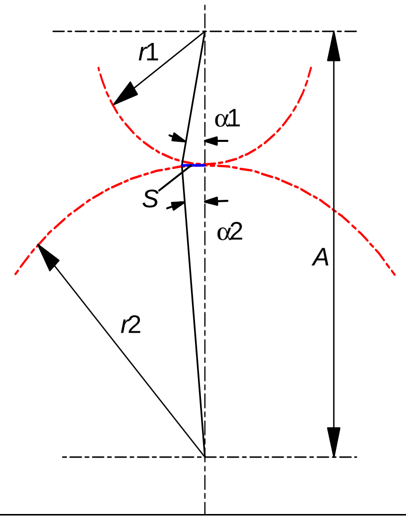

Fig. 50.1.2
Simplified geometric representation of the effect of tooth clearance *S* on the torsional offset at the pinion α1 and gearwheel α2

The derivations in [5.2] indicate that the torsional offset is highly dependent on the shaft-centre distance (i.e. on the gear unit size) and that backlash has a relatively more pronounced effect on small gear units than on large gear units. The influence of the reduction ratio is relatively small (Fig. 50.1.3).

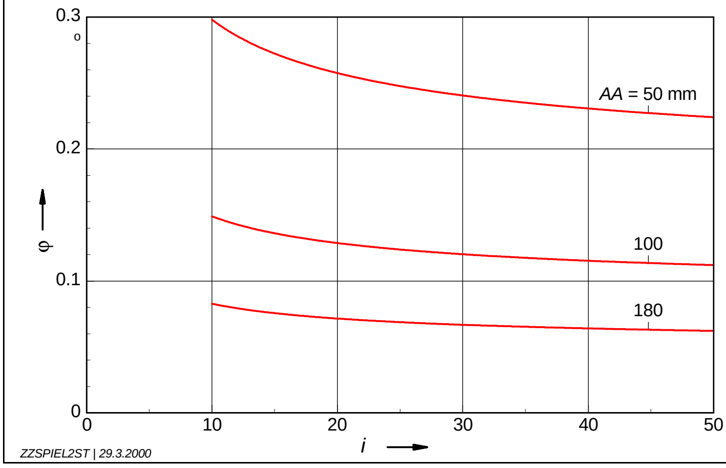

Fig. 50.1.3
Guide values for the torsional offset (φ) on the output shaft of 2-stage helical-gear units in relation to the reduction ratio *i* and shaft-centre distance *AA*

If calculations are approximate, the following values can be used for the torsional offset on the output shaft when the rotor shaft is locked, regardless of the reduction ratio:

- ☐ ***Small gear unit:*** ***approximately 0.3*** °
- ☐ ***Medium-size gear unit:*** ***approximately 0.15*** °
- ☐ ***Large gear unit:*** ***approximately 0.1*** °

50.2 Effect on linear motion

The effects on linear motion as a function of the effective diameter of the power transmission components as shown in Fig. 50.2 can be calculated using these guide values.
Where the power transmission components have standard effective diameters (below approximately 250 mm), the tolerances remain below approximately 0.5, i.e. within very tight limits, due to backlash.

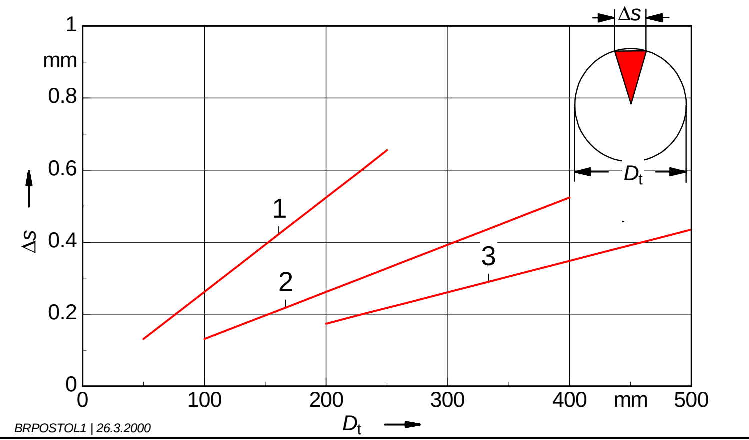

Fig. 50.2
Effect of backlash on deviation Δ*s* from a position as a function of the effective diameter of power transmission components D_t;
applicable to all reduction ratios

1 Small gear units
2 Medium-size gear units
3 Large gear units

manufactured by Danfoss Bauer

51 1:2 speed ratio (Dahlander connection)

Pole-changing in the ratio of 1 : 2 is particularly frequently used as the direction of the current in the part-phases of the winding can be altered simply by switching the connections on the terminals to produce two rotating field speeds in the ratio 1:2. This type of connection is termed the "Dahlander connection" after its discoverer.
The entire slot cross section is active at both speeds, unlike two separate windings (section 52) – resulting in relatively high model utilization. Although this benefit is also given by special connections, these require either a very high number of terminals or a very complicated multi-stepped winding. Dahlander connection is a relatively cheap way to achieve speed-stepping, even if this is only in the ratio of 1:2, thus making it unsuitable where high demands are placed on positioning accuracy.

51.1 External and internal current and field direction with Dahlander connection

Fig. 51.1 provides a highly simplified overview of how the current and magnetization direction in the respective half-phases of each phase winding are reversed simply by changing the terminal connection and how a different field distribution (number of poles) is created.

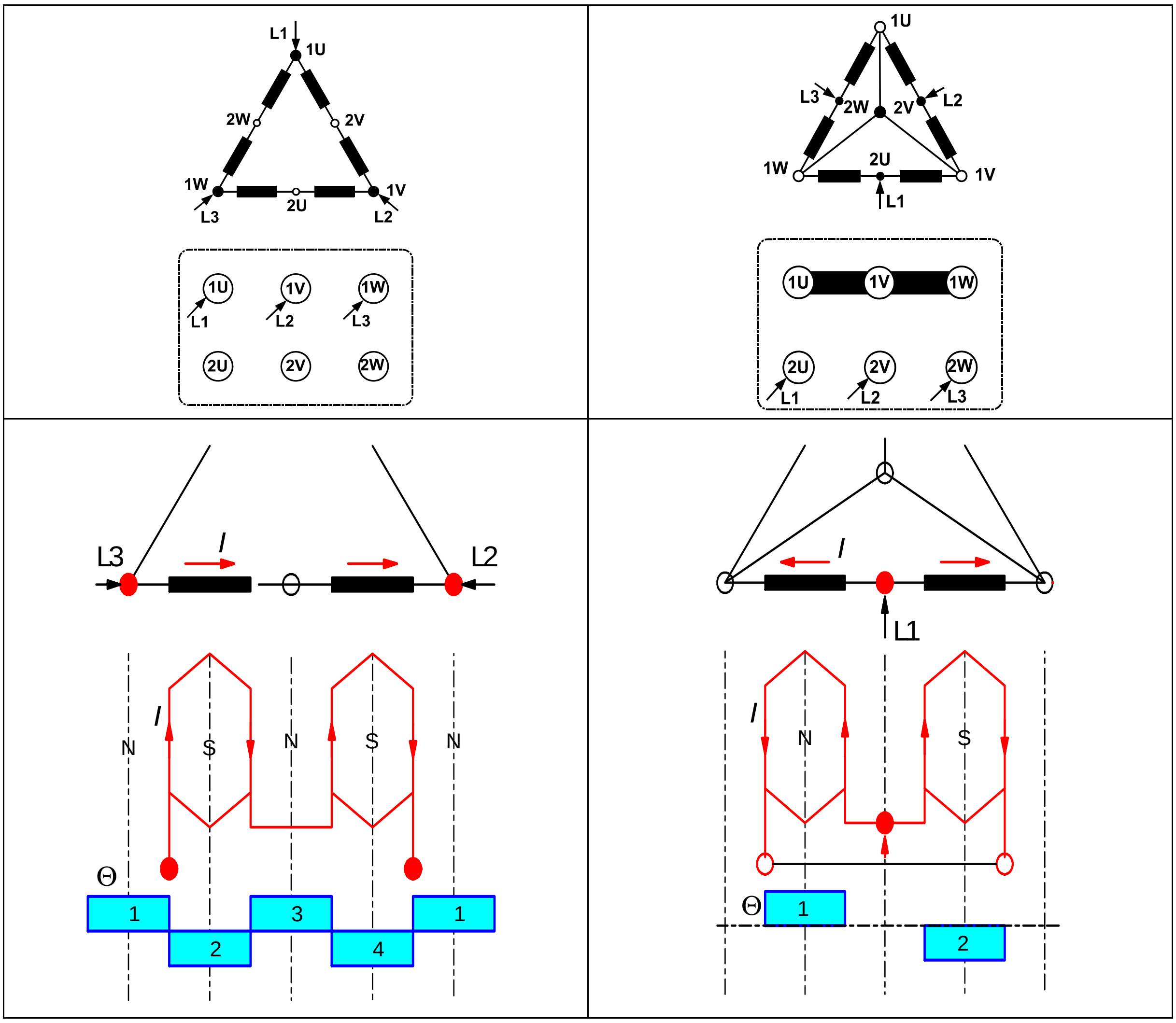

Fig. 51.1 Simplified overview of the terminal connection and the direction of the current *I* and magnetization Θ with delta/double-star Dahlander connection for 4/2 poles

51.2 Type utilization with Dahlander connection

The fixed switch-over provision described in section 51.1 permits only a highly imperfect adaptation of the winding for the layout to optimize it for every individual number of poles. Furthermore, the laminated core dimensions – i.e. the rotor diameter and the back height for a given outside diameter – can only be a compromise between the opposing requirements of the two pole numbers. Finally, the winding for the low number of poles is relatively heavily chorded and so has a poor winding factor. In view of these facts, the model utilization on a pole-changing motor is only about 60 ... 80 % of the output of an equivalent fixed-speed motor.

51.3 Relative height of the torque characteristic curves

With Dahlander connection, the relative height of the magnetic flux, and consequently the torque characteristic curve for the two pole numbers, is fixed.
The examples in Fig. 51.3.1 shows that the absolute torque values in star-star connection (high speed) are usually somewhat lower that in delta (Δ) configuration (low speed).

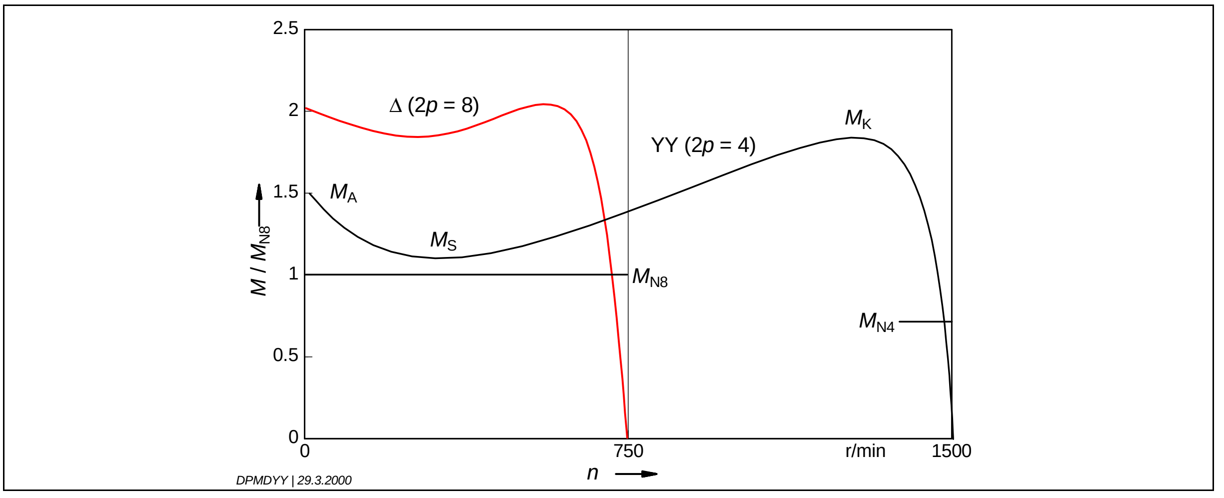

Fig. 51.3.1 Example of the relative height of the torque characteristic curves with Dahlander connection
Δ (2p = 8): Delta connection for a high number of poles (e.g. 8 – low speed)
YY (2p = 4): Double-star connection for a low number of poles (e.g. 4 – high speed)

The rated torque at the high speed (the 4-pole characteristic curve M_{N4} in our example) must be reduced somewhat below the basic connection (8-pole, M_{N8}, in our example) to ensure reliable starting and the necessary overload capacity (breakdown torque/rated torque ratio, M_K/M_N). For thermal reasons, this reduction always appears greater than ought to be required judging from the torque characteristic curves. This yields roughly the following output and torque gradation for pole-changing three-phase geared motors with standard numbers of poles for model utilization within the limits set by the IEC Standard specifications:

Pole-changing Δ/YY	Relative torques Low speed	High speed	Relative outputs Low speed	High speed
4/2	100 %	approx. 65 %	100 %	approx. 130 %
8/4	100 %	approx. 75 %	100 %	approx. 150 %
12/6	100 %	approx. 75 %	100 %	approx. 150 %

Table 51.3.2 Guide values for the gradation of torque and output on pole-changing three-phase motors in delta/star-star (Δ/YY) Dahlander connection with full thermal model utilization

Whilst the maximum permissible thermal output is given in the catalogues for three-phase standard motors (without gear units), this may not always be the most cost-effective solution for geared motors. If one sets the torque for high speed at 100 %, the torque at the low speed for a 4/2-pole motor will be approximately 150 % (1/0.65 = 1.5).
The gear unit must be rated for this 150 % torque.
With slow-running drives, it may be assumed that the torque requirement is used primarily to overcome friction or a hoisting load; in other words, it is approximately the same for both (linear) speeds.
The potential torque at the low speed (150 %) is far too high. The gear unit could be rated for 100 % the torque and thus be more cost-effective.

For this reason Danfoss Bauer catalogues quote the following cheaper gradations for pole-changing motors:

Pole-changing	Relative torques		Relative outputs	
Δ/YY	Low speed	High speed	Low speed	High speed
4/2	100 %	approx. 100 %	100 %	approx. 200 %
8/4	100 %	approx. 100 %	100 %	approx. 200 %

Table 51.3.3 Gradation of torque and power rating for pole-changing three-phase geared motors in Dahlander connection with more cost-effective gear utilization for a constant torque

52 Other speed ratios (separate windings)

Two separate windings inserted in one stator are usually used to obtain two speeds which differ in the ratio 1:2. The effort associated with the winding technology required, comprising insertion work, wiring and insulation (coil from coil and winding from winding), is large.
Machine winding is usually not possible; the proportion of manual labour (i.e. the labour component of the costs) is relatively high.
In spite of the high cost and the poor use of the model, pole-changing motors with two separate windings are very widespread. They have a far simpler mechanical system than change speed gearboxes and a more elegant (electrical) method of control.
It has not generally been accepted to implement special configurations which utilize the full slot area available because the winding technology involved is even more complicated; see [5.2].

52.1 Terminal configuration

The mains connections may be connected to the two windings if desired on motors with two separate windings and various pole numbers.
The windings are normally connected inside the motor in star configuration and terminated with three ends.
Additional delta/star (Δ/Y) tap changing is possible as an option but is limit to special cases as 12 terminals and usually an enlarged terminal box are required.

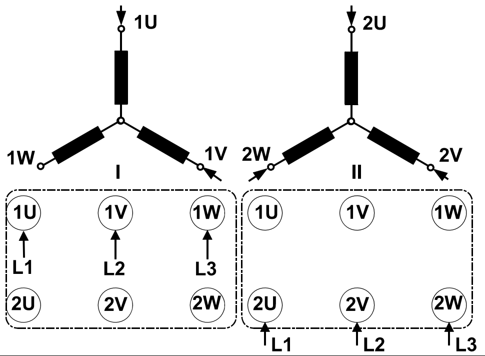

Fig. 52.1.1
Circuit diagram for two separate windings,
two speeds, I and II

52.2 Possible speed ratios

There are physical and manufacturing limits on the possible number of poles. The lowest number of poles is 2 (3000 r/min). The highest number of poles possible at a justifiable cost depends on the frame size of the motor.
The following applies for a three-phase single-layer winding:

Number of coils = 1.5 · number of poles
This gives a
minimum number of slots = 2 · number of coils = 3 · number of poles

Number of poles	8	12	16	20
Minimum number of slots	24	36	48	60

Table 52.2.1 Minimum number of slots as a function of the number of poles

The problem of accommodating the minimum number of slots on the existing circumference arises with small stator bores, i.e. a problem of stamping, insulating and winding.
Fig. 52.2.2 illustrates the space requirements by way of an example.

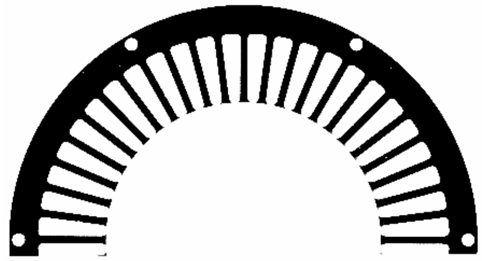

Fig. 52.2.2
Section through motor with a frame size of 80, rotor diameter of 70 mm and 48 slots

The following maximum pole numbers have been determined for Danfoss Bauer three-phase motors in view of the manufacturing constraints mentioned above.

Danfoss Bauer Type	Corresponding IEC shaft height	Maximum number of poles
D05.	56	8
D06..	63	12
D08..	80	12
D09..	90	12
D11..	112	16
D13..	132	20
D16..	160	20
D18..	180	20
DNF22	225	20
DNF25	250	20
DNF28	280	20

Table 52.2.3 Maximum possible number of poles on Danfoss Bauer three-phase motor according to type (shaft height)

Pole numbers of 10, 14 and 18 – which should theoretically be offered in the 2 to 20-pole range – are not used as they do not permit a convenient winding arrangement with other numbers of poles.
This results in the following speed ratios:

Numbers of poles	Synchronous motor speeds in r/min at 50 Hz	Speed ratio
8/6	750/1000	1:1.33
6/4	1000/1500	1:1.5
12/8	500/750	1:1.5
6/2	1000/3000	1:3
12/4	500/1500	1:3
8/2	750/3000	1:4
16/4	375/1500	1:4
20/4	300/1500	1:5
12/2	500/3000	1:6
16/2	375/3000	1:8
20/2	300/3000	1:10

Table 52.2.4 Possible pole numbers, speeds and speed ratios for the 2 ... 20 pole number range (note the restrictions on use according to the type size as shown in Table 52.2.3)

The speed ratios given in Fig. 52.2.5 are standard for positioning motors.

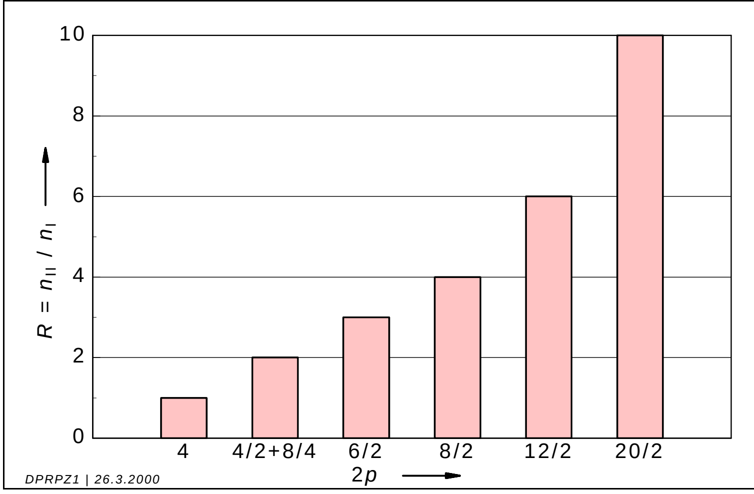

Fig. 52.2.5
Speed ratio *R* of pole-changing positioning motors with two speeds;

Dahlander connection or two separate windings

52.3 Model utilization with separate windings

While the laminated core dimensions and slot shapes of single-speed motors can be optimized for the particular number of poles, a compromise must be made for two separate windings (two pole numbers). Furthermore, roughly half of the winding space in the slot remains unused. The model utilization is therefore relatively low compared to that of single-speed motors.

Pole-changing	Output at high speed
6/2	approx. 70 ... 90 %
8/2	approx. 70 ... 90 %
12/2	approx. 55 ... 75 %
16/2	approx. 30 ... 60 %
20/2	approx. 30 ... 60 %

Table 52.3 Guide values for the model utilization with two separate windings compared to that for 4-pole motors of the same model size

52.4 Relative height of the torque characteristic curves

The relative height of the torque characteristic curves can, within broad limits, be selected as required – unlike the rigid link associated with Dahlander connection. Standard motors with two separate windings are designed for a constant rated torque at both speed stages.

Number of poles	Relative overload capacity at low speed		high speed	
	M_A/M_N	M_K/M_N	M_A/M_N	M_K/M_N
6/2	1.6 ... 2.1	2.0 ... 2.2	1.8 ... 2.3	2.0 ... 2.8
8/2	1.6 ... 2.1	1.9 ... 2.1	1.8 ... 2.3	2.0 ... 2.8
12/2	1.6 ...1.9	1.8 ... 1.8	1.8 ... 2.6	2.0 ... 2.8

Table 52.4.1 Guide values for the relative overload capacity of pole-changing motors with two separate windings

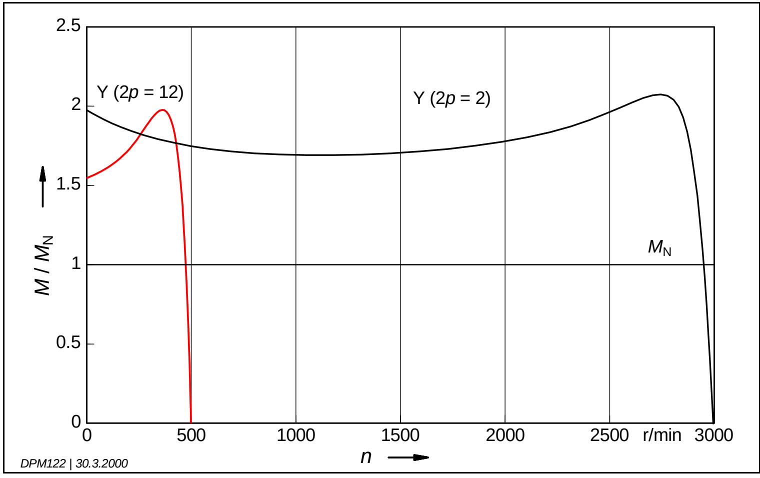

Fig. 52.4.2
Example of the relative height of the torque characteristic curves with two separate windings

The example shows that typically, if not universally, the torque overload capacity (breakaway torque and pull-out torque) at the low pole number (high speed) is usually a little higher than at the low speed stage.

52.5 Cost comparison

The following cost comparison is based on geared motors with a speed of approximately 100 r/min in the highest speed stage. The rated output also relates to the highest speed stage. The comparison can give only a rough ***idea*** of the relative costs of drives; the additional costs of control units and switchgear are included.

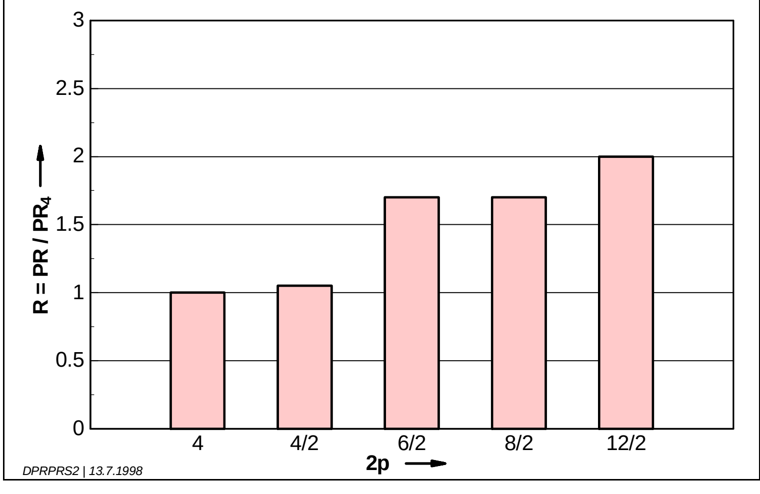

Fig. 52.5.2
Guide values for the costs of pole-changing geared motors with speed ratios of
1:2 (4/2-pole),
1:3 (6/2-pole),
1:4 (8/2-pole),
1:6 (12/2-pole)
compared to a geared motor with a fixed speed (4-pole).

53 Possibilities and limits of pole-changing

Fig. 53.1 provides guide values for the total number of overtravel revolutions of the rotor of a 8/2-pole positioning motor with run-out braking. Unfavourable conditions have been selected intentionally.

- ☐ Factor of inertia *FI* = 2
- ☐ Braking torque the same as the motor's rated torque
- ☐ No braking assistance from the load

The graph is not a substitute for recalculation for the particular case in question; however, it should serve to point out that the total overtravel when using the positioning speed (I) declines in the ratio of approximately 8:1 whereas the speed ratio is only 4:1 (8/2-pole).

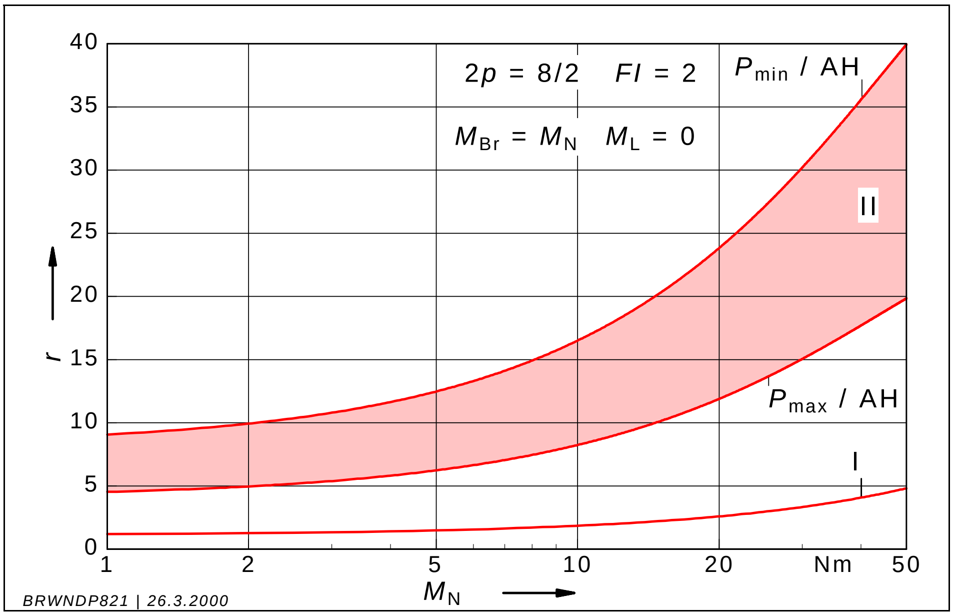

Fig. 53.1
Total overtravel revolutions *r* on the rotor of 8/2-pole positioning motors with rated torques of $M_{N;}$ braking from a high (II) or low (I) speed

P_{min}/AH - lowest output for one particular shaft height
P_{max}/AH - highest output for one particular shaft height

Fig. 53.2 shows the effect of the number of poles – i.e. the choice of positioning speed – on the reduction of the total overtravel.

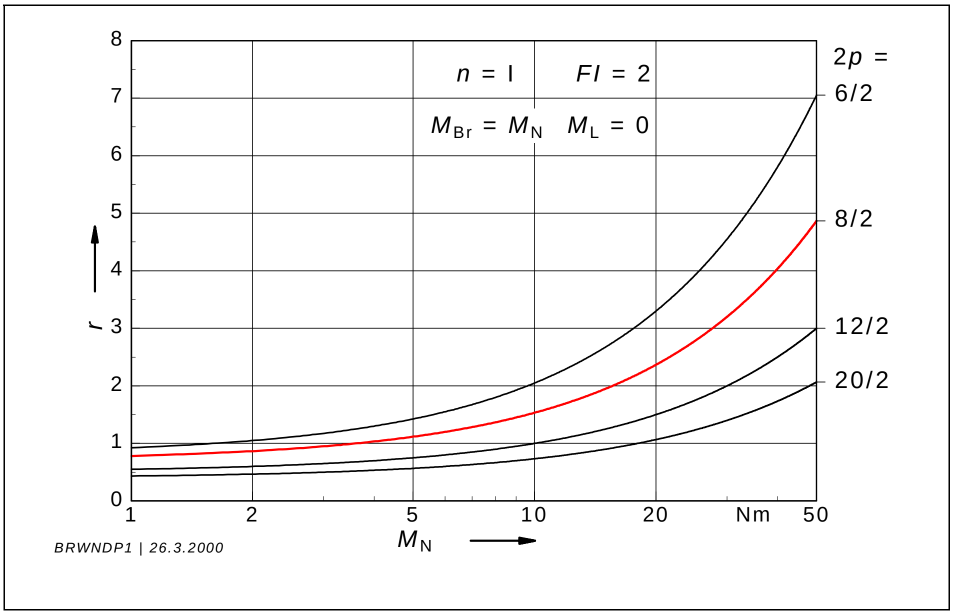

Fig. 53.2 Total overtravel revolutions *r* on the rotor of positioning motor with rated torques M_N for various pole number ratios 2*p* braking from the low speed and *FI* = 2 in each case

Fig. 53.2 can be further simplified to obtain a rough estimate. Fig. 53.3 applies regardless of the pole number at which the motor operates at the positioning speed. It expresses the overtravel distance as a percentage *p* of the distance travelled at the positioning speed in one second. The following can be calculated from this:

$$s_N = \frac{p \cdot v}{100}$$

s_N	-	overtravel distance in m
p	-	percentage from graph 53.3
v	-	positioning speed in m/s

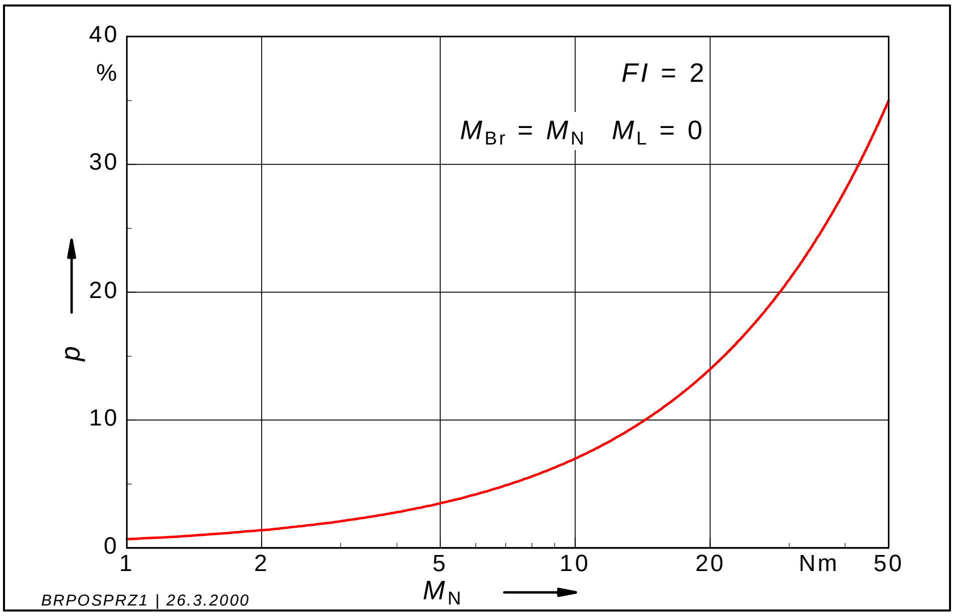

Fig. 53.3 Guide value for the overtravel distance for motors having nominal torques M_N (explanations given in the text)

54 Inverter-fed motors

The higher the running speed and the lower the permissible stopping tolerance, the greater the speed ratio required. Fig. 54.1 provides empirical values; however, these are no substitute for recalculation on a case by case basis.

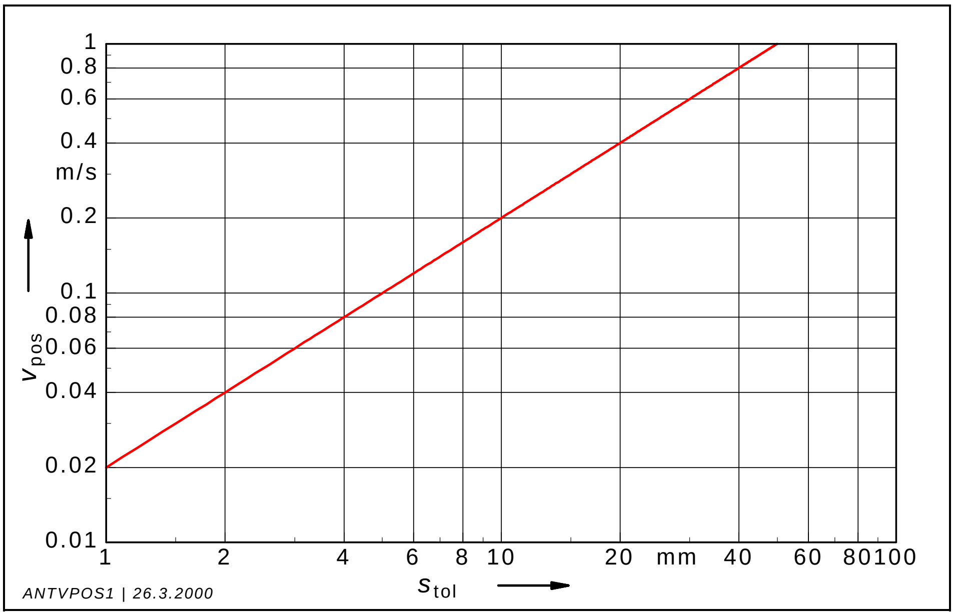

Fig. 54.1 Guide values for the positioning speed v_{pos} in relation to the expected stopping tolerance s_{tol}

Fig. 54.2 shows the limits of drive systems:

- Speed ratios $R \leq 4$ allow the conventional pole-changing PU solution to be used.
- Speed ratios $R > 10$ generally necessitate the variable frequency VF solution.
- In the $4 < R \leq 10$ range, the two solutions compete with VF having the advantage in terms of technology and PU the advantage in terms of cost.

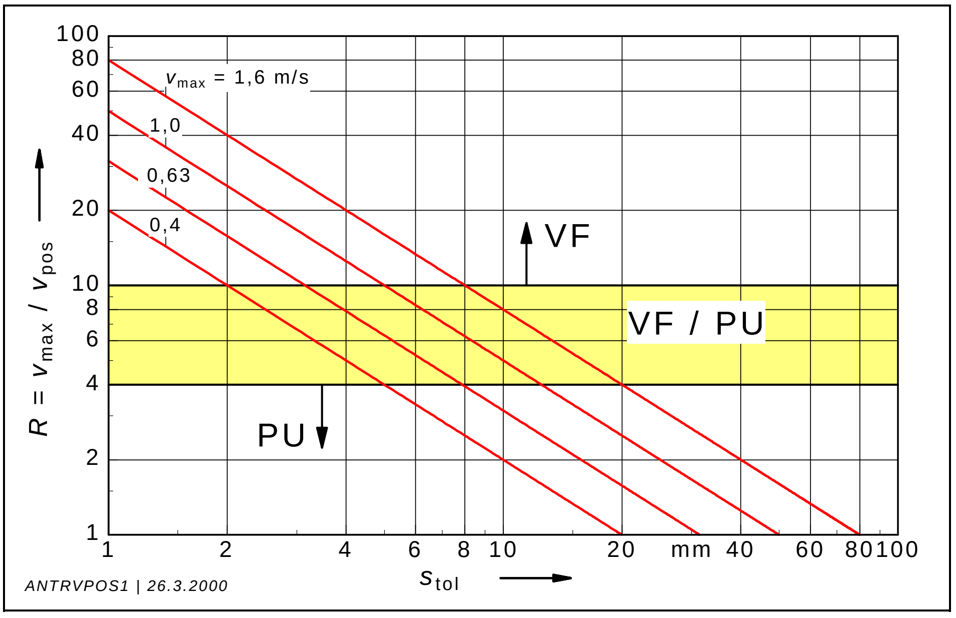

Fig. 54.2 Limits of use in relation to the expected stopping tolerance s_{tol} and to the running speed v_{max}

PU - pole-changing VF - variable frequency

In addition to technical considerations, cost is also decisive in the decision-making process, but not only in the transitional range. The development of a compact solution that can be integrated into the motor terminal box (Fig. 54.4) makes the selection of inverter feed easier, particularly in the important power range up to 3 kW, as shown in Fig. 54.3.
This price comparison is based on the following assumptions which may need to be modified to suit the particular case but should be borne in mind as far as switchgear and control units are concerned.

- Speed ratio 1:6
- Cyclic duration factor (*ED*) 60 % with VF and 25/75 % with PU
- Thermal motor protection (TMS) by means of thermistors (a circuit-breaker is supplied as standard with the inverter)
- Contactors for pole-changing (not required with inverters)
- Wiring and installation costs have not been taken into account (higher with PU than with VF).

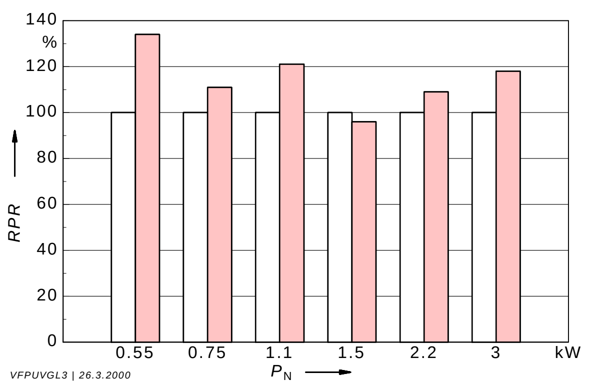

Fig. 54.3
Guide values for the relative price (*RPR*) of drive solutions with pole-changing (PU) and integrated inverter (VF)

See the text for marginal conditions

Fig. 54.4
“Eta-K”
Three-phase geared motor with built-on frequency inverter to form a compact drive
Rated outputs
P_N to 7.5 kW
Integrated protective devices against overload, overcurrent, phase failure, overvoltage and undervoltage.
Thermal monitoring for the motor and inverter.
Connected by a plug to the motor unit
Degree of protection IP65.

55 Positioning control using frequency inverters

Danfoss series 5000 VLT® frequency inverter with integrated SyncPos movement control to increase capacity and simplify the control systems of palleting machines which stack crates of bottles. The crates are unloaded using a stacking gripper. The vertical and horizontal movements of the gripper are controlled by two series 5000 VLT® drives which receive feedback signals from two encoders. These are some of the benefits of such a system:

- Greater output thanks to the greater dynamic response of the palleting machine
- Gentler product movement with greater accuracy
- Simple wiring and programming: the series 5000 VLT® drive is an intelligent drive that can control all aspects of the application. This does away with the need for a PLC or similar external control unit, for example.
- Compact design requires less space on the mounting plate
- Communication via a field bus interface

Index positioning is the ideal solution for palleting machines in many sectors. However, it is also suitable for:

- Indexing tables
- Depaletting machines
- Storage systems
- Pick-and-place systems

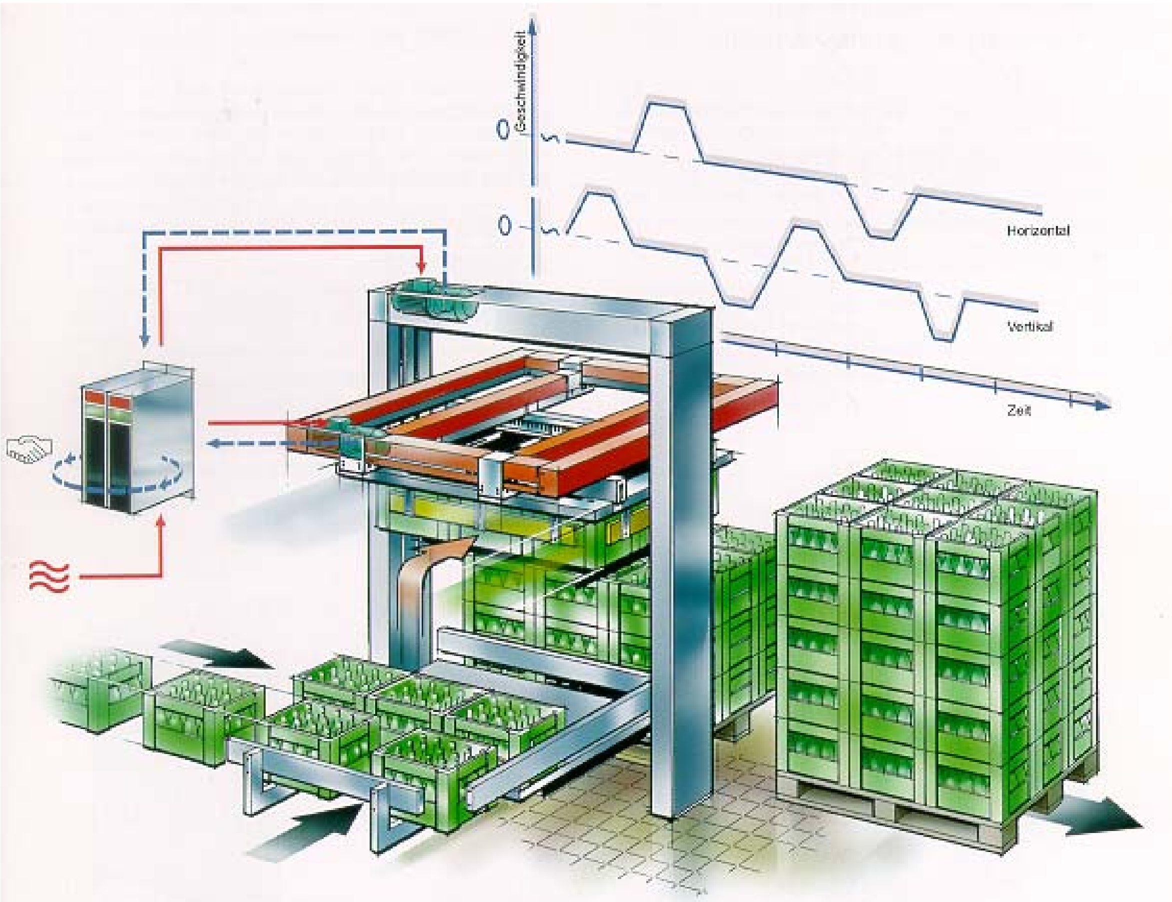

Fig. 55.1 Schematic depiction of the application of inverter-fed motors with SynchPos control for positioning on a palleting machine

Bibliography

Part II

2.1 IEC 60034-1
Rotating electrical machines; Part 1: Rating and performance

2.2 EN 60034-1
Rotating electrical machines; Part 1: Rating and performance

2.3 IEC 60034-12
Rotating electrical machines; Part 12: Starting performance of single-speed three-phase cage induction motors with voltages up to and including 690 V

2.4 NEMA MG1
Motors and generators

2.5 National Electrical Code (NEC) Handbook
NFPA USA (1993)

2.6 *Rentzsch, H.:*
Elektromotoren [Electric motors]
ABB manual (1992)

2.7 *Falk, K.:*
Der Drehstrommotor – Ein Lexikon für die Praxis [The three-phase motor – A practical lexicon]
VDE Verlag Berlin Offenbach (1997)

2.8 *Kümmel, F.:*
Elektrische Antriebstechnik [Electrical drive systems]
Springer Verlag Berlin Heidelberg New York (1971)

2.9 *Greiner, H.:*
Auswahl von Rollgangs-Antrieben [Selection of roller table drives]
Special imprint SD 807 by Danfoss Bauer GmbH

2.10 *Vogel, J.:*
Elektrische Antriebstechnik [Electrical drive systems]
Hüthig Verlag Heidelberg (1998)

2.11 *Greiner, H.:*
Schutzmaßnahmen bei Drehstrom-Getriebemotoren [Protective measures for three-phase geared motors]
Published by Danfoss Bauer GmbH (2000)

2.12 *Seifert, D.; Strangmüller, Th.:*
Stoßmoment und Stoßstrom der Asynchronmaschine [Shock torque and inrush current of the induction motor]
etz Archiv volume 11 (1989) no. 9

2.13 *Wüthrich, W.:*
Übersicht über die Einschaltmomente bei Asynchronmotoren im Stillstand [Overview of the starting torques of induction motors at rest]
ETZ-A volume 88 (1967) no. 22

Parts III + IV:

3.1 *Fischer, R.:*
Elektrische Maschinen [Electrical machines]
Carl Hanser Verlag Munich Vienna (1995)

3.2 *Geisweid, R.:*
Elektrotechnik und elektrische Antriebe [Electrical engineering and electical drives]
Springer-Verlag Heidelberg Berlin New York (1973)

3.3 Danfoss A/S:
Wissenswertes über Frequenzumrichter [Facts worth knowing about frequency converters] (1997)

3.4 *Bedenke, H.J.; Pfassek, R.; Rothenbach, G.; Vaske, P.:*
Elektrische Antriebe und Steuerungen [Electrical drives and control systems]
B.G. Teubner Stuttgart (1969)

Parts V + VI:

5.1 *Greiner, H.:*
Elektrische Antriebe mit Getriebemotoren [Electrical drives with geared motors]
Publikation by Danfoss Bauer GmbH

5.2 *Greiner, H.:*
Bremsen und Positionieren mit polumschaltbaren Getriebe-Motoren [Braking and positioning with pole-changing geared motors]
Special imprint SD 2688 by Danfoss Bauer GmbH

5.3 *Greiner, H.:*
Anlauf und elektrodynamische Auslaufbremsung bei Käfigläufer-Motoren [Starting and dynamic braking with cage motors]
Special imprint SD 3095 by Danfoss Bauer GmbH

5.4 Technische Akademie Esslingen [Esslingen Technical Academy]:
Bremsen und Positionieren mit Drehstromantrieben [Braking and positioning with three-phase drives]
Teaching notes for TAE course 20281/64.110

5.5 *Severin, D.; Musiol, F.:*
Der Reibungsmechanismus in Sicherheitsbremsen von Kranen [The mechanism of friction in the safety brakes of cranes]
DHF 1/2-89

5.6 *Weiss, U.:*
Reibungsbremsen und ihre Innovationsgrenzen [Friction brakes and their limits of innovation]
Der Konstrukteur [The Designer] 12/1978

5.7 VDI code of practice VDI 2241 Sheet 1:
Schaltbare fremdbetätigte Reibkupplungen und -bremsen [Switching externally-operated friction clutches and brakes]

Index of keywords

A	Section
A.C. solenoid	33
ABR single-disc spring-loaded brake	35.5
Additional rotating mass	13
Adjusting	42
Air gap	42
Assessment criterion for soft starting	2
B	
Bar pendulum	28.2
Belt	33
Brake application response time	38
Brake application with A.C. solenoids	38.1
Brake application with D.C. solenoids	38.2
Brake motor	32
Brake release response time	37
Brake release with A.C. solenoids	37.1
Brake release with D.C. solenoids	37.2
Braking energy (selection)	41
Braking force	33
Braking system, classification	33
Braking time	22.3
Braking torque (required)	40.1
Braking torque (selection)	40
Braking torques with PU	23.1
Braking travel	22.3
Built-in brake	34
Built-on brake	34
Calculation (braking time and braking travel)	23.3
Centrifugal clutches	15.1
Changing the direction from full speed	20
Circuit diagram of D.C. braking	22.2, 22.4
Classification of starting behaviour	18
Coefficient of friction	49.2
Coil	35
Cone	33
Cone rotor	35
Cone spring-loaded brake released by the motor field	35.7
Connection (1:1.73 voltage)	36.2
Connection (1:2 voltage)	36.3
Connection (operation from an inverter)	36.6
Connection (pole-changing)	36.4
Connection (sample cases)	36.7
Connection (starting devices)	36.5
Control system (time-dependent)	49.3
Control system (travel-dependent)	49.3
Conversion of moving masses	31
Cost comparison (PU)	52.5
D	
D.C. injection braking	22
D.C. injection braking (thermal rating)	25.4
D.C. solenoid	33
D.C. solenoid releases (rated values)	36.8
D.C. voltage (rated values)	36.8.2
D.C.-circuit break	38
Dahlander connection	36.4
Dahlander connection (model utilization)	51.2
Dahlander connection (principle)	51.1
Damping the braking torques	23.2
Data on the brakes	A1

Deceleration	43.1
Deceleration time	43.1
Delta connection	36.1
Diodes	36
Diodes (circuit configuration)	36.8.3
Direct-on-line switching	5
Disc	33
Disc spring	33
Division of torque according to mass fractions	30
Double-disc	33
Double-disc spring-loaded brake	35.2
Double-disc spring-loaded brake on the fan cowl	35.4
Driver	35
Drum	33
Dual voltage winding	36.2
E	
Electrical feed to the solenoid release	36
Electrodynamic braking (general)	1
Electrodynamic braking, thermal rating	25
Electrodynamic injection braking (general)	III
Electromagnet	33
Electronic D.C. braking units	22.5
Electronic starting circuit	11
Example designs (brakes)	35
Exponential function	37.2
F	
Factor of inertia *FI*	29
FBR single-disc spring-loaded brake	35.6
FI (factor of inertia)	29
Flank clearance	50
Free-wheeling circuit	36.8.3
Frequency control	24
Frequency control (thermal rating)	25.6
Frequency-controlled starting	12
Friction surface	33
G	
Gear backlash	50.1
Gear backlash (linear motion)	50.2
Gear loading according to mass fractions	30
H	
Heavy fan for soft starting	13
High-speed excitation	37.2
Hoist	32
Hydrodynamic couplings	15.2
Hyper-synchronous braking (thermal rating)	25.1
Hyper-synchronous regenerative braking	19
I	
Induction couplings	15.3
Inertial mass (experimental determination)	28
Inertial mass of homogenous bodies	27
Injection braking	40.2
Inverter duty	36.6
Inverter-fed motors	54
K	
Kinetic energy	41.1
KUSA method	10.2
L	
Lifting duty (brake selection)	40.3
Lifting duty (braking time)	43.2
Limit air gap	41.4
Linear motion as a tangent to the circle	31.3

Load characteristic curve	4
Losses with electrodynamic braking methods	25
Lost energy with long release time	37.3
Lowering duty	43.3
M	
Magnetic brake	33.2
Maintenance	34
Maltese cross	32
Mass moment of inertia (experimental)	28
Mass moment of inertia (friction discs)	39
Mass moment of inertia (general)	IV
Mass moment of inertia (rotation)	31.1
Mass moment of inertia (translation)	31.2
Mass moment of inertia for soft starting	13
Mass moment of inertia of cylindrical steel bodies	26.3
Mass moment of inertia of homogenous bodies	27
Mass moment of inertia of the rotor	26
Means of adjustment	42
Modular system	46
Motor characteristic curve	3
Motor field	33
Moving masses as an inertial mass	31
Multiple-disc spring-loaded brake	35.9
Multiple-discs	33
N	
NEMA classification (torque)	18.3
NEMA code letters	18.2
No load operating frequency	37.4
No load operating frequency Z_0	16.2.1
Number of poles (maximum for PU)	52.2
Operating in switching mode	48
Overexcitation	37.2
Overtravel angle	40.3
Overtravel distance	45
Overtravel distance (rotation)	45.2
Overtravel distance (translation)	45.1
Overtravel distance when positioning	53
Overtravel time	44.1, 44.3
P	
Part-winding starting	8
Permanent magnet	33
Permissible on-load operating frequency Z_{lim}	16.2.2
Plugging (reverse-field braking)	21
Plugging (thermal rating)	25.3
Plug-in connection	36.9
Pole-changing	23
Pole-changing (brake connection)	36.4
Pole-changing (possibilities and limits)	53
Pole-changing (stepped starting)	6
Pole-changing (thermal rating)	25.5
Pole-changing positioning motors	52
Positioning (general)	48
Positioning speed (guide value)	54
Potential energy	41
Primary starter	36.5
Proximity switch	49.3.2
PU/VF limitations	54
R	
Rating of the D.C. brake	22.3
Recommended deceleration	23.4
Regenerative braking	19

Regenerative braking from the inverter	24
Releasing force	33
Remanence	38.1
Repair	34
Reserve stocks	34
Response time	44.1
Response time (contactor)	49.3.1
Reverse-field braking	21
Reversing	20
Reversing (thermal rating)	25.2
Ripple	36.8.3
Robotics	48
Rotating table	32
Rotation travel	45
Rotor mass	26
Rotor mass moment of inertia	26
Run-down test	28.3
Run-up time	17
Run-up time, calculation	17
S	
Safety brake	33.2
Self-adjustment	42
Separate windings	36.4
Separate windings (model utilization)	52.3
Series resistors	10
Service life	41.4
Setting, braking torque	42
Shaft-centre distance	50
Shoe spring-loaded brake with A.C. solenoid release	35.8
Shoes	33
Single-disc spring-loaded brake	35.1, 35.10
Single-disc spring-loaded brake on the fan cowl	35.3
Single-phase bridge circuit	36.8.3
Single-phase series resistance (KUSA resistance)	10.2
Slewing gear	32
Slip on a conveyor belt	2.1
Slipring motors	14
Soft starting	36.5
Soft starting or braking (criteria)	2
Solenoid casing	35
Special rotors with increased slip	14
Speed ratio ≠ 1:2	52
Speed ratio = 1:2	51
Speed ratios (possible)	52.2
Speed ratios (separate windings)	52
SPR electronic soft deceleration	23.5
Spring	33
Spring-loaded brake	33, 33.2
Spring-loaded brakes (technical data)	A1
Star connection	36.1
Star-delta starting	7
Starting (general)	II
Starting and electrical braking (general)	1
Starting and electrical braking (introduction)	I
Starting behaviour in accordance with IEC 60034-12	18.1
Starting behaviour, classification	18
Starting circuit, electronic	11
Starting classes	18.4
Starting clutches	15
Starting cycle (basic differences)	37.3.1
Starting device (wiring diagram of the brake)	36.5

Starting transformer (soft starting)	9
Starting transformer (wiring diagram of the brake)	36.5
Starting using series resistors	10
Starting using stepped winding	8
Stepped starting by pole-changing	6
Swinging of a load	2.3
Switching delay	36.8.3
Switching duty (predominant acceleration)	16.2
Switching duty (predominant output)	16.2
Switching duty (thermal rating)	16
Switching duty types (designation)	16.1
Switching energy	41
Switching energy (reduction)	41.3
Switching energy per braking operation	41.1
Switching energy per friction element	41.3
T	
Technical data for spring-loaded brakes	A1
Terminal connection (PU separate windings)	52.1
Thermal load relief on the motor	37.4
Thermal rating of the braking methods	25
Thermal rating of the switching duty	16
Thermally equivalent switching frequency Z_{th}	16.2.3
Thermally permissible switching energy	41.2
Three-phase series resistors	10.1
Thrust plate	35
Time constant	37.2
Timer relay	49
Tipping on a conveyor belt	2.2
Tolerances	49
Tolerances (control system)	49.3
Tolerances (mechanical brake)	49.2
Tolerances (PLC)	49.4
Tolerances (proximity switch)	49.3.2
Tolerances (response times of contactors)	49.3.1
Tolerances (timer relay)	49.3.3
Tolerances (wear)	49.1
Torque characteristic curves (relative height)	52.4
Torque-speed characteristic curve of the load	4
Torque-speed characteristic curve of the motor	3
Torsional offset	50
Torsional pendulum	28.1
Transformers for starting	9
Transitional behaviour	2.4
Translation travel	45
Travelling gear	32
Type test for switching duty	16.2.4
V	
Variable frequency	36.6
Voltage spikes	36.8.1
W	
Wear	42
Working capacity	42
Working capacity of large brakes	47
Z	

The three-phase cage induction motor owes its good reputation as a rugged, problem-free drive unit not least to its good starting characteristics. With starting torques of 1.5 to 2.5 times their rated torque, these machines are able to start up even heavy-duty driven machinery under full load and ensure rapid acceleration.
Although this ability is of positive benefit in most applications, there are a number of driven machines where sudden acceleration can cause problems. For example, oscillation of a load on a crane hook, tipping of bottles on a conveyor belt or sudden over-stressing of mechanical transmission components. Efforts to "improve the starting properties" of three-phase cage motors are therefore seldom aimed at increasing the acceleration, but are more often aimed at ***reducing the run-up torque***.

The development of electric drives shows a clear trend towards ***more frequent switching*** and to ***greater precision in the positioning*** of the load. Previously, motors were designed for continuous operation and the conveyed material or the driven tools were controlled by mechanical systems which provided stepwise movement. Nowadays, braked motors can be accurately positioned by a combination of braking and pulse control. Mechanical braking and stopping from the positioning speed is provided by an auxiliary spring-loaded ***mechanical brake***. This also works as a safety brake, securing the load in a stationary position in the event of a power outage.
Where very high speeds and extremely accurate stopping positions are required, motors with stepplessly adjustable speeds are used, preferably three-phase inverter motors where the ***frequency is varied by a static converter.***

Starting, braking and positioning – these are important aspects of the duties required of electric drives in the context of automation and rationalization.

This book is aimed at all those working in the field of drive technology.
It aims to provide answers to those questions concerning drive technology which the author has most frequently encountered over his many years of experience in the planning and use of three-phase geared motors.

Danfoss Bauer GmbH

Eberhard-Bauer-Straße 36-60
D-73734 Esslingen
Telefon 0711 – 3 51 80
Telefax 0711 – 3 51 83 51

The Gear Motor Specialist